
Electronic Thesis and Dissertation Repository

11-12-2018 11:00 AM

White Matter Inflammation And Executive Dysfunction: Implications For Alzheimer Disease And Vascular Cognitive Impairment

Alexander Levit
The University of Western Ontario

Supervisor
Whitehead, Shawn N.
The University of Western Ontario Co-Supervisor
Hachinski, Vladimir
The University of Western Ontario

Graduate Program in Anatomy and Cell Biology

A thesis submitted in partial fulfillment of the requirements for the degree in Doctor of
Philosophy Follow this and additional works at: <https://ir.lib.uwo.ca/etd>



Part of the [Alexander Levit 2018](#) [Neurobiology Commons](#), [Behavior and Behavior Mechanisms Commons](#), [Medical Neurobiology Commons](#), [Mental Disorders Commons](#), [Molecular and Cellular Neuroscience Commons](#), [Nervous System Diseases Commons](#), [Neurology Commons](#), [Neurosciences Commons](#), [Other Neuroscience and Neurobiology Commons](#), [Pathology Commons](#), [Psychiatric and Mental Health Commons](#), and the [Psychiatry Commons](#)

Recommended Citation

Levit, Alexander, "White Matter Inflammation And Executive Dysfunction: Implications For Alzheimer Disease And Vascular Cognitive Impairment" (2018). *Electronic Thesis and Dissertation Repository*. 5824. <https://ir.lib.uwo.ca/etd/5824>

This Dissertation/Thesis is brought to you for free and open access by Scholarship@Western. It has been accepted for inclusion in Electronic Thesis and Dissertation Repository by an authorized administrator of Scholarship@Western. For more information, please contact wlsadmin@uwo.ca.

White Matter Inflammation And Executive Dysfunction: Implications For Alzheimer Disease And Vascular Cognitive Impairment

Alexander Levit

Supervisor

Whitehead, Shawn N.

The University of Western Ontario

Co-Supervisor

Hachinski, Vladimir

The University of Western Ontario

Graduate Program in Anatomy and Cell Biology

A thesis submitted in partial fulfillment of the requirements for the degree in Doctor of Philosophy

© Alexander Levit 2018

Follow this and additional works at: <https://ir.lib.uwo.ca/etd>

 Part of the [Behavioral Neurobiology Commons](#), [Behavior and Behavior Mechanisms Commons](#), [Medical Neurobiology Commons](#), [Mental Disorders Commons](#), [Molecular and Cellular Neuroscience Commons](#), [Nervous System Diseases Commons](#), [Neurology Commons](#), [Neurosciences Commons](#), [Other Neuroscience and Neurobiology Commons](#), [Pathology Commons](#), [Psychiatric and Mental Health Commons](#), and the [Psychiatry Commons](#)

Abstract

White matter integrity is crucial to healthy executive function, the cognitive domain that enables functional independence. However, in the ageing brain, white matter is highly vulnerable. White matter inflammation increases with age and Alzheimer disease (AD), which disrupts the normal function of white matter. This may contribute to executive dysfunction, but the relationship between white matter inflammation and executive function has not been directly evaluated in ageing nor AD. White matter is also particularly vulnerable to cerebrovascular disease, corresponding with the common presentation of executive dysfunction in vascular cognitive impairment (VCI). Thus, white matter may be an important substrate by which vascular injury exacerbates the cognitive impact of comorbid AD pathology and cerebrovascular pathology. To study the relationship between age, pathogenic amyloid precursor protein (APP), white matter inflammation, cerebrovascular disease, and executive dysfunction, the transgenic rat model of AD (TgAPP21) was evaluated for astrocytosis, microgliosis and cognitive impairment. The TgAPP21 rat was found to demonstrate spontaneously increased white matter microglia activation, impaired reversal learning, and a regressive impairment of behavioural flexibility, a key subdomain of executive function. The TgAPP21 rat also developed a precocious increase in white matter microglia activation. However, this was not matched by a continued increase in behavioural inflexibility, suggesting a dynamic and age-dependent relationship between white matter inflammation and behavioural flexibility. Hypertension induced by chronic angiotensin-II infusion impaired both wildtype (Wt) and TgAPP21 rats' working memory and behavioural flexibility. However, while Wt rats demonstrated a linear increase in white matter astrocytosis in response to blood pressure elevation, normotensive TgAPP21 rats already had an increased baseline level of white matter astrocytosis and further increase in response to hypertension was not observed. TgAPP21 rats also demonstrated a greater vulnerability to cerebrovascular disease, as focal striatal ischemic injury resulted in reduced set shifting efficiency. Thus, the TgAPP21 rat is an important model for studying the complex relationship between age, pathogenic APP, and cerebrovascular disease and their impact on executive dysfunction. These

findings support the emerging significance of white matter inflammation and executive dysfunction in the pathophysiology of ageing, AD, and VCI.

Keywords

White Matter, Inflammation, Microglia, Cognitive Impairment, Executive Function, Behavioural Flexibility, Alzheimer Disease, Amyloid, Vascular Dementia, Ischemic Stroke, Hypertension, Animal/Rat Model.

Co-Authorship Statement

The work presented in *Chapter 2: The Cognitive and Neuroinflammatory Profile of the TgAPP21 Rat* is under review for *Scientific Reports* under the title *Regressive behavioural inflexibility and white matter microglia activation in the transgenic APP21 rat model* and was coauthored by Aaron M. Regis, Andrew Gibson, Olivia H. Hough, Shikhar Maheshwari, Yuksel Agca, Cansu Agca, Vladimir Hachinski, Brian L Allman, Shawn N Whitehead.

The work presented in *Chapter 3: Behavioural Inflexibility and White Matter Inflammation Across the TgAPP21 Lifespan* is under review for publication in the *Journal of Neuroscience* under the title *Precocious white matter inflammation and behavioural inflexibility precede learning and memory impairment in the TgAPP21 rat*, and was coauthored by Andrew Gibson, Olivia Hough, Youngkyung Jung, Yuksel Agca, Cansu Agca, Vladimir Hachinski, Brian L. Allman, Shawn N Whitehead.

The work presented in *Chapter 4: The Role of Hypertension in Executive Function and White Matter Astrocytosis* is under review for publication in *Hypertension* under the title *Hypertension and pathogenic hAPP independently induce white matter astrocytosis and cognitive impairment in the rat*, and was coauthored by Sonny Cheng, Olivia Hough, Yuksel Agca, Cansu Agca Vladimir Hachinski, Shawn N Whitehead.

The work presented in *Chapter 5: Striatal Ischemic Injury Exacerbates Behavioural Inflexibility* has been published in *Behavioural Brain Research* 333(2017):267-275 with the title *Behavioural inflexibility in a comorbid rat model of striatal ischemic injury and mutant hAPP overexpression* and was co-authored by Aaron M Regis, Jessica R Garabon, Seung-Hun Oh, Sagar J Desai, Nagalingam Rajakumar, Vladimir Hachinski, Yuksel Agca, Cansu Agca, Shawn N Whitehead, Brian L Allman.

The work presented in *Appendix F: PET/MRI Study* included work presented at the 2018 Imaging Network Ontario Annual Symposium in Toronto, ON, with the title *Correcting the Arterial Input Function for Dynamic ¹⁸F-FEPPA PET in Transgenic Fischer 344 Rats with Manual Blood Sampling* and was co-authored by Qi Qi (presenter), Matthew S. Fox,

Shawn N. Whitehead, Ting-Yim Lee, Jonathan D. Thiessen. This appendix also included work presented at the American Academy of Neurology 2018 Annual Meeting in Los Angeles, California, for which the abstract was published in *Neurology* 90(15 Supplement) with the title *Multimodal Imaging of White Matter Inflammation in a Rat Model of Striatal Ischemic Stroke (P2.226)*; this presentation was co-authored by Matthew S. Fox, Qi Qi, Vladimir Hachinski, Jonathan D. Thiessen, Shawn N. Whitehead.

Dedication

To Boris & Larisa Levit, my parents – you worked so hard and sacrificed so much so that I could have the best opportunities for success. You taught me to challenge the status quo and to be persistent; I am so lucky to have learned from the best, and I am forever grateful.

To Yan David Levit, my brother – thank you for teaching me to put integrity, meaning and soul into my work. You remind me to take care of myself and everyone we love.

To Natanya Russek, my wife – I am so incredibly blessed to have your support behind all my endeavours. Your love for your grandmother, Dora Russek z”l, always reminds me of why our work matters, and I aspire to echo the care and compassion that you bring to this world.

My family has always inspired my curiosity and my drive for discovery. In searching of answers about our biology, I’ve learned so much more about myself. This thesis is dedicated to you all.

Acknowledgments

It has been such a pleasure to work in the Vulnerable Brain Lab. The technical support and guidance of Dr Lynn Wang, Dr Nina Weishaupt, and ACVS staff were crucial to all of the work described in this thesis. Sharing the adventures of graduate school with my incredible colleagues has made work so much more memorable and enjoyable: Mona Alshaikh, Jennifer Au, Dr Brittany Balint, Dr Sarah Caughlin, Ashmahan Elsariti, Jessica Garabon, Aaron Harris, Nadia Ivanova, Victoria Jaramek, Hayley Nell, Dr Seung-Hun Oh, Dae Hee Park, Aaron Regis, Austyn Roseborough, Victoria Thorburn, Jasmine Wang, and Ryan Wong – I will always look forward to working with you. I'm very grateful of my colleagues that have contributed directly to the research presented in this thesis: Murad Ahmad, Vineeth Bhoadi, Sonny Cheng, Andrew Gibson, Olivia Hough, Stella Iankov, Youngkyung Jung, Qingfan Liu, Shikhar Maheshwari, Rahul Mor, Berk Rasheed, Michelle Shin, John Paul Trudell, and Matthew Zhou.

Learning and working in the Department of Anatomy and Cell Biology was always very gratifying – thank you to all the students, faculty, and staff that have fostered such a friendly environment. My Comprehensive Exam mentors & committee helped me learn to be simultaneously critical of and confident in my scientific convictions – thank you Dr Jonathan Thiessen, Dr Brian Allman, Dr Stephen Pasternak, and Dr David Cechetto. I am also very grateful for the guidance of my supervisory committee, Dr Raj Rajakumar & Dr Brian Allman – you taught me of the importance of professionalism and have been incredibly helpful in shaping my research directions. I also want to thank Dr Raj Rajakumar for acting as my thesis reader. I also want to thank Yuksel Agca and Cansu Agca for generously providing us access to working with the TgAPP21 rat model.

Of course, I am so grateful to have had such incredible supervisors: Dr Vladimir Hachinski and Dr Shawn Whitehead. It has been such a privilege to work in the research environments that you have developed. Your approaches to research and mentorship are unparalleled. Thank you for trusting and challenging me to take on our research questions, and thank you for all of your mentorship at every turn in this adventure.

Finally, the work in this thesis was made possible by external sources of funding from the Heart & Stroke Foundation, the Canadian Institute of Health Research (CIHR), the Ontario Graduate Scholarship (OGS), and the Schulich Foundation.

Table of Contents

Abstract	i
Co-Authorship Statement	iii
Dedication	v
Acknowledgments	vi
Table of Contents	vii
List of Tables	xii
List of Figures	xiii
List of Appendices	xv
List of Abbreviations	xvi
Chapter 1: Introduction	1
1.1 White Matter and Cognitive Function	1
1.1.1 White Matter Integrity	2
1.1.1.1 White Matter Vascular Insufficiency	3
1.1.1.2 White Matter Gliosis and Inflammation	4
1.1.2 Executive Function	5
1.1.2.1 Inhibitory Control	6
1.1.2.2 Working Memory	7
1.1.2.3 Cognitive/Behavioural Flexibility	8
1.2 Alzheimer Disease	10
1.2.1 Clinical Profile of Alzheimer Disease	10
1.2.2 Neuropathology of Alzheimer Disease	13
1.2.2.1 Current Diagnostic Criteria	14
1.2.2.2 Role of Glia in Alzheimer Disease	15
1.2.2.3 White Matter Changes in Alzheimer Disease	17
1.3 Vascular Cognitive Impairment	20
1.3.1 Clinical Profile of Vascular Cognitive Disorders	21
1.3.2 Neuropathology of Vascular Cognitive Disorders: Cerebrovascular Disease	22

1.4	The Neurovascular Hypothesis of Alzheimer disease	24
1.4.1	The Neurovascular Unit and Blood-Brain-Barrier	24
1.4.2	NVU Dysfunction	25
1.4.2.1	Hypertension	26
1.4.2.2	Ischemic Stroke and Silent Brain Infarcts	27
1.4.2.3	Abluminal Injury: Alzheimer Disease Pathology	27
1.4.3	White Matter Pathology and the Neurovascular Hypothesis of Alzheimer Disease	28
1.5	Rationale and Objectives	30
1.6	References	32
 Chapter 2: The Cognitive and Neuroinflammatory Profile of the TgAPP21 Rat		50
2.1	Abstract	50
2.2	Introduction	51
2.3	Methods	53
2.3.1	Animals	53
2.3.2	Set Shift & Reversal	53
2.3.2.1	Apparatus	54
2.3.2.2	Food Restriction & Initial Operant Conditioning	54
2.3.2.3	Side Bias Determination	55
2.3.2.4	Visual Cue Discrimination	55
2.3.2.5	Set-shifting: Response Discrimination	56
2.3.2.6	Set-shifting Behavioural Measures	56
2.3.2.7	Reversal	57
2.3.3	Morris Water Maze	60
2.3.4	Open Field	61
2.3.5	Immunohistochemistry & Image Processing	61
2.3.6	Data Analyses	62
2.4	Results	64
2.4.1	Set Shift & Reversal	64
2.4.2	Morris Water Maze	69
2.4.3	Open Field	75

2.4.4	Activated Microglia in White Matter	77
2.5	Discussion	82
2.6	References	84

Chapter 3: Behavioural Inflexibility and White Matter Inflammation Across the TgAPP21 Lifespan		87
3.1	Abstract	87
3.2	Introduction	88
3.3	Methods	90
3.3.1	Animals	90
3.3.2	Set Shift & Reversal	93
3.3.3	Morris Water Maze	94
3.3.4	Open Field	95
3.3.5	Immunohistochemistry & Image Processing	95
3.3.6	Data Analysis	97
3.4	Results	98
3.4.1	Set Shift	98
3.4.1.1	Visual Cue Discrimination	98
3.4.1.2	Response Discrimination	100
3.4.1.3	Reversal	104
3.4.1.4	Omission Trials	106
3.4.1.5	Exclusions & Outliers	108
3.4.2	Morris Water Maze	110
3.4.2.1	Navigational Learning	110
3.4.2.1	Navigational Memory	110
3.4.2.3	Regressive Platform Search	111
3.4.2.4	Cued Trials & Swim Speed	113
3.4.3	Open Field	118
3.4.4	Activated Microglia	120
3.4.5	Reactive Astrocytes	124
3.5	Discussion	128
3.6	References	131

Chapter 4: The Role of Hypertension in Executive Function and White Matter Astrocytosis	134
4.1 Abstract	134
4.2 Introduction	135
4.3 Methods	137
4.3.1 Animals	137
4.3.2 Blood Pressure Elevation & Measurement	137
4.3.3 Morris Water Maze	138
4.3.4 Open field	138
4.3.5 Immunohistochemistry & Image Processing	139
4.3.6 Data Analysis	140
4.4 Results	141
4.4.1 Blood Pressure Elevation and Measurement	141
4.4.2 Reactive Astrocytes	143
4.3.3 Activated Microglia	146
4.3.4 Open Field	148
4.3.5 Morris Water Maze	150
4.5 Discussion	152
4.6 References	154
Chapter 5: Striatal Ischemic Injury Exacerbates Behavioural Inflexibility	158
5.1 Abstract	158
5.2 Introduction	159
5.3 Methods	161
5.3.1 Animals	161
5.3.2 Endothelin-1 Focal Ischemic Injury	161
5.3.3 Thionine Histochemistry	162
5.3.4 Microscopy and Striatal Injury Analysis	162
5.3.5 Set-Shifting	163
5.3.4 Data Analyses	165

5.4	Results	166
5.4.1	Striatal Ischemic Injury	166
5.4.2	Visual Cue Discrimination	168
5.4.3	Set-shifting: Response Discrimination	170
5.4.4	Logistic Modelling: Exposure-Response Curve	173
5.5	Discussion	175
5.5.1	Comorbidity of AD and Stroke	175
5.5.2	Logistic Modelling: Exposure-Response Curve	176
5.5.3	Clinical Relevance of Comorbid Model	177
5.6	References	179
Chapter 6: Discussion		183
6.1	Summary	183
6.2	Regressive Behavioural Inflexibility	184
6.3	White Matter Inflammation	186
6.4	Mixed Pathology	187
6.5	Limitations	187
6.6	Future Directions	190
6.7	Conclusion	192
6.7	References	194
Appendices		200
Curriculum Vitae		247

List of Tables

Table 2-1: Global activation of microglia across anatomical regions	Error! Bookmark not defined.
Table 3-1: Experimental group characteristics	92
Table 3-2: Stage of Exclusion from Set Shifting Results	109

List of Figures

Figure 2-1: Testing behavioral flexibility in an operant based set-shifting task	58
Figure 2-2: TgAPP21 rats demonstrate unimpaired learning and memory of visual cue discrimination	65
Figure 2-3: TgAPP21 rats demonstrate increased regressive behaviour during extradimensional set shifting and impaired spatial reversal	68
Figure 2-4: TgAPP21 rats demonstrate regressive inflexibility during the Morris Water Maze probe test	71
Figure 2-5: Supplementary MWM behavioural analysis	73
Figure 2-6: TgAPP21 rats exhibited less exploratory behaviour in the open field	76
Figure 2-7: Increased microglia activation in TgAPP21 white matter correlates with reversal impairments	80
Figure 3-1: Impaired visual cue discrimination learning & memory in aged rats.	99
Figure 3-2: Set shifting in aged transgenic rats facilitated by impaired memory of visual cue discrimination.	102
Figure 3-3: Regressive inflexibility in transgenic rats peaked at 8 months of age	103
Figure 3-4: Reversal impairment in transgenic rats peaked at 8 months of age, increased with age in wildtype rats	105
Figure 3-5: Neither genotype nor age affected frequency of omission trials.	107
Figure 3-6: Age impaired Morris Water Maze learning	114
Figure 3-7: Age-dependent memory impairment in the Morris Water Maze probe was preceded by a regressive-like inflexibility	115
Figure 3-8: Regressive behaviour consistent across response discrimination and Morris Water Maze probe	117

Figure 3-9: Decreased open field exploration in aged and transgenic Rats	119
Figure 3-10: Precocious corpus callosum inflammation in transgenic rats	123
Figure 3-11: Reduced forceps minor astrocyte reactivity in aged TgAPP21	126
Figure 3-12: Significant positive correlation between regressive errors and astrocyte reactivity in the forceps minor.	127
Figure 4-1: Mean Arterial Pressure during 8 weeks of normal saline or AngII infusion.	142
Figure 4-2: Increased white matter reactive astrocytosis in transgenic rats is unresponsive to blood pressure elevation.	145
Figure 4-3: Increased white matter and hippocampal microglia activation in transgenic rats.	147
Figure 4-4: Reduced exploratory behaviour in transgenic rats.	149
Figure 4-5: AngII infusion impaired behavioural flexibility.	151
Figure 5-1: Wt-ET1 and Tg-ET1 have equal infarct areas in the ipsilateral striatum	167
Figure 5-2: Visual cue discrimination learning and memory retrieval	169
Figure 5-3: Response discrimination learning and number of errors committed during set-shifting	171
Figure 5-4: Set-shift error profile	172
Figure 5-5: Logistic modelling of incongruent trial error rates	174

List of Appendices

Appendix A: Set Shift Data Extraction	203
Appendix B: MWM Regressive Preference for Target Quadrant	210
Appendix C: Immunohistochemistry Protocols	211
Appendix D: Microscopy and Image Analysis Protocols	214
Appendix E: Rat Tail Cuff Blood Pressure Measurement Protocol	226
Appendix F: PET/MRI Study	237
Appendix G: Animal Use Protocol	246

List of Abbreviations

A β	amyloid- β / β -amyloid
AD	Alzheimer disease
ADL	activities of daily living
AngII	Angiotensin II
ANCOVA	analysis of covariance (statistical method)
ANOVA	analysis of variance (statistical method)
APP	amyloid precursor protein; see also hAPP
CCCDTD4	4 th Canadian Consensus Conference on the Diagnosis and Treatment of Dementia
CERAD	Consortium to Establish a Registry for Alzheimer's Disease
COX	cyclooxygenase
CT	computerized tomography
DAB	3,3'-diaminobenzidine-tetrahydrochloride
DLPFC	dorsolateral prefrontal cortex
DSM-V	5 th edition of the Diagnostic and Statistical Manual of Mental Disorders
DTI	diffusion tensor imaging
DW-MRI	diffusion weighted magnetic resonance imaging
EOAD	early onset Alzheimer disease (diagnosed at <65 years of age)
FA	fractional anisotropy
GFAP	glial fibrillary acidic protein
hAPP	human amyloid precursor protein (with Swedish and Indiana mutations in the context of this thesis)

IADL	instrumental activities of daily living
IHC	immunohistochemistry
LOAD	late onset Alzheimer disease (diagnosed at ≥ 65 years of age)
LRP	Lipoprotein receptor-related protein
MCI	mild cognitive impairment
MHC	major histocompatibility complex
MRI	magnetic resonance imaging
MTM	mean transit time
MWM	Morris Water Maze
NFTs	neurofibrillary tangles
NIA-AA	National Institute of Aging – Alzheimer’s Association
NSAID	non-steroidal anti-inflammatory drug
NVU	neurovascular unit
OFC	orbital frontal cortex
PCET	Penn conditional exclusion test
PET	positron emission tomography
PFC	prefrontal cortex
RD	response discrimination (set shifting)
SD	standard deviation
SEM	standard error of the mean
SVD	small vessel disease
Tg/TgAPP21	transgenic rat model of Alzheimer disease; Fischer 344 homozygous for pathogenic hAPP with Swedish and Indiana mutations.

TNF- α	tumour necrosis factor- α
VaD	vascular dementia
VASCOG	International Society for Vascular Behavioural and Cognitive Disorders
VCD	visual cue discrimination (set shifting)
VCIND	vascular mild cognitive impairment
VLPFC	ventrolateral prefrontal cortex
VMPFC	ventromedial prefrontal cortex
WCST	Wisconsin card sorting test
Wt	wildtype rat (Fischer 344)

Chapter 1: Introduction

This chapter outlines the current literature pertaining to white matter integrity, neuroinflammation, and cognitive impairment in the context of Alzheimer disease (AD) and vascular cognitive impairment (VCI). AD and vascular pathology frequently occur together and important intersections of these two conditions are observed in white matter tissue. Investigating this link between AD and vascular pathology will develop our understanding of the early pathophysiology of the two leading causes of dementia.

1.1 White Matter and Cognitive Function

Neuroscience and behavioural neurology has traditionally focused on grey matter even though white matter occupies 40-50% of the adult human brain¹. Although Jean-Martin Charcot described the white matter lesions observed in multiple sclerosis and amyotrophic lateral sclerosis in the 19th century², it would not be until 1965 that the notion of “cerebral disconnection” as a more general mechanism for cognitive impairment would be introduced by Norman Geschwind¹. Today, white matter continues to be understood generally as tissue that mediates the *transfer* of information, in contrast to the *processing* of information which is attributed to grey matter. This applies to all levels of cognition, but the striking abundance of white matter in the frontal lobes, the seat of integration and coordination, underscores the importance of white matter for higher-level domains of cognition,¹ including inhibition, cognitive flexibility, planning, problem solving, reasoning, abstract thinking, complex social processing, and creativity. Comparative neuroanatomy identifies our species’ unique proportion of white matter volume, featuring an exceptional quantity of thick myelinated fibres, as crucial to our ability to excel in higher-level cognition³.

Conversely, impairments of higher level cognition can be attributed to white matter disruptions, including lesions that are far subtler than what Jean-Martin Charcot could detect¹. Aided by developments in neuroimaging, the term white matter dementia was introduced in 1988 to expand the scope of dementia research³. Similarly, recent decades

saw an increased interest in the role of glial cells in normal and disordered neurological function^{4,5}. White matter is defined by a preponderance of axons, myelin, and oligodendrocytes but also includes an abundance of astrocytes, microglia, and blood vessels³, so the roles of glial cells in disorders of the central nervous system (CNS) would naturally direct more research to white matter⁴⁻⁷. The following sections will review current literature on the cognitive correlates of white matter and the general impairments observed with white matter dysfunction. Thereafter, white matter dysfunction will be described in the context of AD and VaD.

1.1.1 White Matter Integrity

Healthy white matter function depends on thick and well-organized myelination of axons⁸. White matter structure is also experience dependent, with ongoing white matter reorganization playing an important role in supporting cognitive plasticity⁹. White matter degeneration can present clearly in the form of volume loss, measured with neuroimaging or as gross atrophy on post-mortem studies. More subtle forms of white matter degeneration include microstructural changes that alter molecular diffusion characteristics as measured by diffusion-weighted magnetic resonance imaging (DW-MRI), including an early form of this technique, diffusion tensor imaging (DTI)¹⁰. In short, DTI relies on differences in the displacements of water molecules depending on tissue type¹¹. One of the most commonly metrics used in DTI is fractional anisotropy (FA), which quantifies how restricted water molecule diffusion is in a given voxel. FA measures range from 0 to 1, with low values seen in the CSF-filled ventricles where water diffusion is unrestricted in all directions, and high values in myelinated white matter tracts such as the corpus callosum, where water movement is greatly restricted to move primarily along the direction of the axons^{11,12}.

A loss of FA in white matter tissue, where FA is expected to be high, indicates microstructural changes that are presumed to be predominantly the result of demyelination or alterations in myelin structure¹¹⁻¹³. However, FA also reflects axonal caliber, injury, and density, as well as uniformity of fibre direction and gliosis; research continues to identify the histopathological correlates of DTI metrics, including FA, and

how these radiological-histopathological correlates change in different disease contexts¹². Despite this, and with some controversy¹⁰, DTI measures such as FA are widely inferred as a measure of white matter integrity. The limitations of this interpretation are well detailed by Jones et al¹⁰, but the appeal to inferring deleterious microstructural changes based on DTI measurements is supported by cognitive correlates¹². In normal aging^{9,14-21} and many different neurodegenerative conditions²²⁻²⁸, loss of FA in white matter has been correlated with cognitive impairments, most often with processing speed and executive function.

The clinical utility of measuring microstructural white matter changes is further demonstrated by the potentially diagnostic and prognostic value of leukoaraiosis. Also known as white matter hyperintensities, leukoaraiosis is a radiological phenomenon of diffuse hypodense (on CT) or hyperintense (on T2 MRI) white matter²⁹⁻³⁴. Leukoaraiotic white matter has reduced white matter integrity, as measured by DW-MRI^{35,36} and leukoaraiosis is an important risk factor for stroke, dementia, and death³⁷⁻³⁹. The term leukoaraiosis, derived from the Greek *leuko* (white) and *araiosis* (rarefaction) was coined intentionally so as not to assume any particular disease etiology;⁴⁰ still to this day, the exact processes that causes leukoaraiosis has not been determined. Vascular pathology is commonly proposed as the underlying mechanism of leukoaraiosis⁴¹⁻⁴⁴, although dysregulation of glial cells and inflammation have also been implicated^{45,46}.

1.1.1.1 *White Matter Vascular Insufficiency*

White matter is particularly sensitive to vascular disruption^{44,47-52}. When mild hypercapnia was induced in healthy subjects to produce systemic vasodilation, a significant steal phenomenon was observed that resulted in reduced blood flow to white matter⁵⁰. The very regions that had reduced blood flow matched the common neuroanatomical locations of leukoaraiosis matter, namely periventricular^{44,50}. This was also supported by a previous study of subjects with leukoaraiosis that had normal blood flow to grey matter but reduced white matter blood flow⁵². Reduced blood flow indicates a poorer cerebrovascular reserve in white matter, and the white matter regions that are relatively

more prone to leukoaraiotic changes indeed fall in the “watershed” regions in between the major arterial zones of the brain^{50,51,53,54}. Moreover, white matter has been shown to be highly vulnerable to ischemic injury, with increased susceptibility seen with age⁵¹. The greater white matter vulnerability to ischemia is attributed to a relative paucity of collaterals in deep white matter⁵³ and the high sensitivity of oligodendrocyte precursor cells to ischemia-induced oxidative stress⁵¹. In a rat model maintained on a high saturated fat, salt, and refined sugar diet, hypertension and cerebral small vessel blockage was associated with white matter atrophy⁵⁵.

Hypertension also correlates with disruptions of white matter structure^{49,56} and is a key risk factor for leukoaraiosis^{47,57}. At the same time, the presence of leukoaraiosis is more common in subjects with orthostatic hypotension⁵⁸ and increased pulse pressure^{59,60}. Cerebral small vessel disease (SVD) is an umbrella term for pathologies of perforating cerebral arterioles, capillaries, and venules⁴², and is associated with systemic vascular risk factors such as hypertension, atherosclerosis, diabetes mellitus, and atrial fibrillation⁶¹; cerebral SVD also often manifests as leukoaraiosis⁴¹⁻⁴⁴. Thus, due to the organization of the cerebrovasculature^{50,53}, white matter is extremely susceptible to common systemic cardiovascular conditions. A lot of histopathological heterogeneity has been observed in leukoaraiosis, so that in general, any vascular conditions that cause cerebral hypoperfusion, blood brain barrier (BBB) disruption, chronic ischemia, microinfarcts, venous collagenosis, vessel tortuosity, or vessel wall thickening is also thought to cause leukoaraiosis^{43,54,62}.

1.1.1.2 White Matter Gliosis and Inflammation

In addition to the large variety of vascular abnormalities observed in leukoaraiotic white matter, many active and dystrophic glial cells are also observed⁴³. This includes dysfunctional oligodendrocytes, clasmatodendritic astrocytes (abnormal astrocytes with swollen soma and short blunt processes), and activated microglia^{44,62,63}. As glial cells actively maintain white matter integrity and homeostasis, they may be important targets for therapeutic intervention^{64,65}. Neuroinflammation in neurodegenerative diseases is

thought to be driven primarily by microglia, which are involved in both cytokine secretion and phagocytosis^{4,66,67}; microglia-mediated inflammation affects white matter in particular, both in normal aging and in neurodegenerative disease⁶⁸. Indeed, experimental studies have shown that the inhibition of white matter microgliosis improves white matter integrity after cerebral hypoperfusion⁶⁹⁻⁷⁶, thus microglia play an important role in the vascular vulnerability of white matter. **Although microglia activation does not capture the entire scope of neuroinflammation, microglial activation is a strong indicator of a proinflammatory environment⁶⁷ and will be used as the key measure of neuroinflammation in this thesis.** Astrocytes also interact with microglia in inflammatory conditions and are an important factor in both white matter maintenance inflammation^{5-7,66,77}. Despite the importance of both microglia and astrocytes in maintaining white matter in neurodegenerative disease and in health, there is a paucity of literature on how dysregulation of these white matter glial cells affect cognition. In two recent rodent studies, white matter microglial activation was associated with executive dysfunction^{78,79}, and two recent post-mortem studies of dementia pugilistica and alcohol-related neuropathology also demonstrated an association between executive dysfunction with white matter astrocytosis^{80,81}. The prevalence and burden of diseases that can induce dysregulation of white matter microglia and astrocytes, and consequentially, impair white matter integrity and executive function, warrants more research.

1.1.2 Executive Function

Executive function refers to a group of inter-dependent cognitive functions that enable planning, mental manipulation, and control over goal-directed behaviour. The core subdomains of executive function are inhibitory control, working memory, and cognitive flexibility⁸², which all rely on information processing in the prefrontal cortex (PFC) and its extensive connections with other cortical and subcortical brain regions. Although specific locations of leukoaraiosis do associate with impairments of specific subdomains²⁸, leukoaraiosis in any region is also correlated with hypometabolism in the PFC and global impairments of executive function^{21,28,83}. The substantial convergence of fibre pathways that connect the PFC¹ may explain how pathology in even a small focal white matter

lesion could affect metabolism in the entire frontal cortex and cause broad impairments of executive function³¹.

Of all cognitive domains, executive function is often the most sensitive to both environmental and physiological stressors⁸². Accordingly, executive function declines in late adulthood^{82,84}, which has been linked to disruptions of white matter integrity¹⁴⁻²¹. Even in normal aging, white matter volume shows a greater decline than grey matter volume^{12,85}. For patients diagnosed with dementia or at risk of dementia, one of the most difficult challenges is the loss of functional independence, which is strongly dependent on executive function⁸⁶⁻⁸⁸. In a clinical setting, functional independence is most often evaluated according to an individual's capacity for activities of daily living (ADLs), including personal hygiene, mobility, and eating⁸⁸. More complex ADLs such as the management of finances and medications, cooking, housekeeping, often referred to as instrumental ADLs (IADLs), are also evaluated to offer a more sensitive measure of cognitive impairment in earlier stages of neurodegenerative diseases⁸⁸. Indeed, the cognitive domain that best predicts current and future functional independence, as measured by ADLs and IADLS, is executive function⁸⁶⁻⁸⁸. This emphasizes the importance of supporting general white matter health for maintaining executive function as well as functional independence.

1.1.2.1 Inhibitory Control

Inhibitory control of attention, thought, behaviour, and emotions constitutes one of the core subdomains of executive function⁸². Inhibitory control of attention can occur involuntarily, as with the filtering of stimuli at the level of perception such as background noise at a cocktail party. Inhibitory control of attention can also occur voluntarily, as when effort is made to ignore stimuli that distract from goal-directed behaviour⁸². The inhibition of both mental representations and behaviour can be best appreciated in conditions where such inhibition is impaired; intrusive memories and thoughts are a core component of post-traumatic stress disorder^{89,90}, substance addiction⁹¹, and the obsessive component of obsessive-compulsive disorder⁹², while impairments of behavioural

inhibition are also seen in substance addiction⁹¹ and the compulsions seen in obsessive-compulsive disorder⁹². Lastly, inhibitory control of emotions is regularly required in social interaction and maintaining motivation while delaying gratification through arduous tasks, such as writing a dissertation⁸².

The PFC is responsible for regulating and inhibitory control over attention, thought, behaviour, and emotions. The inferior frontal gyrus in the ventrolateral PFC (VLPFC) plays an important role in inhibition via direct connections to other cerebral cortices, basal ganglia, the subthalamic nucleus, and cerebellar cortices^{93,94}. In particular, the right VLPFC has been associated with behavioural inhibition, whereas the bilateral actions of the VLPFC contribute more to inhibition of attention and thoughts⁹³⁻⁹⁵. Inhibition of emotions appears to be more directly regulated by both the ventromedial PFC (VMPFC), which have extensive connections with the amygdala, hypothalamus, nucleus accumbens, and brainstem nuclei^{93,94}. Both the VMPFC and VLPFC are considered to initiate top-down control of inhibition but other structures downstream are also crucial to inhibitory control, namely the basal ganglia and supplementary motor areas⁹⁴. While focal lesions in any of these structures may cause specific impairments of inhibition, white matter lesions in any of the circuits that connect these structures will also impair inhibitory control⁹³.

1.1.2.2 *Working Memory*

Another core domain of executive function is working memory, defined as the function of holding and manipulating information that is not perceptually present (mental representations)⁸². Working memory is often further distinguished by verbal and non-verbal (visual-spatial) content, and is utilized in all instances of mental math, mental reorganization or revision of information, and relating different pieces of information such as verbal translation; working memory is essential for reasoning. Working memory may often be miscategorized as a type of short-term memory rather than a subdomain of executive function, but working memory is more closely linked to executive function in terms of neuroanatomy, childhood development, and function⁸².

There is considerable controversy over whether working memory is a dissociable cognitive domain. Of course, working memory and short-term memory are highly inter-related. This is demonstrated by short-term memory tasks that require a longer (suprathreshold) number of information items, wherein working memory is automatically engaged to organize the information. The key distinction between working memory and short-term memory is that the former involves manipulations of information in addition to the mental holding of that information. Holding information activates the VLPFC during tasks that require either working memory or short-term memory, while working memory dependent tasks involving the manipulation of information are also associated with activation of the dorsolateral PFC (DLPFC)⁸². Similarly, working memory and inhibitory control are often functionally inter-dependent and show high neural co-activation⁸². Working memory directs inhibitory control, while inhibitory control regulates the information that can occupy working memory. This has led many to view inhibitory control as derivative, with working memory enhancement of specific goals or thoughts considered to be sufficient to automatically repress unwanted goals or thoughts, that is, inhibitory control. Others still maintain that working memory and inhibitory control are dissociable domains, and that mental suppression requires more than just a relative lack of mental enhancement. While this debate continues⁸², most will agree that all subdomains of executive function are highly interdependent, including the subdomain of cognitive or behavioural flexibility.

1.1.2.3 Cognitive/Behavioural Flexibility

Cognitive flexibility, often referred to as behavioural flexibility in the context of rodent studies, builds on both inhibitory control and working memory. Cognitive flexibility describes the ability to change perspectives or goals, which involves the inhibition of current thoughts or goal-directed behaviours and the engagement of new ones⁸². Representative tasks that require cognitive flexibility include design fluency, verbal fluency, and category fluency, wherein a subject is asked to, respectively, think of different uses of a table, different words that begin with a certain letter, or alternate sequentially between letters and numbers⁸². Accordingly, cognitive flexibility is considered to be crucial

for creativity. Lesions of the dorsomedial PFC (DMPFC) produce the most consistent impairments of different types of fluency^{96,97}.

Another common task that requires cognitive flexibility is task switching. A relatively simple form of task switching is known as reversal, such as when a rewarding option is changed from a left switch to a right switch. Lesions of the orbitofrontal cortex (OFC), located between the VMPFC and VLPFC⁹⁸, result in reversal impairments^{99,100}. A more complex form of task switching is known as set shifting, which requires a subject to redirect their attention between different sets of cues; this is exemplified by the Wisconsin Card Sorting Task, wherein subjects need to shift between sorting rules that depend on shape, colour, or number¹⁰¹. In contrast to reversal, set shifting is impaired by lesions of the DLPFC^{99,100}.

Both reversal and set-shifting tests have also been adapted for rodent studies, wherein maze-based or operant-based challenges require rodents to reverse behaviour or shift behaviour according to attentional sets¹⁰⁰. Although the functional divisions of the PFC do not arrange in the same neuroanatomical topography in rodents, reversal and set shifting impairments are similarly doubly dissociated in rats¹⁰². Additional pathways between the PFC, thalamus, and striatum that also contribute to set shifting behaviour are also conserved across species¹⁰², further supporting the interpretation that behavioural flexibility in rats is still very informative for the study of cognitive flexibility in humans^{98,100}. Though there certainly are limitations to the human-rodent homology of cognitive-behavioural flexibility, other executive functions, and underlying neural correlates, the experimental possibilities of rodent studies are still crucial to identifying the neural substrates and disease mechanisms of neurodegenerative cognitive impairments^{100,103}.

1.2 Alzheimer Disease

Alzheimer disease (AD) is a devastating condition of progressive neurodegeneration and the most common cause of dementia¹⁰⁴. AD is a terminal illness and no current therapies can stop or reverse disease progression. As with many diseases of advanced age, there is heterogeneity in disease presentation and progression, and there are many environmental and lifestyle factors that are considered to modify the risk of incidence¹⁰⁴. Neuropathologically, AD presents with protein-rich plaques, neurofibrillary tangles (NFTs), and gliosis, but disease etiology remains undetermined. The following sections will outline the clinical and neuropathological features that currently define AD and explore emerging research on the role of glia and white matter pathology.

1.2.1 Clinical Profile of Alzheimer Disease

Patients with symptoms of dementia can be evaluated in a clinical setting and if the pattern of cognitive impairment and biomarkers are characteristic of AD, a diagnosis of “probable AD” can be made¹⁰⁵. As current clinical diagnoses are not sufficiently sensitive nor specific for AD, diagnosis of AD is not confirmed until post-mortem evaluation¹⁰⁶; currently, there are no cognitive impairments or biomarkers that can provide definitive clinical diagnosis. However, the most recent criteria put forward by National Institute of Aging-Alzheimer’s Association (NIA-AA) and the International Working Group for New Research Criteria for the Diagnosis of AD (IWG2) have endorsed the use of some biomarkers in aiding clinical diagnosis^{105,107}. Though biomarkers are an active area of development¹⁰⁷⁻¹⁰⁹, recommendations from NIA-AA and the 4th Canadian Consensus Conference on the Diagnosis and Treatment of Dementia (CCCDTD4) do not recommend regular use of biomarkers in the diagnosis of AD until more definitive evidence of safety and benefit is available¹¹⁰. Current treatments offer only modest delays of symptom progression^{111,112}, but early and accurate diagnosis does improve care planning and symptom management¹¹².

Memory impairment is considered to be a cardinal symptom of AD and different types of memory are affected in a typical sequence as the disease progresses¹¹³. As

neurodegeneration typically begins in the structures of the medial temporal lobe including the hippocampus, episodic memory is often the earliest to be impaired¹¹⁴. Episodic memory describes memory of autobiographical events. Episodic memory of recent events tends to be affected prior to impairments of remote memory recall and immediate recall, which rely more on extra-hippocampal structures¹¹⁴. For example, a patient with mild-moderate AD may have difficulty recalling a family visit from a day prior but could recall childhood memories or the meal that they just completed. As the disease progresses, semantic memory becomes impaired as well, which are memories of non-autobiographical facts such as the capital of a country. Procedural memory, which describes non-declarative memories including motor skills such as playing the piano, is spared until late in disease progression. More recently, several other cognitive domains have been recognized as important features of early AD: visuospatial, language, and executive. Since 2011, the NIA-AA has recommended that symptoms of amnesia are not required for a diagnosis of probable AD¹⁰⁵. This also applies to recent versions of two other widely used diagnostic criteria: the 5th edition of the Diagnostic and Statistical Manual of Mental Disorders (DSM-V)¹¹⁵ and the IWG2¹⁰⁷. Executive dysfunction is observed in the majority of early AD patients, with complex attentional functions as the most commonly affected: working memory, dual processing, attentional control, and response selection¹¹⁶.

The global prevalence of AD was estimated to be 35.6 million in 2010; this figure is projected to nearly double every 20 years, due to the expected growth of the elderly population¹¹⁷. Early onset AD (EOAD), defined as the onset of dementia before 65 years of age, is rare but follows strong inheritance patterns^{118,119}. Late onset AD (LOAD; diagnosed after the age of 65) is also considered to be a genetic disorder but with complex interactions with environmental factors¹²⁰. After the age of 65, 17% of women and 9% of men are predicted to be diagnosed with AD in their lifetime, with risk increasing with age¹²¹. Overall, AD contributes to 60-80% of all dementia cases¹⁰⁴. Common genetic variation of Apolipoprotein E (ApoE), which is involved in cholesterol and lipid transport throughout the body, is the strongest known genetic risk factor specific to LOAD¹²². In particular, an estimated 27% of the general population carries at least one allele for the ApoE ϵ 4 isoform; carriers of a single ϵ 4 variant have a 2-3 fold increased risk of LOAD,

while the rare 2% of the public that are $\epsilon 4/\epsilon 4$ carriers have a 12-fold increased risk^{104,123,124}. Though ApoE has been implicated in AD by direct CNS dysregulation, it may also affect AD pathophysiology indirectly by cerebrovascular dysregulation, as ApoE is also a major risk factor for cardiovascular morbidity¹²⁵. However, variations in ApoE only account for 1/4 of the genetic variance that contributes to LOAD diagnosis, and genetics overall can only account for 1/2 of the variance in LOAD diagnosis¹²⁶. Thus, potentially modifiable environmental factors may play an important role for the majority of the population.

Mild cognitive impairment (MCI) is a clinical diagnosis that identifies patients with relatively minor functional challenges due to cognitive impairments. MCI is primarily distinguished from dementia in that ADLs are not severely impaired, despite impairments in one or more cognitive domains¹²⁷. Though MCI is not attributed to any particular neuropathology and can progress to different forms of dementia¹²⁸, of which AD is only one form of dementia, the NIA-AA identifies *MCI due to AD* as the symptomatic prodementia phase of AD¹²⁷. As with the use of emerging diagnostic biomarkers, the CCCDTD4 recommends that MCI due to AD is only diagnosed in specialized clinical practice and for research purposes. Patients with MCI are at increased risk of developing dementia¹²⁹, but this is controversial as the annual conversion rate is highly variable (3-20%) and the majority of MCI diagnosed patients might not progress to a diagnosis of dementia even after 10 years of follow up¹³⁰⁻¹³⁴. Ongoing research on MCI is focused on identifying factors that distinguish MCI from cognitively unimpaired older adults and factors that predict conversion to the different forms of dementia. A large range of clinical factors and biomarkers have been found to predict conversion to AD, offering insight into the early pathophysiology and trajectory of AD:^{127,128,134} multidomain impairment¹³⁵⁻¹³⁹, vascular risk factors¹⁴⁰, ApoE isoforms¹³⁹, plasma and CSF biomarkers¹⁴¹, and neuroimaging biomarkers^{142,143} including white matter hyperintensities^{144,145}.

1.2.2 Neuropathology of Alzheimer Disease

The pathophysiology of AD remains undetermined and the disease has considerable pathological heterogeneity. However, all presentations of AD feature aggregates of amyloid protein and NFTs, attributed to increased production and/or impaired protein clearance.

Amyloid precursor protein (APP) is expressed widely throughout the brain and in many other organs^{146,147}, but its physiological functions have not been fully identified¹⁴⁸. Mutations of APP and key enzymes involved in the amyloidogenic cleavage pathway of APP (PSEN1/2) have been linked to autosomal dominant forms of EOAD, though not all mutations are fully penetrant¹¹⁸. Two post-translational cleavage pathways have been identified for APP, with the amyloidogenic pathway producing an extracellular amyloid- β (A β) fragment. A β aggregates into several forms, ranging in size from soluble oligomers to insoluble fibrils that can form plaques. More recently, soluble A β oligomers, also known as also known as A β -derived diffusible ligands (ADDLs), have been considered to be a key player in the neurotoxic mechanism of AD as A β oligomers can bind a range of synaptic receptors and induce synaptic loss¹⁴⁹. Interestingly, A β oligomers also elicit pro-inflammatory responses and impairment of essential glial functions¹⁴⁹. Moreover, neurons are no longer considered to be the sole source of A β ; reactive astrocytes can also contribute significantly to A β production¹⁵⁰.

Tau protein is another important molecular factor in the pathophysiology of AD. Under physiological conditions, tau protein stabilizes neuronal microtubules. Pathological stressors induce hyperphosphorylation of tau, which then aggregates to form neurotoxic NFTs¹⁵¹. In AD, NFTs present after the accumulation of A β plaques but are a stronger neuropathological correlate of cognitive impairment¹⁵². NFTs accumulate first in the entorhinal cortex, and as the disease progresses, NFTs propagate into hippocampal regions, the lateral temporal cortex, association cortices, and lastly to primary unimodal cortices¹⁵³⁻¹⁵⁵. This contrasts the propagation of A β plaques which follow a more inward direction, first accumulating in the neocortical association regions before spreading to allocortical structures, the limbic regions, diencephalon, and lastly, the brainstem and

cerebellum¹⁵⁵⁻¹⁵⁷. Despite this difference in neuropathological propagation, direct interactions of A β and tau protein are thought to be synergistically deleterious and central to the development of dementia¹⁵⁸⁻¹⁶⁰, with glial cells playing an important role in mediating the interaction of A β and tau dysregulation^{161,162}.

1.2.2.1 *Current Diagnostic Criteria*

Although post-mortem evaluation continues to be considered the gold-standard for verifying a clinical diagnosis of AD, many cases of autopsy-identified AD do not have a clinical history of dementia¹⁰⁶. While such cases may indicate pre-symptomatic AD, which was intended by design¹⁶³, neuropathological criteria continue to be refined to improve correlation with clinical history¹⁶⁴. Currently, the most widely recognized guidelines were put forward by the NIA-AA¹⁶⁵, which determines the neuropathological stage of AD according to:

- Extracellular A β deposits, also known as senile plaques, scored according to the *Thal* phases¹⁵⁶.
- Intracellular NFTs that feature aggregates of hyperphosphorylated tau protein, scored by Braak stages¹⁵⁴
- Dense aggregates of A β and dystrophic neurites known as neuritic plaques, scored according to the Consortium to Establish a Registry for Alzheimer Disease (CERAD) criteria¹⁶⁶. These represent a subset of senile plaques and are more closely associated with neuronal injury.

The scores of these 3 neuropathological features are combined to determine whether brain tissue has low, intermediate, or high levels of AD neuropathological changes. Senile plaques in the *Thal* phases include diffuse A β plaques, which are usually not associated with glial responses or synaptic loss¹⁶⁷. Though diffuse A β plaques are a sensitive indicator of AD dementia, they are also common in elderly individuals without dementia. However, characterizing the distribution and density of all forms of senile plaques continues to play a role in the NIA-AA guidelines by improving sensitivity for cognitive

impairment¹⁶⁸ and detection of early disease^{156,164}. The Thal phases are also recommended for correlation with neuroimaging studies¹⁶⁵. To offer improved diagnostic specificity for cognitive impairment, the CERAD criteria excludes diffuse plaques and emphasizes neuritic plaques, which are more closely associated with cognitive impairment¹⁶⁷. The Braak distribution of NFTs provides even stronger clinicopathological correlation, as neocortical NFT burden provides the strongest neuropathological correlate for cognitive impairment^{152,167}. However, NIA-AA guidelines clearly state that A β deposits, NFTs, and neuritic plaques should not be considered the comprehensive molecular profile of AD neuropathology¹⁶⁵. Rather, the guidelines prompt further research into elucidating the unknown mechanisms by which amyloid and tau proteins are dysregulated and identifying the specific molecular processes that lead to neurodegeneration. Experimental animal models continue to be recommended for this line of research¹⁶⁵.

1.2.2.2 *Role of Glia in Alzheimer Disease*

Both neuritic plaques and NFTs are associated with astrocytosis and microgliosis¹⁶⁹. Whereas A β load plateaus early after symptom onset^{169,170}, astrocytosis and microgliosis continue to increase linearly as the disease progresses¹⁶⁹. Moreover, astrocytosis and microgliosis are correlated with NFT burden and loss of cortical thickness¹⁶⁹, raising the question of whether these glial responses are merely reacting to the AD pathology or playing a central role in the disease mechanism⁶⁶. As glial cells are fundamental to the maintenance of CNS homeostasis, including inflammatory processes, glial cells present a favorable therapeutic target for modifying the course of AD^{64,65}.

Neuroinflammation in AD is thought to be driven primarily by microglia, the brain's resident myeloid cells, which are involved in both cytokine secretion and phagocytosis⁶⁶. This is distinct from the conditions that are traditionally defined as neuroinflammatory diseases, namely multiple sclerosis and the different forms of encephalitis, which are driven by peripheral leukocytes that migrate into the CNS from systemic circulation⁶⁶. The adaptive immune response, mediated primarily by T- and B-lymphocytes, has not been implicated in AD neuroinflammation, so mechanisms seen in most autoimmune conditions are

unlikely to be observed in AD. Furthermore, astrocytes are also directly involved with AD neuroinflammation^{66,77}. Unlike in MS, traumatic injury, or ischemic stroke, astrocytes in AD do not typically form glial scars even though they upregulate expression of glial fibrillary acidic protein (GFAP)⁶⁶. Instead, reactive astrocytes appear to modulate microglial function and play an important role in A β degradation^{66,77,171}. This is further complicated by the observation of senescent or dystrophic microglia and astrocytes associated with prolonged exposures of high A β concentrations, which may indicate a crucial decompensation in the course of AD^{66,172,173}. It remains to be determined which specific processes in AD neuroinflammation are protective and which are detrimental⁶⁶.

Both preclinical and clinical studies suggest a critical role of glial-mediated inflammation in AD. Cognitive and neuropathological profiles of transgenic mouse models of AD have been improved by a breadth of molecules with anti-inflammatory properties: rapamycin, minocycline, pioglitazone, thalidomide, etanercept, and celestrol, all of which modulate tumour necrosis factor- α (TNF- α) signalling and the activation of pro-inflammatory microglia and astrocytes¹⁷⁴⁻¹⁷⁶. TNF- α is a pro-inflammatory cytokine that plays a pivotal role in inflammation throughout the body, and its expression is increased by both neurons and glial cells during both acute and chronic brain injury.¹⁷⁶ A β activates several TNF- α dependent pathways, including cyclooxygenase (COX)-mediated inflammatory processes¹⁷⁷. Non-steroidal anti-inflammatory drugs (NSAIDs) reduce these inflammatory processes by inhibiting COX in neurons, microglia, and astrocytes^{178,179}, and NSAIDs may also offer neuroprotection by COX-independent pathways such as the direct promotion of non-amyloidogenic processing of APP¹⁷⁹⁻¹⁸¹. Cohort studies of have shown promise in reducing the risk of AD, with the most recent meta-analysis of 236 000 participants from 16 cohort studies citing a 19% relative risk reduction of AD diagnosis¹⁷⁹. This supports the potential of anti-inflammatory drugs as a disease modifying therapy but the optimal NSAID type, dose, and the duration and timing of treatment have yet to be identified. Skepticism over this direction of research is raised by several studies that showed an increased incidence of AD among NSAID cohorts¹⁷⁹. The only randomized-controlled trial of NSAID intervention did find reduced AD incidence if treatment was initiated in asymptomatic individuals, but increased incidence if treatment was initiated in patients

with cognitive impairment or dementia¹⁸², suggesting that the timing of NSAID intervention with regard to disease stage is a crucial factor. This consideration is likely to extend to other anti-inflammatory drug trials, such as the phase-II trial of the anti-TNF- α biologic, etanercept, which showed favourable but non-significant trends in patients with mild to moderate AD¹⁸³.

In AD, glial cell density increases throughout grey matter tissue, but also in white matter¹⁸⁴. Oligodendrocytes provide important trophic supports to neurons, but A β is toxic to oligodendrocytes *in vitro*^{185,186}. Histological changes of white matter are commonly observed in AD; while oligodendrocyte density is decreased, post-mortem evaluation has found astrocyte and microglia numbers to be increased in the white matter of patients with AD dementia^{187,188}. PET studies have also identified increased white matter inflammation in AD patients^{68,189}.

1.2.2.3 *White Matter Changes in Alzheimer Disease*

Much of AD continues to be defined by pathological changes in grey matter but white matter degeneration is also observed in AD, both on imaging and in histological samples^{23,190-193}. In AD, white matter degeneration can range from demyelination to atrophy^{32,190,194}. The specific patterns of white matter atrophy may also be crucial to differentiating potentially distinct forms of AD¹⁹¹. Whereas LOAD more typically featured white matter atrophy in the medial temporal regions, EOAD features greater cingulate atrophy¹⁹¹. Atypical variants of AD include the logopenic variant of primary progressive aphasia (lv-PPA), which features more left parietal white matter atrophy, and posterior cortical atrophy (PCA), which features more occipital white matter atrophy. Compared to LOAD, more white matter atrophy in the lateral temporal cortex, parietal cortex, cingulum, and corpus callosum were observed in EOAD, lv-PPA, and PCA¹⁹¹. Thus, specific patterns of white matter atrophy may aid in characterizing specific forms of AD.

This has prompted the possibility that white matter disease may be a core feature of AD¹⁸⁶. However, whether white matter atrophy is due to local degenerative changes or secondary to remote neuronal injury, i.e., due to Wallerian or anterograde degeneration

has not been determined¹⁹⁰. Currently, there is more evidence in favour of white matter atrophy as a secondary process, as grey matter and white matter volume loss are usually correlated¹⁹⁰. However, primary local damage and retrograde damage due to AD cannot be ruled out¹⁹⁰. Oligodendrocytes may be sensitive to the increased concentrations of A β seen in the brains of patients with AD, and loss of oligodendrocytes due to increased concentrations of A β could contribute to white matter demyelination and consequent degeneration^{185,186}. Moreover, the specific patterns of diffusion tensor changes seen in AD are not indicative of primarily Wallerian degeneration^{190,195,196}. While grey matter and white matter volume loss may be correlated in AD, white matter damage seen in MCI showed no relationship with grey matter atrophy^{190,194}. This suggests that especially in the early stages of disease, white matter may undergo atrophy due to local injury and retrograde degeneration as well as secondary degeneration due to grey matter injury and anterograde degeneration¹⁹⁰. The growing evidence of glial dysregulation as a common feature of AD also suggests potential inflammatory mechanisms by which white matter could be damaged directly^{68,186,197}, independent of grey matter senile plaques and NFTs¹⁶⁷.

Any observed primary local damage could also be attributed to vascular injury, as white matter is particularly sensitive to vascular disruption⁴⁹⁻⁵¹ and cerebrovascular disease is highly comorbid with AD^{198,199}. However, there is considerable overlap in the findings that are conventionally attributed to purely AD and purely vascular neuropathologies²⁰⁰⁻²⁰⁴, with many proposing that vascular disruption may be central to AD as well^{31,33,34,202,205,206}. The intersection of AD and VaD may be most apparent in leukoaraiosis, the radiological phenomenon of diffuse hypodense (on CT) or hyperintense (on T2 MRI) white matter²⁹⁻³⁴. Leukoaraiosis is associated with disruptions of white matter integrity^{35,36} and vascular pathology^{41,45,50,207-211}, but leukoaraiosis is also an important risk factor for AD³⁷⁻³⁹ and leukoaraiosis volume has also been correlated directly with the severity of cognitive and functional impairment in AD²¹²⁻²¹⁴. Recently, CSF concentrations of A β were found to correlate with leukoaraiosis volume^{215,216}. In the Dominantly Inherited Alzheimer Network (DIAN) study, which follows a cohort of carriers of genetic mutations known to cause EOAD (*PSEN1/2*, *APP*), leukoaraiosis volume began to increase significantly 6 years

prior to estimated symptom onset³². Specifically, in the parietal and occipital lobe, leukoaraiosis was significantly increased as early as 22 years prior to estimated symptom onset. This offers strong support for leukoaraiosis as a core feature of AD and a potential biomarker as opposed to an observation that is commonly coincidental due to chance alone³². However, the pathological basis of leukoaraiosis has yet to be identified. While many studies suggest a vascular etiology for leukoaraiosis⁴¹, dysregulation of astrocytes in the BBB⁴⁵ and genetic variation related to inflammation has also been implicated⁴⁶. Though dysregulation of astrocytes and aberrant inflammation can certainly be initiated by vascular pathology, AD-related proteinopathies may also drive the dysregulation of glial cells and neuroinflammation, as discussed above. While leukoaraiosis may already be an informative predictor for dementia, further experimentation is needed to identify the etiology of leukoaraiosis in the context of AD.

1.3 Vascular Cognitive Impairment

Cerebrovascular disease is highly heterogeneous and the second most prevalent cause of dementia^{104,199,217}. When cerebrovascular disease causes cognitive and functional impairment, Vascular dementia (VaD) is diagnosed. However, in many patients, cerebrovascular disease may result in cognitive impairment but not functional impairment²¹⁷, analogous to MCI with cerebrovascular etiology^{218,219}. In recognition of this, broader diagnostic categories have been proposed: major Canadian and US associations endorse *vascular cognitive impairment* (VCI)^{217,220}, the International Society for Vascular Behavioural and Cognitive Disorders (VASCOG) endorse *vascular cognitive disorder*²²¹, and the DSM-V uses the term *vascular neurocognitive disorders*¹¹⁵. While the terminology will continue to evolve in research and clinical settings, this thesis will refer to the term VCI to include both VCI-no dementia (VCIND)^{218,219} and VaD. VCIND and VaD exist on a spectrum of cognitive manifestations of cerebrovascular disease, with VaD only diagnosed when cognitive impairment causes severe functional impairment. In the Canadian Study of Health and Aging, following a diagnosis of VCIND, 58% died and 46% developed dementia within 5 years; of patients that progressed to dementia and were alive at follow-up, 35% had AD, 15% had mixed dementia, 42% had VaD, and 8% had an unclassified form of dementia²²². Since effective prevention and treatment for cerebrovascular disease exists, there is growing interest in reliably identifying VCI to limit disease progression^{217,222}.

Unlike AD, there is not a defined set of pathological criteria for the post-mortem diagnosis of VaD, and clinical diagnostic criterion are applied inconsistently²²³. Moreover, increased recognition of the comorbidity of AD and VaD has made it difficult to distinguish the two diseases, with growing recognition of mixed dementia as the most prevalent form of dementia^{199,224}. Mixed dementia will refer to the prevalent case in which both AD and cerebrovascular disease contribute to cognitive impairment^{199,224}, although comorbidity of other forms of neurodegenerative disease are also common.

1.3.1 *Clinical Profile of Vascular Cognitive Disorders*

Generally, VCI can result from overt symptomatic cerebrovascular disease, such as ischemic or hemorrhagic stroke, or from “covert” cerebrovascular disease, such as asymptomatic lacunar infarcts or small vessel disease¹⁹⁹. Particularly in patients with covert cerebrovascular disease, thorough physical examination, neuropsychological assessment, and neuroimaging play an important role in diagnosing VCI. Due to the vascular nature of VCI, functional and cognitive impairments evolve suddenly, in contrast to the relatively gradual progression of impairments seen in AD. Any cognitive domain can be impaired and multidomain impairment is common in VCI. As the frontal lobes and white matter are particularly susceptible to cerebrovascular disease, executive functions are the most commonly affected¹⁹⁹. Deficits in ADLs only contribute to the diagnosis of VCI if they are due to cognitive impairments; functional impairments as a result of any motor or sensory sequelae related to cerebral infarcts are not considered, emphasizing the cognitive component of VCI²²⁰.

The epidemiological estimates of VCI vary greatly but offer important insights into the complex relationships between cerebrovascular disease and dementia. Risk factors for VCI are generally the same risk factors identified for stroke and cardiovascular disease: smoking, atrial fibrillation, hypertension, diabetes, hyperlipidemia, and ApoE ϵ 4, while regular exercise confers protection²²⁰. After the age of 55, lifetime risk of stroke is 21% in women and 17% in men¹²¹, while estimates for the proportion of patients that develop cognitive impairment after a symptomatic stroke ranges greatly, from 6-41%^{225,226}. With regard to covert cerebrovascular disease, 67-76% of elderly subjects without a history of cognitive impairment exhibit cerebrovascular pathology in post-mortem evaluation, with small vessel disease being the most common^{198,227}. Thus, even in the absence of overt cognitive symptoms, cerebrovascular disease is highly prevalent. Both overt and covert cerebrovascular disease contribute to an overall prevalence of VaD in 1.6% of individuals over the age of 65, with prevalence increasing exponentially with age²²⁸. Though there are no direct studies of the lifetime risk of VaD, lifetime risk of all-cause dementia is 22% in women and 14% in men over the age of 65¹²¹, of which 15-20% is attributed to VaD^{225,228-230}. Similarly, VaD accounts for 18% of early dementia cases diagnosed prior

to 65 years of age²²⁸. However, cerebrovascular disease is estimated to contribute 33% of the risk of *all-cause dementia*^{199,217}; cerebrovascular disease is highly comorbid with AD, such that mixed dementia is estimated to be more prevalent than either “pure” AD or VCI^{199,224}.

1.3.2 Neuropathology of Vascular Cognitive Disorders: Cerebrovascular Disease

Cerebrovascular disease, the underlying neuropathology of VCI, is very heterogeneous, and multiple types of cerebrovascular lesions can be observed in a single brain. Universally accepted neuropathological criteria for VCI do not exist^{221,223}, and the correlations between the breadth of cerebrovascular disease and its range of clinical manifestation is an area of ongoing research^{226,231,232}. However, it is informative to classify cerebrovascular disease according to major etiological categories^{199,226}:

- *Large vessel disease* or atherosclerosis: proliferation of the intima (atheroma) in medium and large arteries, with accumulation of cholesterol and leukocytes that can lead to plaque formation and calcification. Plaques can rupture, causing local thrombosis and a single large brain infarct or produce emboli and multiple infarcts.
- *Small vessel disease*: reduced compliance in arterioles and capillaries due to arteriosclerosis, lipohyalinosis, arteriolosclerosis, and amyloid angiopathy, resulting in lacunar infarcts, even smaller microinfarcts, small hemorrhages, and extravasations of blood known as microbleeds.
- *Cardiac*: cardioembolic injury, commonly attributed to atrial fibrillation, as well as any condition that impairs cerebral perfusion such as cardiomyopathy, cardiogenic shock.
- *Other Systemic*: sickle cell disease, autoimmune conditions such as vasculitis, circulatory shock.

Cerebrovascular lesions can be further categorized according to distribution: focal, multifocal, or diffuse. Focal lesions can be attributed to any of the etiologies described above, but focal lesions that result in VCI are usually the result of an infarct in functionally

important regions. Focal lesions affecting the mesial temporal lobe, anterior cingulate cortex, caudate, thalamus, angular gyrus of the dominant hemisphere, and key white matter areas can result in strategic infarct dementia²²³. Multifocal lesions of large vessel etiology can result in multiple infarct dementia²²³. Multifocal or diffuse lesions of small vessel etiology are particularly heterogeneous and are seen in VCI attributed to multiple lacunar infarcts, Binswanger disease, hypertensive angiopathy, and cerebral amyloid angiopathy²²³. In two hereditary cerebrovascular conditions that can result in VCI, dominant arteriopathy with subcortical infarcts and leukoencephalopathy (CADASIL)²³³ and Moya Moya disease²³⁴, both small and large vessel disease are seen in a multifocal/diffuse distribution. The categories of cerebrovascular pathologies outlined here are far from exhaustive but do capture some of the breadth of factors involved. Further considerations related to neuropathological staging include lesion severity, location(s), and sampling strategies are also in ongoing development, and will likely play an important role in correlating cerebrovascular disease and VCI^{226,231,232}.

The high co-occurrence of AD and cerebrovascular disease^{199,224} has generated research on whether the two diseases may have synergistic neuropathological and cognitive effects²³⁵⁻²³⁹. This is supported by the Nun Study, which found that AD pathology was far more likely to correlate with dementia if cortical infarcts or lacunar strokes were also present²⁴⁰. This has been replicated, with a recent metanalysis of 2856 from 10 studies finding that compared to patients with post-mortem evidence of AD, patients with both AD neuropathology and cerebrovascular disease were three times more likely to have had dementia²⁴¹. In a large post-mortem study from the National Alzheimer's Coordinating Centre, 80% of patients diagnosed with AD were also found to have cerebrovascular pathology, significantly greater than the 67% of subjects that had cerebrovascular pathology but no cognitive impairment¹⁹⁸. Furthermore, a recent large cross-sectional study with participants of the Religious Orders Study and the Rush Memory and Aging Project found the odds of a clinical diagnosis of AD to be increased in participants that had cerebral atherosclerosis or cerebral arteriosclerosis, confirmed post-mortem²³⁹. Thus, the prevention and treatment of cerebrovascular disease is likely to play an important role in reducing the burden of dementia by addressing both AD and VCI²⁴¹⁻²⁴³.

1.4 The Neurovascular Hypothesis of Alzheimer disease

In recognition of the high comorbidity between AD and VCI, the Neurovascular Hypothesis of AD proposes that the interaction of amyloid pathology and cerebrovascular disease is a core mechanism that leads to neuronal injury and cognitive impairment²³⁶. The Neurovascular Hypothesis directs focus to neurovascular unit (NVU), which is composed of neurons, astrocytes, endothelial cells, myocytes, pericytes, crucial extracellular components, and resident immune cells²⁴⁴. A crucial component of the NVU is the BBB, which segregates the interstitial microenvironment of the CNS and regulates the clearance of neurotoxic molecules such as A β . The NVU also regulates the coupling of blood flow and local metabolic demands, known as hyperaemia or neurovascular coupling^{203,245}. Thus, the NVU is crucial to protecting the brain from both AD pathology and cerebrovascular disease. At the same time, the NVU can be directly disrupted by both of these diseases as well as systemic vascular conditions^{203,237,238,246-248}. Experimental studies have generated evidence in support of the Neurovascular Hypothesis, identifying potential therapeutic targets that may prevent important neurodegenerative disease mechanisms^{203,237,246-251}.

1.4.1 *The Neurovascular Unit and Blood-Brain-Barrier*

Autoregulation of large vessels maintains near-constant blood flow to a large vascular territory, accomplished by intravascular regulation of the luminal diameter to compensate for fluctuations in systemic blood pressure. In contrast, coupling occurs at the microscopic level of the vascular bed, accomplished through a complex coordination between NVU cells responding to fluctuations in the metabolic demands of the local parenchyma²⁴⁴. Myocytes are the smooth muscle cells that make autoregulation of arteries and arterioles possible, and myocytes communicate with downstream pericytes via gap junctions²⁵². Pericytes are also contractile cells that regulate blood flow at the level of capillary beds and individual capillaries, and pericytes have been found to communicate with both endothelial cells and astrocytes²⁴⁴. Astrocytes are considered to be the key detector of abluminal metabolic demands, receiving glutamatergic signals from neurons and

interneurons²⁴⁴. To relay these signals and affect local blood flow, astrocyte endfeet release vasoactive substances such as eicosanoids which directly stimulate or inhibit the contraction of pericytes²⁵³. Additionally, astrocyte endfeet release potassium ions into blood vessels and onto myocytes, inducing vasodilation²⁵³. Endothelial cells also modulate vascular tone, and relay signals of vascular tone to astrocytes²⁴⁴. Importantly, cells of the NVU are mutually dependent on crucial extracellular trophic factors during both development, maintenance, and microstructural remodelling²⁴⁴. The NVU directs the formation, maintenance, and remodelling of the BBB, which regulates the passive and active diffusion of molecules and ions both into and out of the brain parenchyma. The physical barrier of the BBB is formed in part by the complex basement membrane that is maintained by both endothelial cells and astrocytes²⁴⁸. More recently, the primary inflammatory cells of the brain, microglia, have also been found to respond to ischemia and contribute to BBB and vascular remodelling by cytokine signalling. Dysregulation of any of the NVU cells or microglia can contribute to a dysfunctional BBB.

1.4.2 NVU Dysfunction

The NVU maintains neurovascular coupling and the microenvironment of the CNS, promoting healthy CNS function. However, vascular conditions can lead to dysregulation of the NVU, disrupting CNS homeostasis. Hypertension, ischemic stroke, and covert or 'silent' brain infarcts (SBI) are among the most prevalent vascular etiologies that can cause NVU dysfunction. The NVU is essentially the site at which small vessel disease occurs; arteriosclerosis, lipohyalinosis, microbleeds, and microhemorrhages indicate profound disruption of the NVU²⁵⁴. Due to the diffuse nature of small vessel disease, NVU dysregulation is likely to exist well beyond the immediate temporal or anatomical proximity of detectable cerebrovascular lesions, such as SBI. Impaired coupling results in oligoemia, hypoxia²³⁷, and mitochondrial-mediated oxidative stress²³⁷, with further injury propagated by dysregulated inflammation^{248,255,256}. Meanwhile, a 'leaky' BBB can result in extravasation of circulating molecules and proteins that have toxic and pro-inflammatory effects in the brain^{237,254}. Interestingly, peripheral sources of circulating A β can enter the CNS, induce A β -related pathology, and disrupt neuronal function^{237,246,257};

this can be prevented by molecular interventions that target specific molecules in the NVU²⁴⁶. Thus, NVU dysfunction can exacerbate or result in AD pathology. In turn, abluminal pathology such as AD can also propagate dysregulation of the NVU and BBB, creating a self-propagating pathological cycle.

1.4.2.1 *Hypertension*

Hypertension is a highly prevalent condition, affecting 23% of Canadian adults, of whom only 68% have controlled blood pressure²⁵⁸. Hypertension is also recognized as a leading vascular risk factor for stroke and dementia^{259,260}, including AD²⁶¹⁻²⁶³. Experimental animal models of comorbid hypertension to exacerbate AD-related pathology^{251,264-268}. However, while the connection between hypertension and cerebrovascular disease is well established^{259,260}, it remains inconclusive whether anti-hypertensive therapy reduces AD incidence²⁶⁹⁻²⁷⁴. In addition to dysregulating cerebrovascular autoregulation, hypertension can also disrupt neurovascular coupling²⁰³. This was observed in an experimental hypertensive rodent model that had an attenuated blood flow response to whisker stimulation²⁷⁵, which was further exacerbated by neocortical application of A β or by transgenic expression of pathogenic APP²⁷⁶. Similarly, in a clinical cohort study using PET imaging, hypertensive subjects demonstrated a reduced hemodynamic change during a memory task²⁷⁷. Moreover, hypertension has been shown to cause BBB leakiness and the pro-inflammatory activation of microglia and astrocytes²⁷⁸. Perivascular macrophages, resident immune cells that are distinct from microglia, have also been found to release reactive oxygen species in response to hypertension, resulting in neurovascular and cognitive dysfunction²⁷⁹. These are some of the mechanisms by which hypertension can disrupt the NVU and CNS function, even in the absence of detectable cerebrovascular disease²⁰³.

1.4.2.2 *Ischemic Stroke and Silent Brain Infarcts*

The lifetime risk of ischemic stroke in the Framingham study was found to be 18% for women and 15% for men at 55 years of age²⁸⁰. In a recent retrospective cohort study in London, Ontario, cardioembolic etiology accounted for 56% and large artery atherosclerosis accounted for 26% of ischemic stroke cases²⁸¹. Small vessel disease can also result in ischemic lesions, including microinfarcts and lacunar infarcts; when these infarcts do not cause symptoms, they are classified as an SBI. By their nature, SBIs are found incidentally on neuroimaging or in post-mortem evaluation, most often affecting subcortical white matter, basal ganglia, thalamus, and the infratentorial region²⁸². Disturbingly, SBI are found in 10-20% of the general elderly population, increasing with age and hypertension^{283,284} to as high as 62% in select elderly populations with other significant morbidity²⁸⁵. While the chronic impact of SBI on proximal intact NVUs is difficult to investigate, it is likely to demonstrate similar processes seen in ischemic strokes and small vessel disease. Following ischemic stroke, autoregulation and coupling are impaired even in brain regions that appear uninjured²⁰³. Similarly, in a transient middle cerebral artery occlusion model, BBB disruption can be observed 30 days after injury, even on the contralateral hemisphere²⁸⁶. When striatal lacunar infarcts were modelled in a transgenic mouse model of AD, increased APP, tau, and inflammatory microglia were observed in the cortex and hippocampus²⁸⁷. In this same study, anti-inflammatory treatment reduced the area and density of APP near the injury site. Thus, inflammation may play an important role in propagating AD-related pathology following NVU injury by ischemic stroke and SBI.

1.4.2.3 *Abluminal Injury: Alzheimer Disease Pathology*

A β is generally cleared from the brain by enzymatic degradation or by active clearance across the BBB, mediated by the low-density lipoprotein receptor-related proteins (LRP) pathway. Endothelial cell LRP1 binds and initiates clearance of abluminal unbound A β as well as ApoE-bound A β ; interestingly, ApoE ϵ 4 inhibits this active transport of A β out of the brain²³⁷. By impairing the clearance of A β , reduced expression of LRP1 in blood

vessels has been associated with AD in both preclinical and clinical studies²³⁷. However, A β can impair its own clearance by oxidizing LRP1, which was observed in the hippocampal tissue of AD patients²⁸⁸. As A β is toxic to virtually all cell types in the NVU, increased concentrations of A β , as seen in AD, can directly disrupt the NVU^{289,290}. Additionally, dysregulated inflammation induced by AD pathology can further disrupt the NVU, while failure of perivascular macrophages to clear A β can contribute to its accumulation in the brain^{279,289,291}. Thus, the disruption of the NVU may be either a cause of AD, a consequence of AD, or both. In any case, there is strong indication that the NVU has a central role in neurodegenerative disease.

1.4.3 White Matter Pathology and the Neurovascular Hypothesis of Alzheimer Disease

The Neurovascular Hypothesis offers a potential understanding of AD that is non-neuron-centric²³⁶, as it draws attention to the important role of non-neuronal cells in the NVU. Similarly, the often-overlooked factor of white matter disease may also play an important role in the Neurovascular Hypothesis; disruption of NVUs in periventricular white matter, which is particularly vulnerable to cerebrovascular pathology^{44,47-52}, may contribute to the accumulation of cerebral A β and in turn, AD. Both in preclinical and clinical studies, AD pathology is associated with impaired coupling^{235,245}. Dramatic pericyte loss is observed in the white matter of patients that had AD, which is also accompanied with demyelination²⁹². This was further investigated in transgenic mice lacking cerebral pericytes, which developed white matter dysfunction, white matter atrophy, hippocampal and cortical atrophy, and cognitive impairments²⁹². Furthermore, a transgenic mouse model of AD treated with simvastatin, a cholesterol lowering drug, showed improved coupling and cognition²⁹³.

The role of proinflammatory astrocytes and microglia in NVU injury, white matter integrity, and cognitive impairment is also strongly supported; 5 recent experimental animal studies showed that targeted modulation of astrocyte- and microglia-mediated inflammation protected white matter microstructure, white matter function, and cognition following chronic hypertension, hypoperfusion, and ischemic injury⁷²⁻⁷⁶. These studies did not

evaluate whether protecting white matter integrity had beneficial effects on executive function, but this link has been demonstrated in humans. In elderly individuals with hypertension and/or diabetes mellitus type 2, neurovascular coupling was measured by changes in blood flow velocity in the middle cerebral artery during a series of cognitive evaluations; more responsive coupling was correlated with better scores on cognitive flexibility tasks and higher white matter FA, an indicator of white matter integrity²⁹⁴. In the same study, consumption of flavanol-cocoa for 30 days improved coupling and behavioural flexibility scores, which was attributed to the beneficial effects of cocoa flavanols on systemic and cerebral vascular function²⁹⁴. Altogether, these studies strongly indicate that white matter inflammation and cerebrovascular disease play an important role in the pathogenesis of executive dysfunction and AD. However, with regard to executive function, this has yet to be evaluated in an experimental model of AD.

1.5 Rationale and Objectives

White matter is highly susceptible to ageing^{12,85}, as both amyloid pathology and cerebrovascular disease can initiate white matter inflammation and dysfunction^{44,68,186,215,216,292}. In recent studies, microglia- and astrocyte-mediated inflammation of white matter was shown to impair executive function⁷⁸⁻⁸¹, a major cognitive domain that is crucial for maintaining functional independence⁸⁶⁻⁸⁸. However, the relationship between white matter inflammation and executive function in the contexts of ageing or AD has not been directly evaluated, even though both increased inflammation and executive dysfunction are common in advanced age and AD^{68,84,116,190,191,193}. Thus, we hypothesized that **ageing and pathogenic APP induce white matter inflammation, resulting in executive dysfunction**. Furthermore, as white matter is particularly vulnerable to cerebrovascular disease^{44,47-52}, chronic dysfunction of the NVU can result in reduced clearance of A β ²³⁷ and further exacerbation of white matter inflammation^{248,255,256}. Thus, **vascular injury exacerbates white matter inflammation and executive dysfunction induced by ageing and pathogenic APP**. A transgenic rat model of AD was studied to test these hypotheses and address the following research objectives:

- 1) To determine the effect of pathogenic APP on white matter inflammation and executive function ([Chapter 2](#) and [Chapter 3](#))
- 2) To characterize the temporal relationship between age, pathogenic APP expression, white matter inflammation, and executive function ([Chapter 3](#))
- 3) To evaluate the impact of comorbid pathogenic APP and cerebrovascular stress (hypertension; [Chapter 4](#)) or injury (ischemia; [Chapter 5](#)) on executive function

The attributes of the transgenic model, the TgAPP21 rat, permitted the investigation of pre-A β -plaque dysfunction²⁹⁵⁻²⁹⁸, modelling the early stages of AD-related pathology. Evaluation of inflammation was focused on microglia and astrocytes, as these cells are central to the neuroinflammatory processes observed in neurodegenerative disease⁶⁶. Testing paradigms for rat behavioural flexibility have been well established^{100,299,300}, and behavioural flexibility is considered to be the most integrated cognitive subdomain of

executive function⁸². Thus, evaluation of executive function in the TgAPP21 rat was focused on behavioural flexibility.

1.6 References

1. Filley CM. White matter and behavioral neurology. *Ann N Y Acad Sci.* 2005;1064:162-183.
2. Kumar DR, Aslinia F, Yale SH, Mazza JJ. Jean-Martin Charcot: the father of neurology. *Clin Med Res.* 2011;9(1):46-49.
3. Filley CM. White Matter Dementia: Origin, Development, Progress, and Prospects. *J Neuropsychiatry Clin Neurosci.* 2016:appineuropsych16010003.
4. Jakel S, Dimou L. Glial Cells and Their Function in the Adult Brain: A Journey through the History of Their Ablation. *Front Cell Neurosci.* 2017;11:24.
5. Kaminsky N, Bihari O, Kanner S, Barzilai A. Connecting Malfunctioning Glial Cells and Brain Degenerative Disorders. *Genomics Proteomics Bioinformatics.* 2016;14(3):155-165.
6. Matute C, Ransom BR. Roles of white matter in central nervous system pathophysiologies. *ASN Neuro.* 2012;4(2).
7. Lundgaard I, Osorio MJ, Kress BT, Sanggaard S, Nedergaard M. White matter astrocytes in health and disease. *Neuroscience.* 2014;276:161-173.
8. Fields RD. Neuroscience. Change in the brain's white matter. *Science.* 2010;330(6005):768-769.
9. de Lange AG, Brathen AC, Grydeland H, et al. White matter integrity as a marker for cognitive plasticity in aging. *Neurobiol Aging.* 2016;47:74-82.
10. Jones DK, Knosche TR, Turner R. White matter integrity, fiber count, and other fallacies: the do's and don'ts of diffusion MRI. *Neuroimage.* 2013;73:239-254.
11. Soares JM, Marques P, Alves V, Sousa N. A hitchhiker's guide to diffusion tensor imaging. *Front Neurosci.* 2013;7:31.
12. Salat DH, Tuch DS, Greve DN, et al. Age-related alterations in white matter microstructure measured by diffusion tensor imaging. *Neurobiol Aging.* 2005;26(8):1215-1227.
13. Jung RE, Grazioplene R, Caprihan A, Chavez RS, Haier RJ. White matter integrity, creativity, and psychopathology: disentangling constructs with diffusion tensor imaging. *PLoS One.* 2010;5(3):e9818.
14. Gunning-Dixon FM, Raz N. The cognitive correlates of white matter abnormalities in normal aging: a quantitative review. *Neuropsychology.* 2000;14(2):224-232.
15. Sasson E, Doniger GM, Pasternak O, Tarrasch R, Assaf Y. White matter correlates of cognitive domains in normal aging with diffusion tensor imaging. *Front Neurosci.* 2013;7(7 MAR):32.
16. Rabin JS, Perea RD, Buckley RF, et al. Global White Matter Diffusion Characteristics Predict Longitudinal Cognitive Change Independently of Amyloid Status in Clinically Normal Older Adults. *Cereb Cortex.* 2018(February):1-12.
17. Hedden T, Gabrieli JD. Insights into the ageing mind: a view from cognitive neuroscience. *Nat Rev Neurosci.* 2004;5(2):87-96.

18. Grieve SM, Williams LM, Paul RH, Clark CR, Gordon E. Cognitive aging, executive function, and fractional anisotropy: a diffusion tensor MR imaging study. *AJNR Am J Neuroradiol*. 2007;28(2):226-235.
19. Head D, Buckner RL, Shimony JS, et al. Differential vulnerability of anterior white matter in nondemented aging with minimal acceleration in dementia of the Alzheimer type: evidence from diffusion tensor imaging. *Cereb Cortex*. 2004;14(4):410-423.
20. Van Petten C, Plante E, Davidson PS, Kuo TY, Bajuscak L, Glisky EL. Memory and executive function in older adults: relationships with temporal and prefrontal gray matter volumes and white matter hyperintensities. *Neuropsychologia*. 2004;42(10):1313-1335.
21. Madden DJ, Bennett IJ, Song AW. Cerebral white matter integrity and cognitive aging: contributions from diffusion tensor imaging. *Neuropsychol Rev*. 2009;19(4):415-435.
22. Bozzali M, Franceschi M, Falini A, et al. Quantification of tissue damage in AD using diffusion tensor and magnetization transfer MRI. *Neurology*. 2001;57(6):1135-1137.
23. Lin YC, Shih YC, Tseng WY, et al. Cingulum correlates of cognitive functions in patients with mild cognitive impairment and early Alzheimer's disease: a diffusion spectrum imaging study. *Brain Topogr*. 2014;27(3):393-402.
24. Atkinson-Clement C, Pinto S, Eusebio A, Coulon O. Diffusion tensor imaging in Parkinson's disease: Review and meta-analysis. *Neuroimage Clin*. 2017;16:98-110.
25. Alves GS, Sudo FK, Alves CEO, et al. Diffusion tensor imaging studies in vascular disease: A review of the literature. *Dement Neuropsychol*. 2012;6(3):158-163.
26. Metzler-Baddeley C, Cantera J, Coulthard E, Rosser A, Jones DK, Baddeley RJ. Improved Executive Function and Callosal White Matter Microstructure after Rhythm Exercise in Huntington's Disease. *J Huntingtons Dis*. 2014;3(3):273-283.
27. Cesar B, Dwyer MG, Shucard JL, et al. Cognitive and White Matter Tract Differences in MS and Diffuse Neuropsychiatric Systemic Lupus Erythematosus. *AJNR Am J Neuroradiol*. 2015;36(10):1874-1883.
28. Smith EE, Salat DH, Jeng J, et al. Correlations between MRI white matter lesion location and executive function and episodic memory. *Neurology*. 2011;76(17):1492-1499.
29. Clarke R, Joachim C, Esiri M, et al. Leukoaraiosis at presentation and disease progression during follow-up in histologically confirmed cases of dementia. *Ann N Y Acad Sci*. 2000;903:497-500.
30. Pettersen JA, Sathiyamoorthy G, Gao FQ, et al. Microbleed topography, leukoaraiosis, and cognition in probable Alzheimer disease from the Sunnybrook dementia study. *Arch Neurol*. 2008;65(6):790-795.
31. Brickman AM, Guzman VA, Gonzalez-Castellon M, et al. Cerebral autoregulation, beta amyloid, and white matter hyperintensities are interrelated. *Neurosci Lett*. 2015;592:54-58.
32. Lee S, Viqar F, Zimmerman ME, et al. White matter hyperintensities are a core feature of Alzheimer's disease: Evidence from the dominantly inherited Alzheimer network. *Ann Neurol*. 2016;79(6):929-939.
33. Kalaria RN, Akinyemi R, Ihara M. Does vascular pathology contribute to Alzheimer changes? *J Neurol Sci*. 2012;322(1-2):141-147.

34. Cai Z, Wang C, He W, et al. Cerebral small vessel disease and Alzheimer's disease. *Clin Interv Aging*. 2015;10:1695-1704.
35. O'Sullivan M, Morris RG, Huckstep B, Jones DK, Williams SC, Markus HS. Diffusion tensor MRI correlates with executive dysfunction in patients with ischaemic leukoaraiosis. *J Neurol Neurosurg Psychiatry*. 2004;75(3):441-447.
36. Altamura C, Scarscia F, Quattrocchi CC, et al. Regional MRI Diffusion, White-Matter Hyperintensities, and Cognitive Function in Alzheimer's Disease and Vascular Dementia. *J Clin Neurol*. 2016;12(2):201-208.
37. Debette S, Markus HS. The clinical importance of white matter hyperintensities on brain magnetic resonance imaging: systematic review and meta-analysis. *BMJ*. 2010;341(jul26 1):c3666.
38. Brickman AM, Provenzano FA, Muraskin J, et al. Regional white matter hyperintensity volume, not hippocampal atrophy, predicts incident Alzheimer disease in the community. *Arch Neurol*. 2012;69(12):1621-1627.
39. Brickman AM. Contemplating Alzheimer's disease and the contribution of white matter hyperintensities. *Curr Neurol Neurosci Rep*. 2013;13(12):415.
40. Hachinski VC, Potter P. Leuko-Araiosis. 2015.
41. Wardlaw JM, Valdés Hernández MC, Muñoz-Maniega S, Valdes Hernandez MC, Munoz-Maniega S. What are white matter hyperintensities made of? Relevance to vascular cognitive impairment. *J Am Heart Assoc*. 2015;4(6):1140-1140.
42. Shi Y, Wardlaw JM. Update on cerebral small vessel disease: a dynamic whole-brain disease. *Stroke Vasc Neurol*. 2016;1(3):83-92.
43. Ter Telgte A, van Leijsen EMC, Wiegertjes K, Klijn CJM, Tuladhar AM, de Leeuw FE. Cerebral small vessel disease: from a focal to a global perspective. *Nat Rev Neurol*. 2018;14(7):387-398.
44. Black S, Gao F, Bilbao J. Understanding white matter disease: imaging-pathological correlations in vascular cognitive impairment. *Stroke*. 2009;40(3 Suppl):S48-52.
45. Huang J, Li J, Feng C, et al. Blood-Brain Barrier Damage as the Starting Point of Leukoaraiosis Caused by Cerebral Chronic Hypoperfusion and Its Involved Mechanisms: Effect of Agrin and Aquaporin-4. *Biomed Res Int*. 2018;2018:2321797.
46. Raz N, Yang Y, Dahle CL, Land S. Volume of white matter hyperintensities in healthy adults: contribution of age, vascular risk factors, and inflammation-related genetic variants. *Biochim Biophys Acta*. 2012;1822(3):361-369.
47. Raz N, Rodrigue KM, Acker JD. Hypertension and the brain: vulnerability of the prefrontal regions and executive functions. *Behav Neurosci*. 2003;117(6):1169-1180.
48. Vicario A, Martinez CD, Baretto D, Diaz Casale A, Nicolosi L. Hypertension and cognitive decline: impact on executive function. *J Clin Hypertens (Greenwich)*. 2005;7(10):598-604.
49. Li X, Ma C, Sun X, et al. Disrupted white matter structure underlies cognitive deficit in hypertensive patients. *Eur Radiol*. 2016;26(9):2899-2907.
50. Mandell DM, Han JS, Poublanc J, et al. Selective reduction of blood flow to white matter during hypercapnia corresponds with leukoaraiosis. *Stroke*. 2008;39(7):1993-1998.

51. Wang Y, Liu G, Hong D, Chen F, Ji X, Cao G. White matter injury in ischemic stroke. *Prog Neurobiol.* 2016;141:45-60.
52. Markus HS, Lythgoe DJ, Ostegaard L, O'Sullivan M, Williams SC. Reduced cerebral blood flow in white matter in ischaemic leukoaraiosis demonstrated using quantitative exogenous contrast based perfusion MRI. *J Neurol Neurosurg Psychiatry.* 2000;69(1):48-53.
53. Iadecola C, Park L, Capone C. Threats to the mind: aging, amyloid, and hypertension. *Stroke.* 2009;40(3 Suppl):S40-44.
54. Lin J, Wang D, Lan L, Fan Y. Multiple Factors Involved in the Pathogenesis of White Matter Lesions. *Biomed Res Int.* 2017;2017:9372050.
55. Langdon KD, Cordova CA, Granter-Button S, et al. Executive dysfunction and blockage of brain microvessels in a rat model of vascular cognitive impairment. *Journal of Cerebral Blood Flow & Metabolism.* 2017:0271678X1773921-0271678X1773921.
56. Skoog I. A review on blood pressure and ischaemic white matter lesions. *Dement Geriatr Cogn Disord.* 1998;9 Suppl 1:13-19.
57. van Dijk EJ, Breteler MM, Schmidt R, et al. The association between blood pressure, hypertension, and cerebral white matter lesions: cardiovascular determinants of dementia study. *Hypertension.* 2004;44(5):625-630.
58. Oh YS, Kim JS, Lee KS. Orthostatic and supine blood pressures are associated with white matter hyperintensities in Parkinson disease. *J Mov Disord.* 2013;6(2):23-27.
59. Wang Z, Wong A, Liu W, et al. Pulse Pressure and Cognitive Decline in Stroke Patients With White Matter Changes. *J Clin Hypertens (Greenwich).* 2015;17(9):694-698.
60. Kim CK, Lee SH, Kim BJ, Ryu WS, Yoon BW. Age-independent association of pulse pressure with cerebral white matter lesions in asymptomatic elderly individuals. *J Hypertens.* 2011;29(2):325-329.
61. van Norden AG, de Laat KF, Gons RA, et al. Causes and consequences of cerebral small vessel disease. The RUN DMC study: a prospective cohort study. Study rationale and protocol. *BMC Neurol.* 2011;11:29.
62. Gouw AA, Seewann A, van der Flier WM, et al. Heterogeneity of small vessel disease: a systematic review of MRI and histopathology correlations. *J Neurol Neurosurg Psychiatry.* 2011;82(2):126-135.
63. Joutel A, Chabriat H. Pathogenesis of white matter changes in cerebral small vessel diseases: beyond vessel-intrinsic mechanisms. *Clin Sci (Lond).* 2017;131(8):635-651.
64. Di Benedetto B, Rupprecht R. Targeting glia cells: novel perspectives for the treatment of neuropsychiatric diseases. *Curr Neuropharmacol.* 2013;11(2):171-185.
65. Ahmed S, Gull A, Khuroo T, Aqil M, Sultana Y. Glial Cell: A Potential Target for Cellular and Drug Based Therapy in Various CNS Diseases. *Curr Pharm Des.* 2017;23(16):2389-2399.
66. Heppner FL, Ransohoff RM, Becher B. Immune attack: the role of inflammation in Alzheimer disease. *Nat Rev Neurosci.* 2015;16(6):358-372.

67. Harry GJ, Kraft AD. Neuroinflammation and microglia: considerations and approaches for neurotoxicity assessment. *Expert Opin Drug Metab Toxicol*. 2008;4(10):1265-1277.
68. Raj D, Yin Z, Breur M, et al. Increased White Matter Inflammation in Aging- and Alzheimer's Disease Brain. *Front Mol Neurosci*. 2017;10(June):206.
69. Wolf G, Lotan A, Lifschytz T, et al. Differentially Severe Cognitive Effects of Compromised Cerebral Blood Flow in Aged Mice: Association with Myelin Degradation and Microglia Activation. *Front Aging Neurosci*. 2017;9:191.
70. Hase Y, Horsburgh K, Ihara M, Kalaria RN. White matter degeneration in vascular and other ageing-related dementias. *J Neurochem*. 2018;144(5):617-633.
71. Shobin E, Bowley MP, Estrada LI, et al. Microglia activation and phagocytosis: relationship with aging and cognitive impairment in the rhesus monkey. *Geroscience*. 2017;39(2):199-220.
72. Lan LF, Zheng L, Yang X, Ji XT, Fan YH, Zeng JS. Peroxisome proliferator-activated receptor-gamma agonist pioglitazone ameliorates white matter lesion and cognitive impairment in hypertensive rats. *CNS Neurosci Ther*. 2015;21(5):410-416.
73. Fowler JH, McQueen J, Holland PR, et al. Dimethyl fumarate improves white matter function following severe hypoperfusion: Involvement of microglia/macrophages and inflammatory mediators. *Journal of Cerebral Blood Flow and Metabolism* 2017.
74. Qin C, Fan WH, Liu Q, et al. Fingolimod Protects Against Ischemic White Matter Damage by Modulating Microglia Toward M2 Polarization via STAT3 Pathway. *Stroke*. 2017;48(12):3336-3346.
75. Manso Y, Holland PR, Kitamura A, et al. Minocycline reduces microgliosis and improves subcortical white matter function in a model of cerebral vascular disease. *Glia*. 2018;66(1):34-46.
76. Miyanohara J, Kakae M, Nagayasu K, et al. TRPM2 Channel Aggravates CNS Inflammation and Cognitive Impairment via Activation of Microglia in Chronic Cerebral Hypoperfusion. *J Neurosci*. 2018;38(14):3520-3533.
77. von Bernhardi R, Eugenin J. Microglial reactivity to beta-amyloid is modulated by astrocytes and proinflammatory factors. *Brain Res*. 2004;1025(1-2):186-193.
78. Kim DH, Choi BR, Jeon WK, Han JS. Impairment of intradimensional shift in an attentional set-shifting task in rats with chronic bilateral common carotid artery occlusion. *Behav Brain Res*. 2016;296:169-176.
79. Janova H, Arinrad S, Balmuth E, et al. Microglia ablation alleviates myelin-associated catatonic signs in mice. *J Clin Invest*. 2018;128(2):734-745.
80. Saing T, Dick M, Nelson PT, Kim RC, Cribbs DH, Head E. Frontal cortex neuropathology in dementia pugilistica. *J Neurotrauma*. 2012;29(6):1054-1070.
81. de la Monte SM, Kril JJ. Human alcohol-related neuropathology. *Acta Neuropathol*. 2014;127(1):71-90.
82. Diamond A. Executive functions. *Annu Rev Psychol*. 2013;64:135-168.
83. Tullberg M, Fletcher E, DeCarli C, et al. White matter lesions impair frontal lobe function regardless of their location. *Neurology*. 2004;63(2):246-253.

84. Harada CN, Natelson Love MC, Triebel KL. Normal cognitive aging. Vol 29: NIH Public Access; 2013:737-752.
85. Guttmann CR, Jolesz FA, Kikinis R, et al. White matter changes with normal aging. *Neurology*. 1998;50(4):972-978.
86. Johnson JK, Lui LY, Yaffe K. Executive Function, More Than Global Cognition, Predicts Functional Decline and Mortality in Elderly Women. *The Journals of Gerontology Series A: Biological Sciences and Medical Sciences*. 2007;62(10):1134-1141.
87. Razani J, Casas R, Wong JT, Lu P, Alessi C, Josephson K. Relationship between executive functioning and activities of daily living in patients with relatively mild dementia. *Appl Neuropsychol*. 2007;14(3):208-214.
88. Mlinac ME, Feng MC. Assessment of Activities of Daily Living, Self-Care, and Independence. *Arch Clin Neuropsychol*. 2016;31(6):506-516.
89. Falconer E, Bryant R, Felmingham KL, et al. The neural networks of inhibitory control in posttraumatic stress disorder. *J Psychiatry Neurosci*. 2008;33(5):413-422.
90. Levy BJ, Anderson MC. Individual differences in the suppression of unwanted memories: the executive deficit hypothesis. *Acta Psychol (Amst)*. 2008;127(3):623-635.
91. Baler RD, Volkow ND. Drug addiction: the neurobiology of disrupted self-control. *Trends Mol Med*. 2006;12(12):559-566.
92. Penades R, Catalan R, Rubia K, Andres S, Salamero M, Gasto C. Impaired response inhibition in obsessive compulsive disorder. *Eur Psychiatry*. 2007;22(6):404-410.
93. Arnsten AF, Rubia K. Neurobiological circuits regulating attention, cognitive control, motivation, and emotion: disruptions in neurodevelopmental psychiatric disorders. *J Am Acad Child Adolesc Psychiatry*. 2012;51(4):356-367.
94. Chambers CD, Garavan H, Bellgrove MA. Insights into the neural basis of response inhibition from cognitive and clinical neuroscience. *Neurosci Biobehav Rev*. 2009;33(5):631-646.
95. Garavan H, Ross TJ, Stein EA. Right hemispheric dominance of inhibitory control: an event-related functional MRI study. *Proc Natl Acad Sci U S A*. 1999;96(14):8301-8306.
96. Robinson G, Shallice T, Bozzali M, Cipolotti L. The differing roles of the frontal cortex in fluency tests. *Brain*. 2012;135(Pt 7):2202-2214.
97. Chapados C, Petrides M. Impairment only on the fluency subtest of the Frontal Assessment Battery after prefrontal lesions. *Brain*. 2013;136(Pt 10):2966-2978.
98. Carlen M. What constitutes the prefrontal cortex? *Science*. 2017;358(6362):478-482.
99. Dalley JW, Cardinal RN, Robbins TW. Prefrontal executive and cognitive functions in rodents: neural and neurochemical substrates. *Neurosci Biobehav Rev*. 2004;28(7):771-784.
100. Bizon JL, Foster TC, Alexander GE, Glisky EL. Characterizing cognitive aging of working memory and executive function in animal models. *Front Aging Neurosci*. 2012;4:19.
101. Robinson AL, Heaton RK, Lehman RA, Stilson DW. The utility of the Wisconsin Card Sorting Test in detecting and localizing frontal lobe lesions. *J Consult Clin Psychol*. 1980;48(5):605-614.

102. Floresco SB, Zhang Y, Enomoto T. Neural circuits subserving behavioral flexibility and their relevance to schizophrenia. *Behav Brain Res*. 2009;204(2):396-409.
103. Chudasama Y. Animal models of prefrontal-executive function. *Behav Neurosci*. 2011;125(3):327-343.
104. Alzheimer's A. 2016 Alzheimer's disease facts and figures. *Alzheimers Dement*. 2016;12(4):459-509.
105. McKhann GM, Knopman DS, Chertkow H, et al. The diagnosis of dementia due to Alzheimer's disease: recommendations from the National Institute on Aging-Alzheimer's Association workgroups on diagnostic guidelines for Alzheimer's disease. *Alzheimers Dement*. 2011;7(3):263-269.
106. Beach TG, Monsell SE, Phillips LE, Kukull W. Accuracy of the clinical diagnosis of Alzheimer disease at National Institute on Aging Alzheimer Disease Centers, 2005-2010. *J Neuropathol Exp Neurol*. 2012;71(4):266-273.
107. Dubois B, Feldman HH, Jacova C, et al. Advancing research diagnostic criteria for Alzheimer's disease: the IWG-2 criteria. *Lancet Neurol*. 2014;13(6):614-629.
108. Huynh RA, Mohan C. Alzheimer's Disease: Biomarkers in the Genome, Blood, and Cerebrospinal Fluid. *Front Neurol*. 2017;8:102.
109. Sabbagh MN, Lue LF, Fayard D, Shi J. Increasing Precision of Clinical Diagnosis of Alzheimer's Disease Using a Combined Algorithm Incorporating Clinical and Novel Biomarker Data. *Neurol Ther*. 2017;6(Suppl 1):83-95.
110. Gauthier S, Patterson C, Chertkow H, et al. Recommendations of the 4th Canadian Consensus Conference on the Diagnosis and Treatment of Dementia (CCCDTD4). *Can Geriatr J*. 2012;15(4):120-126.
111. Casey DA, Antimisiaris D, O'Brien J. Drugs for Alzheimer's disease: are they effective? *P T*. 2010;35(4):208-211.
112. Herman L, Atri A, Salloway S. Alzheimer's Disease in Primary Care: The Significance of Early Detection, Diagnosis, and Intervention. *Am J Med*. 2017;130(6):756.
113. Hennekes C, Reed C, Chen YF, Dell'Agnello G, Lebec J. Describing the Sequence of Cognitive Decline in Alzheimer's Disease Patients: Results from an Observational Study. *J Alzheimers Dis*. 2016;52(3):1065-1080.
114. Gold CA, Budson AE. Memory loss in Alzheimer's disease: implications for development of therapeutics. *Expert Rev Neurother*. 2008;8(12):1879-1891.
115. American Psychiatric Association., American Psychiatric Association. DSM-5 Task Force. *Diagnostic and statistical manual of mental disorders : DSM-5*. 5th ed. Washington, D.C.: American Psychiatric Association; 2013.
116. Stokholm J, Vogel A, Gade A, Waldemar G. Heterogeneity in executive impairment in patients with very mild Alzheimer's disease. *Dement Geriatr Cogn Disord*. 2006;22(1):54-59.
117. Prince M, Bryce R, Albanese E, Wimo A, Ribeiro W, Ferri CP. The global prevalence of dementia: a systematic review and metaanalysis. *Alzheimers Dement*. 2013;9(1):63-75 e62.

118. Ridge PG, Mukherjee S, Crane PK, Kauwe JS, Alzheimer's Disease Genetics C. Alzheimer's disease: analyzing the missing heritability. *PLoS One*. 2013;8(11):e79771.
119. Barber RC. The genetics of Alzheimer's disease. *Scientifica (Cairo)*. 2012;2012:246210.
120. Ridge PG, Ebbert MT, Kauwe JS. Genetics of Alzheimer's disease. *Biomed Res Int*. 2013;2013:254954.
121. Seshadri S, Wolf PA. Lifetime risk of stroke and dementia: current concepts, and estimates from the Framingham Study. *Lancet Neurol*. 2007;6(12):1106-1114.
122. Liu CC, Liu CC, Kanekiyo T, Xu H, Bu G. Apolipoprotein E and Alzheimer disease: risk, mechanisms and therapy. *Nat Rev Neurol*. 2013;9(2):106-118.
123. Raber J, Huang Y, Ashford JW. ApoE genotype accounts for the vast majority of AD risk and AD pathology. *Neurobiol Aging*. 2004;25(5):641-650.
124. Michaelson DM. APOE epsilon4: the most prevalent yet understudied risk factor for Alzheimer's disease. *Alzheimers Dement*. 2014;10(6):861-868.
125. Kim J, Basak JM, Holtzman DM. The role of apolipoprotein E in Alzheimer's disease. *Neuron*. 2009;63(3):287-303.
126. Ridge PG, Hoyt KB, Boehme K, et al. Assessment of the genetic variance of late-onset Alzheimer's disease. *Neurobiol Aging*. 2016;41:200 e213-200 e220.
127. Albert MS, DeKosky ST, Dickson D, et al. The diagnosis of mild cognitive impairment due to Alzheimer's disease: recommendations from the National Institute on Aging-Alzheimer's Association workgroups on diagnostic guidelines for Alzheimer's disease. *Alzheimers Dement*. 2011;7(3):270-279.
128. Petersen RC. Mild cognitive impairment as a diagnostic entity. *J Intern Med*. 2004;256(3):183-194.
129. Roberts RO, Knopman DS, Mielke MM, et al. Higher risk of progression to dementia in mild cognitive impairment cases who revert to normal. *Neurology*. 2014;82(4):317-325.
130. Mitchell AJ, Shiri-Feshki M. Rate of progression of mild cognitive impairment to dementia--meta-analysis of 41 robust inception cohort studies. *Acta Psychiatr Scand*. 2009;119(4):252-265.
131. Farias ST, Mungas D, Reed BR, Harvey D, DeCarli C. Progression of mild cognitive impairment to dementia in clinic- vs community-based cohorts. *Arch Neurol*. 2009;66(9):1151-1157.
132. Burke D. Review: long-term annual conversion rate to dementia was 3.3% in elderly people with mild cognitive impairment. *Evid Based Med*. 2009;14(3):90.
133. Ward A, Tardiff S, Dye C, Arrighi HM. Rate of conversion from prodromal Alzheimer's disease to Alzheimer's dementia: a systematic review of the literature. *Dement Geriatr Cogn Dis Extra*. 2013;3(1):320-332.
134. Schott JM, Petersen RC. New criteria for Alzheimer's disease: which, when and why? *Brain*. 2015;138(Pt 5):1134-1137.
135. Tabert MH, Manly JJ, Liu X, et al. Neuropsychological prediction of conversion to Alzheimer disease in patients with mild cognitive impairment. *Arch Gen Psychiatry*. 2006;63(8):916-924.

136. Summers MJ, Saunders NL. Neuropsychological measures predict decline to Alzheimer's dementia from mild cognitive impairment. *Neuropsychology*. 2012;26(4):498-508.
137. Kirova AM, Bays RB, Lagalwar S. Working memory and executive function decline across normal aging, mild cognitive impairment, and Alzheimer's disease. *Biomed Res Int*. 2015;2015:748212.
138. Cloutier S, Chertkow H, Kergoat MJ, Gauthier S, Belleville S. Patterns of Cognitive Decline Prior to Dementia in Persons with Mild Cognitive Impairment. *J Alzheimers Dis*. 2015;47(4):901-913.
139. Michaud TL, Su D, Siahpush M, Murman DL. The Risk of Incident Mild Cognitive Impairment and Progression to Dementia Considering Mild Cognitive Impairment Subtypes. *Dement Geriatr Cogn Dis Extra*. 2017;7(1):15-29.
140. Li J, Wang YJ, Zhang M, et al. Vascular risk factors promote conversion from mild cognitive impairment to Alzheimer disease. *Neurology*. 2011;76(17):1485-1491.
141. Lehallier B, Essioux L, Gayan J, et al. Combined Plasma and Cerebrospinal Fluid Signature for the Prediction of Midterm Progression From Mild Cognitive Impairment to Alzheimer Disease. *JAMA Neurol*. 2016;73(2):203-212.
142. Sun Z, van de Giessen M, Lelieveldt BP, Staring M. Detection of Conversion from Mild Cognitive Impairment to Alzheimer's Disease Using Longitudinal Brain MRI. *Front Neuroinform*. 2017;11:16.
143. Frolich L, Peters O, Lewczuk P, et al. Incremental value of biomarker combinations to predict progression of mild cognitive impairment to Alzheimer's dementia. *Alzheimers Res Ther*. 2017;9(1):84.
144. Smith EE, Egorova S, Blacker D, et al. Magnetic resonance imaging white matter hyperintensities and brain volume in the prediction of mild cognitive impairment and dementia. *Arch Neurol*. 2008;65(1):94-100.
145. Silbert LC, Dodge HH, Perkins LG, et al. Trajectory of white matter hyperintensity burden preceding mild cognitive impairment. *Neurology*. 2012;79(8):741-747.
146. Nalivaeva NN, Turner AJ. The amyloid precursor protein: a biochemical enigma in brain development, function and disease. *FEBS Lett*. 2013;587(13):2046-2054.
147. Uhlen M, Fagerberg L, Hallstrom BM, et al. Proteomics. Tissue-based map of the human proteome. *Science*. 2015;347(6220):1260419.
148. Puig KL, Combs CK. Expression and function of APP and its metabolites outside the central nervous system. *Exp Gerontol*. 2013;48(7):608-611.
149. Ferreira ST, Lourenco MV, Oliveira MM, De Felice FG. Soluble amyloid-beta oligomers as synaptotoxins leading to cognitive impairment in Alzheimer's disease. *Front Cell Neurosci*. 2015;9:191.
150. Frost GR, Li YM. The role of astrocytes in amyloid production and Alzheimer's disease. *Open Biol*. 2017;7(12).
151. Avila J, Lucas JJ, Perez M, Hernandez F. Role of tau protein in both physiological and pathological conditions. *Physiol Rev*. 2004;84(2):361-384.
152. Nelson PT, Alafuzoff I, Bigio EH, et al. Correlation of Alzheimer disease neuropathologic changes with cognitive status: a review of the literature. *J Neuropathol Exp Neurol*. 2012;71(5):362-381.

153. Braak H, Braak E. Neuropathological staging of Alzheimer-related changes. *Acta Neuropathol.* 1991;82(4):239-259.
154. Braak H, Alafuzoff I, Arzberger T, Kretschmar H, Del Tredici K. Staging of Alzheimer disease-associated neurofibrillary pathology using paraffin sections and immunocytochemistry. *Acta Neuropathol.* 2006;112(4):389-404.
155. Iaccarino L, Tammewar G, Ayakta N, et al. Local and distant relationships between amyloid, tau and neurodegeneration in Alzheimer's Disease. *Neuroimage Clin.* 2018;17:452-464.
156. Thal DR, Rub U, Orantes M, Braak H. Phases of A beta-deposition in the human brain and its relevance for the development of AD. *Neurology.* 2002;58(12):1791-1800.
157. Thal DR. Clearance of amyloid beta-protein and its role in the spreading of Alzheimer's disease pathology. *Front Aging Neurosci.* 2015;7:25.
158. Manczak M, Reddy PH. Abnormal interaction of oligomeric amyloid-beta with phosphorylated tau: implications to synaptic dysfunction and neuronal damage. *J Alzheimers Dis.* 2013;36(2):285-295.
159. Do TD, Economou NJ, Chamas A, Buratto SK, Shea JE, Bowers MT. Interactions between amyloid-beta and Tau fragments promote aberrant aggregates: implications for amyloid toxicity. *J Phys Chem B.* 2014;118(38):11220-11230.
160. Pascoal TA, Mathotaarachchi S, Shin M, et al. Synergistic interaction between amyloid and tau predicts the progression to dementia. *Alzheimers Dement.* 2017;13(6):644-653.
161. Leyns CEG, Holtzman DM. Glial contributions to neurodegeneration in tauopathies. *Mol Neurodegener.* 2017;12(1):50.
162. Garwood CJ, Pooler AM, Atherton J, Hanger DP, Noble W. Astrocytes are important mediators of Abeta-induced neurotoxicity and tau phosphorylation in primary culture. *Cell Death Dis.* 2011;2:e167.
163. Jack CR, Jr., Bennett DA, Blennow K, et al. NIA-AA Research Framework: Toward a biological definition of Alzheimer's disease. *Alzheimers Dement.* 2018;14(4):535-562.
164. Thal DR, von Arnim C, Griffin WS, et al. Pathology of clinical and preclinical Alzheimer's disease. *Eur Arch Psychiatry Clin Neurosci.* 2013;263 Suppl 2:S137-145.
165. Hyman BT, Phelps CH, Beach TG, et al. National Institute on Aging-Alzheimer's Association guidelines for the neuropathologic assessment of Alzheimer's disease. *Alzheimers Dement.* 2012;8(1):1-13.
166. Mirra SS, Heyman A, McKeel D, et al. The Consortium to Establish a Registry for Alzheimer's Disease (CERAD). Part II. Standardization of the neuropathologic assessment of Alzheimer's disease. *Neurology.* 1991;41(4):479-486.
167. Serrano-Pozo A, Frosch MP, Masliah E, Hyman BT. Neuropathological alterations in Alzheimer disease. *Cold Spring Harb Perspect Med.* 2011;1(1):a006189.
168. Boluda S, Toledo JB, Irwin DJ, et al. A comparison of Abeta amyloid pathology staging systems and correlation with clinical diagnosis. *Acta Neuropathol.* 2014;128(4):543-550.
169. Serrano-Pozo A, Mielke ML, Gomez-Isla T, et al. Reactive glia not only associates with plaques but also parallels tangles in Alzheimer's disease. *Am J Pathol.* 2011;179(3):1373-1384.

170. Jack CR, Jr., Wiste HJ, Lesnick TG, et al. Brain beta-amyloid load approaches a plateau. *Neurology*. 2013;80(10):890-896.
171. Pascual O, Ben Achour S, Rostaing P, Triller A, Bessis A. Microglia activation triggers astrocyte-mediated modulation of excitatory neurotransmission. *Proc Natl Acad Sci U S A*. 2012;109(4):E197-205.
172. Streit WJ, Xue QS, Tischer J, Bechmann I. Microglial pathology. *Acta Neuropathol Commun*. 2014;2:142.
173. Thal DR. The role of astrocytes in amyloid beta-protein toxicity and clearance. *Exp Neurol*. 2012;236(1):1-5.
174. Corbett A, Williams G, Ballard C. Drug repositioning in Alzheimer's disease. *Front Biosci (Schol Ed)*. 2015;7:184-188.
175. Calsolaro V, Edison P. Neuroinflammation in Alzheimer's disease: Current evidence and future directions. *Alzheimers Dement*. 2016;12(6):719-732.
176. Decourt B, Lahiri DK, Sabbagh MN. Targeting Tumor Necrosis Factor Alpha for Alzheimer's Disease. *Curr Alzheimer Res*. 2017;14(4):412-425.
177. Medeiros R, Figueiredo CP, Pandolfo P, et al. The role of TNF-alpha signaling pathway on COX-2 upregulation and cognitive decline induced by beta-amyloid peptide. *Behav Brain Res*. 2010;209(1):165-173.
178. Krause DL, Muller N. Neuroinflammation, microglia and implications for anti-inflammatory treatment in Alzheimer's disease. *Int J Alzheimers Dis*. 2010;2010.
179. Zhang C, Wang Y, Wang D, Zhang J, Zhang F. NSAID Exposure and Risk of Alzheimer's Disease: An Updated Meta-Analysis From Cohort Studies. *Front Aging Neurosci*. 2018;10:83.
180. Sanz-Blasco S, Calvo-Rodriguez M, Caballero E, Garcia-Durillo M, Nunez L, Villalobos C. Is it All Said for NSAIDs in Alzheimer's Disease? Role of Mitochondrial Calcium Uptake. *Curr Alzheimer Res*. 2018;15(6):504-510.
181. Kukar T, Golde TE. Possible mechanisms of action of NSAIDs and related compounds that modulate gamma-secretase cleavage. *Curr Top Med Chem*. 2008;8(1):47-53.
182. Breitner JC, Baker LD, Montine TJ, et al. Extended results of the Alzheimer's disease anti-inflammatory prevention trial. *Alzheimers Dement*. 2011;7(4):402-411.
183. Butchart J, Brook L, Hopkins V, et al. Etanercept in Alzheimer disease: A randomized, placebo-controlled, double-blind, phase 2 trial. *Neurology*. 2015;84(21):2161-2168.
184. Andrade-Moraes CH, Oliveira-Pinto AV, Castro-Fonseca E, et al. Cell number changes in Alzheimer's disease relate to dementia, not to plaques and tangles. *Brain*. 2013;136(Pt 12):3738-3752.
185. Roth AD, Ramirez G, Alarcon R, Von Bernhardi R. Oligodendrocytes damage in Alzheimer's disease: beta amyloid toxicity and inflammation. *Biol Res*. 2005;38(4):381-387.
186. Sachdev PS, Zhuang L, Braidy N, Wen W. Is Alzheimer's a disease of the white matter? *Curr Opin Psychiatry*. 2013;26(3):244-251.

187. Sjobeck M, Englund E. Glial levels determine severity of white matter disease in Alzheimer's disease: a neuropathological study of glial changes. *Neuropathol Appl Neurobiol*. 2003;29(2):159-169.
188. Tomimoto H, Akiguchi I, Suenaga T, et al. Alterations of the blood-brain barrier and glial cells in white-matter lesions in cerebrovascular and Alzheimer's disease patients. *Stroke*. 1996;27(11):2069-2074.
189. Jeong YJ, Yoon HJ, Kang DY. Assessment of change in glucose metabolism in white matter of amyloid-positive patients with Alzheimer disease using F-18 FDG PET. *Medicine (Baltimore)*. 2017;96(48):e9042.
190. Agosta F, Pievani M, Sala S, et al. White matter damage in Alzheimer disease and its relationship to gray matter atrophy. *Radiology*. 2011;258(3):853-863.
191. Migliaccio R, Agosta F, Possin KL, Rabinovici GD, Miller BL, Gorno-Tempini ML. White matter atrophy in Alzheimer's disease variants. *Alzheimers Dement*. 2012;8(5 Suppl):S78-87 e71-72.
192. Bronge L, Bogdanovic N, Wahlund LO. Postmortem MRI and histopathology of white matter changes in Alzheimer brains. A quantitative, comparative study. *Dement Geriatr Cogn Disord*. 2002;13(4):205-212.
193. Zhang Y, Schuff N, Jahng GH, et al. Diffusion tensor imaging of cingulum fibers in mild cognitive impairment and Alzheimer disease. *Neurology*. 2007;68(1):13-19.
194. Maier-Hein KH, Westin CF, Shenton ME, et al. Widespread white matter degeneration preceding the onset of dementia. *Alzheimers Dement*. 2015;11(5):485-493 e482.
195. Pierpaoli C, Barnett A, Pajevic S, et al. Water diffusion changes in Wallerian degeneration and their dependence on white matter architecture. *Neuroimage*. 2001;13(6 Pt 1):1174-1185.
196. Song SK, Sun SW, Ramsbottom MJ, Chang C, Russell J, Cross AH. Dysmyelination revealed through MRI as increased radial (but unchanged axial) diffusion of water. *Neuroimage*. 2002;17(3):1429-1436.
197. Goldberg MP, Ransom BR. New light on white matter. *Stroke*. 2003;34(2):330-332.
198. Toledo JB, Arnold SE, Raible K, et al. Contribution of cerebrovascular disease in autopsy confirmed neurodegenerative disease cases in the National Alzheimer's Coordinating Centre. *Brain*. 2013;136(Pt 9):2697-2706.
199. Smith EE. Clinical presentations and epidemiology of vascular dementia. *Clin Sci (Lond)*. 2017;131(11):1059-1068.
200. Kalaria RN, Ballard C. Overlap between pathology of Alzheimer disease and vascular dementia. *Alzheimer Dis Assoc Disord*. 1999;13 Suppl 3:S115-123.
201. Groves WC, Brandt J, Steinberg M, et al. Vascular dementia and Alzheimer's disease: is there a difference? A comparison of symptoms by disease duration. *J Neuropsychiatry Clin Neurosci*. 2000;12(3):305-315.
202. de la Torre JC. Is Alzheimer's disease a neurodegenerative or a vascular disorder? Data, dogma, and dialectics. *The Lancet Neurology*. 2004;3(3):184-190.

203. Girouard H, Iadecola C. Neurovascular coupling in the normal brain and in hypertension, stroke, and Alzheimer disease. *J Appl Physiol (1985)*. 2006;100(1):328-335.
204. Rodrigue KM. Contribution of cerebrovascular health to the diagnosis of Alzheimer disease. *JAMA Neurol*. 2013;70(4):438-439.
205. Moody DM, Brown WR, Challa VR, Ghazi-Birry HS, Reboussin DM. Cerebral microvascular alterations in aging, leukoaraiosis, and Alzheimer's disease. *Ann N Y Acad Sci*. 1997;826:103-116.
206. de la Torre JC. Alzheimer Disease as a Vascular Disorder: Nosological Evidence. *Stroke*. 2002;33(4):1152-1162.
207. Pantoni L, Garcia JH. Pathogenesis of leukoaraiosis: a review. *Stroke*. 1997;28(3):652-659.
208. Wardlaw JM, Sandercock PA, Dennis MS, Starr J. Is breakdown of the blood-brain barrier responsible for lacunar stroke, leukoaraiosis, and dementia? *Stroke*. 2003;34(3):806-812.
209. Basile AM, Pantoni L, Pracucci G, et al. Age, hypertension, and lacunar stroke are the major determinants of the severity of age-related white matter changes. The LADIS (Leukoaraiosis and Disability in the Elderly) Study. *Cerebrovasc Dis*. 2006;21(5-6):315-322.
210. Conklin J, Silver FL, Mikulis DJ, Mandell DM. Are acute infarcts the cause of leukoaraiosis? Brain mapping for 16 consecutive weeks. *Ann Neurol*. 2014;76(6):899-904.
211. Bernbaum M, Menon BK, Fick G, et al. Reduced blood flow in normal white matter predicts development of leukoaraiosis. *J Cereb Blood Flow Metab*. 2015;35(10):1610-1615.
212. Diaz JF, Merskey H, Hachinski VC, et al. Improved recognition of leukoaraiosis and cognitive impairment in Alzheimer's disease. *Arch Neurol*. 1991;48(10):1022-1025.
213. Stout JC, Jernigan TL, Archibald SL, Salmon DP. Association of dementia severity with cortical gray matter and abnormal white matter volumes in dementia of the Alzheimer type. *Arch Neurol*. 1996;53(8):742-749.
214. Ble A, Ranzini M, Zurlo A, et al. Leukoaraiosis is associated with functional impairment in older patients with Alzheimer's disease but not vascular dementia. *J Nutr Health Aging*. 2006;10(1):31-35.
215. van Westen D, Lindqvist D, Blennow K, et al. Cerebral white matter lesions - associations with Abeta isoforms and amyloid PET. *Sci Rep*. 2016;6:20709.
216. Pietroboni AM, Scarioni M, Carandini T, et al. CSF beta-amyloid and white matter damage: a new perspective on Alzheimer's disease. *J Neurol Neurosurg Psychiatry*. 2018;89(4):352-357.
217. Hachinski V, Iadecola C, Petersen RC, et al. National Institute of Neurological Disorders and Stroke-Canadian Stroke Network vascular cognitive impairment harmonization standards. *Stroke*. 2006;37(9):2220-2241.
218. Stephan BC, Matthews FE, Khaw KT, Dufouil C, Brayne C. Beyond mild cognitive impairment: vascular cognitive impairment, no dementia (VCIND). *Alzheimers Res Ther*. 2009;1(1):4.
219. Roman GC, Sachdev P, Royall DR, et al. Vascular cognitive disorder: a new diagnostic category updating vascular cognitive impairment and vascular dementia. *J Neurol Sci*. 2004;226(1-2):81-87.

220. Gorelick PB, Scuteri A, Black SE, et al. Vascular contributions to cognitive impairment and dementia: a statement for healthcare professionals from the american heart association/american stroke association. *Stroke*. 2011;42(9):2672-2713.
221. Sachdev P, Kalaria R, O'Brien J, et al. Diagnostic criteria for vascular cognitive disorders: a VASCOG statement. *Alzheimer Dis Assoc Disord*. 2014;28(3):206-218.
222. Wentzel C, Rockwood K, MacKnight C, et al. Progression of impairment in patients with vascular cognitive impairment without dementia. *Neurology*. 2001;57(4):714-716.
223. Korczyn AD, Vakhapova V, Grinberg LT. Vascular dementia. *J Neurol Sci*. 2012;322(1-2):2-10.
224. Korczyn AD. Mixed Dementia-the Most Common Cause of Dementia. *Annals of the New York Academy of Sciences*. 2002;977(1):129-134.
225. Black SE. Vascular cognitive impairment: epidemiology, subtypes, diagnosis and management. *J R Coll Physicians Edinb*. 2011;41(1):49-56.
226. Jellinger KA. Pathology and pathogenesis of vascular cognitive impairment-a critical update. *Front Aging Neurosci*. 2013;5:17.
227. Neuropathology Group. Medical Research Council Cognitive F, Aging S. Pathological correlates of late-onset dementia in a multicentre, community-based population in England and Wales. Neuropathology Group of the Medical Research Council Cognitive Function and Ageing Study (MRC CFAS). *Lancet*. 2001;357(9251):169-175.
228. van der Flier WM, Scheltens P. Epidemiology and risk factors of dementia. *J Neurol Neurosurg Psychiatry*. 2005;76 Suppl 5:v2-7.
229. Lobo A, Launer LJ, Fratiglioni L, et al. Prevalence of dementia and major subtypes in Europe: A collaborative study of population-based cohorts. Neurologic Diseases in the Elderly Research Group. *Neurology*. 2000;54(11 Suppl 5):S4-9.
230. Canadian study of health and aging: study methods and prevalence of dementia. *CMAJ*. 1994;150(6):899-913.
231. Kalaria RN, Kenny RA, Ballard CG, Perry R, Ince P, Polvikoski T. Towards defining the neuropathological substrates of vascular dementia. *J Neurol Sci*. 2004;226(1-2):75-80.
232. Kalaria RN. Neuropathological diagnosis of vascular cognitive impairment and vascular dementia with implications for Alzheimer's disease. *Acta Neuropathol*. 2016;131(5):659-685.
233. Choi EJ, Choi CG, Kim JS. Large cerebral artery involvement in CADASIL. *Neurology*. 2005;65(8):1322-1324.
234. Yamashita M, Oka K, Tanaka K. Histopathology of the brain vascular network in moyamoya disease. *Stroke*. 1983;14(1):50-58.
235. Kisler K, Nelson AR, Montagne A, Zlokovic BV. Cerebral blood flow regulation and neurovascular dysfunction in Alzheimer disease. *Nat Rev Neurosci*. 2017;18(7):419-434.
236. Zlokovic BV. Neurovascular mechanisms of Alzheimer's neurodegeneration. *Trends Neurosci*. 2005;28(4):202-208.

237. Zlokovic BV. Neurovascular pathways to neurodegeneration in Alzheimer's disease and other disorders. *Nat Rev Neurosci*. 2011;12(12):723-738.
238. Iadecola C. Neurovascular regulation in the normal brain and in Alzheimer's disease. *Nat Rev Neurosci*. 2004;5(5):347-360.
239. Arvanitakis Z, Capuano AW, Leurgans SE, Bennett DA, Schneider JA. Relation of cerebral vessel disease to Alzheimer's disease dementia and cognitive function in elderly people: a cross-sectional study. *Lancet Neurol*. 2016;15(9):934-943.
240. Snowdon DA, Greiner LH, Mortimer JA, Riley KP, Greiner PA, Markesbery WR. Brain infarction and the clinical expression of Alzheimer disease. The Nun Study. *JAMA*. 1997;277(10):813-817.
241. Azarpazhooh MR, Avan A, Cipriano LE, Munoz DG, Sposato LA, Hachinski V. Concomitant vascular and neurodegenerative pathologies double the risk of dementia. *Alzheimer's & Dementia*. 2018;14:148-156.
242. Pase MP, Satizabal CL, Seshadri S. Role of Improved Vascular Health in the Declining Incidence of Dementia. *Stroke*. 2017;48(7):2013-2020.
243. Hachinski V, Sposato LA. Dementia: from muddled diagnoses to treatable mechanisms. *Brain*. 2013;136(Pt 9):2652-2654.
244. Muoio V, Persson PB, Sendeski MM. The neurovascular unit - concept review. *Acta Physiol (Oxf)*. 2014;210(4):790-798.
245. Tarantini S, Tran CHT, Gordon GR, Ungvari Z, Csiszar A. Impaired neurovascular coupling in aging and Alzheimer's disease: Contribution of astrocyte dysfunction and endothelial impairment to cognitive decline. *Exp Gerontol*. 2017;94:52-58.
246. Deane R, Singh I, Sagare AP, et al. A multimodal RAGE-specific inhibitor reduces amyloid beta-mediated brain disorder in a mouse model of Alzheimer disease. *J Clin Invest*. 2012;122(4):1377-1392.
247. Halliday MR, Rege SV, Ma Q, et al. Accelerated pericyte degeneration and blood-brain barrier breakdown in apolipoprotein E4 carriers with Alzheimer's disease. *J Cereb Blood Flow Metab*. 2016;36(1):216-227.
248. Zenaro E, Piacentino G, Constantin G. The blood-brain barrier in Alzheimer's disease. *Neurobiol Dis*. 2017;107:41-56.
249. Jin SJ, Liu Y, Deng SH, et al. Protective effects of activated protein C on neurovascular unit in a rat model of intrauterine infection-induced neonatal white matter injury. *J Huazhong Univ Sci Technol Med Sci*. 2015;35(6):904-909.
250. D. Williams P, V. Zlokovic B, H. Griffin J, E. Pryor K, P. Davis T. Preclinical Safety and Pharmacokinetic Profile of 3K3A-APC, a Novel, Modified Activated Protein C for Ischemic Stroke. *Current Pharmaceutical Design*. 2012;18(27):4215-4222.
251. Carnevale D, Mascio G, D'Andrea I, et al. Hypertension induces brain beta-amyloid accumulation, cognitive impairment, and memory deterioration through activation of receptor for advanced glycation end products in brain vasculature. *Hypertension*. 2012;60(1):188-197.

252. Borysova L, Wray S, Eisner DA, Burdyga T. How calcium signals in myocytes and pericytes are integrated across in situ microvascular networks and control microvascular tone. *Cell Calcium*. 2013;54(3):163-174.
253. MacVicar BA, Newman EA. Astrocyte regulation of blood flow in the brain. *Cold Spring Harb Perspect Biol*. 2015;7(5).
254. Rosenberg GA. Extracellular matrix inflammation in vascular cognitive impairment and dementia. *Clin Sci (Lond)*. 2017;131(6):425-437.
255. Thurgur H, Pinteaux E. Microglia in the Neurovascular Unit: Blood–Brain Barrier–microglia Interactions After Central Nervous System Disorders. *Neuroscience*. 2018.
256. Barakat R, Redzic Z. The Role of Activated Microglia and Resident Macrophages in the Neurovascular Unit during Cerebral Ischemia: Is the Jury Still Out? *Med Princ Pract*. 2016;25 Suppl 1:3-14.
257. Bu XL, Xiang Y, Jin WS, et al. Blood-derived amyloid-beta protein induces Alzheimer's disease pathologies. *Mol Psychiatry*. 2017.
258. Padwal RS, Bienek A, McAlister FA, Campbell NR, Outcomes Research Task Force of the Canadian Hypertension Education P. Epidemiology of Hypertension in Canada: An Update. *Can J Cardiol*. 2016;32(5):687-694.
259. Tzourio C. Hypertension, cognitive decline, and dementia: an epidemiological perspective. *Dialogues Clin Neurosci*. 2007;9(1):61-70.
260. Kennelly SP, Lawlor BA, Kenny RA. Blood pressure and dementia - a comprehensive review. *Ther Adv Neurol Disord*. 2009;2(4):241-260.
261. Oveisgharan S, Hachinski V. Hypertension, executive dysfunction, and progression to dementia: the canadian study of health and aging. *Arch Neurol*. 2010;67(2):187-192.
262. Iadecola C. Hypertension and dementia. *Hypertension*. 2014;64(1):3-5.
263. Livingston G, Sommerlad A, Orgeta V, et al. Dementia prevention, intervention, and care. *Lancet*. 2017;390(10113):2673-2734.
264. Diaz-Ruiz C, Wang J, Ksiazak-Reding H, et al. Role of Hypertension in Aggravating Abeta Neuropathology of AD Type and Tau-Mediated Motor Impairment. *Cardiovasc Psychiatry Neurol*. 2009;2009:107286.
265. Gentile MT, Poulet R, Di Pardo A, et al. Beta-amyloid deposition in brain is enhanced in mouse models of arterial hypertension. *Neurobiol Aging*. 2009;30(2):222-228.
266. Csiszar A, Tucsek Z, Toth P, et al. Synergistic effects of hypertension and aging on cognitive function and hippocampal expression of genes involved in beta-amyloid generation and Alzheimer's disease. *Am J Physiol Heart Circ Physiol*. 2013;305(8):H1120-1130.
267. Cifuentes D, Poittevin M, Dere E, et al. Hypertension accelerates the progression of Alzheimer-like pathology in a mouse model of the disease. *Hypertension*. 2015;65(1):218-224.
268. Carnevale D, Perrotta M, Lembo G, Trimarco B. Pathophysiological Links Among Hypertension and Alzheimer's Disease. *High Blood Press Cardiovasc Prev*. 2016;23(1):3-7.

269. Lithell H, Hansson L, Skoog I, et al. The Study on COgnition and Prognosis in the Elderly (SCOPE); outcomes in patients not receiving add-on therapy after randomization. *J Hypertens*. 2004;22(8):1605-1612.
270. Peters R, Beckett N, Forette F, et al. Incident dementia and blood pressure lowering in the Hypertension in the Very Elderly Trial cognitive function assessment (HYVET-COG): a double-blind, placebo controlled trial. *Lancet Neurol*. 2008;7(8):683-689.
271. McGuinness B, Todd S, Passmore P, et al. Blood pressure lowering in patients without prior cerebrovascular disease for prevention of cognitive impairment and dementia. *Cochrane Database Syst Rev*. 2009(4):CD004034-CD004034.
272. Sörös P, Whitehead S, Spence JD, et al. Antihypertensive treatment can prevent stroke and cognitive decline. *Nat Rev Neurol*. 2013;9(3):174-178.
273. Perrotta M, Lembo G, Carnevale D. Hypertension and Dementia: Epidemiological and Experimental Evidence Revealing a Detrimental Relationship. *Int J Mol Sci*. 2016;17(3):347.
274. Walker V, Davies N, Kehoe P, Martin R. Can treatments for hypertension be repurposed for the treatment of dementia? *Revue d'Épidémiologie et de Santé Publique*. 2018;66:S262-S262.
275. Kazama K, Wang G, Frys K, Anrather J, Iadecola C. Angiotensin II attenuates functional hyperemia in the mouse somatosensory cortex. *Am J Physiol Heart Circ Physiol*. 2003;285(5):H1890-1899.
276. Faraco G, Park L, Zhou P, et al. Hypertension enhances Abeta-induced neurovascular dysfunction, promotes beta-secretase activity, and leads to amyloidogenic processing of APP. *J Cereb Blood Flow Metab*. 2016;36(1):241-252.
277. Jennings JR, Muldoon MF, Ryan C, et al. Reduced cerebral blood flow response and compensation among patients with untreated hypertension. *Neurology*. 2005;64(8):1358-1365.
278. Setiadi A, Korim WS, Elsaafien K, Yao ST. The role of the blood-brain barrier in hypertension. *Exp Physiol*. 2018;103(3):337-342.
279. Faraco G, Sugiyama Y, Lane D, et al. Perivascular macrophages mediate the neurovascular and cognitive dysfunction associated with hypertension. *J Clin Invest*. 2016;126(12):4674-4689.
280. Seshadri S, Beiser A, Kelly-Hayes M, et al. The lifetime risk of stroke: estimates from the Framingham Study. *Stroke*. 2006;37(2):345-350.
281. Bogiatzi C, Hackam DG, McLeod AI, Spence JD. Secular trends in ischemic stroke subtypes and stroke risk factors. *Stroke*. 2014;45(11):3208-3213.
282. Vilar-Bergua A, Riba-Llena I, Nafria C, et al. Blood and CSF biomarkers in brain subcortical ischemic vascular disease: Involved pathways and clinical applicability. *J Cereb Blood Flow Metab*. 2016;36(1):55-71.
283. Fanning JP, Wong AA, Fraser JF. The epidemiology of silent brain infarction: a systematic review of population-based cohorts. *BMC Med*. 2014;12:119.
284. Vermeer SE, Longstreth WT, Jr., Koudstaal PJ. Silent brain infarcts: a systematic review. *Lancet Neurol*. 2007;6(7):611-619.
285. Nakagawa T, Sekizawa K, Nakajoh K, Tanji H, Arai H, Sasaki H. Silent cerebral infarction: a potential risk for pneumonia in the elderly. *J Intern Med*. 2000;247(2):255-259.

286. Garbuzova-Davis S, Haller E, Williams SN, et al. Compromised blood-brain barrier competence in remote brain areas in ischemic stroke rats at the chronic stage. *J Comp Neurol*. 2014;522(13):3120-3137.
287. Whitehead SN, Massoni E, Cheng G, et al. Triflusal reduces cerebral ischemia induced inflammation in a combined mouse model of Alzheimer's disease and stroke. *Brain Res*. 2010;1366:246-256.
288. Owen JB, Sultana R, Aluise CD, et al. Oxidative modification to LDL receptor-related protein 1 in hippocampus from subjects with Alzheimer disease: implications for Abeta accumulation in AD brain. *Free Radic Biol Med*. 2010;49(11):1798-1803.
289. Erickson MA, Banks WA. Blood-brain barrier dysfunction as a cause and consequence of Alzheimer's disease. *J Cereb Blood Flow Metab*. 2013;33(10):1500-1513.
290. Veszelka S, Toth AE, Walter FR, et al. Docosahexaenoic acid reduces amyloid-beta induced toxicity in cells of the neurovascular unit. *J Alzheimers Dis*. 2013;36(3):487-501.
291. Hawkes CA, JoAnne M. Selective targeting of perivascular macrophages for clearance of β amyloid in cerebral amyloid angiopathy. 2009;106(4):1261-1266.
292. Montagne A, Nikolakopoulou AM, Zhao Z, et al. Pericyte degeneration causes white matter dysfunction in the mouse central nervous system. *Nat Med*. 2018;24(3):326-337.
293. Tong XK, Lecrux C, Rosa-Neto P, Hamel E. Age-dependent rescue by simvastatin of Alzheimer's disease cerebrovascular and memory deficits. *J Neurosci*. 2012;32(14):4705-4715.
294. Sorond FA, Hurwitz S, Salat DH, Greve DN, Fisher ND. Neurovascular coupling, cerebral white matter integrity, and response to cocoa in older people. *Neurology*. 2013;81(10):904-909.
295. Agca C, Klakotskaia D, Schachtman TR, Chan AW, Lah JJ, Agca Y. Presenilin 1 transgene addition to amyloid precursor protein overexpressing transgenic rats increases amyloid beta 42 levels and results in loss of memory retention. *BMC Neurosci*. 2016;17(1):46.
296. Agca C, Fritz JJ, Walker LC, et al. Development of transgenic rats producing human beta-amyloid precursor protein as a model for Alzheimer's disease: transgene and endogenous APP genes are regulated tissue-specifically. *BMC Neurosci*. 2008;9:28.
297. Rosen RF, Fritz JJ, Dooyema J, et al. Exogenous seeding of cerebral beta-amyloid deposition in betaAPP-transgenic rats. *J Neurochem*. 2012;120(5):660-666.
298. Silverberg GD, Miller MC, Pascale CL, et al. Kaolin-induced chronic hydrocephalus accelerates amyloid deposition and vascular disease in transgenic rats expressing high levels of human APP. *Fluids Barriers CNS*. 2015;12(1):2.
299. Brady AM, Floresco SB. Operant procedures for assessing behavioral flexibility in rats. *J Vis Exp*. 2015(96):e52387.
300. Floresco SB, Block AE, Tse MTL. Inactivation of the medial prefrontal cortex of the rat impairs strategy set-shifting, but not reversal learning, using a novel, automated procedure. *Behav Brain Res*. 2008;190(1):85-96.

Chapter 2: The Cognitive and Neuroinflammatory Profile of the TgAPP21 Rat

This study set out to determine the effect of pathogenic APP on white matter inflammation and executive function (Objective 1) and is currently under review for *Scientific Reports*.

2.1 Abstract

Executive dysfunction and white matter pathology continue to be relatively understudied in Alzheimer's disease (AD). The TgAPP21 rat model of AD expresses hAPP with swe/ind mutations but does not spontaneously develop plaques; however, previous studies of this model suggest a spontaneous impairment of behavioural flexibility, an important subdomain of executive function. In this study, 7 – 8-month-old male TgAPP21 rats were tested for behavioural flexibility, learning, and memory using an operant conditioning chamber and the Morris Water Maze (MWM). TgAPP21 rats demonstrated a regressive behavioral inflexibility during set shifting in an operant conditioning chamber, and regressive behaviour was also demonstrated in the MWM probe test; this behavioural phenotype has not been previously described in the MWM. Clinical research of prodromal AD suggests that white matter pathology may underlie impairment of executive functions such as behavioural flexibility. Diffuse microglia activation was increased in the white matter of TgAPP21, which was found to correlate with the number of reversal errors in the operant conditioning chamber. TgAPP21 rats are therefore an instrumental model of behavioural inflexibility and plaque-independent extrahippocampal changes of early AD-related amyloidopathy.

2.2 Introduction

Patients with mild cognitive impairment that exhibit executive dysfunction are more likely to progress to Alzheimer's disease (AD)¹⁻⁷. Executive dysfunction can also be detected early in AD, even prior to diagnosis⁸⁻¹¹. Particular subdomains of executive function that are important predictors of progressive cognitive decline include cognitive flexibility and working memory¹⁻⁵. Despite this, behavioural characterization of rodent models of AD has largely focused on hippocampal dependent cognition such as memory and spatial processing¹²⁻¹⁴. To advance our understanding of the early mechanisms underlying AD and other dementias, further characterization of executive functions in rodent models is needed¹⁵.

The TgAPP21 transgenic Fischer 344 rat (hAPP with Swedish and Indiana mutations) is ideal for modelling the prodromal phase of AD. TgAPP21 rats do not spontaneously develop plaques^{16,17}, but while amyloid aggregates are absent in naïve TgAPP21 rats, aggregates can be induced by cerebral stressors¹⁶⁻¹⁹. No behavioural changes have been found in previous studies of naïve TgAPP21 rats, which have only evaluated hippocampal dependent spatial learning and memory¹⁷. In contrast, TgAPP21 rats with ischemic injury of the dorsal striatum demonstrated significantly more behavioural inflexibility than injured wildtype (control) rats and uninjured TgAPP21 rats, characterized by a specific increase of regressive errors on an extradimensional set shifting task²⁰. While the interaction of ischemic striatal injury and transgene expression produced a synergistic increase of behavioural inflexibility, the transgene alone had an overall effect of increased regressive behaviour. This warrants closer investigation of spontaneous regressive behaviour in TgAPP21 rats. Mild cortical pathology has only been observed in naïve TgAPP21 rats that were aged to 18 – 19 months of age and was absent in younger rats and would therefore be unlikely to underlie spontaneous behavioural inflexibility in younger rats. However, significant dysregulation of membrane lipids has been found in TgAPP21 white matter by 12 months of age²¹. Recent clinical research on the early stages of dementia have found white matter pathology to be linked to executive dysfunction, including behavioural inflexibility²²⁻³². As features of both white matter pathology and executive dysfunction have been observed independently in the TgAPP21 rat, this model may

present an important opportunity to study the link between white matter changes and executive function.

To better characterize spontaneous behavioural changes in TgAPP21 rats, a complement of behavioural tests was performed in the present study. We found that TgAPP21 rat demonstrated behavioural inflexibility in an operant-chamber-based test of extradimensional set shifting³³. This manifested as increased regressive behaviour and reversal impairments in an operant conditioning chamber. To corroborate previous findings of normal hippocampal-dependent function in TgAPP21 rats, the Morris Water Maze (MWM) was used to evaluate spatial learning, memory, and working memory³⁴⁻³⁸. MWM tests confirmed that TgAPP21 rats had unimpaired spatial learning and memory, but we were surprised to also observe a previously undescribed regressive-like behaviour during the MWM probe test. These observations demonstrate how tests of behavioural inflexibility can inform tests of hippocampal function, such as learning and memory. Lastly, as white matter inflammation has been linked to executive dysfunction, we analyzed brain tissue for activation of microglia and astrocytes in the plaque-free TgAPP21 rat. While astrocyte activation was not increased in TgAPP21 rat, widespread activation of white matter microglia was significantly increased. Microglia activation in the supraventricular corpus callosum (SVCC) was also significantly correlated with reversal impairment. Our findings identify the TgAPP21 rat as having the behavioural and neuropathological profile that reflects some of the earliest observable neurological changes that precede diagnosis of dementia.

2.3 Methods

2.3.1 Animals

Animal ethics and procedures were approved by the Animal Care Committee at Western University (protocol 2014-016) and are in compliance with Canadian and National Institute of Health Guides for the Care and Use of Laboratory Animals (NIH Publication #80-23). All rats used in this study were housed in facilities maintained by Western University Animal Care and Veterinary Services on a 12:12 hour light/dark cycle alternating at 1AM/PM; behavioural testing was conducted during the rats' dark cycle. Homozygous transgenic Fischer 344-APP21 rats (TgAPP21) were studied to model the effect of increased brain concentrations of amyloid protein. Developed by lentiviral infection of zygotes, TgAPP21 rats overexpress a pathogenic human APP sequence with Swedish and Indiana mutations, and produce high levels of beta-amyloid (both 1-40 and 1-42), but do not deposit beta-amyloid plaques¹⁶. TgAPP21 rats were bred and aged in house, alongside wildtype Fischer 344. TgAPP21 homozygosity was validated using tissue samples from pups. 10 male TgAPP21 rats and 10 male wildtype Fischer 344 (Wt) rats with body masses ranging from 300-430 g were aged to an average of 6.7 months (SD = 0.3) before behavioural studies began; rats were euthanized at 7.5 months of age (SD = 0.3). This age range was selected to allow for some age-dependent pathology of hAPP expression and to minimize other health variables expected in more advanced age.

2.3.2 Set Shift & Reversal

Behavioral flexibility was assessed using an operant conditioning based set-shifting task as developed by Floresco et al³⁹. As described in our recent publication⁴⁰, the set-shifting task required rats to perform an extradimensional strategy shift, in which they had to transition from a learned visual cue-dependent strategy to a newly-rewarding egocentric spatial strategy (Figure 2-1). The overall experimental series included acclimation and training, initial set formation (visual cue discrimination task) and finally, set-shifting (response discrimination task). Throughout these experimental steps, animals were

tested during their dark cycle at regular individual times, completing all training and testing in the same apparatus.

2.3.2.1 Apparatus

Two operant conditioning chambers (Med Associates; St. Albans, VT) were fitted in separate sound attenuating boxes. The operant conditioning chambers were equipped with two retractable response levers which were located on either side of a central food pellet receptacle. A bright stimulus light was located above each lever (Figure 2-1), and there was a house light at the back of the apparatus at roof level. All operant conditioning chamber inputs and outputs were handled using MED-PC software (Med Associates; St. Albans, VT) with customized programs that automated control of the chamber and data recording. Immediately following a correct lever press, a 45 mg sucrose pellet (Dustless precision pellets, Bio-Serv; Burlington, ON) was dispensed into the central pellet receptacle as a positive reinforcement.

2.3.2.2 Food Restriction & Initial Operant Conditioning

To ensure motivation for food reinforcement, food restriction was initiated 6 days before lever-press training and continued throughout testing. Feed quantity was adjusted individually to maintain rat body mass at 85% of initial free-feed mass. Rats were weighed regularly during food restriction, and there was no difference in loss of body mass between groups. Water was provided freely during food restriction.

Three days prior to training, pellets were placed daily in the rat's cage to allow for acclimation to the future reinforcement used in testing. Rats were habituated to the operant conditioning chamber for 20 min, followed by daily training of lever pressing; lever presses were reinforced with a pellet using a fixed-ratio 1 (FR1) schedule. Rats were trained under manual control of lever extension & retraction using operant conditioning strategies until they could consecutively alternate between 15 left and 15 right lever presses. They were then trained daily on an automated 90-trial program that pseudo-

randomly alternated lever presentation; each trial allowed the rat 10 s to press an extended lever, followed by a 20 s inter-trial period. The training program was repeated daily until the rat completed 90 trials with 5 or fewer omissions.

2.3.2.3 *Side Bias Determination*

The side bias determination program was run immediately after training was complete. Both levers were presented on all trials, and rats were granted a 10 s response period with a 20 s inter-trial period. Initially, either lever was rewarded with a pellet, but the following reward would only be given when the opposite lever was pressed. This was repeated until the rat completed 7 pairs of lever alternations (a pair could be initiated on either side). A side bias was identified if one lever was pressed twice as many times as the other lever, otherwise the lever-side that initiated 4 or more of 7 alternation pairs was classified as the biased side. Each rat's side bias was used for the response discrimination task, where the lever opposite the rat's side bias was always considered the correct lever.

2.3.2.4 *Visual Cue Discrimination*

One day after completion of side bias determination, rats began the visual cue discrimination (VCD) task (Figure 2-1). On each trial, illumination of one stimulus light preceded the extension of both levers by 3 s and remained illuminated when both levers were extended. The rat then had 10 s to press the lever associated with the illuminated stimulus to receive a pellet. If no lever was pressed (omission), then no pellet was granted, levers were retracted, and lights were turned off. The location of the stimulus light was counterbalanced and presented equally over both levers during the test. All animals were presented with 100 trials on a testing day, with 20 s inter-trial periods. 8 correct consecutive responses were needed to achieve test criterion, and if this was not met within the allotted trial limit, the animal was placed in its home cage and retested the next day. Omissions were not considered to disrupt a streak of correct responses.

2.3.2.5 *Set-shifting: Response Discrimination*

On the day after the VCD task performance criterion was achieved, rats were given 20 VCD trials to test for retention of the learned rule (i.e., “follow the light”). On the 21st trial, the paradigm was switched to a response discrimination (RD) task in which only the lever opposite the rat’s side bias was always considered correct despite the location of the stimulus light. The RD task continued for 120 trials, with a performance criterion set at 8 correct consecutive responses.

It is important to note that half of the RD task trials could be considered as ‘congruent’ and the other half were ‘incongruent’, occurring in a counterbalanced and pseudorandom sequence. ‘Congruent trials’ occurred when the visual cue distractor was illuminated above the correct lever, so that a rat would be rewarded whether it was responding in accordance with the previously-correct VCD strategy or the new RD strategy (Figure 2-1). Hence, success on a congruent trial was not informative of the rat’s behavioural strategy. In contrast, ‘incongruent trials’ occurred when the visual cue distractor was illuminated above the incorrect lever, so that a rat would only receive a pellet if it responded in accordance with the new RD strategy (Figure 2-1). Thus, success on an incongruent trial was informative of the rat’s behavioural strategy. In this study, we also included a 24 h delayed 20 trial retrieval test for response discrimination.

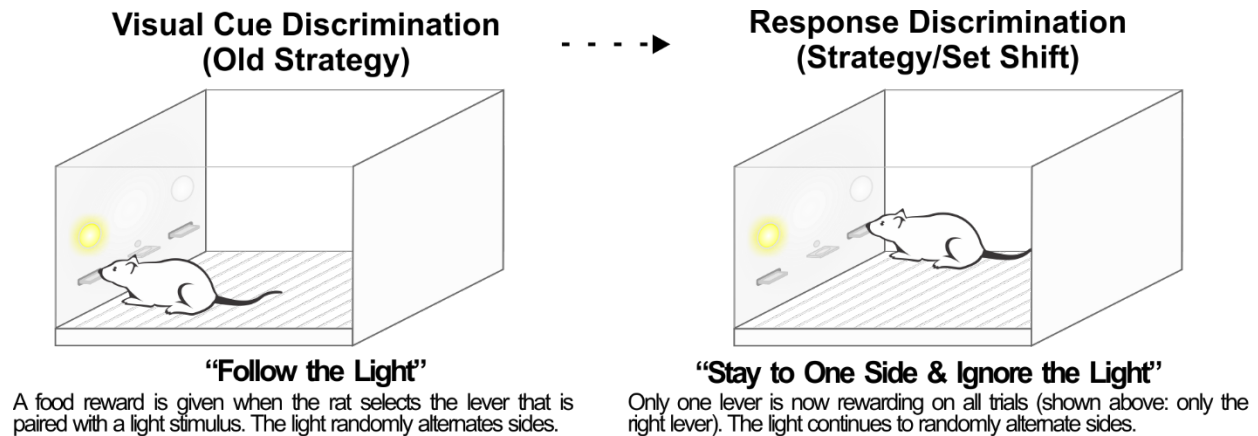
2.3.2.6 *Set-shifting Behavioural Measures*

Traditional measures for assessing set-shifting behaviour during the RD task included the number of trials to criterion, number of errors to criterion, and error profiling, namely by perseverative, never-reinforced, or regressive error types (Figure 2-1)^{39,40}. Errors made on incongruent trials were deemed either perseverative or regressive. ‘Perseverative’ errors were scored earlier in the RD task when rats continued to adhere to the original VCD strategy (i.e., “follow the light”), so long as 6 or more incorrect lever responses were observed in a block of 8 incongruent trials (which randomly occurred over a block of 16 trials that also included 8 interspersed congruent trials). Later in the RD task, rats successfully disengaged from the previously-correct VCD strategy. Once 5 or fewer

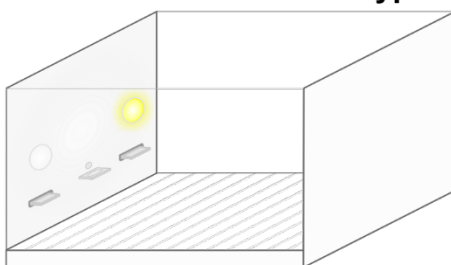
incorrect lever responses were observed in a block of 8 incongruent trials, all incorrect responses to incongruent trials in that block and on all subsequent blocks were scored as 'regressive' errors. Thus, perseverative errors were an indicator of the rat's failure to inhibit the previously-learned strategy, whereas regressive errors indicated the rat's failure to engage or maintain a new strategy³⁹. Incorrect responses made on congruent trials, when the rat's response did not follow either the VCD or RD strategies, were scored as 'never-reinforced' errors (Figure 2-1). Never-reinforced errors reflected the rat's exploration of new operant strategies and provided an index of a rat's ability to filter out non-rewarding options³⁹.

2.3.2.7 *Reversal*

Immediately after the Response Discrimination Retrieval test, a 120-trial session of spatial reversal was initiated, wherein the opposite lever became the only rewarding lever; the cue light continued to pseudorandomly alternate during the reversal trials to ensure sufficient cognitive challenge.

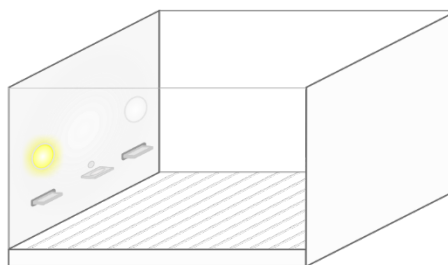


Types of Set-Shifting Trials



Congruent

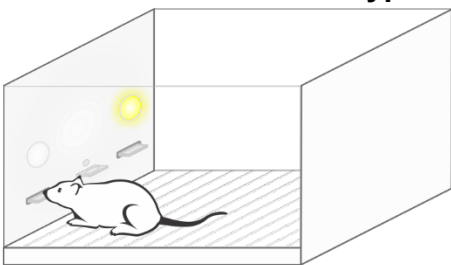
The rat would be rewarded if it responded in accordance with either the no-longer rewarding visual cue strategy or the newly rewarding strategy of pressing the lever on one side only (in this case, the right lever). Hence, *congruent trials are not informative of behavioural strategy*. Half of all trials were congruent.



Incongruent

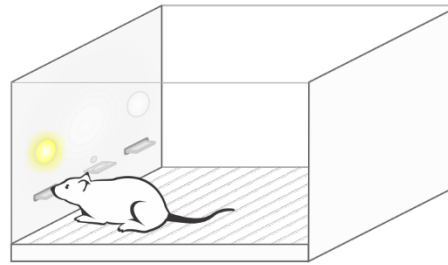
The rat would only be rewarded if it abandoned the no-longer rewarding visual cue strategy and responded in accordance with the newly rewarding strategy of pressing the lever on one side only (in this case, the right lever). Hence, *incongruent trials are informative of behavioural strategy*. Half of all trials were congruent.

Types of Set-Shifting Errors



Never-Reinforced

Reflect exploration of new strategies, and also an index of the rat's ability to filter out non-rewarding options.



Perseverative or Regressive

Perseverative errors reflect a failure to disengage from the old “visual cue” strategy. Regressive errors reflect a failure to engage or maintain the new strategy, “response discrimination”

Figure 2-1: Testing behavioral flexibility in an operant based set-shifting task

During the final day of testing, rats were first exposed to 20 visual cue discrimination (VCD) trials that required them to retrieve the strategy learned the day earlier, i.e., pressing the lever under the randomly illuminated light for a pellet. On the 21st trial, rats were then challenged to shift from the original, no-longer rewarding strategy (VCD) towards a new strategy (lever position; response discrimination). In this shift, errors on

congruent trials were characterized as never-reinforced, while errors on incongruent trials were either perseverative or regressive. Perseverative errors occurred early in the shift, when rats persisted with the old strategy on 75% or more of incongruent trials, failing to disengage from the no-longer rewarding strategy. Regressive errors occurred later in the shift, when rats had already disengaged from the old strategy and followed it on less than 75% of incongruent trials but regressed back to the old strategy, failing to fully engage and/or maintain the new strategy.

2.3.3 *Morris Water Maze*

Following set shifting and recovery of normal body weight, rats were tested in the MWM. In a dimly lit room, a water tank (144 cm diameter) was filled with room temperature water, dyed with black non-toxic acrylic paint, and a target platform (12 cm diameter) was submerged below 3 cm of water. To allow for multiple tolerances of navigational error, the 'target quadrant' and a 7.5 cm vicinity to the platform designated as the 'platform region' were both evaluated in swim path analysis (Figure 2-4A). Rats were placed in a fixed start location and had to locate the hidden platform to be removed from the water tank. The rats were given six 90 s learning trials (with 1 h inter-trial rest intervals) to learn the location of the submerged platform; this learning schedule was adapted from Roof et al⁴¹. Twenty-four hours after the last learning trial, the rats' swim behaviour was again recorded during the probe test, wherein the platform was removed.

In addition to tracking the rat's location over time, swim strategies were analyzed according to swim time in key regions. Swim time in the annulus (Figure 2-4A), a 27cm wide ring corresponding to the location and diameter of the platform region, approximated the use of an egocentric strategy based on distance from the wall, also known as 'chaining'³⁸. Swim time in a subset of the annulus outside of the target quadrant (Figure 2-4A) was also analyzed to determine if egocentric navigation to a platform generalized to the rest of the maze. The thigmotactic region designated a 10 cm proximity to the tank walls; swim time in this region indicated thigmotactic behaviour. The 'goal directed corridor' was a subjective interpretation of the rats' intended swim path, based on video recordings of swim behaviour and heading as judged by a blinded rater. When the corridor was directed at the platform location, the rater scored the amount of time that the rat demonstrated 'allocentric navigation' (Figure 2-4A)³⁸. Working spatial memory is another crucial component of navigation, and can be dissociated by testing trial-dependent learning as in match-sample testing^{35,37}. Three days after the probe test, 5 consecutive days of delayed match-sample testing assessed spatial working memory. Each day, during the 'sample trial', a new start location and a new platform location was used. 6 h later, the rats were tested on these new spatial parameters during the 'match trial' and were assessed for improvement in their latency to locate the platform (schematic location

of platforms can be found in [Figure 4-5B](#)). The 6 h delay was used to create a greater working memory challenge³⁷.

After MWM testing was complete, potentially confounding differences in visual perception or swim speed were evaluated on 4 cued trials (2 different start locations for 2 different platform locations) wherein the location of the platform was visibly marked. All swim paths were tracked using ANYmaze tracking software, version 4.70 (Stoelting Company; Wood Dale, IL), with a top-view webcam (C525, Logitech, Newark, CA). The experimenter was not visible to the rats during testing.

2.3.4 Open Field

The day after MWM testing was complete, rat behaviour in the open field was evaluated. Rats were placed in a square 45 cm open field with 40 cm black walls and a black floor and permitted to explore freely for 20 mins. A top-view webcam was used for behavioural tracking with ANYmaze software, version 4.70. Active time was measured as the sum of time spent on both locomotor and non-locomotor movement. The experimenter was not visible to the rats during testing.

2.3.5 Immunohistochemistry & Image Processing

After all behavioural testing was complete, rats were euthanized with intraperitoneal injection of pentobarbital (Euthanyl, Bimeda MTC Animal Health Inc; Cambridge, ON) and after transcardiac perfusion with 200 ml of 0.01 PBS followed by 200 ml of freshly depolymerized and buffered 4% paraformaldehyde solution (PFA), brain tissue was collected and stored in 4% PFA for 24 h before transfer to 30% sucrose solution (n = 10 for both groups). 30 µm coronal sections were prepared using a cryostat (CryoStar NX50, Thermo Fischer Scientific; Ottawa, ON) and stored in cryoprotectant until all tissue was available for IHC. Standard protocols were followed for DAB-mediated IHC of free floating sections, using an ABC-HRP kit (Thermo Fischer Scientific #32020; Ottawa, ON), a 1:1000 concentration of OX6 primary antibody to identify activated microglia (BD

Pharmingen #554926; Mississauga)⁴², and a 1:2000 concentration of GFAP primary antibody to identify reactive astrocytes (Sigma-Aldrich #G3893; Oakville, ON)⁴³. Stained brain sections were mounted onto slides (VWR #16004-368; Mississauga, ON), air-dried, dehydrated in baths of progressive concentrations of ethanol and Xylene, and cover-slipped with DePex mounting medium (BDH Chemicals; Mississauga, ON).

Stitched micrographs of slides were prepared using a 10x objective lens on an upright microscope (Nikon Eclipse Ni-E, Nikon DS Fi2 colour camera, NIS Elements Imaging; Mississauga, ON); light source intensity, exposure, aperture, and diaphragm parameters were fixed for all imaging. Prior to each scan, white balance was automated using an off-tissue reference point and a focus plane was programmed for the micrograph. Anatomical regions of interest (Figure 2-7A; forceps minor, cingulum, corpus callosum, internal capsule, hippocampus) were captured at coronal sections: Bregma +3.00mm, +2.00mm, +0.00mm, -3.00mm, and -5.50mm⁴⁴. The subset of the corpus callosum, the supraventricular corpus callosum (SVCC), was of particular interest and outlined on the anterior two coronal planes of the corpus callosum, excluding the portion of the corpus callosum that was medial to the lateral ventricles. Micrographs were processed and analyzed using ImageJ, version 1.50b; after regions of interest were outlined using the polygon tool, images were converted to 8-bit, processed using the *subtract background* command, and then thresholded with a fixed grayscale cut-off value of 237. Area coverage (%) was recorded for each region of interest. For anatomical regions that spanned multiple coronal sections (corpus callosum, cingulum, hippocampus), an average area coverage was calculated, weighted by cross-sectional area at each coronal plane.

2.3.6 Data Analyses

Graphpad Prism 7.0 software was used to generate figures and for statistical comparisons of group means; equal variances were not assumed for group comparisons (Welch's t-test), which were corrected for multiplicity using the Holm-Sidak method. Bonferroni correction was used for one-sample t-tests. Where dependent measures were

repeated over time, 2-way repeated measures ANOVA was performed, followed by Sidak's post hoc tests. IBM SPSS, version 23, was used for regression and partial correlation analysis. Group statistics were summarized in figures as means with error bars = SEM; all errors noted in text indicate SEM. Significance was determined with $\alpha = 0.05$. The datasets generated and analysed for the current study are available from the corresponding author on reasonable request.

2.4 Results

2.4.1 *Set Shift & Reversal*

Attentional set shifting, an important component of behavioural flexibility, was tested in an operant conditioning chamber using appetitive conditioning with sucrose pellet reinforcement. Wt and TgAPP21 rats were first food restricted until they respectively lost 13.5 +/- 0.7% and 13.8 +/- 0.3% of ad libitum weight. On the visual cue discrimination task, rats were first trained to press the lever that was associated with a cue light. This cue light would be activated on every trial above one of two levers, alternating sides in pseudorandom fashion (Figure 2-2A). The number of trials needed to achieve a learning criterion of 8 correct consecutive lever presses was not significantly different between groups (Figure 2-2B), indicating no differences in learning. 24 h after the learning criterion was achieved, a 20-trial test was run for retrieval of visual cue discrimination. Again, no group differences were observed on this visual cue retrieval test (Figure 2-2C), suggesting that visual cue memory was unimpaired in the TgAPP21 rats. No group differences in the number of omissions were observed throughout discrimination trials, indicating no group differences in motivation to lever press.

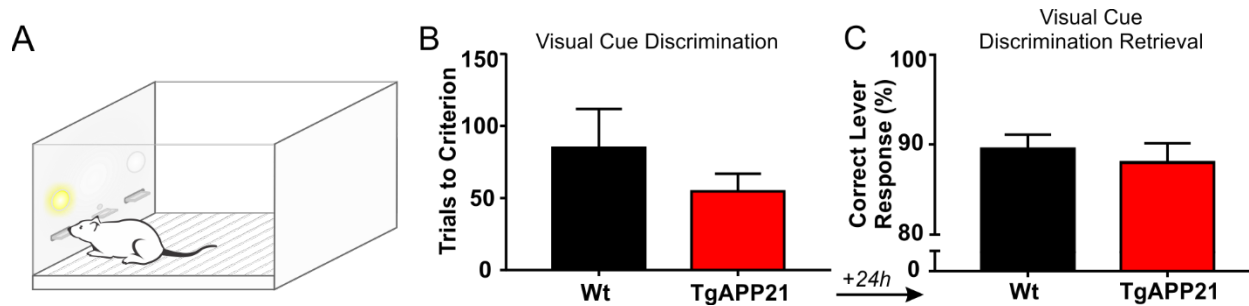


Figure 2-2: TgAPP21 rats demonstrate unimpaired learning and memory of visual cue discrimination

(A) When a rat pressed the lever associated with the cue light, which pseudorandomly alternated sides, they were rewarded with a sucrose pellet.

(B) The number of learning trials needed to achieve a criterion of 8 correct consecutive responses and **(C)** the number of correct lever presses (out of 20 trials) after a 24 h delay were not significantly different between Wt and TgAPP21 rats.

n = 10 for both groups, error bars = SEM.

Immediately after the 20 trials of the visual cue retrieval test, attentional set shifting was evaluated over 120 response discrimination trials wherein sucrose pellet reinforcement was now determined by a spatial strategy. This extradimensional shift challenged rats to ignore the cue light, which continued to pseudorandomly alternate sides, and learn that only one of the levers would yield a food pellet. No group differences were observed in the number of trials needed to achieve the learning criterion of 8 correct consecutive responses during response discrimination (Figure 2-3A). We then evaluated the types of errors committed, which can be categorized as never reinforced, perseverative, or regressive²¹. *Never reinforced errors* occur when a lever press follows neither the previously learned rewarding visual cue strategy (i.e., “follow the light”) nor the new spatial strategy (e.g., “always press the left lever”). Never reinforced errors tend to occur in the early-middle trials of response discrimination and reflect a failure to filter out non-rewarding operant behaviour. *Perseverative errors* occur early during response discrimination, when rats persist in following the no-longer rewarding visual cue strategy. Once rats disengage from the visual cue strategy, that is, when <75% of responses follow the old strategy, subsequent errors following the old strategy are considered *regressive*. TgAPP21 rats demonstrated a nonsignificant trend for fewer perseverative errors, which were negatively correlated with regressive errors ($r = -0.81$, $p = 0.005$, $F(1,8) = 15.11$; no correlation seen in Wt rats). This shift in the error profile of TgAPP21 rats reflected a significant increase in the number regressive errors (Figure 2-3B; $p = 0.046$, $t = 2.256$, $df = 10.9$). Furthermore, TgAPP21 rats committed significantly more errors even after achieving the response discrimination learning criterion of 8 correct consecutive trials (Figure 2-3C; $p = 0.01$, $t = 2.793$, $df = 15.66$). Errors after reaching criterion are uncommon and suggest a very aberrant regressive behavioural phenotype.

To test for retrieval of response discrimination, a retrieval test of 20 trials was run after a 24 h delay; no group differences were observed in the proportion of correct lever presses (Figure 2-3D). Immediately after the response discrimination retrieval test, 120 trials of a spatial reversal task were run, wherein the rewarding lever was now on the side opposite to the previously rewarding lever. As the cue light continued to alternate pseudorandomly during this task, profiling the errors types was not possible. However, TgAPP21 rats performed significantly more total errors on this task (Figure 2-3E; $p = 0.02$, $t = 2.538$, df

= 15.25). No group differences in the number of omissions were observed throughout response discrimination and reversal trials, indicating no group differences in motivation to lever press.

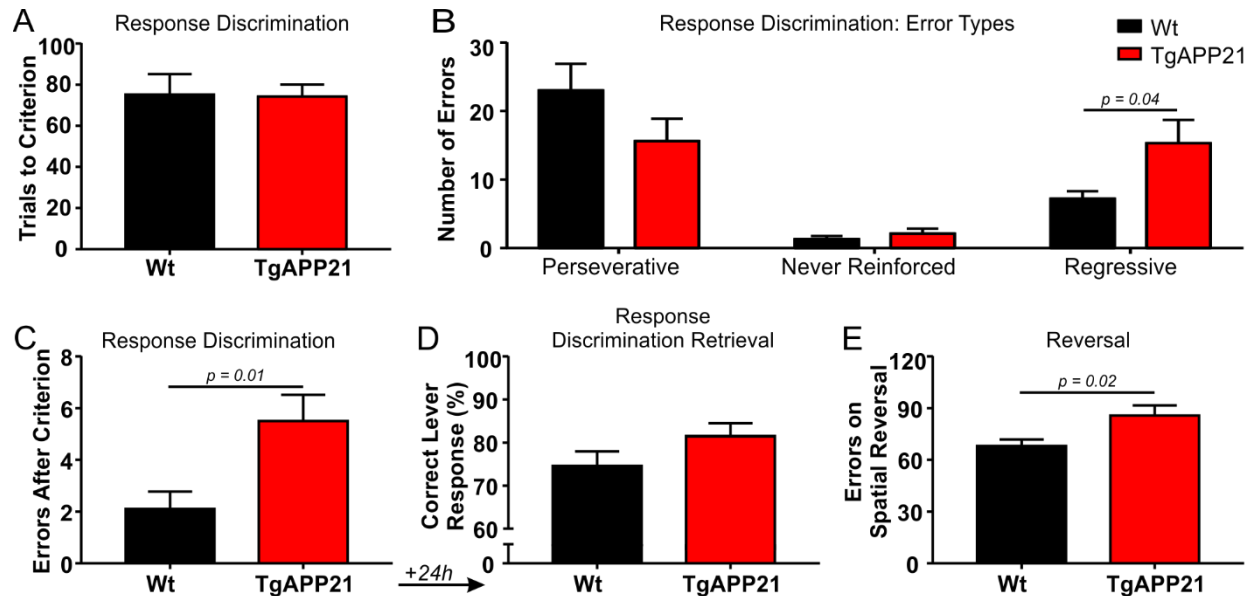


Figure 2-3: TgAPP21 rats demonstrate increased regressive behaviour during extradimensional set shifting and impaired spatial reversal

Immediately after visual cue retrieval, rats were challenged to ignore the cue light, which continued to pseudorandomly alternate sides, and learn that only one of the levers would always yield a food pellet.

(A) The number of trials required to achieve 8 correct consecutive responses under the new spatial strategy was not different between Wt and TgAPP21 rats.

(B) However, the types of errors committed over the 120 trials allotted for the set shift differed. Never reinforced errors were committed when a rat's response was not in accordance with the visual cue strategy or the new correct spatial strategy and reflect a failure to filter out non-rewarding operant behaviour. Perseverative errors were committed when a rat continued to follow the no-longer rewarding visual cue strategy. Once a rat had begun to disengage from the visual cue strategy (<75% of responses following the old strategy), subsequent responses following the visual cue strategy were considered regressive errors; TgAPP21 rats committed significantly more regressive errors.

(C) This paralleled a significant increase in the subset of regressive errors that were committed after criterion for response discrimination was met (8 correct consecutive responses), further suggesting a highly regressive behavioural phenotype.

(D) After a 24 h delay, there was no difference in the retrieval of response discrimination, as inferred by the correct number of responses out of 20 trials.

(E) When the rewarding strategy was again changed, so that only the opposite lever would now yield a sucrose pellet on all trials (reversal), TgAPP21 rats committed more errors.

n = 10 for both groups, error bars = SEM.

2.4.2 Morris Water Maze

To test for spatial learning capacity, rats were trained on a modified MWM protocol⁴¹. Six 90 s learning trials with 1 h intervals allowed both Wt and TgAPP21 rats to learn the location of the submerged platform (Figure 2-4B). No differences in MWM learning efficiency was observed; navigational strategies were similar except TgAPP21 demonstrated a greater reliance on egocentric navigation during trials 4-6 (Figure 2-5D; $p = 0.049$, $F(1,18) = 4.421$).

The probe test identified clearer distinctions in navigational behaviour. 24 h after the last learning trial, the platform was removed, and the rats' memory of the platform location during a 90 s probe test was inferred by latency to enter the platform region and preference for the target quadrant in which the platform was previously located (Figure 2-4C). No significant differences were observed in the latency to enter the platform region, suggesting that TgAPP21 rats have no spatial memory impairments; 1 outlier Wt rat is not represented in Figure 2-4C (ROUT method, $Q = 0.1\%$), but was still included in all statistical analyses. Both groups showed a significant preference for the target quadrant (Wt: $p = 0.04$, $t = 2.758$, $df = 9$; Tg: $p = 0.01$, $t = 4.27$, $df = 9$; compared to a chance value of 25% of swim time), indicating that both groups formed a true allocentric map of the MWM³⁸. However, when the probe test was parsed into 30 s segments, TgAPP21 rats demonstrated a significantly increased preference for the target quadrant during the last 30 s segment of the probe test (Figure 2-4D; see supplementary online files for representative video recordings; Appendix B). This behaviour was unusual in that a preference for the target quadrant should normally remain level or extinguish over the course of the probe test.

During the probe test, TgAPP21 rats also demonstrated abnormal search strategies that further indicate impairments of behavioural flexibility. No group differences were observed in thigmotaxis during the learning trials (Figure 2-5A), but while Wt rats showed an increase of thigmotaxis during the probe test, TgAPP21 rats did not (Figure 2-4E, Figure 2-5E; $p = 0.004$, $t = 3.597$, $df = 18$). Furthermore, TgAPP21 rats spent significantly more time in both egocentric search for the platform (time spent in the annulus) and allocentric platform-directed swim (Figure 2-4E). Only in the final 30 s segment of the probe test,

TgAPP21 rats normalized the proportion of time in egocentric navigation, though they continued to favour allocentric search for the platform ($p = 0.001$, $t = 3.773$, $df = 54$). The group differences in egocentric and allocentric navigation help characterize the group differences in thigmotactic response; TgAPP21 rats continued to navigate according to the allocentric and egocentric cues associated with the learned platform location, while Wt rats employed a broader search strategy which involved more swim time in the thigmotactic region.

Comparing across behavioural testing paradigms, the TgAPP21 rats' impairment on spatial reversal (Figure 2-3E) and greater adherence to search strategies favouring the last known platform location despite platform removal (Figure 2-4E) indicate impairments of behavioural flexibility. More specifically, the TgAPP21 rats' regressive behaviour on response discrimination (Figure 2-3BC) and increased target quadrant preference late in the probe test (Figure 2-4D) identifies a primarily regressive inflexibility.

No significant group differences were observed in average swim time improvement on match-sample testing (Figure 2-5F), so working memory is unlikely to have played a role in behavioural differences seen in MWM navigational behaviour. After MWM tests were completed, potentially confounding differences in visual perception or swim speed were evaluated on 4 cued trials wherein the location of the platform was visibly marked. No differences were observed in swim time to the platform, and no differences in swim speed were observed

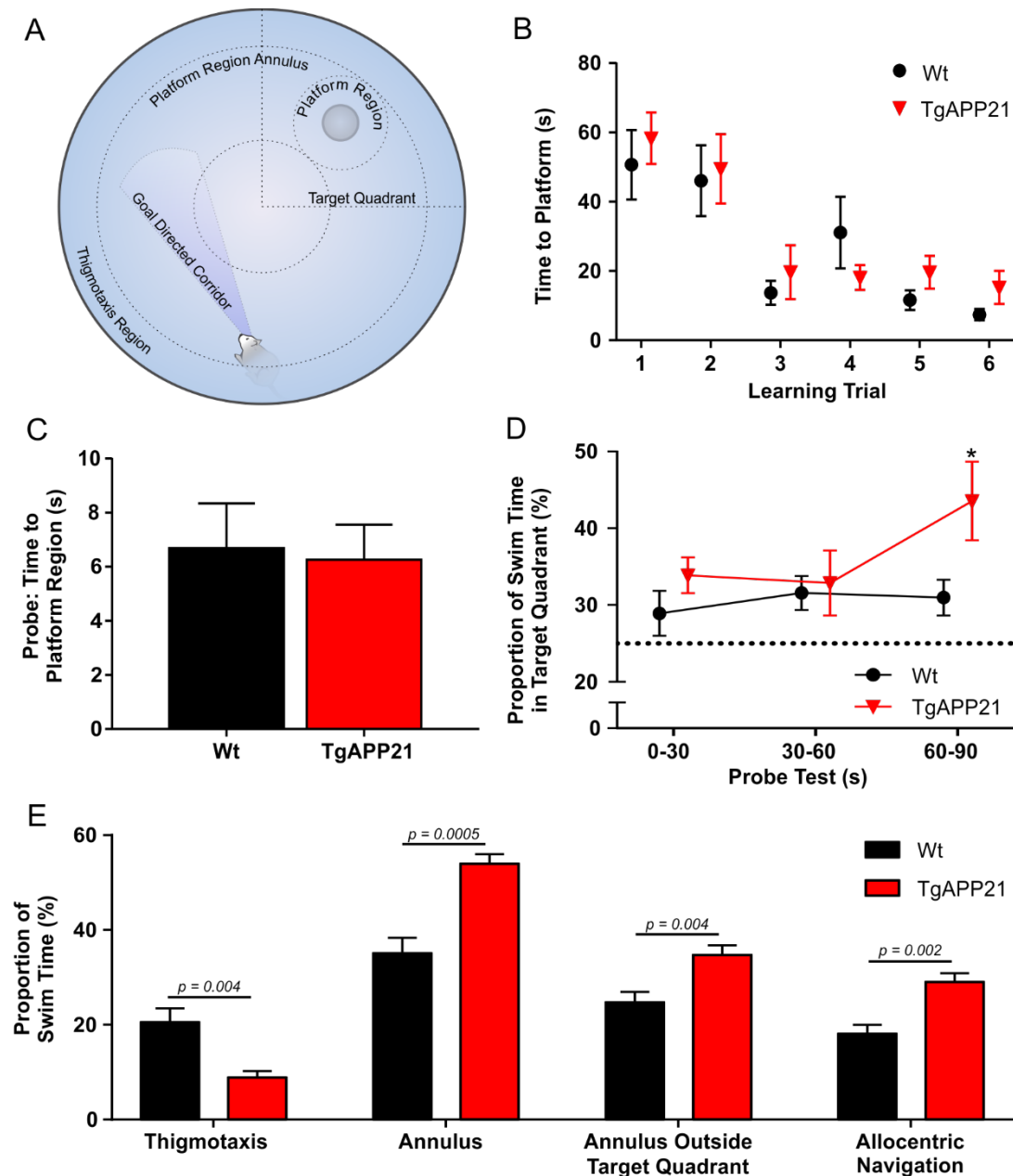


Figure 2-4: TgAPP21 rats demonstrate regressive inflexibility during the Morris Water Maze probe test

(A) Apparatus schematic of start location, region designations, and platform location; the platform (grey) was submerged below 3 cm of water. The schematic is not to scale.

(B) Wt and TgAPP21 showed no significant differences in learning to locate the platform.

(C) During the 24 h delayed probe test, the platform was removed before observation of swim behaviour. Recall of the learned platform location, as inferred by latency to enter the platform region, was not significantly different between Wt and TgAPP21 rats.

(D) TgAPP21 rats spent more swim time in the target quadrant during the last 30 s segment of the probe test. * The TgAPP21 rats' increased preference in this final segment of the test was significant in comparison to the first two segments ($p < 0.02$) and in comparison with the Wt rats ($p = 0.03$). The dotted horizontal line indicates the time in the target quadrant that would be expected by chance.

(E) TgAPP21 rats demonstrated atypical swim strategies following the removal of the platform during the delayed probe test: TgAPP21 rats did not increase swim time in the thigmotaxis region; TgAPP21 rats spent more time in egocentric navigation to the platform region, as demonstrated by the greater preference for both the annulus and the annulus outside of the target quadrant; TgAPP21 rats spent more time in allocentric navigation to the learned platform location.

The increased preference for the target quadrant (D) and swim strategies favouring the platform's last known location (E) indicate a regressive inflexibility in the TgAPP21 rats.

n = 10 for both groups, error bars = SEM.

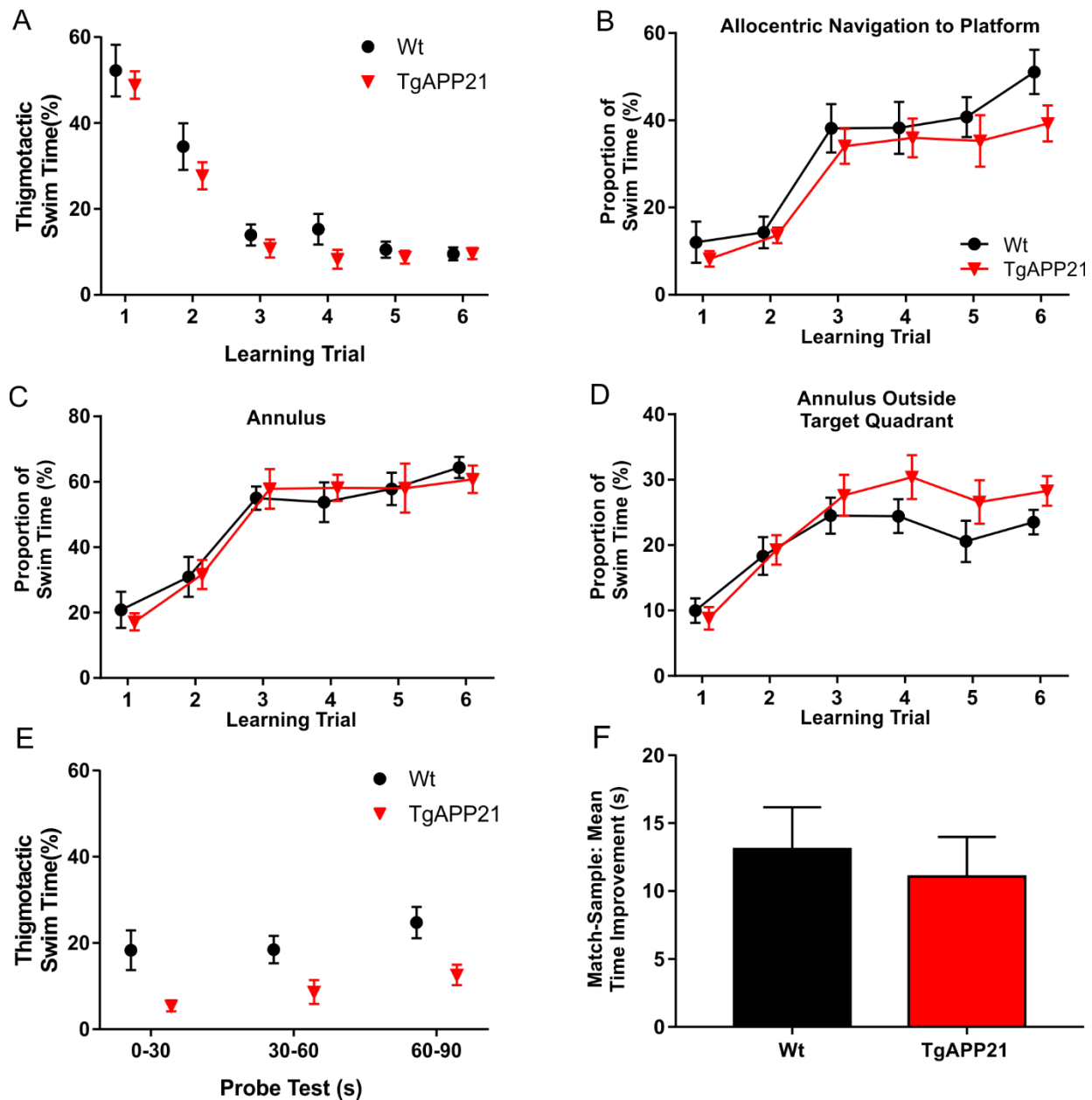


Figure 2-5: Supplementary MWM behavioural analysis

(A) During MWM learning trials, repeat exposure had a significant effect on thigmotactic behaviour, progressively reducing thigmotaxis in both groups ($p < .0001$, $F(5,90) = 56.73$). Wt and TgAPP21 showed no significant differences in (B) allocentric navigation or (C-D) egocentric navigation during learning. However, TgAPP21 rats did tend to spend more time in the annulus outside of the target quadrant; while this trend was not statistically significant across all learning trials ($p = 0.053$), it was significant when only trials 4 – 6 were analyzed ($p = 0.049$, $F(3,36) = 4.421$). This suggests that TgAPP21 have an increased reliance on egocentric spatial navigation as this measure captures a search strategy that relies on swimming a fixed distance from the maze wall, even when outside of the target quadrant.

(E) Thigmotaxis over the full 90 s of the probe test was significantly affected by genotype ($p = 0.002$, $F(1,18) = 12.8$). Over the course of the probe test, all rats demonstrated increasing thigmotaxis ($p = 0.04$, $F(2,36) = 3.63$).

(F) On delayed match-sample testing for working memory, no group differences were observed.

$n = 10$ for both groups, error bars = SEM.

2.4.3 Open Field

Potentially confounding behavioural variables such as exploratory behaviour and anxiety were evaluated in the open field. The day after MWM testing was complete, rat behaviour in the open field was evaluated; the first 5 min of the 20 min test are considered to be relatively more anxiogenic for the rats. TgAPP21 demonstrated reduced exploration in the open field with significantly less travel distance over the full 20 min duration of the test ($p < 0.0001$, $t = 6.981$, $df = 36$), and reduced active time during both the first 5 min ($p = 0.003$, $t = 3.421$, $df = 36$) and full 20 min duration of the test ($p = .002$, $t = 3.691$, $df = 36$; [Figure 2-6AB](#)). A generalized reduction in exploratory behaviour may be a relevant factor in the TgAPP21 rats' MWM target quadrant preference during the probe test, but distance travelled in the target quadrant during the MWM probe had no correlation with distance travelled in the open field. Moreover, reduced exploration would not explain the increased goal-oriented return to the target quadrant and no rat was immobile at any time in MWM testing.

Group differences in anxiety are unlikely to have affected operant conditioning chamber or MWM behaviour, as no differences in anxiety were observed in the open field ([Figure 2-6C](#)). TgAPP21 rats showed a nonsignificant trend ($p = 0.06$) for reduced time in the open field centre during the full 20 min test period; this is more likely to be due to the TgAPP21 rats' reduced locomotion than an increased level of anxiety, as time in the centre of the field correlated with total distance travelled ($r = 0.69$, $p = 0.0008$; $F(1,18) = 16.26$). The absence of group differences in open field centre avoidance disputes the possibility that Wt rats exhibited more thigmotaxis during the MWM probe ([Figure 2-4E](#)) test suggesting increased levels of anxiety; time spent in the centre of the open field did not correlate with thigmotactic swim time.

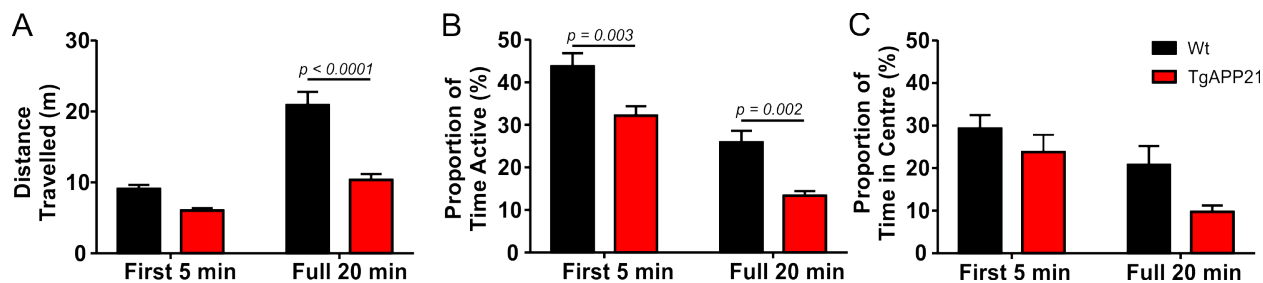


Figure 2-6: TgAPP21 rats exhibited less exploratory behaviour in the open field

(A) TgAPP21 rats demonstrated reduced locomotion over the full 20 min test and (B) reduced active time during both the first 5 min and the full 20 min test, indicating reduced exploratory behaviour.

(C) The relatively exposed centre of the open field is considered to be anxiogenic, particularly during initial exploration of the open field. No significant group differences were observed for the avoidance of the centre, suggesting no differences of anxiety in response to novel environments.

n = 10 for both groups, error bars = SEM.

2.4.4 Activated Microglia in White Matter

Qualitative observations of increased concentrations of activated OX6-positive microglia⁴² informed which anatomical regions of interest to analyze quantitatively (Figure 2-7AB): the forceps minor, corpus callosum, cingulum, internal capsule, and hippocampus. A subset of the corpus callosum, the supraventricular corpus callosum (SVCC; immediately superior and anterior to the lateral ventricles) was also analyzed separately, as it was observed to have particularly increased concentrations of OX6-positive microglia in TgAPP21 rats. Interestingly, this same region has also been found to have some of the greatest age-dependent dysregulation of membrane lipids²¹.

Significantly more area coverage by OX6-positive microglia was observed in the white matter tracts of TgAPP21 rats (Figure 2-7D): corpus callosum, SVCC, cingulum, and internal capsule. Nonsignificant trends for increased OX6-positive microglia area coverage was also observed for the forceps minor ($p = 0.08$, $t = 2.26$, $df = 18$) and hippocampus ($p = 0.08$, $t = 2.025$, $df = 18$). Within individual brains, increased microglia activation was highly correlated across anatomical regions, even when controlling for genotype (Table 2-1). This suggests a pro-inflammatory cue that is diffuse, consistent with broad over-expression of pathogenic hAPP. To avoid collinearity in modelling relationships between white matter microglia activation and behavioural findings, stepwise regression was used to identify the most informative predictors. Only reversal errors in the operant conditioning chamber were found to be significantly related to white matter area coverage by OX6-positive microglia, for which the SVCC was identified as the most informative predictor (Figure 2-7C; $R^2 = 0.42$, $p = 0.002$, $F(1,18) = 12.794$). Independently, both genotype and SVCC microglia activation were significant predictors of reversal errors ($\beta = 0.513$, $p = 0.02$, $t = 2.538$, $df = 18$; ; $\beta = 0.645$, $p = 0.002$, $t = 3.577$, $df = 18$). When genotype and SVCC microglia activation were both included in a linear regression model, SVCC microglia activation was still a significant predictor of reversal errors ($\beta = 0.544$, $p = 0.04$, $t = 2.212$, $df = 17$) while genotype was not, suggesting that the relationship between genotype and reversal errors was primarily mediated by white matter microglia activation ($p = 0.005$, Sobel statistic = 2.600). No group differences in

morphology or area coverage by reactive GFAP-positive astrocytes⁴³ were observed (Figure 2-7E).

Table 2-1: Global activation of microglia across anatomical regions

	Forceps Minor	Corpus Callosum	SVCC	Cingulum	Internal Capsule	Hippocampus
Forceps Minor	-	0.62 0.005	0.55 0.014	0.56 0.014	0.61 0.005	0.47 0.044
Corpus Callosum		-	0.95 <0.0001	0.85 <0.0001	0.73 <0.0001	0.56 0.013
SVCC			-	0.78 <0.0001	0.63 0.004	0.48 0.0383
Cingulum				-	0.70 0.001	0.70 0.001
Internal Capsule					-	0.61 0.006
Hippocampus						-

Strong positive partial correlations indicate that microglia activation increased globally within individual rats' brains; values shown indicate Pearson's r and corresponding p values for correlations of OX6+ microglia activation (% Area) between anatomical regions of interest. These correlations were controlled for genotype, so increases in microglia activation were seen globally for both Wt and TgAPP21 rats. n = 20. SVCC = Supraventricular Corpus Callosum

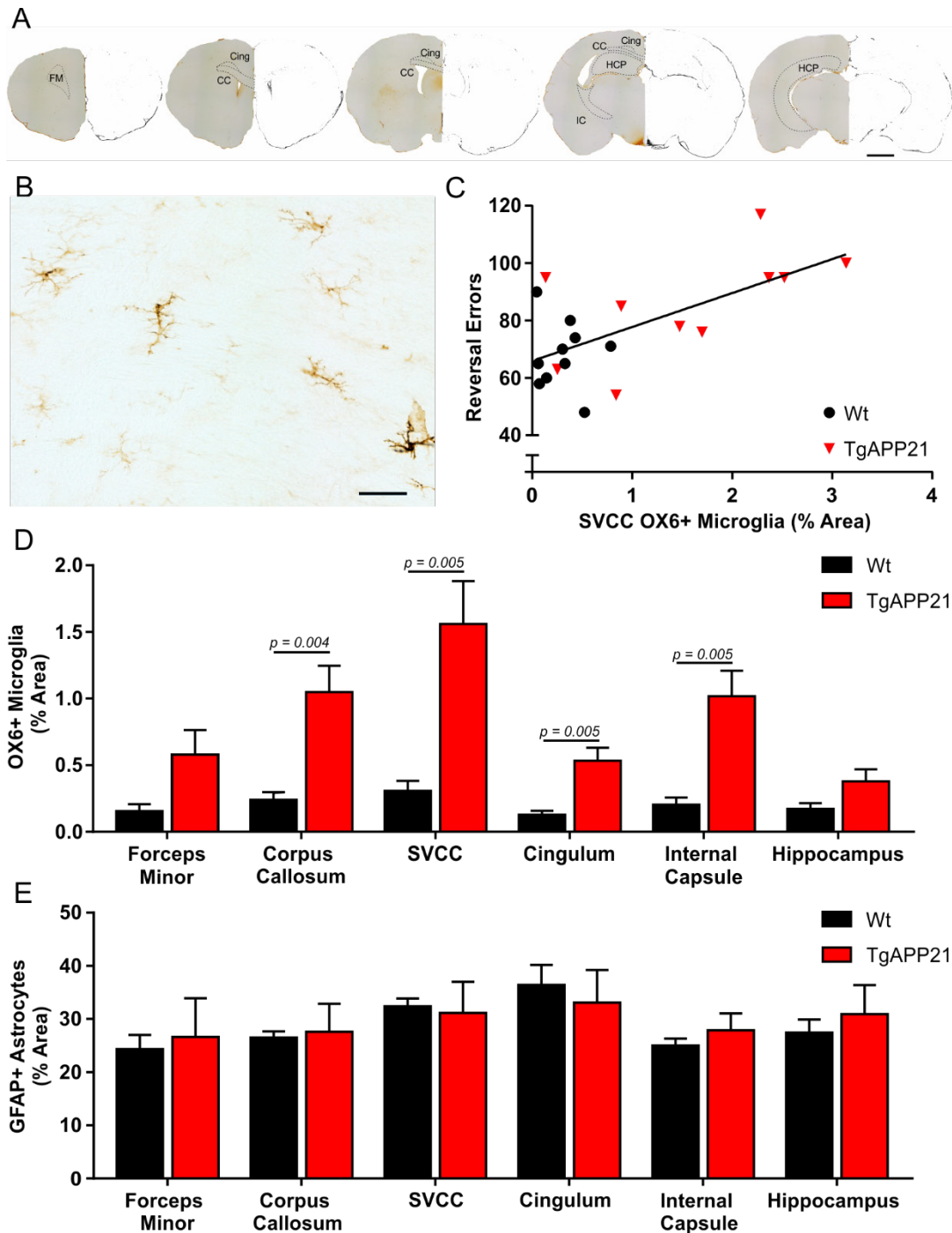


Figure 2-7: Increased microglia activation in TgAPP21 white matter correlates with reversal impairments

(A) Representative coronal sections developed with DAB-immunohistochemistry and an OX6 primary antibody, with anatomical regions of interest outlined on the left hemisphere and digitally processed images overlaid on the right hemisphere; FM = forceps minor, CC = corpus callosum, Cing = cingulum, IC = internal capsule, HCP = hippocampus. The

supraventricular corpus callosum (SVCC) was a subsection of the corpus callosum that was directly superior and anterior to the lateral ventricles. Scale bar = 2 mm.

(B) Representative DAB-immunohistochemistry image of corpus callosum tissue with 1.3% area coverage by OX6-positive microglia. Scale bar = 50 μ m. (C) A significant linear relationship was found between OX6-positive microglia area coverage in the SVCC and the number of spatial reversal errors in the operant conditioning chamber ($R^2 = 0.42$, $p = 0.002$). Microglia activation throughout the brain was highly correlated (Table 2-1) and using stepwise linear regression, OX6+ microglia area coverage in the SVCC was identified as the most informative predictor of reversal errors.

(D) Microglia activation was significantly increased in the white matter tracts of TgAPP21 rats; cross-sectional area coverage by OX6+ microglia was increased in the corpus callosum, SVCC, cingulum, and internal capsule.

(E) No group differences were observed for cross-sectional area occupied by GFAP-positive astrocytes.

$n = 10$ for both groups, error bars = SEM.

2.5 Discussion

Our findings replicate the absence of learning and memory deficits in naïve TgAPP21 rats but capture a spontaneous increase of regressive behavioural inflexibility, reversal impairments, a reduction of exploratory locomotor behaviour. Although TgAPP21 rats do not develop amyloid plaques¹⁶⁻²⁰, we have found a spontaneous increase of white matter activation of microglia. Microglia activation in the supraventricular corpus callosum was also a significant mediator of reversal impairment, even when accounting for genotype. The globally increased activation of white matter microglia suggests that TgAPP21 rats spontaneously develop an inflammatory response to the widespread overexpression of pathogenic hAPP, which may have precipitated the cognitive impairments and amyloidopathy seen in previous studies when TgAPP21 rats were exposed to cerebral stressors¹⁸⁻²⁰. The initiation of pathology at the axon is consistent with previous findings of neurofibrillary tangles appearing spontaneously in 18 – 19-month-old TgAPP21 rats¹⁷. Microglia activation in the white matter of TgAPP21 is also consistent with clinical studies that have found increased white matter pathology in early stages of AD^{30,31}, which likely involves inflammatory processes^{23,29,31,32}.

The TgAPP21 rats' increased reversion to the learned target quadrant during the final third of the MWM probe test paralleled our observations of regressive behaviour during response discrimination. To our knowledge, this behaviour in the MWM probe test has not been previously reported, perhaps because of previous recommendations to perform probe tests for only 30 – 60 s to avoid extinction^{34,45}. One possible interpretation is informed by our finding that TgAPP21 rats exhibited reduced exploration in the open field, so it is possible that TgAPP21 rats were less motivated to explore the water maze during the probe test. However, TgAPP21 rats were never immobile during the probe test and a reduced exploratory drive would not explain the increased goal-oriented return to the target quadrant during the last third of the probe test. Another interpretation is that TgAPP21 rats had a more accurate spatial recall of the platform location. This is unlikely as there were no group differences in the time required to swim to the platform region and both groups demonstrated a significant preference for the target quadrant. Moreover, this would not account for the TgAPP21 rats' significantly increased preference for the target

quadrant in only the *last third* of the probe test. It is the timing of the TgAPP21 rats' preference for the target quadrant that is particularly indicative of a regressive behavioural inflexibility, whereas a persistently greater preference could be expected with perseverative behavioural inflexibility. The increase in thigmotaxis in Wt rats was more likely a consequence of a swim strategy that involved more 'random search' and 'scanning', as evidenced by reduced 'direct swim' and 'chaining' patterns of swim. Random search and scanning patterns of swim result in more crossing into the thigmotactic region, but are still generally successful strategies for finding new platform locations⁴⁶. In contrast, TgAPP21 demonstrated less navigational flexibility following the removal of the platform. Our MWM probe results highlight how behavioural inflexibility in rodents could lead to misinterpretation of increased target quadrant preference as an indication of better memory. Tests for behavioural flexibility can inform performance on memory tests³⁸, and our findings reaffirm the need to develop a better understanding of how executive dysfunction can confound measures of memory.

We demonstrate in this study that the TgAPP21 rat is a highly relevant model as it demonstrates both executive dysfunction and white matter pathology, which have been linked in the early stages of neurodegenerative diseases²²⁻³². While cerebral amyloid deposits are not observed spontaneously in TgAPP21 rats across their lifespan¹⁸, we have shown that TgAPP21 rats have increased microglia activation in white matter and impairments of behavioural flexibility by the age of 7 – 8 months. Therefore, the TgAPP21 rat is useful to the study of these early disease processes that precede the canonical features of AD.

2.6 References

1. Chen P, Ratcliff G, Belle SH, Cauley JA, DeKosky ST, Ganguli M. Cognitive tests that best discriminate between presymptomatic AD and those who remain nondemented. *Neurology*. 2000;55(12):1847-1853.
2. Saunders NL, Summers MJ. Longitudinal deficits to attention, executive, and working memory in subtypes of mild cognitive impairment. *Neuropsychology*. 2011;25(2):237-248.
3. Johns EK, Phillips NA, Belleville S, et al. The profile of executive functioning in amnesic mild cognitive impairment: disproportionate deficits in inhibitory control. *J Int Neuropsychol Soc*. 2012;18(3):541-555.
4. Summers MJ, Saunders NL. Neuropsychological measures predict decline to Alzheimer's dementia from mild cognitive impairment. *Neuropsychology*. 2012;26(4):498-508.
5. Clement F, Gauthier S, Belleville S. Executive functions in mild cognitive impairment: emergence and breakdown of neural plasticity. *Cortex*. 2013;49(5):1268-1279.
6. Kirova AM, Bays RB, Lagalwar S. Working memory and executive function decline across normal aging, mild cognitive impairment, and Alzheimer's disease. *Biomed Res Int*. 2015;2015:748212.
7. Cloutier S, Chertkow H, Kergoat MJ, Gauthier S, Belleville S. Patterns of Cognitive Decline Prior to Dementia in Persons with Mild Cognitive Impairment. *J Alzheimers Dis*. 2015;47(4):901-913.
8. Fabrigoule C, Rouch I, Taberly A, et al. Cognitive process in preclinical phase of dementia. *Brain*. 1998;121 (Pt 1)(1):135-141.
9. Baudic S, Barba GD, Thibaudet MC, Smagghe A, Remy P, Traykov L. Executive function deficits in early Alzheimer's disease and their relations with episodic memory. *Arch Clin Neuropsychol*. 2006;21(1):15-21.
10. Grober E, Hall CB, Lipton RB, Zonderman AB, Resnick SM, Kawas C. Memory impairment, executive dysfunction, and intellectual decline in preclinical Alzheimer's disease. *J Int Neuropsychol Soc*. 2008;14(2):266-278.
11. Belleville S, Fouquet C, Duchesne S, Collins DL, Hudon C. Detecting early preclinical alzheimer's disease via cognition, neuropsychiatry, and neuroimaging: Qualitative review and recommendations for testing. Vol 422014:S375-S382.
12. Teuber A, Sundermann B, Kugel H, et al. MR imaging of the brain in large cohort studies: feasibility report of the population- and patient-based BiDirect study. *Eur Radiol*. 2017;27(1):231-238.
13. Do Carmo S, Cuello AC. Modeling Alzheimer's disease in transgenic rats. *Mol Neurodegener*. 2013;8(1):37.
14. Webster SJ, Bachstetter AD, Nelson PT, Schmitt FA, Van Eldik LJ. Using mice to model Alzheimer's dementia: an overview of the clinical disease and the preclinical behavioral changes in 10 mouse models. *Front Genet*. 2014;5(APR):88.
15. Bizon JL, Foster TC, Alexander GE, Glisky EL. Characterizing cognitive aging of working memory and executive function in animal models. *Front Aging Neurosci*. 2012;4:19.

16. Agca C, Fritz JJ, Walker LC, et al. Development of transgenic rats producing human beta-amyloid precursor protein as a model for Alzheimer's disease: transgene and endogenous APP genes are regulated tissue-specifically. *BMC Neurosci.* 2008;9:28.
17. Agca C, Klakotskaia D, Schachtman TR, Chan AW, Lah JJ, Agca Y. Presenilin 1 transgene addition to amyloid precursor protein overexpressing transgenic rats increases amyloid beta 42 levels and results in loss of memory retention. *BMC Neurosci.* 2016;17(1):46.
18. Rosen RF, Fritz JJ, Dooyema J, et al. Exogenous seeding of cerebral beta-amyloid deposition in betaAPP-transgenic rats. *J Neurochem.* 2012;120(5):660-666.
19. Silverberg GD, Miller MC, Pascale CL, et al. Kaolin-induced chronic hydrocephalus accelerates amyloid deposition and vascular disease in transgenic rats expressing high levels of human APP. *Fluids Barriers CNS.* 2015;12(1):2.
20. Levit A, Regis AM, Garabon JR, et al. Behavioural inflexibility in a comorbid rat model of striatal ischemic injury and mutant hAPP overexpression. *Behav Brain Res.* 2017;333(June):267-275.
21. Caughlin S, Maheshwari S, Agca Y, et al. Membrane-lipid homeostasis in a prodromal rat model of Alzheimer's disease: Characteristic profiles in ganglioside distributions during aging detected using MALDI imaging mass spectrometry. *Biochim Biophys Acta.* 2018;1862(6):1327-1338.
22. Buckner RL. Memory and executive function in aging and AD: multiple factors that cause decline and reserve factors that compensate. *Neuron.* 2004;44(1):195-208.
23. Rosenberg GA. Inflammation and white matter damage in vascular cognitive impairment. *Stroke.* 2009;40(3 Suppl):S20-23.
24. Rabin JS, Perea RD, Buckley RF, et al. Global White Matter Diffusion Characteristics Predict Longitudinal Cognitive Change Independently of Amyloid Status in Clinically Normal Older Adults. *Cereb Cortex.* 2018(February):1-12.
25. Chen TF, Chen YF, Cheng TW, Hua MS, Liu HM, Chiu MJ. Executive dysfunction and periventricular diffusion tensor changes in amnesic mild cognitive impairment and early Alzheimer's disease. *Hum Brain Mapp.* 2009;30(11):3826-3836.
26. Grambaite R, Selnes P, Reinvang I, et al. Executive dysfunction in mild cognitive impairment is associated with changes in frontal and cingulate white matter tracts. *J Alzheimers Dis.* 2011;27(2):453-462.
27. Smith EE, Salat DH, Jeng J, et al. Correlations between MRI white matter lesion location and executive function and episodic memory. *Neurology.* 2011;76(17):1492-1499.
28. Prins ND, Scheltens P. White matter hyperintensities, cognitive impairment and dementia: an update. *Nat Rev Neurol.* 2015;11(3):157-165.
29. Wardlaw JM, Valdés Hernández MC, Muñoz-Maniega S, Valdés Hernández MC, Muñoz-Maniega S. What are white matter hyperintensities made of? Relevance to vascular cognitive impairment. *J Am Heart Assoc.* 2015;4(6):1140-1140.
30. Maier-Hein KH, Westin CF, Shenton ME, et al. Widespread white matter degeneration preceding the onset of dementia. *Alzheimers Dement.* 2015;11(5):485-493 e482.

31. Lee S, Viqar F, Zimmerman ME, et al. White matter hyperintensities are a core feature of Alzheimer's disease: Evidence from the dominantly inherited Alzheimer network. *Ann Neurol*. 2016;79(6):929-939.
32. Raj D, Yin Z, Breur M, et al. Increased White Matter Inflammation in Aging- and Alzheimer's Disease Brain. *Front Mol Neurosci*. 2017;10(June):206.
33. Brady AM, Floresco SB. Operant procedures for assessing behavioral flexibility in rats. *J Vis Exp*. 2015(96):e52387.
34. Vorhees CV, Williams MT. Morris water maze: procedures for assessing spatial and related forms of learning and memory. *Nat Protoc*. 2006;1(2):848-858.
35. Kealy J, Diviney M, Kehoe E, et al. The effects of overtraining in the Morris water maze on allocentric and egocentric learning strategies in rats. *Behav Brain Res*. 2008;192(2):259-263.
36. Bizon JL, LaSarge CL, Montgomery KS, McDermott AN, Setlow B, Griffith WH. Spatial reference and working memory across the lifespan of male Fischer 344 rats. *Neurobiol Aging*. 2009;30(4):646-655.
37. Vorhees CV, Williams MT. Assessing spatial learning and memory in rodents. *ILAR J*. 2014;55(2):310-332.
38. Rogers J, Churilov L, Hannan AJ, Renoir T. Search strategy selection in the Morris water maze indicates allocentric map formation during learning that underpins spatial memory formation. *Neurobiol Learn Mem*. 2017;139:37-49.
39. Floresco SB, Block AE, Tse MTL. Inactivation of the medial prefrontal cortex of the rat impairs strategy set-shifting, but not reversal learning, using a novel, automated procedure. *Behav Brain Res*. 2008;190(1):85-96.
40. Desai SJ, Allman BL, Rajakumar N. Combination of behaviorally sub-effective doses of glutamate NMDA and dopamine D1 receptor antagonists impairs executive function. *Behav Brain Res*. 2017;323:24-31.
41. Roof RL, Schielke GP, Ren X, Hall ED. A comparison of long-term functional outcome after 2 middle cerebral artery occlusion models in rats. *Stroke*. 2001;32(11):2648-2657.
42. Wong WT. Microglial aging in the healthy CNS: phenotypes, drivers, and rejuvenation. *Front Cell Neurosci*. 2013;7:22.
43. Sofroniew MV, Vinters HV. Astrocytes: biology and pathology. *Acta Neuropathol*. 2010;119(1):7-35.
44. Paxinos G, Watson C. *The rat brain in stereotaxic coordinates*. 6th ed. Amsterdam ; Boston ;; Academic Press/Elsevier; 2007.
45. Blokland A, Geraerts E, Been M. A detailed analysis of rats' spatial memory in a probe trial of a Morris task. *Behav Brain Res*. 2004;154(1):71-75.
46. Graziano A, Petrosini L, Bartoletti A. Automatic recognition of explorative strategies in the Morris water maze. *J Neurosci Methods*. 2003;130(1):33-44.

Chapter 3: Behavioural Inflexibility and White Matter Inflammation Across the TgAPP21 Lifespan

This chapter expands the experiments described in Chapter 2 to an additional 3 age points, characterizing the temporal relationship between age, pathogenic APP expression, white matter inflammation, and executive function (Objective 1 & 2). Data from the 8-month-old rats in Chapter 2 was included in this study. While delayed matching to sample testing in the MWM was performed in this study, it could not be completed in the oldest cohort and no informative results were observed in the younger cohorts, thus delayed matching to sample test results are not presented in this chapter. The manuscript of this study is under review for publication in the *Journal of Neuroscience*.

3.1 Abstract

Neuroinflammation and behavioural inflexibility are common in late adulthood but far more profound in Alzheimer disease (AD). To investigate the relationship between neuroinflammation, behavioural flexibility, ageing, and AD, male wildtype Fischer 344 and the TgAPP21 rats were aged to 4, 8, 13, and 22 months and evaluated for neuroinflammation and cognitive impairment. TgAPP21 rats overexpress a pathogenic variant of the human amyloid precursor protein (Swedish and Indiana mutations) but do not spontaneously develop overt pathology related to AD. In both genotypes, learning and memory were similarly impaired in older rats. However, at 8 months of age, TgAPP21 rats demonstrated behavioural inflexibility in set shifting, reversal, and the Morris Water Maze, while wildtype rats showed inflexibility at 13 and 22 months of age. This early inflexibility in TgAPP21 rats was accompanied by a precocious increase in activated microglia within the corpus callosum; 8- and 13-month-old TgAPP21 rats had similar levels of microglia activation as 13- and 22-month-old wildtype rats, respectively. However, while neuroinflammation within the white matter continued to progress with age, behavioural inflexibility peaked in 8-month old TgAPP21 rats. These findings suggest that prior to the onset of learning and memory impairments, age-dependent white matter inflammation has an important but dynamic effect on behavioural inflexibility.

3.2 Introduction

Executive functions are necessary for maintaining functional independence¹. Inhibition, working memory, and behavioural flexibility are core subdomains of executive function, but these cognitive subdomains decline with age^{2,3}. This has been linked to disruptions of white matter integrity, which are observed even in “healthy” elderly individuals⁴⁻⁷, as white matter tract integrity is important for executive function^{6,8}. White matter volume also shows a greater age-dependent decline than grey matter volume⁹, emphasizing the importance of white matter changes in ageing. Therefore, developing a better understanding of the processes that affect white matter integrity will be crucial to supporting healthier aging.

Experimental studies have found that white matter microgliosis is associated with disruption of white matter integrity, resulting in cognitive impairments¹⁰⁻¹⁷. Age-associated dysregulation of microglia leads to a pro-inflammatory environment in the brain¹⁸, and this process appears to be particularly pronounced in white matter¹⁹. While this association has been well established, the specific processes that incite dysregulation of microglia remains unclear. Since amyloid pathology is highly prevalent and also progresses with age²⁰, amyloid has been widely considered a common culprit in age-associated microglial dysregulation^{18,21,22}. This may account for the observations of neuroinflammation^{19,23}, white matter disruption^{24,25}, and executive dysfunction²⁶⁻²⁹ in the early stages of Alzheimer disease (AD). To determine the temporal sequence and molecular links between dysregulation of amyloid and microglia, longitudinal preclinical studies are needed.

Previous studies of microglia-mediated disruption of white matter integrity were limited in investigating impairments of executive function, such as behavioural flexibility. Although experimental animal studies have demonstrated a strong association between white matter microgliosis, disruption of white matter integrity, and cognitive impairments, the combined role of age and pathogenic human amyloid precursor protein (hAPP) in white matter microgliosis is not clear. The transgenic APP21 (TgAPP21) rat was developed from the Fischer 344 strain and overexpresses a pathogenic variant of hAPP³⁰. TgAPP21 rats do not spontaneously develop AD-associated pathology but are more vulnerable to

acute cerebral stressors, which can induce amyloid aggregation and a regressive form of behavioural inflexibility³¹⁻³³.

In this study, male wildtype Fischer 344 (Wt) and TgAPP21 rats were aged to 4, 8, 13, and 22 months of age and evaluated for cognitive impairments and white matter microglia activation. As amyloid can trigger the activation of microglia and chronic neuroinflammation localizes to white matter in the aging brain¹⁹, we predicted an earlier increase in the activation of microglia in the white matter of TgAPP21 rats. Accordingly, microglia-mediated disruption of white matter integrity would cause impairments of behavioural flexibility in TgAPP21 rats at a younger age. Indeed, we found a precocious age-dependent increase of microglia activation in the corpus callosum of TgAPP21 rats, and in an operant-conditioning chamber, regressive forms of behavioural inflexibility during set shifting and reversal impairments peaked in TgAPP21 rats at 8 months of age. Regressive target quadrant preference in the MWM also peaked in 8-month-old TgAPP21 rats. These findings suggest that pathogenic hAPP expression can accelerate white matter microgliosis and affect behavioural flexibility, a core component of executive function.

3.3 Methods

3.3.1 Animals

Animal ethics and procedures were approved by the Animal Care Committee at Western University (protocol 2014-016) and are in compliance with Canadian and National Institute of Health Guides for the Care and Use of Laboratory Animals (NIH Publication #80-23). All rats used in this study were housed in facilities maintained by Western University Animal Care and Veterinary Services on a 12:12 hour light/dark cycle alternating at 1AM/PM; behavioural testing was conducted during the rats' dark cycle. Homozygous transgenic Fischer 344-APP21 (TgAPP21) rats were studied to model the effect of increased brain concentrations of amyloid protein. Developed by lentiviral infection of zygotes, TgAPP21 rats overexpress a pathogenic hAPP with Swedish and Indiana mutations and produce high levels of beta-amyloid (both 1-40 and 1-42) but do not spontaneously develop β -amyloid plaques³⁰. hAPP homozygosity was validated using tissue samples from pups.

Male TgAPP21 and wildtype (Wt) Fischer 344 rats were bred and aged to form four different age cohorts (n = 10 – 13 for each genotype at each age cohort; see

Table 3-1 for sample size details). From herein, the four age points will be referred to as 4M, 8M, 13M, and 22M, corresponding to the mean age in months at which the cohorts were euthanized. Ages were well matched between genotypes, with no significant differences in the age at which behavioural testing was initiated or the age at which rats were euthanized and brain tissue was collected (

Table 3-1). Rats that failed training, visual cue discrimination (VCD), or did not achieve at least 75% correct lever presses on VCD retrieval trials would be excluded from all set

shifting analyses, as these rats' motivation to lever press and for food could not be ensured. Additionally, 22M rats that were not resilient to the stress of food restriction and behavioural testing were excluded from subsequent behavioural testing.

Table 3-1: Experimental group characteristics

Cohort	4M		8M		13M		22M	
	Wt	Tg	Wt	Tg	Wt	Tg	Wt	Tg
N	12	12	11	12	13	13	9	10
Age at set shifting	3.2 (0.3)	3.0 (0.3)	6.6 (0.4)	7.0 (0.1)	12.6 (0.3)	12.5 (0.3)	21.3 (0.3)	21.5 (0.2)
Age at perfusion	3.8 (0.3)	3.7 (0.3)	7.4 (0.4)	7.7 (0.1)	13.4 (0.3)	13.3 (0.3)	21.9 (0.8)	22.2 (0.6)
Included in VCD analysis	11	12	11	10	13	13	8	9
Included in RD analysis	11	12	11	10	13	12	8	8
Included in Reversal results	8	11	5	7	10	8	4	6
Included in MWM analysis	12	12	11	12	13	13	5	9
Included in OF analysis	12	12	11	12	13	13	6	10

Values in parenthesis indicate SD.

3.3.2 *Set Shift & Reversal*

The set shifting protocol, which includes side bias determination, is detailed in [2.3.2 Set Shift & Reversal on page 53](#). Briefly, rats were food restricted and maintained at 85-87% of free-feed mass to ensure motivation for 45 mg sucrose pellets (Dustless precision pellets, Bio-Serv; Burlington ON) during behavioural reinforcement in a sound-attenuated operant-conditioning chamber (Med Associates; St. Albans, VT). During all training and testing, each correct lever press was reinforced with a single sucrose pellet (fixed-ratio 1 schedule). Habituation to the operant-conditioning chamber was followed by initial lever-press training; rats were required to lever press on at least 85 of 90 trials of lever presentations, pseudorandomly alternating sides, before progressing to VCD.

Twenty-four h after initial training, rats were given 100 trials to learn the VCD task. In each trial, both levers were extended but only the lever paired with the cue light, which pseudorandomly alternated sides, would yield a sucrose pellet reward when pressed. The passing criterion for visual discrimination was 8 correct consecutive responses, based on methods used by Floresco et al³⁴. Twenty-four h after meeting criterion, a VCD retrieval session of 20 trials was run to evaluate retention. Immediately after the VCD retrieval session, 120 trials of response discrimination (RD) were initiated: only one lever would yield a sucrose pellet on all trials, even though the cue light continued to alternate sides. For each rat, the lever opposite a previously determined side bias was selected to be rewarding during RD (as described previously)³³. This challenged the rats to ignore the previously learned VCD strategy and to acquire a spatial strategy, constituting an extra-dimensional set shift. As described previously³³, RD trials were binned into 16 trials of 8 congruent and 8 incongruent trials. Perseverative errors were scored when rats reverted to the VCD strategy on incongruent trials; once rats demonstrated disengagement from VCD (5 or fewer errors in a block of 8 incongruent trials), subsequent reversions to the VCD strategy on incongruent trials was scored as regressive errors. Incorrect lever presses on congruent trials were scored as never-reinforced errors. The passing criterion for RD was 8 correct consecutive responses. We departed from common approaches to operant-conditioning chamber based set shifting³⁵ in that we allowed rats to complete all 120 trials of RD instead of removing them from the chamber once they achieved criterion.

This allowed us to quantify the number of errors committed after criterion, offering a more complete measure of regressive behaviour. We also conducted a 24 h delayed 20 trial RD retrieval test. This was immediately followed by a 120-trial session of spatial reversal, wherein the opposite lever became the only rewarding lever; the cue light continued to pseudorandomly alternate during the reversal trials to ensure sufficient cognitive challenge.

During all discrimination tests (VCD, RD, reversal), rats were granted a 10 s response period during which the chamber was illuminated. If the correct lever was pressed, the chamber remained illuminated for another 4 s so that rats could retrieve the sucrose pellet reward. This was followed by a dark inter-trial period so that trials lasted a total of 30 s. Cue lights were presented 3 s before lever extension and extinguished upon lever press or the end of the 10 s response period. Omissions (no lever press) were not treated as errors and did not reset a count of correct consecutive lever presses.

In this chapter, rats that failed to achieve a correct lever press rate of at least 75% on the visual cue discrimination (VCD) retrieval test were excluded from all set-shifting results, whereas results in Chapter 2 focused only on rats that could achieve the higher threshold of at least 80%. This parameter was modified to maintain sufficient sample size in the oldest cohort; 5/17 22MO rats achieved only 75%. Similarly, only rats that achieved at least 75% correct lever press on the response discrimination (RD) retrieval trials were evaluated in reversal. Exclusions are detailed in [3.4.1.5 Exclusions & Outliers](#) on page 108 and [Table 3-2](#).

3.3.3 Morris Water Maze

Following set shift & reversal, rats' body weights were restored to ad libitum feed levels (5 – 7 days), before proceeding to MWM testing. In a dimly lit room, a water tank (144 cm diameter) was filled with room temperature water, dyed with black non-toxic acrylic paint, and a target platform (12 cm diameter) was submerged below 3 cm of water. Rats were placed in a fixed start location and had to locate the hidden platform to be removed from the water tank. The rats were given six 90 s learning trials (with 1 h inter-trial rest intervals)

to learn the location of the submerged platform; this learning schedule was adapted from Roof et al³⁶. Twenty-four hours after the last learning trial, the rats' swim behaviour was again recorded during the probe test, wherein the platform was removed. To allow for multiple tolerances of navigational error, the 'target quadrant' and a 7.5 cm vicinity to the platform location designated as the 'platform region' were both evaluated in swim path analysis.

After MWM testing was complete, potentially confounding differences in visual perception or swim speed were evaluated on 4 cued trials (2 different start locations for 2 different platform locations) wherein the location of the platform was visibly marked. All swim paths were tracked using ANYmaze tracking software, version 4.70 (Stoelting Company; Wood Dale, IL), with a top-view webcam (C525, Logitech; Newark, CA). The experimenter was not visible to the rats during testing. Several 22M rats were not fit for MWM testing (failure to restore ad libitum body weight after food restriction for set shifting or failure to swim safely) and were excluded from analysis (4 Wt rats and 1 TgAPP21 rat), leaving a reduced sample size of $n = 5$ Wt and $n = 9$ TgAPP21 rats from the 22M cohort.

3.3.4 Open Field

The day after MWM testing was complete, rat behaviour in the open field was evaluated. Rats were placed in a square 45 cm open field with 40 cm black walls and a black floor and permitted to explore freely for 20 mins. A top-view webcam was used for behavioural tracking with ANYmaze software, version 4.70 (Stoelting Company). Active time was measured as the sum of time spent on both locomotor and non-locomotor movement. The experimenter was not visible to the rats during testing.

3.3.5 Immunohistochemistry & Image Processing

After all behavioural testing was complete, rats were euthanized with intraperitoneal injection of pentobarbital (Euthanyl, Bimeda MTC Animal Health Inc; Cambridge, ON) and after transcardiac perfusion with 200 ml of 0.01 PBS followed by 200 ml of freshly

depolymerized and buffered 4% paraformaldehyde solution (PFA), brain tissue was collected and stored in 4% PFA for 24 h before transfer to 30% sucrose solution ($n = 5$ for all 8 groups). 30 μm coronal sections were prepared using a cryostat (CryoStar NX50, Thermo Fischer Scientific; Ottawa, ON) and stored in cryoprotectant until all tissue was available for IHC. Standard protocols were followed for DAB-mediated IHC of free floating sections, using an ABC-HRP kit (Thermo Fischer Scientific #32020; Ottawa, ON), a 1:1000 concentration of OX6 primary antibody for MHC II to identify activated microglia (BD Biosciences #554926; Mississauga, ON³⁷), and a 1:2000 concentration of GFAP primary antibody to identify reactive astrocytes (Sigma-Aldrich #G3893; Oakville, ON³⁸). Stained brain sections were mounted onto slides (VWR #16004-368; Mississauga, ON), air-dried, dehydrated in baths of progressive concentrations of ethanol and Xylene, and cover-slipped with DePex mounting medium (BDH Chemicals; Mississauga, ON).

Stitched micrographs of slides were prepared using a 10x objective lens on an upright microscope (Nikon Eclipse Ni-E, Nikon DS Fi2 colour camera, NIS Elements Imaging; Mississauga, ON); light source intensity, exposure, aperture, and diaphragm parameters were fixed for all imaging. Prior to each scan, white balance was automated using an off-tissue reference point and a focus plane was programmed for the micrograph. Anatomical regions of interest (forceps minor, cingulum, corpus callosum, internal capsule, hippocampus) were captured at coronal sections: Bregma +3.00, +2.00, +0.00, -3.00, and -5.50 mm³⁹. The subset of the corpus callosum, the supraventricular corpus callosum (SVCC), was of particular interest⁴⁰ and outlined on the anterior two coronal planes of the corpus callosum, excluding the portion of the corpus callosum that was medial to the lateral ventricles. Micrographs were processed and analyzed using ImageJ, version 1.50b; after regions of interest were outlined using the polygon tool, images were converted to 8-bit, processed using the subtract background command, and then thresholded with a fixed grayscale cut-off value of 237. Percentage of area coverage was recorded for each region of interest. For anatomical regions that spanned multiple coronal sections, an average area coverage was calculated, weighted by cross-sectional area at each coronal plane; the corpus callosum and cingulum were analyzed across 3 coronal planes (Bregma +2.00, +0.00, and -3.00 mm) and the hippocampus was analyzed across 2 coronal planes (Bregma -3.00 and -5.50 mm).

3.3.6 *Data Analysis*

Two-way ANOVA were used to test the effects of age and genotype on outcome measures using GraphPad Prism 7.0 software (La Jolla, CA). The conservative Dunnett's post-hoc analysis was used to compare outcome measures across age cohorts within either genotype. When comparing genotype groups at a given age, Sidak's post-hoc analysis was used. Microglia activation in separate brain regions were also analyzed with two-way MANOVA models using IBM SPSS version 23 (Armonk, NY). Partial correlations between outcome measures, controlling for age and genotype, were also calculated in SPSS; outcome measures were evaluated for normality to determine whether Spearman or Pearson correlations were more appropriate. Binary outcome measures such as exclusions and meeting test criteria were analyzed in SPSS using logistic regression with age and genotype as independent variables. Any exclusion of outliers from figures or analyses is noted; statistical outliers on any outcome measures were identified using the robust regression and outlier method (ROUT)⁴¹. All errors bars shown in figures indicate standard error of the mean (SEM); probability values of statistical tests were only reported for significant comparisons.

3.4 Results

3.4.1 Set Shift

3.4.1.1 Visual Cue Discrimination

Learning and memory were analyzed in an operant-conditioning chamber. On VCD, food reward would be given when rats pressed the lever associated with a visual cue, which would pseudorandomly present over the left or the right lever. VCD learning was impaired only in 22M rats ([Figure 3-1A](#)); genotype did not affect VCD performance, but age was a significant factor ($p = 0.0001$, $F(3,79) = 7.9$; 2-Way ANOVA). The age-dependent impairment of VCD learning was significant in TgAPP21 rats, as 22M TgAPP21 rats required significantly more trials to reach VCD criterion than 4M TgAPP21 ($p = 0.002$, $q = 3.454$, $df = 78$), 8M TgAPP21 ($p = 0.003$, $q = 3.371$, $df = 78$), and 13M TgAPP21 rats ($p = 0.0001$, $q = 4.394$, $df = 78$; Dunnett's post-hoc test). A similar trend was observed for 22M Wt rats but was not significant. The exclusion of a single statistical outlier within the 8M Wt group (identified as an outlier using the ROUT method with $Q = 0.5\%$) this did not alter the interpretation of any statistical comparisons.

Similarly, on the 24 h delayed VCD retrieval trials, only 22M rats demonstrated an impairment of memory ([Figure 3-1B](#)). Again, only age was a significant factor ($p < 0.0001$, $F(3,79) = 10.22$; 2-Way ANOVA). The age-dependent impairment on VCD retrieval was significant in both 22M Wt rats (compared to 4M Wt: $p = 0.05$, $q = 2.398$, $df = 79$; and 13M Wt rats: $p = 0.004$, $q = 3.288$, $df = 79$) and in 22M TgAPP21 rats (compared to 4M TgAPP21: $p = 0.0005$, $q = 3.963$, $df = 79$; and 13M TgAPP21 rats: $p = 0.0009$, $q = 3.973$, $df = 79$; Dunnett's post-hoc test). Although this indicates a memory impairment in 22M rats, all rats included in these results were still able to press the correct lever on at least 75% of the 20 trials. The exclusion of rats that failed to meet the 75% criterion ([Table 3-2](#)) did not alter findings of statistical significance in either VCD learning or retrieval, but these rats were still excluded from all set shifting and reversal results as their motivation to lever press was uncertain; exclusion was not associated with age (Wald's $\chi^2(3) = 1.082$; logistic regression). Thus, although 22M rats performed significantly worse on the VCD retrieval trials, they could still access learned memory that enabled VCD.

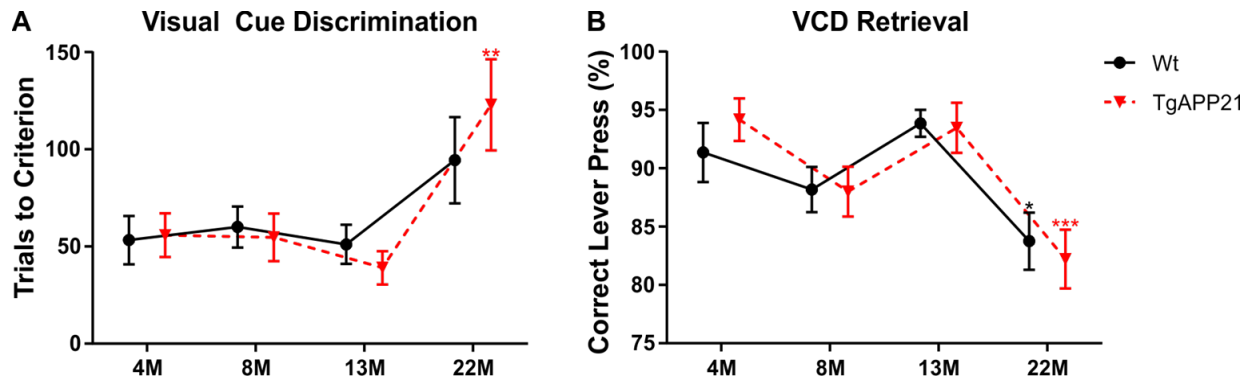


Figure 3-1: Impaired visual cue discrimination learning & memory in aged rats.

(A) Learning performance on VCD was scored by the number of trials needed to reach a criterion of 8 correct consecutive lever presses. Only age had an effect on learning performance ($p = 0.0001$). ** 22M TgAPP21 rats required more trials to criterion than all younger TgAPP21 rats ($p < 0.01$); a similar but non-significant trend was observed for 22M Wt rats.

(B) Memory of VCD was evaluated after a 24 h delay on a 20-trial test, scoring the proportion of correct lever presses. Again, only age had a significant effect on the 24 h delayed retrieval test ($p < 0.0001$). * 22M Wt rats performed worse than the 4M and 13M Wt rats ($p < 0.05$); *** and 22M TgAPP21 rats also performed worse than 4M and 13M TgAPP21 rats ($p < 0.001$). This indicated a memory impairment in 22M rats but not a complete absence of memory for VCD as all rats included in these results pressed the correct lever on at least 75% of the 20 trials.

Rats that did not press the correct lever on at least 75% of VCD retrieval ($n = 4/91$) were excluded from all analyses of set shifting and reversal behaviour. Error bars indicate SEM; $n = 8 - 13$.

3.4.1.2 *Response Discrimination*

Immediately after VCD retrieval, rats were challenged to ignore the visual cue and learn that only one of the levers would yield a food reward on all trials (RD); the rats' ability to demonstrate RD depended on their ability to shift between attentional sets. Wt and TgAPP21 performed similarly in RD, as the number of trials needed to achieve the criterion of 8 correct consecutive responses did not differ between Wt and TgAPP21 rats (Figure 3-2A). However, age was a significant factor in the number of trials to reach criterion ($p = 0.03$, $F(3,77) = 3.096$, 2-Way ANOVA). Unexpectedly, 22M TgAPP21 rats required significantly fewer trials to reach criterion than 4M ($p = 0.04$, $q = 2.534$, $df = 77$) and 13M TgAPP21 rats ($p = 0.02$, $q = 2.690$, $df = 77$; Dunnett's post-hoc test). This was not observed in Wt rats. Age was also the only significant factor in the total number of errors committed over the entire 120-trial RD session (Figure 3-2B; $p = 0.01$, $F(3,77) = 3.782$; 2-Way ANOVA). Again, 22M TgAPP21 rats unexpectedly committed a fewer total amount of errors than 4M ($p = 0.004$, $q = 3.286$, $df = 77$) and 13M TgAPP21 rats ($p = 0.02$, $q = 2.708$, $df = 77$; Dunnett's post-hoc test). The reduced number of trials and errors to RD criterion was attributed to the 22M rats' partially impaired memory for VCD, which therefore presented less interference in engaging the spatially-determined reward strategy.

Despite age-dependent differences in RD performance, no significant differences were observed in performance on the 24 h delayed RD retrieval task (Figure 3-2C). While 22M rats demonstrated partial memory impairments in VCD retrieval, they did not demonstrate any impairment in RD retrieval. This may indicate a dissociable impairment for distinct forms of memory (visual cue association vs spatial association) or may reflect the reduced level of locomotor effort required with a spatially-fixed rewarding lever. A total of 26 rats failed to press the correct lever on at least 75% of RD retrieval trials (Table 3-2). As RD is more challenging than VCD, and the focus of RD testing is on set shifting, these rats were still included in the analyses of RD results and were excluded only from subsequent reversal results & analyses.

Though genotype did not have an overall effect on the number of RD errors committed, genotype did play a role in the types of errors committed. Early in RD, persistence in

following the visual cue constitutes a perseverative error; once a rat has already begun to disengage from VCD, subsequent errors are deemed regressive. Thus, errors committed after criterion, which should indicate complete disengagement from VCD, are a particularly aberrant form of regressive error. Never-reinforced errors occur when rats follow neither the visual nor spatial strategy, indicating a failure to filter out non-rewarding options. Age had no overall effect on the different types of errors committed during response discrimination (Figure 3-3). However, genotype was a significant factor in the number of errors after criterion ($p = 0.05$, $F(3,77) = 4.013$; 2-Way ANOVA; Figure 3-3D). Unexpectedly, the number of regressive errors peaked in 8M TgAPP21 rats and then decreased in older TgAPP21 cohorts (compared to 22M TgAPP21: $p = 0.03$, $q = 2.66$, $df=77$; Dunnett's test). Though the number of regressive errors was not increased in all TgAPP21 age cohorts, the persistently greater number of errors committed after criterion still indicates a generally regressive phenotype in TgAPP21 rats.

The number of perseverative errors and regressive errors were negatively correlated, even when controlling for age and genotype ($p < 0.0001$, Spearman's $\rho = -0.447$, $df = 81$). This suggests that there is a generalizable trade-off between errors committed early and late in RD; a rat that initially appears to shift away from the VCD strategy more quickly (a decrease in perseverative errors) is likely to require more time to fully acquire response discrimination (an increase in regressive errors).

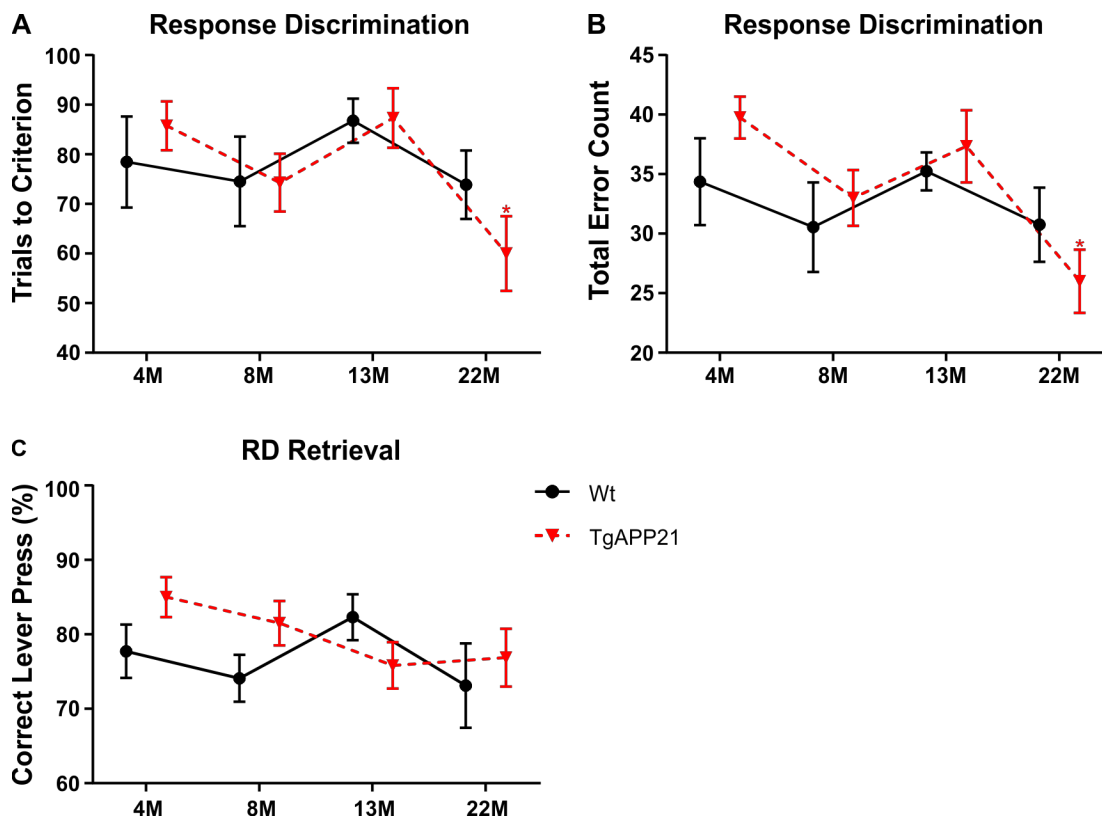


Figure 3-2: Set shifting in aged transgenic rats facilitated by impaired memory of visual cue discrimination.

Rats' set shifting performance during response discrimination was measured by **(A)** the number of trials needed before 8 correct consecutive responses and **(B)** the total number of errors committed across all 120 trials. Age was a significant factor in both the number of trials needed to achieve criterion and the total number of errors ($p < 0.05$). * 22M TgAPP21 rats required fewer trials to achieve criterion than 4M and 13M rats ($p < 0.05$), and * 22M TgAPP21 rats committed fewer errors than 4M and 13M rats ($p < 0.05$).

(C) Neither genotype nor age were significant factors in the number of correct lever presses during the 24 h delayed RD retrieval session.

Error bars indicate SEM; $n = 8 - 13$.

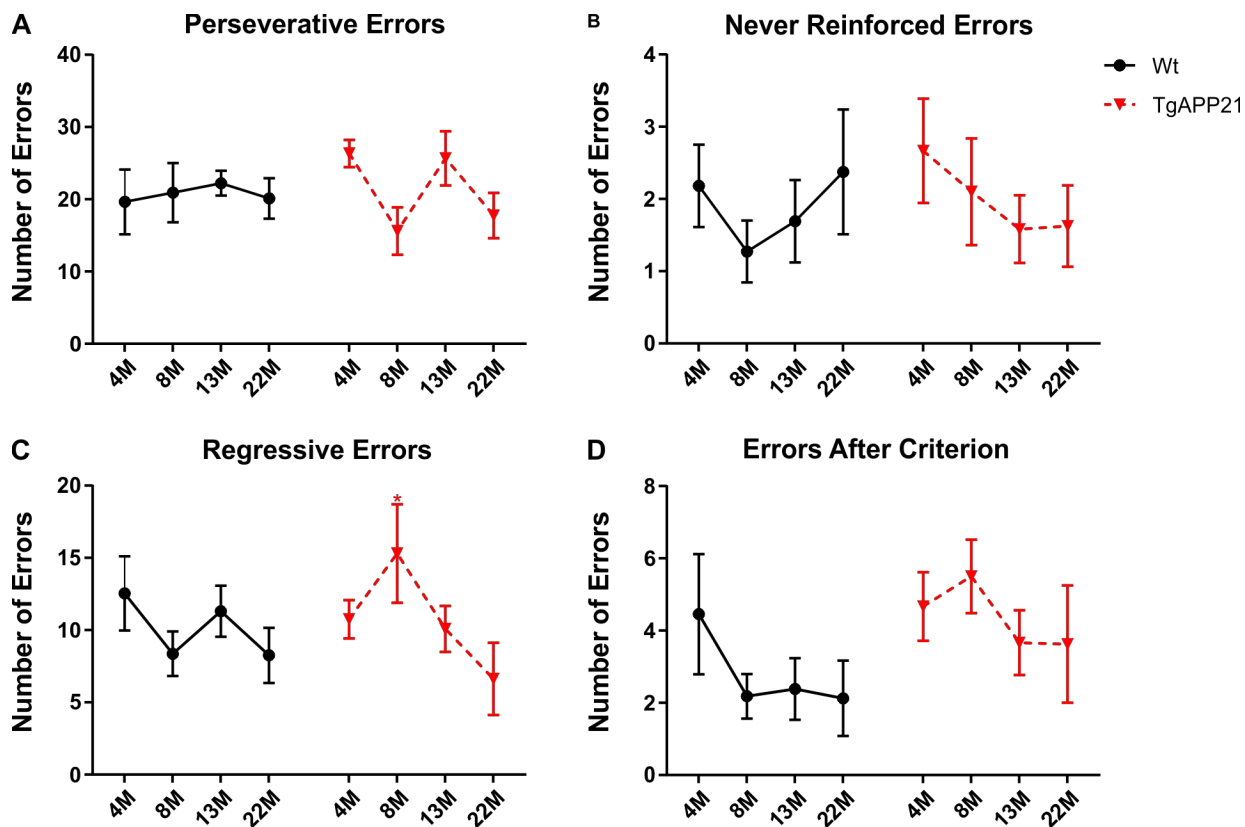


Figure 3-3: Regressive inflexibility in transgenic rats peaked at 8 months of age

Errors made during RD can be categorized as (A) perseverative, (B) never reinforced, or (C) Regressive. * 8M TgAPP21 rats committed more regressive errors than 22M TgAPP21 rats ($p < 0.05$).

(D) Regressive inflexibility is also quantified by the number of errors committed after achieving RD criterion (8 consecutive correct responses). Genotype was a significant factor in the number of errors committed after criterion ($p = 0.05$).

$n = 8 - 13$; error bars = SEM

3.4.1.3 *Reversal*

Neither age nor genotype were had significant overall effect on the number of errors committed during reversal. However, 8M TgAPP21 committed significantly more reversal errors than 4M ($p = 0.02$, $q = 2.729$, $df = 51$) and 22M TgAPP21 rats ($p = 0.05$, $q = 2.432$, $df = 51$; Dunnett's post-hoc test; [Figure 3-4A](#)). In contrast, Wt rats committed more reversal errors with age, demonstrating a significant linear trend ($R^2 = 0.16$, $p = 0.04$, $F(1,23) = 4.599$; post-hoc test for linear trend). Due to the high rate of omission trials during reversal ([Figure 3-5](#)), especially in Wt rats, the error rate on reversal as a proportion of non-omission trials was also evaluated ([Figure 3-4B](#)). This yielded similar results, but with a more robust effect of age in Wt rats ($R^2 = 0.32$, $p = 0.003$) and an error rate significantly increased in 22M Wt compared to 4M Wt rats ($p = 0.03$, $q = 2.477$, $df = 51$; Dunnett's post-hoc test). Only age was a significant predictor for meeting the criterion of 8 correct consecutive lever presses on the reversal task ([Figure 3-4C](#); $p = 0.004$, Wald's $\chi^2_{(3)} = 13.223$; Logistic Regression). Reversal results & analyses included only the rats that pressed the correct lever on at least 75% of RD retrieval trials. The peak reversal impairment in 8M TgAPP21 rats, with a concurrent peak in regressive errors, further suggests that TgAPP21 rats' behavioural inflexibility was greatest at 8 months of age.

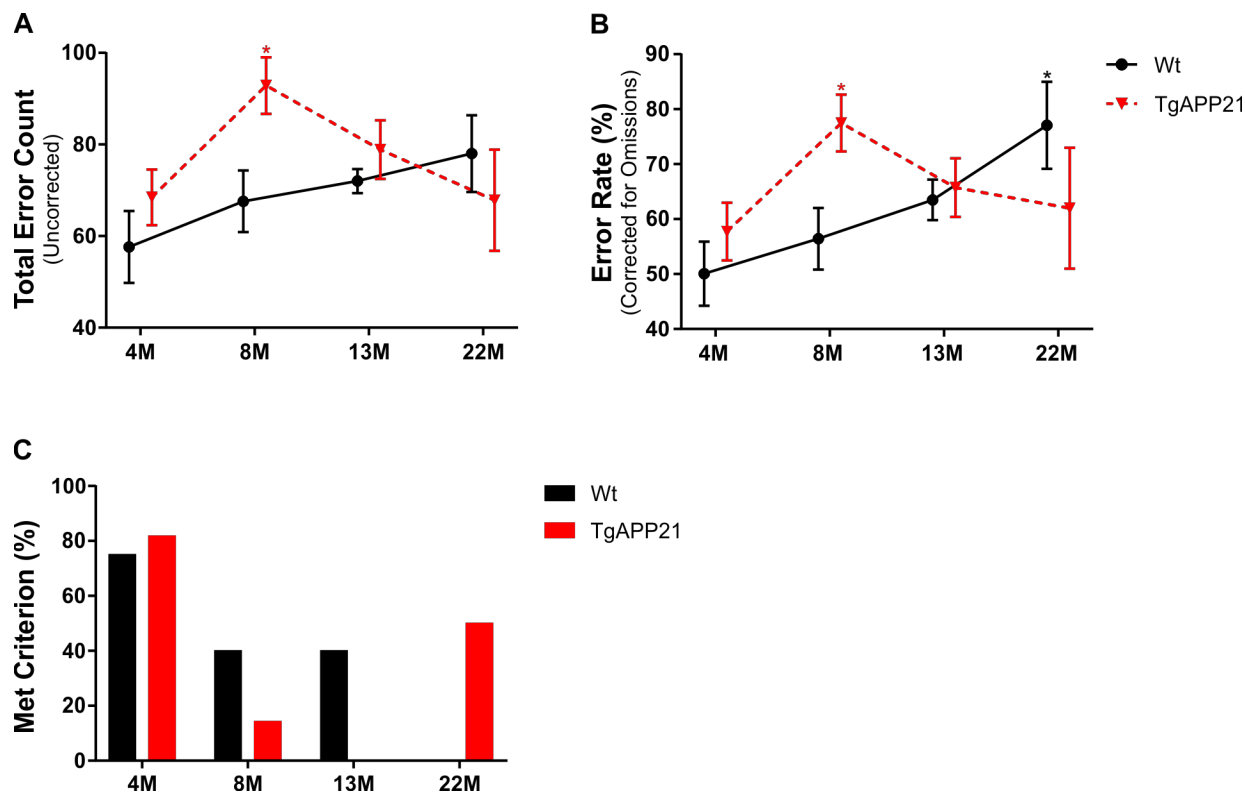


Figure 3-4: Reversal impairment in transgenic rats peaked at 8 months of age, increased with age in wildtype rats

(A) While Wt rats demonstrated a linear trend for a greater number of errors with age ($R^2 = 0.16$, $p = 0.04$), * reversal impairment peaked in 8M TgAPP21 rats, committing significantly more reversal errors than 4M and 22M TgAPP21 rats ($p < 0.05$).

(B) To correct for a high frequency of omission trials, error rates were calculated as the proportion of lever presses that were incorrect, excluding omission trials. With this correction, the age-dependent linear trend for Wt rats became more robust ($R^2 = 0.32$, $p = 0.003$) and * 22M Wt rats showed a significantly greater error rate than 4M Wt rats ($p < 0.05$). * Reversal impairment in TgAPP21 rats still peaked in the 8M group, which had a greater error rate than 4M TgAPP21 rats ($p < 0.05$).

(C) Age, but not genotype, was a significant factor in meeting the reversal criterion of 8 correct consecutive lever presses ($p = 0.008$).

Error bars indicate SEM; $n = 4 - 11$.

3.4.1.4 *Omission Trials*

To verify whether motivation might have played a role in set shifting, especially in aged rats, rates of omission trials were analyzed. When rats did not press either lever on a given trial, the trial was scored as an omission; omission trials can indicate indecision, stress, anxiety, or a lack of motivation to lever press or for food reward. Omissions were more common towards the end of a testing session, such as the combined 140 trials of VCD retrieval followed by RD learning. No groups omitted significantly more trials at any specific stage of set shifting (Figure 3-5). Individual corrections for omissions did not alter any findings of significant differences in VCD nor RD but did reveal a clear age-dependent trend in reversal (Figure 3-4B). Overall, motivation as measured by omission trials did not confound the effects of age nor genotype.

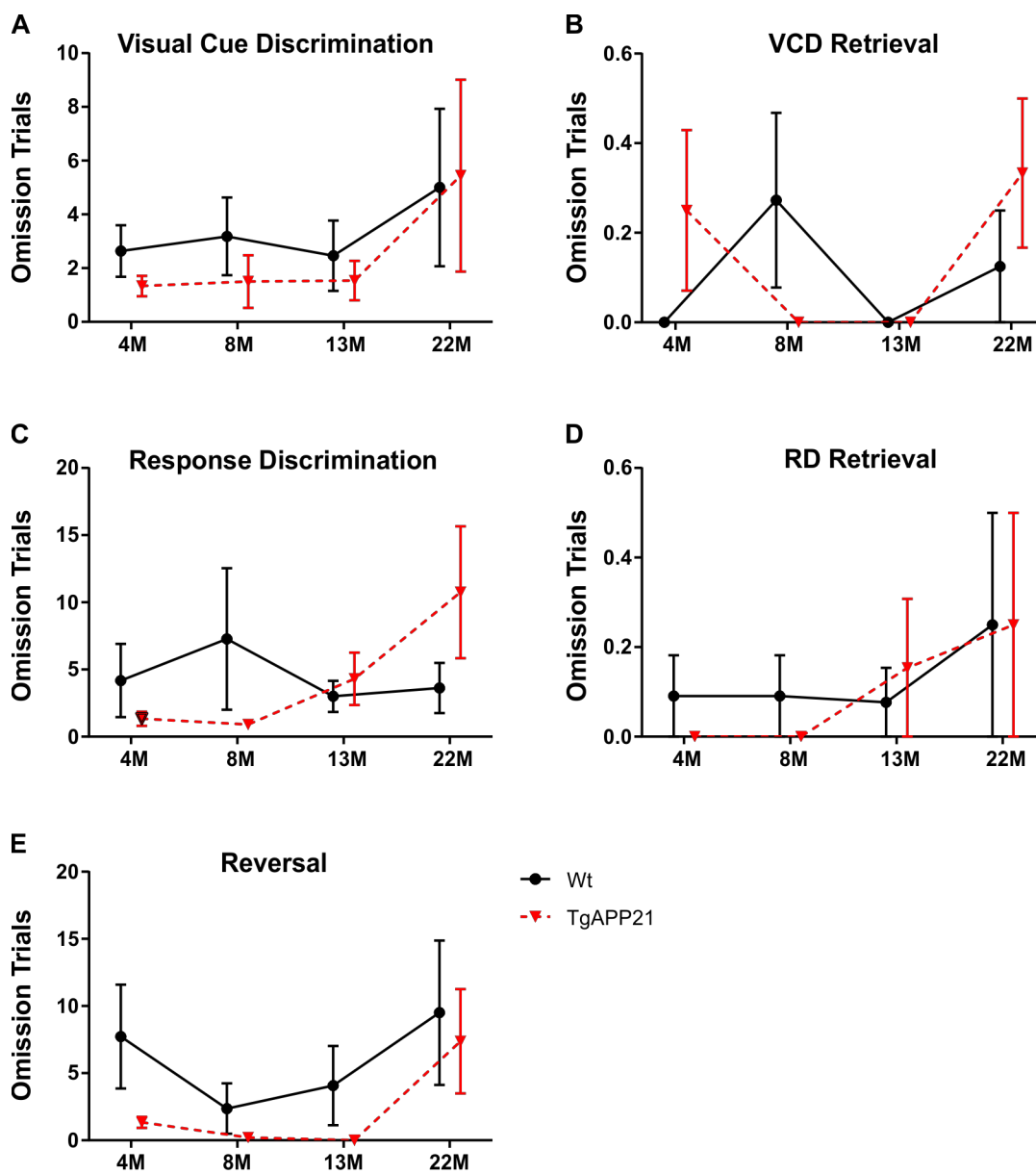


Figure 3-5: Neither genotype nor age affected frequency of omission trials.

When rats did not press either lever on a given trial, the trial was scored as an omission; omission trials can indicate either a lack of motivation, indecision, stress, or anxiety. Neither age nor genotype had a significant effect on the frequency of omission trials.

Error bars indicate SEM; n = 4 – 13.

3.4.1.5 Exclusions & Outliers

As failing any of the set shifting criteria would impact performance on subsequent stages, once a rat was excluded from a given stage, it was also excluded from subsequent stages (Table 3-2). Rats did not advance to VCD learning if they could not complete initial lever press training. All rats that began VCD learning were able to achieve VCD criterion. A single statistical outlier in the 8M Wt group that required 308 trials to criterion on VCD learning (identified as an outlier using the ROUT method with $Q = 0.5\%$) was excluded from analyses of VCD learning only; this did not alter the interpretation of any statistical comparisons but clarified behavioural trends. A single 13M TgAPP21 rat that did not meet RD criterion and 1 22M TgAPP21 rat that was not active during RD (88 omission trials out of 120 RD trials) were excluded from all RD and reversal results & analyses. Twenty-six rats failed to press the correct lever on at least 75% of RD retrieval trials but these were only excluded from reversal results & analyses. The rates of exclusion did not significantly associate with either genotype or any of the age cohorts for any of the set shifting stages or overall.

Table 3-2: Stage of Exclusion from Set Shifting Results

Cohort	4M		8M		13M		22M	
	Wt	Tg	Wt	Tg	Wt	Tg	Wt	Tg
Initial Training				1				
VCD*	1		1	1			1	1
RD Learning						1		1
Reversal (Failed RD Retrieval)	3	1	6	3	3	4	4	2

Once a rat was excluded, it was also excluded in the analyses of subsequent stages.

* Rats that did not press the correct lever on at least 75% of the 20 trials of VCD retrieval, a relatively simple task, were excluded from all set shifting and reversal results & analyses including VCD learning, as these rats' motivation to lever press was uncertain.

Tg = TgAPP21

3.4.2 Morris Water Maze

3.4.2.1 Navigational Learning

Learning performance was measured by the rats' latencies to find the hidden platform across trials 2-6 only, as the first trial reflected the rats' chance discovery of the platform location. Age was the only significant factor in MWM learning (Figure 3-6; $p < 0.0001$, $F(3,79) = 25.162$; 2-Way RM-ANOVA). Compared to 4M rats, both 13M (Wt $p = 0.0003$, $q = 4.103$, $df = 79$; TgAPP21 $p = 0.001$, $q = 3.722$, $df = 79$) and 22M rats (Wt $p < 0.0001$, $q = 5.171$, $df = 79$; TgAPP21 $p < 0.0001$, $q = 5.970$, $df = 79$; Dunnett's post-hoc test) required more time to reach the platform when averaging swim time on trials 2-6. However, only 22M rats failed to show any improvement even by trial 6; 13M Wt still reduced swim time by trial 5 ($p = 0.002$, $q = 3.586$, $df = 395$) and 13M TgAPP21 by trial 3 ($p = 0.0006$, $q = 3.906$, $df = 395$; Dunnett's post-hoc test). Thus, while age impaired MWM learning performance, all but 22M rats demonstrated significant improvement in swim time.

3.4.2.1 Navigational Memory

While no genotype differences were observed in MWM learning, genotype differences on the 24 h delayed probe test were observed. During the probe test, the platform was removed, and rat swim behaviour was observed during a 90 s probe. Latency to swim to the platform region, a 7.5 cm vicinity to the learned platform location, was analyzed to evaluate spatial memory. With age, both Wt and TgAPP21 rats required more time to locate the platform (Figure 3-7A; $p < 0.0001$, $F(3,79)=8.761$; 2-Way ANOVA). Genotype was not a significant factor, but the age-dependent trend for increasing latency to the platform region was more robust in TgAPP21 rats ($R^2 = 0.30$, $p < 0.0001$) than Wt rats ($R^2 = 0.17$, $p = 0.009$; post-hoc test for linear trend). Only 22M TgAPP21 rats demonstrated a significant latency increase over 4M TgAPP21 rats ($p < 0.0001$, $q = 4.875$, $df = 79$; Dunnett's post-hoc test).

Memory was also evaluated by analyzing the proportion of time spent in the target quadrant, that is, the quadrant of the MWM in which the platform was previously located. Both age ($p = 0.03$, $F(3,79) = 3.187$) and genotype ($p = 0.05$, $F(1,79) = 4.140$; 2-Way ANOVA) had a significant effect on the proportion of time spent in the target quadrant (Figure 3-7B), with TgAPP21 rats demonstrating a greater preference for the target quadrant in the 4M, 8M, and 13M groups. 13 MO Wt, 22M Wt, and 22M TgAPP21 rats did not spend more than 25% of swim time in the target quadrant (one-sample t-tests), the expected proportion of swim time in the absence of a target preference. 22M TgAPP21 rats showed a significant decrease in target quadrant preference in comparison to 4M TgAPP21 ($p = 0.02$, $q = 2.774$, $df = 79$) and 8M TgAPP21 rats ($p = 0.003$, $q = 2.137$, $df = 79$; Dunnett's post-hoc test). However, none of the groups demonstrated a significant increase in the time needed to locate the platform region (Figure 3-7A) in comparison to the time needed to locate the platform on the last MWM learning trial (Figure 3-6). This makes it less likely that any of the groups failed to recall a learned platform location. Rather, the 22M rats' failure to learn the platform location precluded any preference for the platform region or target quadrant. When only 4M, 8M, and 13M rats were compared on the probe test, genotype was still a significant factor with TgAPP21 rats spending more time in the target quadrant ($p = 0.002$, $F(1,67) = 10.900$; 2-Way ANOVA). Thus, so long as TgAPP21 rats were able to learn and recall the platform location, they would demonstrate a greater target quadrant preference. The traditional interpretation of target preference would suggest that TgAPP21 rats demonstrated a better recall of the platform location.

3.4.2.3 *Regressive Platform Search*

Just as in the previous study that focused on 8M rats only, it was observed again that some rats would demonstrate an increased preference for the target quadrant in the late segment of the probe test. This was unexpected, as preference for the target quadrant should extinguish, not strengthen, during the course of the probe test. To evaluate the role of regressive behavioural inflexibility in target quadrant preference, the proportion of swim time in the target quadrant in the last 30 s segment of the probe test was analyzed

(Figure 3-7C). Age was a significant factor in this late preference ($p = 0.02$, $F(3,79) = 3.404$; 2-Way ANOVA), driven by the difference between 8M and 22M TgAPP21 rats ($p = 0.002$, $q = 3.474$, $df = 79$; Dunnett's post-hoc test). Since the 22M rats never demonstrated that they learned the platform location, a sub-analysis that excluded 22M rats was also performed. When only 4M, 8M, and 13M rats were compared, only genotype was a significant factor with TgAPP21 rats demonstrating a greater late preference for the target quadrant ($p = 0.02$, $F(1,67) = 5.177$; 2-Way ANOVA). Thus, across the ages at which the rats could learn the platform location, TgAPP21 demonstrated a greater preference for the target quadrant in the last 30 s segment of the probe test. For TgAPP21 rats, the late preference for the target quadrant peaked at 8M of age just as the number of regressive errors and errors after criterion in RD peaked in 8M TgAPP21 rats.

To more accurately capture the regressive nature of a late target quadrant preference, it was important to analyze how this compared to target quadrant preferences demonstrated earlier in the probe test. To do this, the *Regressive Index* was calculated for each rat as the difference between the proportion of time in the target quadrant during the last 30 s and the first 60 s of the probe test. Although genotype nor age had significant overall effects on the Regressive Index, 8M TgAPP21 ($p = 0.02$, $t = 3.796$, $df = 11$) and 13M Wt rats ($p=0.002$, $t = 5.258$, $df = 12$) both demonstrated a significant non-zero Regressive Index (one sample-test with Bonferroni correction; Figure 3-7D). This regressive behaviour in the MWM peaked in both genotypes prior to the development of navigational learning impairments, just as TgAPP21 regressive behaviour in RD peaked at 8 months of age prior to the onset of learning and memory impairments in the operant-conditioning chamber.

For both genotypes, the age-dependent trends for the regressive index (Figure 3-7D) replicated the regressive error trends observed in response discrimination (Figure 3-3C). To test whether the regressive-like behaviour in the MWM probe test was related to regressive behaviour in response discrimination, the relationships between regressive error frequency and late target quadrant preference & regressive index scores were analyzed (Figure 3-8). Regressive error frequency was strongly correlated with both late target quadrant preference ($p = 0.009$, $R^2 = 0.71$, $F(1,6) = 14.76$) and the regressive index

($p = 0.03$, $R^2 = 0.55$, $F(1,6) = 7.481$). This reaffirms the interpretation of late target quadrant preference as a regressive behaviour. Altogether, the increased target quadrant preference demonstrated by TgAPP21 rats in the probe is more indicative of a regressive inflexibility than an improved memory. In TgAPP21 rats, regressive inflexibility in the probe test peaked at 8 months of age, paralleling observations in set shifting and reversal, and in Wt rats, regressive inflexibility was observed at 13 months of age.

3.4.2.4 *Cued Trials & Swim Speed*

Distal visual cues enabled the rats to navigate the MWM, assuming that the rats' vision was not a confounding variable. To test this assumption, cued trials were performed at the conclusion of MWM testing, wherein a visible marker was placed on a new platform location with the platform slightly elevated above the water level. Neither age nor genotype were significant factors in the latency or swim distance to the platform, even when correcting for swim speed as a covariate. Thus, vision was unlikely to be a confounding factor in MWM observations. Similarly, neither age nor genotype were significant factors in swim speeds, averaged across all MWM trials.

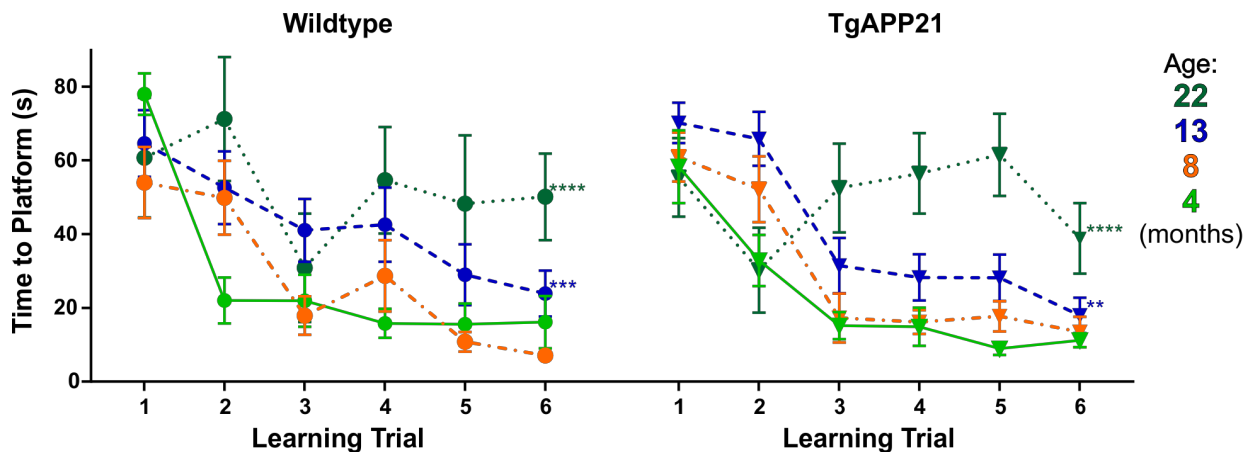


Figure 3-6: Age impaired Morris Water Maze learning

Learning performance was evaluated across trials 2-6. Age had a significant effect on swimming time to platform ($p < 0.0001$).

Compared to 4M Wt rats, *** 13M Wt ($p < 0.001$) and **** 22M Wt rats ($p < 0.0001$) required more time to locate the platform.

Compared to 4M TgAPP21 rats, ** 13M TgAPP21 ($p < 0.01$) and **** 22M TgAPP21 ($p < 0.0001$) rats also required more time to locate the platform.

Only 22M rats failed to show any improvement even by trial 6; 13M Wt still reduced swim time by trial 5 ($p = 0.002$) and 13M TgAPP21 by trial 3 ($p = 0.0006$).

Error bars indicate SEM; $n = 5 - 13$.

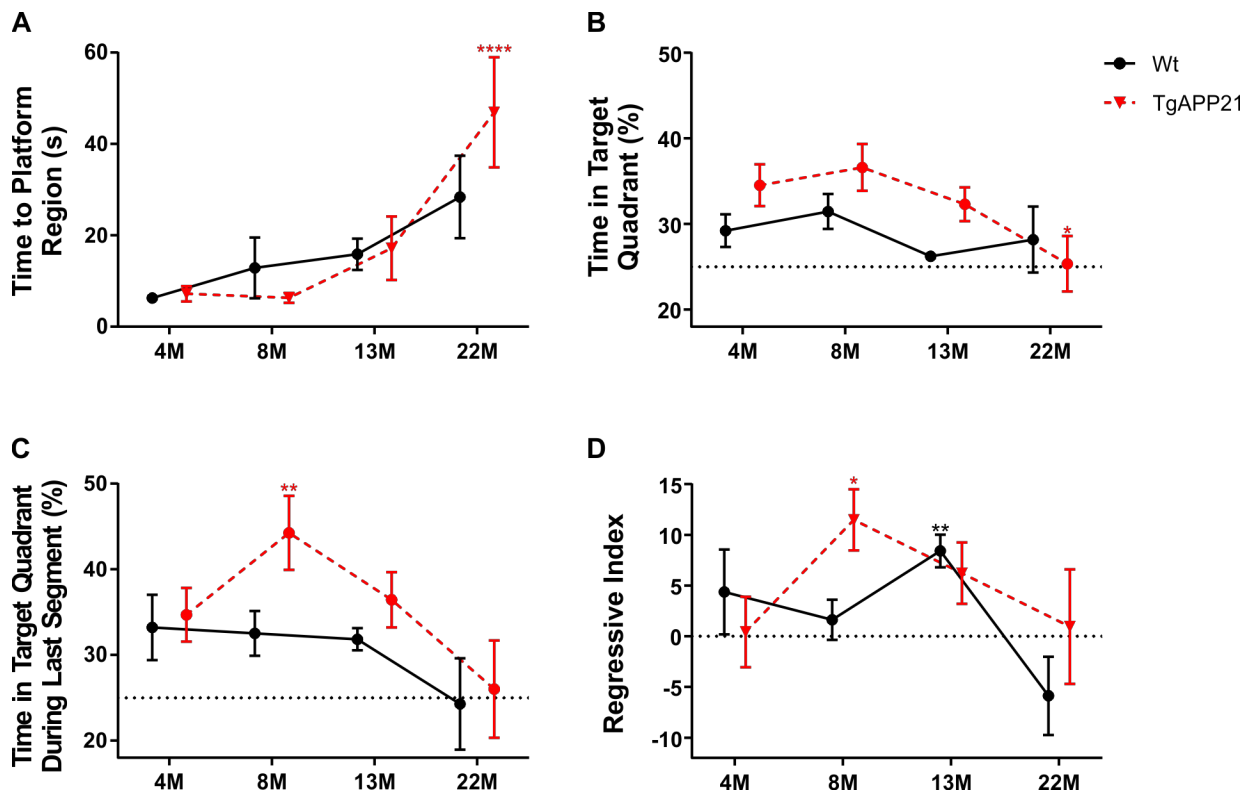


Figure 3-7: Age-dependent memory impairment in the Morris Water Maze probe was preceded by a regressive-like inflexibility

24 h after MWM learning, the platform was removed, and rat swim behaviour was observed during a 90 s probe trial.

(A) Latency to swim to the platform region, a 7.5 cm vicinity to the learned platform location, was analyzed to evaluate spatial memory. With age, both Wt and TgAPP21 rats required more time to locate the platform ($p < 0.0001$). However, **** only 22M TgAPP21 rats showed a significant increase compared to 4M TgAPP21 rats ($p < 0.0001$).

(B) Time in the target quadrant is another commonly used metric to evaluate spatial memory; the dotted line marks the 25% proportion of swim time that would be expected if rats had no bias for the target quadrant. Both age ($p = 0.03$) and genotype ($p = 0.05$) were significant factors in the proportion of time spent in the target quadrant. * 22M TgAPP21 rats spent less time in the target quadrant than 4M and 8M TgAPP21 rats ($p < 0.05$). Traditional interpretation of target preference would suggest that 4M, 8M, and 13M TgAPP21 rats demonstrated a stronger memory for the platform location than age-matched Wt rats.

(C) Age was a significant factor in target quadrant preference during the last 30 s segment of the probe test ($p = 0.02$). This was driven by a ** significantly greater preference in 8M TgAPP21 rats ($p = 0.002$, compared to 22M TgAPP21 rats).

(D) To score the relative increase of a regressive-like preference for the target quadrant, the Regressive Index measures the difference between the proportion of time spent in the target quadrant during the last 30 s segment and the first 60 s segment of the probe

test. * 8M TgAPP21 ($p < 0.05$) and ** 13M Wt rats ($p < 0.01$) both demonstrated a regressive-like preference for the target quadrant.

Error bars indicate SEM; $n = 5 - 13$.

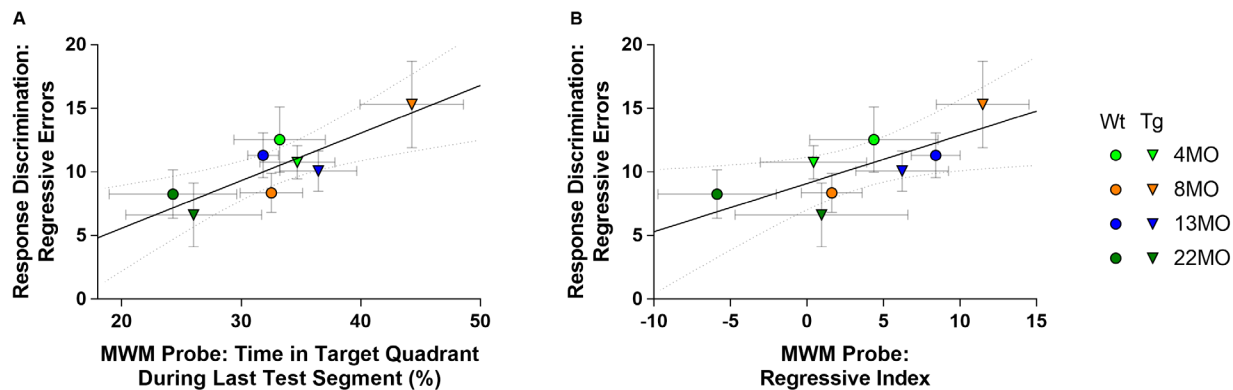


Figure 3-8: Regressive behaviour consistent across response discrimination and Morris Water Maze probe

The group-wise number of regressive errors were significantly correlated with two different measures of regressive like-behaviour in the Morris Water Maze probe: **(A)** the proportion of time spent in the target quadrant last 30 s segment of the probe ($p = 0.009$, Pearson's $R^2 = 0.71$), and **(B)** the regressive index, which is calculated by the difference between the proportion of time spent in the target quadrant during the last 30 s segment compared to the first 60 s of the probe test ($p = 0.03$, Pearson's $R^2 = 0.55$).

Error bars indicate SEM; dotted lines indicate 95% confidence interval of linear regression.

3.4.3 Open Field

The open field evaluates rats' locomotor exploration and avoidance of the anxiogenic field centre. Older and transgenic rats demonstrated less locomotor exploration, with both age and genotype having a significant effect on the total distance travelled during both the first 5 min (Figure 3-9A; Age: $p < 0.0001$, $F(3,81) = 14.12$; Genotype: $p < 0.0001$, $F(1,81) = 54.48$; 2-Way ANOVA) and the full 20 min duration of the open field (Figure 3-9A; Age: $p < 0.0001$, $F(3,81) = 24.73$; Genotype: $p < 0.0001$, $F(1,81) = 71.48$; 2-Way ANOVA). There was also a significant interaction between age and genotype ($p = 0.003$, $F(3,81) = 5.2$; 2-Way ANOVA), with Wt rats showing a greater age-dependent decline in total distance travelled. Overall, TgAPP21 rats demonstrated a profound reduction in locomotor exploration. Avoidance of the centre of the open field is an indicator of anxiety. Neither age nor genotype were significant factors in this measure of anxiety (Figure 3-9B), thus anxiety is unlikely to have confounded behavioural tests.

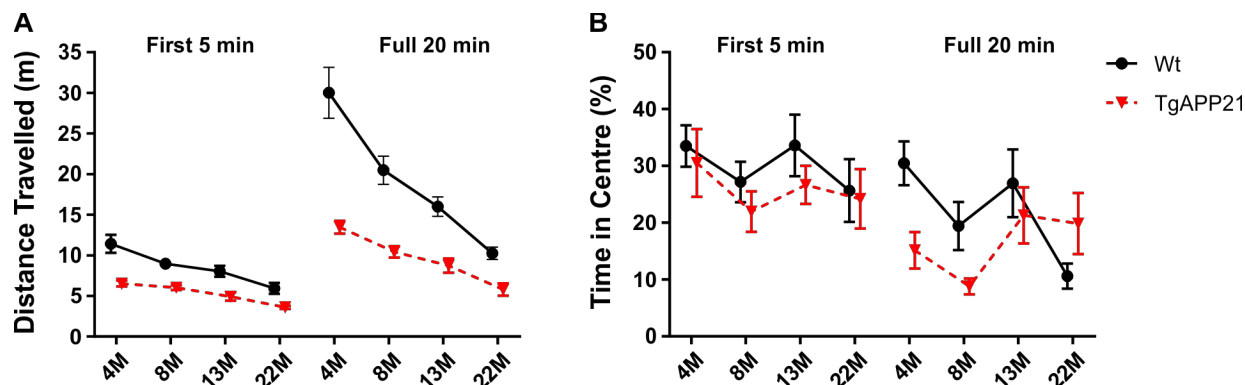


Figure 3-9: Decreased open field exploration in aged and transgenic Rats

(A) Total distance travelled in the open field is a measure of locomotor exploration. Age and genotype were both significant factors in the total distances travelled during both the first 5 min ($p < 0.0001$) and the full 20 min duration of the open field ($p < 0.0001$); older and transgenic rats demonstrated less locomotor exploration. There was also a significant interaction between age and genotype ($p = 0.003$), with Wt rats showing a greater age-dependent decline in total distance travelled. For both the first 5 min and the full 20 min duration of the test, TgAPP21 rats demonstrated significantly less locomotor exploration at the 4M, 8M, and 13M age points ($p < 0.004$), but not at 22 months of age.

(B) Avoidance of the centre of the open field is an indicator of anxiety. Neither age nor genotype were significant factors in this measure of anxiety.

Error bars indicate SEM; $n = 6-13$.

3.4.4 Activated Microglia

The activation of microglia indicates a pro-inflammatory environment. The OX6 antibody for MHC II was used to identify activated microglia. Major white matter tracts, such as the corpus callosum (Figure 3-10A), and the hippocampus were found to be common sites for microglial activation. Though OX6 positive microglia were also observed in the cortex, thalamus, and striatum, their presence was highly sporadic and qualitative observation did not indicate any association with genotype. Thus, only major white matter tracts and the hippocampus were evaluated quantitatively. Older rats demonstrated a significant increase in the cross-sectional area coverage by OX6 positive microglia in the forceps minor, corpus callosum, cingulum, and internal capsule (Figure 3-10B-G; $p < 0.0001$, Wilk's $\Lambda = 0.057$, $F(24,73.109) = 5.112$; 2-way MANOVA). TgAPP21 rats demonstrated greater activated microgliosis ($p < 0.0001$, Wilk's $\Lambda = 0.285$, $F(8,25) = 7.847$), and there was a significant interaction between age and genotype ($p = 0.01$, Wilk's $\Lambda = 0.223$, $F(24,73.109) = 2.067$; 2-Way MANOVA). This interaction was most apparent in the corpus callosum (Figure 3-10D; $p = 0.004$, $F(3,32) = 5.518$) and the supraventricular sub-region of the corpus callosum (Figure 3-10C; $p = 0.002$, $F(3,32) = 6.130$; 2-Way ANOVA). Within these two regions, the age-dependent increase activated microglia was precocious in TgAPP21 rats, so that 8M TgAPP21 rats had as much microglia activation as 13M Wt rats, and 13M TgAPP21 rats had as much microglia activation as 22M Wt rats (Figure 3-10CD). This precocious white matter inflammation was not observed in the forceps minor, cingulum, or internal capsule, but 22M TgAPP21 rats did demonstrate significantly greater activated microglia area coverage than 22M Wt rats in all white matter regions ($p < 0.01$; Sidak's post-hoc test).

In the hippocampus, only age was a significant factor in microglia activation (Figure 3-10G; $p = 0.02$, Wilk's $\Lambda = 0.543$, $F(9,73.163) = 2.319$; 2-Way MANOVA). While 22M TgAPP21 rats demonstrated more neuroinflammation throughout the hippocampus than 4M rats and 22M Wt did not, there was no significant difference between the 22M TgAPP21 and 22M Wt rats. However, in the pooled results for the posterior dorsal and ventral sub-regions of the hippocampus, genotype was a significant factor ($p = 0.005$, $F(1,32) = 8.989$) and interacted significantly with age ($p = 0.0009$, $F(3,32) = 6.997$; 2-Way

ANOVA), such that 22M TgAPP21 rats demonstrated greater neuroinflammation than 22M Wt rats in the posterior hippocampus ($p < 0.0001$, $t = 5.384$, $df = 32$; Sidak's post-hoc test).

Wt rats demonstrated a greater increase of microglia activation in the anterior corpus callosum than the posterior corpus callosum ($p = 0.04$, $F(1,32) = 4.84$; 2-Way ANOVA). In TgAPP21 rats, microglia activation was more widely and diffusely increased, so that there was not a significant anterior-posterior gradient of inflammation in the corpus callosum. This replicates patterns of white matter disruptions observed in healthy elderly control subjects and patients with AD⁴².

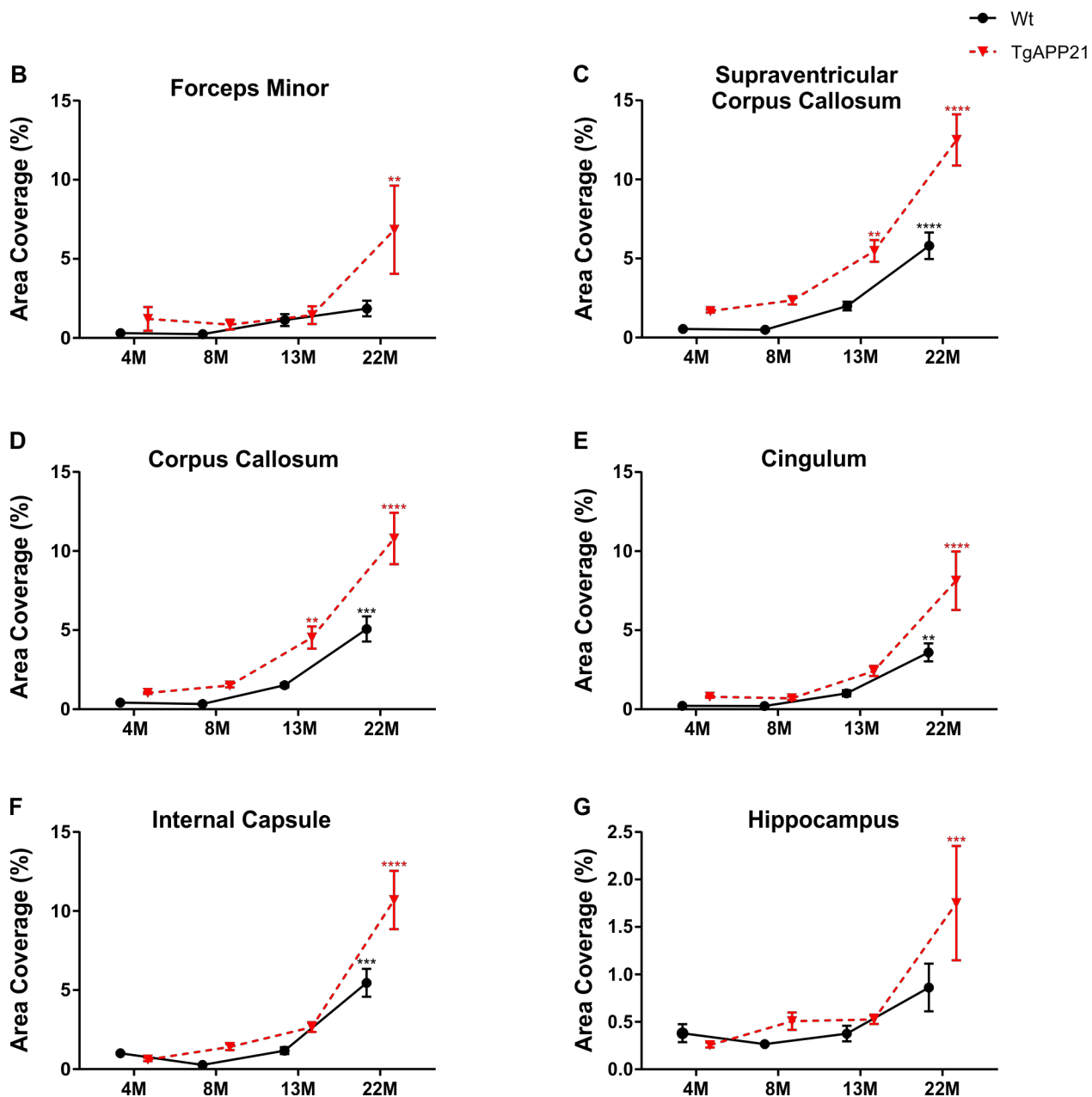
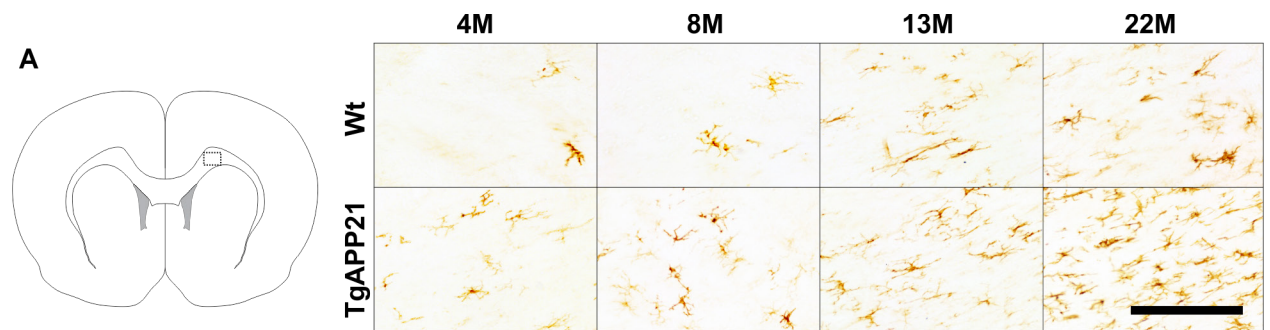


Figure 3-10: Precocious corpus callosum inflammation in transgenic rats

IHC for the OX6 primary antibody for MHC II identified activated pro-inflammatory microglia; white matter areas and the hippocampus were identified as regions with high microglia activation.

(A) The schematic shows one of the coronal planes on which the corpus callosum was analyzed (Bregma +2.0 mm). Representative images of 30 μm thick sections were taken from the dotted outline; 200 μm scale bar.

(B-G) Cross-sectional area coverage by activated microglia was quantified in major white matter tracts and the hippocampus. **(B-F)** Age and genotype were significant factors for microglia activation in white matter ($p < 0.0001$). The interaction between age and genotype was also significant ($p = 0.01$); this interaction was especially apparent in the supraventricular corpus callosum and the corpus callosum ($p < 0.004$). In these regions, the age-dependent increase of white matter inflammation was precocious in TgAPP21 rats, so that 8M and 13M TgAPP21 rats had as much microglia activation as 13M and 22M Wt rats, respectively.

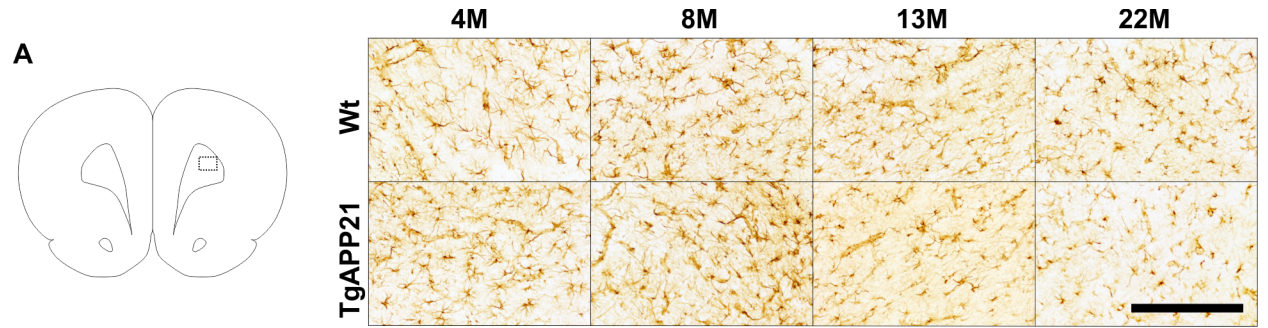
(G) Only age was a significant factor in the activation of microglia in the hippocampus ($p = 0.02$); this also applied to the three subregions of the hippocampus analyzed: anterior dorsal, posterior dorsal, and ventral ($p < 0.007$). ** $p < 0.01$, *** $p < 0.001$, **** $p < 0.0001$: significant increases compared to 4M rats of the same genotype.

Error bars indicate SEM, $n = 5$.

3.4.5 Reactive Astrocytes

To evaluate whether there was an increase of reactive astrocyte in regions with increased microglia activation, cross-sectional area coverage by GFAP-positive astrocytes was evaluated in the same regions (Figure 3-11). Age was a significant factor in astrocyte reactivity in the forceps minor (Figure 3-11B); $p = 0.01$, $F(1,32) = 4.478$), which was also the only region in which genotype was a significant factor ($p = 0.05$, $F(1,32) = 4.346$; 2-way ANOVA). In the forceps minor, 22M TgAPP21 demonstrated a significant decrease in cross sectional area coverage by GFAP-positive astrocytes compared to 8M TgAPP21 ($p = 0.004$, $q = 3.491$, $df = 32$; Dunnett's post-hoc test; Figure 3-11B). This pattern of group differences was significantly correlated with the number of regressive errors committed during response discrimination (group-wise correlation; $p = 0.03$, Pearson's $R^2 = 0.57$, $F(1,6) = 8.036$; Figure 3-12). This relationship was particularly strong in TgAPP21 rats ($p = 0.03$, Pearson's $R^2 = 0.93$, $F(1,2) = 27.33$). Thus, increased astrocyte reactivity in the forceps minor may have played an important role in the 8M TgAPP21 rats' regressive inflexibility.

Age was a significant factor in hippocampal astrocytosis (Figure 3-11G; $p < 0.0001$, Wilk's $\Lambda = 0.330$, $F(9,73.163) = 4.695$; 2-Way MANOVA), but without a clear trend and no differences between the genotypes. This was also observed in the posterior dorsal hippocampus ($p = 0.003$, $F(3,32) = 5.816$) and ventral hippocampus ($p < 0.0001$, $F(3,32) = 10.439$; 2-Way ANOVA), but not the anterior dorsal hippocampus.



● Wt
 ▼ TgAPP21

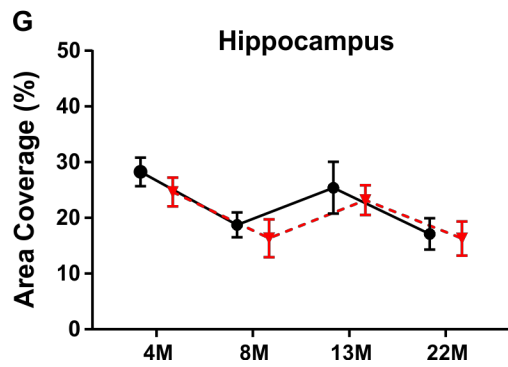
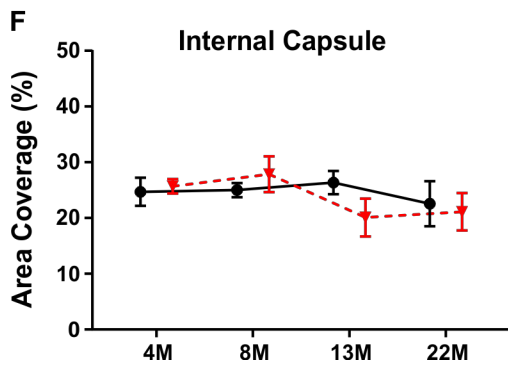
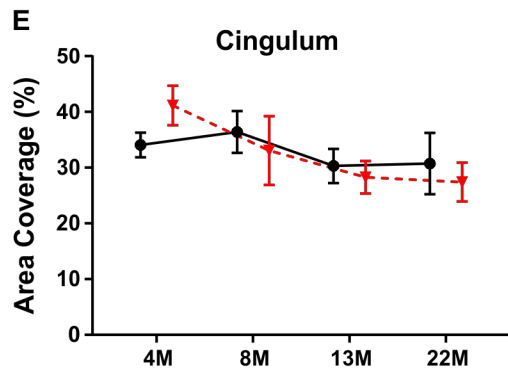
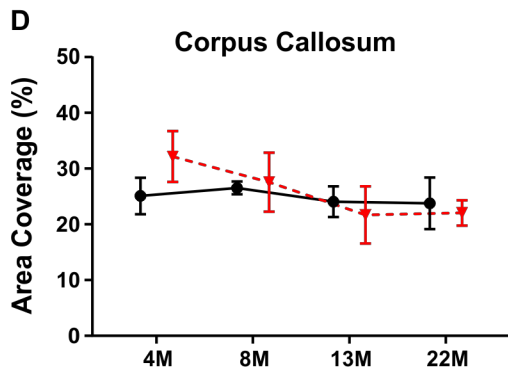
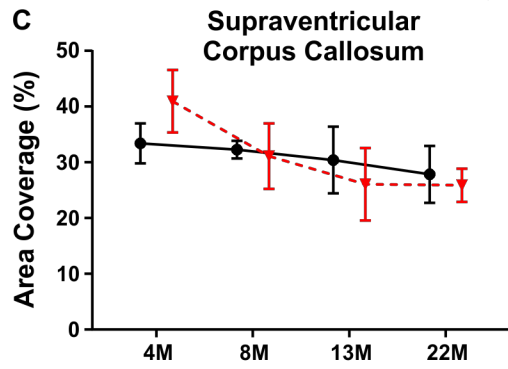
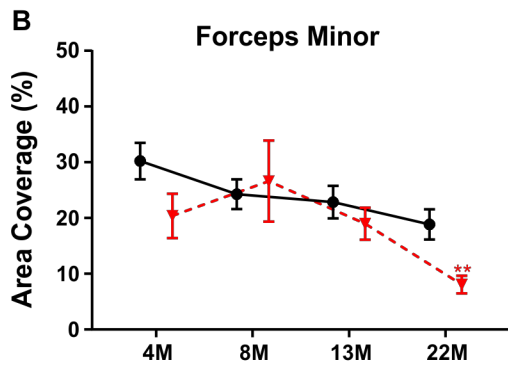


Figure 3-11: Reduced forceps minor astrocyte reactivity in aged TgAPP21

DAB mediated IHC with a primary antibody for GFAP identified reactive astrocytes.

(A) The schematic shows the coronal planes on which the forceps minor was analyzed (Bregma +3.0 mm). Representative images of 30 μm thick sections were taken from the dotted outline; 200 μm scale bar.

(B-G) Cross-sectional area coverage by reactive astrocytes was quantified in regions with increased microglia activation. **(B-F)** Neither age nor genotype were significant factors in astrocyte reactivity across most white matter regions except for the forceps minor, in which both age ($p = 0.01$) and genotype ($p = 0.05$) were significant factors in reactive astrocyte area coverage. ****** In the forceps minor, 22M TgAPP21 rats had a decreased area coverage by reactive astrocytes compared to 8M TgAPP21 rats ($p < 0.01$).

(G) Age was a significant factor in reactive astrocyte area coverage in the hippocampus ($p < 0.0001$).

Error bars indicate SEM, $n = 5$.

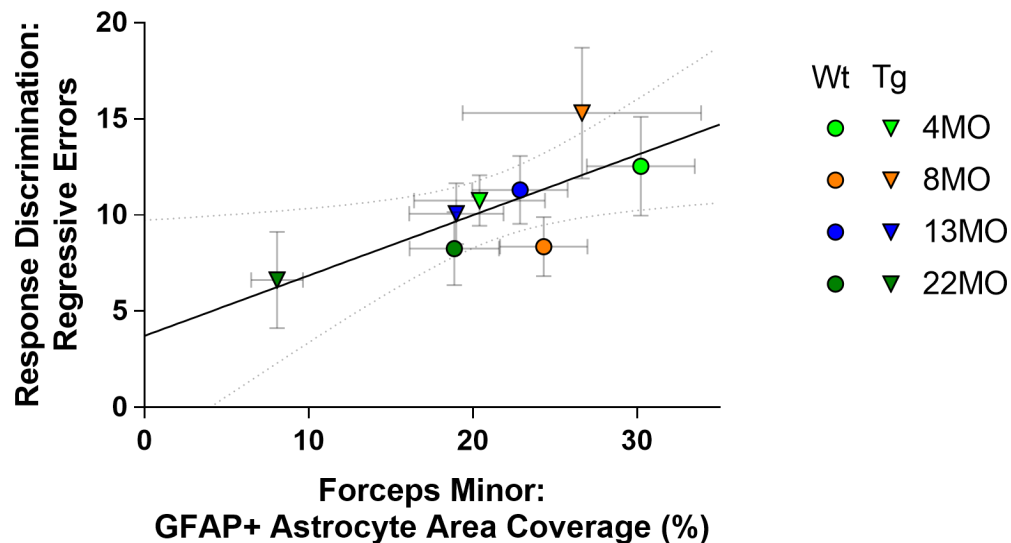


Figure 3-12: Significant positive correlation between regressive errors and astrocyte reactivity in the forceps minor.

The group-wise relationship between the number of regressive errors committed during response discrimination and GFAP-positive reactive astrocyte area coverage in the forceps minor was significant ($p = 0.03$, Pearson's $R^2 = 0.57$).

Error bars indicate SEM; dotted lines indicate 95% confidence interval of linear regression.

3.5 Discussion

The profound acceleration of age-dependent white matter microglia activation builds on previous observations of increased inflammation in the TgAPP21 rats' white matter ([2.4.4 Activated Microglia in White Matter](#) on page 77). Concurrently, the TgAPP21 demonstrated a regressive behavioural phenotype, committing a greater number of errors after criterion during set shifting. This was further evidenced by a greater regressive-like preference for the MWM target quadrant. However, TgAPP21 rats did not show a persistent or progressive increase in regressive behavioural inflexibility across all measures. Instead, behavioural inflexibility peaked in 8M TgAPP21 rats, as measured by the number of regressive errors on set shifting, reversal errors, and the MWM Probe Regressive Index score. Though learning and memory impairments in 22M rats may account for an apparent decrease in inflexibility in 22M TgAPP21 rats, the relative reduction of inflexibility in 13 M TgAPP21 would still be unexpected. Previous studies have observed that environmental enrichment promotes a relatively greater increase of neurogenesis in older than younger rodents⁴³, and that environmental enrichment can promote functional compensation in rodent models of neurodegeneration⁴⁴. This raises the question of whether older TgAPP21 rats may have developed compensatory pathways, which has been described in AD patients with increased paradoxical neural activation⁴⁵; this would need to be investigated with positron emission tomography or functional magnetic resonance imaging.

The TgAPP21 rats' regressive inflexibility could not be attributed directly to their precocious white matter inflammation. However, the amount of astrocytosis in the forceps minor did strongly correlate with the number of regressive errors observed during response discrimination. This complements recent findings that correlated performance on the Stroop color-naming task with white matter integrity in the forceps minor, as measured by fractional anisotropy⁴⁶. In healthy human subjects, fractional anisotropy is negatively correlated with age, particularly in the frontal lobe, and is associated with poorer cognitive performance on an attention-switching task⁵. Our results suggest that pathogenic amyloid and astrocytes may also play important roles in frontal white matter integrity and its behavioural correlates.

Reduced locomotor exploration, as demonstrated by TgAPP21 rats, has been reported in other rodent models of Alzheimer disease⁴⁷. This reduced exploratory behaviour was observed in all age cohorts, and 4M TgAPP21 rats explored the field as little as 22M Wt rats did. Interestingly, in a study on bilateral carotid artery stenosis and white matter injury in aged mice, myelin degradation and microglia activation were associated with reduced social exploration¹⁴. Another study found that mice with white matter injury after bilateral carotid artery stenosis recovered normal exploratory behaviour of a novel object when microglia were inactivated by minocycline and TRPM2 knock-out¹⁷. These studies support the interpretation that white matter inflammation in TgAPP21 rats may have mediated reduced exploratory behaviour.

Several behavioural testing design parameters were crucial to characterizing the TgAPP21 rat, although they are not standard in rodent studies. Allowing rats to continue lever pressing in the operant-conditioning chamber even after achieving criterion allowed us to measure the number of errors committed after criterion during RD. Our MWM test was 90 s long, allowing us to capture a regressive-like target quadrant preference in 8M TgAPP21 and 13M Wt rats. Both the Regressive Index and the time spent in the target quadrant during the last third of the probe test correlated significantly with the number of regressive errors committed during response discrimination learning. This reiterates the potentially confounding role that behavioural flexibility can have on memory testing in the MWM probe. The inherent challenge of maintaining animal wellness in aged rats presents an important limitation in our results; 22M behaviour and neuroinflammation may have been confounded by insidious health factors. Future work should focus on identifying the specific microglia populations that are activated *in vivo* in response to hAPP expression and the specific molecular pathways that link the expression of pathogenic hAPP and microglia activation. Targeted anti-inflammatory intervention or pro-inflammatory challenges will be important for confirming potentially causal links.

The observation of precocious microglia activation in the corpus callosum of TgAPP21 rats reinforces the central role of neuroinflammation in early AD. Increased activation of white matter microglia presented independently of amyloid plaque formation, as amyloid deposits do not develop spontaneously in the TgAPP21 rat^{31,32,48}. Moreover, the onset of

behavioural inflexibility preceded impairments of hippocampal-dependent behaviour, such as spatial and memory impairments. This presents important considerations for future experimental and clinical studies of behavioural inflexibility related to ageing and dementia. In particular, these findings warrant closer investigation of white matter inflammation and regressive forms of inflexibility in the earliest stages of cognitive impairment associated with amyloid pathology.

3.6 References

1. Johnson JK, Lui LY, Yaffe K. Executive Function, More Than Global Cognition, Predicts Functional Decline and Mortality in Elderly Women. *The Journals of Gerontology Series A: Biological Sciences and Medical Sciences*. 2007;62(10):1134-1141.
2. Diamond A. Executive functions. *Annu Rev Psychol*. 2013;64:135-168.
3. Harada CN, Natelson Love MC, Triebel KL. Normal cognitive aging. Vol 29: NIH Public Access; 2013:737-752.
4. Hedden T, Gabrieli JD. Insights into the ageing mind: a view from cognitive neuroscience. *Nat Rev Neurosci*. 2004;5(2):87-96.
5. Grieve SM, Williams LM, Paul RH, Clark CR, Gordon E. Cognitive aging, executive function, and fractional anisotropy: a diffusion tensor MR imaging study. *AJNR Am J Neuroradiol*. 2007;28(2):226-235.
6. Sasson E, Doniger GM, Pasternak O, Tarrasch R, Assaf Y. White matter correlates of cognitive domains in normal aging with diffusion tensor imaging. *Front Neurosci*. 2013;7(7 MAR):32.
7. Rabin JS, Perea RD, Buckley RF, et al. Global White Matter Diffusion Characteristics Predict Longitudinal Cognitive Change Independently of Amyloid Status in Clinically Normal Older Adults. *Cereb Cortex*. 2018(February):1-12.
8. Gunning-Dixon FM, Raz N. The cognitive correlates of white matter abnormalities in normal aging: a quantitative review. *Neuropsychology*. 2000;14(2):224-232.
9. Guttman CR, Jolesz FA, Kikinis R, et al. White matter changes with normal aging. *Neurology*. 1998;50(4):972-978.
10. Lan LF, Zheng L, Yang X, Ji XT, Fan YH, Zeng JS. Peroxisome proliferator-activated receptor-gamma agonist pioglitazone ameliorates white matter lesion and cognitive impairment in hypertensive rats. *CNS Neurosci Ther*. 2015;21(5):410-416.
11. Fowler JH, McQueen J, Holland PR, et al. Dimethyl fumarate improves white matter function following severe hypoperfusion: Involvement of microglia/macrophages and inflammatory mediators. *Journal of Cerebral Blood Flow and Metabolism*2017.
12. Qin C, Fan WH, Liu Q, et al. Fingolimod Protects Against Ischemic White Matter Damage by Modulating Microglia Toward M2 Polarization via STAT3 Pathway. *Stroke*. 2017;48(12):3336-3346.
13. Shobin E, Bowley MP, Estrada LI, et al. Microglia activation and phagocytosis: relationship with aging and cognitive impairment in the rhesus monkey. *Geroscience*. 2017;39(2):199-220.
14. Wolf G, Lotan A, Lifschytz T, et al. Differentially Severe Cognitive Effects of Compromised Cerebral Blood Flow in Aged Mice: Association with Myelin Degradation and Microglia Activation. *Front Aging Neurosci*. 2017;9:191.
15. Hase Y, Horsburgh K, Ihara M, Kalara RN. White matter degeneration in vascular and other ageing-related dementias. *J Neurochem*. 2018;144(5):617-633.
16. Manso Y, Holland PR, Kitamura A, et al. Minocycline reduces microgliosis and improves subcortical white matter function in a model of cerebral vascular disease. *Glia*. 2018;66(1):34-46.

17. Miyanohara J, Kakae M, Nagayasu K, et al. TRPM2 Channel Aggravates CNS Inflammation and Cognitive Impairment via Activation of Microglia in Chronic Cerebral Hypoperfusion. *J Neurosci*. 2018;38(14):3520-3533.
18. Streit WJ, Xue QS, Tischer J, Bechmann I. Microglial pathology. *Acta Neuropathol Commun*. 2014;2:142.
19. Raj D, Yin Z, Breur M, et al. Increased White Matter Inflammation in Aging- and Alzheimer's Disease Brain. *Front Mol Neurosci*. 2017;10(June):206.
20. Jansen WJ, Ossenkoppele R, Knol DL, et al. Prevalence of cerebral amyloid pathology in persons without dementia: a meta-analysis. *JAMA*. 2015;313(19):1924-1938.
21. Prokop S, Miller KR, Heppner FL. Microglia actions in Alzheimer's disease. *Acta neuropathologica*. 2013;126(4):461-477.
22. von Bernhardi R, Eugenin-von Bernhardi L, Eugenin J. Microglial cell dysregulation in brain aging and neurodegeneration. *Front Aging Neurosci*. 2015;7:124.
23. Sudduth TL, Schmitt FA, Nelson PT, Wilcock DM. Neuroinflammatory phenotype in early Alzheimer's disease. *Neurobiol Aging*. 2013;34(4):1051-1059.
24. Maier-Hein KH, Westin CF, Shenton ME, et al. Widespread white matter degeneration preceding the onset of dementia. *Alzheimers Dement*. 2015;11(5):485-493 e482.
25. Lee S, Viqar F, Zimmerman ME, et al. White matter hyperintensities are a core feature of Alzheimer's disease: Evidence from the dominantly inherited Alzheimer network. *Ann Neurol*. 2016;79(6):929-939.
26. Fabrigoule C, Rouch I, Taberly A, et al. Cognitive process in preclinical phase of dementia. *Brain*. 1998;121 (Pt 1)(1):135-141.
27. Baudic S, Barba GD, Thibaudet MC, Smaghe A, Remy P, Traykov L. Executive function deficits in early Alzheimer's disease and their relations with episodic memory. *Arch Clin Neuropsychol*. 2006;21(1):15-21.
28. Grober E, Hall CB, Lipton RB, Zonderman AB, Resnick SM, Kawas C. Memory impairment, executive dysfunction, and intellectual decline in preclinical Alzheimer's disease. *J Int Neuropsychol Soc*. 2008;14(2):266-278.
29. Belleville S, Fouquet C, Duchesne S, Collins DL, Hudon C. Detecting early preclinical alzheimer's disease via cognition, neuropsychiatry, and neuroimaging: Qualitative review and recommendations for testing. Vol 422014:S375-S382.
30. Agca C, Fritz JJ, Walker LC, et al. Development of transgenic rats producing human beta-amyloid precursor protein as a model for Alzheimer's disease: transgene and endogenous APP genes are regulated tissue-specifically. *BMC Neurosci*. 2008;9:28.
31. Rosen RF, Fritz JJ, Dooyema J, et al. Exogenous seeding of cerebral beta-amyloid deposition in betaAPP-transgenic rats. *J Neurochem*. 2012;120(5):660-666.
32. Silverberg GD, Miller MC, Pascale CL, et al. Kaolin-induced chronic hydrocephalus accelerates amyloid deposition and vascular disease in transgenic rats expressing high levels of human APP. *Fluids Barriers CNS*. 2015;12(1):2.

33. Levit A, Regis AM, Garabon JR, et al. Behavioural inflexibility in a comorbid rat model of striatal ischemic injury and mutant hAPP overexpression. *Behav Brain Res.* 2017;333(June):267-275.
34. Floresco SB, Block AE, Tse MTL. Inactivation of the medial prefrontal cortex of the rat impairs strategy set-shifting, but not reversal learning, using a novel, automated procedure. *Behav Brain Res.* 2008;190(1):85-96.
35. Brady AM, Floresco SB. Operant procedures for assessing behavioral flexibility in rats. *J Vis Exp.* 2015(96):e52387.
36. Roof RL, Schielke GP, Ren X, Hall ED. A comparison of long-term functional outcome after 2 middle cerebral artery occlusion models in rats. *Stroke.* 2001;32(11):2648-2657.
37. Wong WT. Microglial aging in the healthy CNS: phenotypes, drivers, and rejuvenation. *Front Cell Neurosci.* 2013;7:22.
38. Sofroniew MV, Vinters HV. Astrocytes: biology and pathology. *Acta Neuropathol.* 2010;119(1):7-35.
39. Paxinos G, Watson C. *The rat brain in stereotaxic coordinates.* 6th ed. Amsterdam ; Boston ;; Academic Press/Elsevier; 2007.
40. Caughlin S, Maheshwari S, Agca Y, et al. Membrane-lipid homeostasis in a prodromal rat model of Alzheimer's disease: Characteristic profiles in ganglioside distributions during aging detected using MALDI imaging mass spectrometry. *Biochim Biophys Acta.* 2018;1862(6):1327-1338.
41. Motulsky HJ, Brown RE. Detecting outliers when fitting data with nonlinear regression - a new method based on robust nonlinear regression and the false discovery rate. *BMC Bioinformatics.* 2006;7(1):123.
42. Head D, Buckner RL, Shimony JS, et al. Differential vulnerability of anterior white matter in nondemented aging with minimal acceleration in dementia of the Alzheimer type: evidence from diffusion tensor imaging. *Cereb Cortex.* 2004;14(4):410-423.
43. Kempermann G, Kuhn HG, Gage FH. Experience-induced neurogenesis in the senescent dentate gyrus. *J Neurosci.* 1998;18(9):3206-3212.
44. Nithianantharajah J, Hannan AJ. Mechanisms mediating brain and cognitive reserve: experience-dependent neuroprotection and functional compensation in animal models of neurodegenerative diseases. *Prog Neuropsychopharmacol Biol Psychiatry.* 2011;35(2):331-339.
45. Buckner RL. Memory and executive function in aging and AD: multiple factors that cause decline and reserve factors that compensate. *Neuron.* 2004;44(1):195-208.
46. Mamiya PC, Richards TL, Kuhl PK. Right Forceps Minor and Anterior Thalamic Radiation Predict Executive Function Skills in Young Bilingual Adults. *Front Psychol.* 2018;9:118.
47. Lalonde R, Fukuchi K, Strazielle C. APP transgenic mice for modelling behavioural and psychological symptoms of dementia (BPSD). *Neurosci Biobehav Rev.* 2012;36(5):1357-1375.
48. Agca C, Klakotskaia D, Schachtman TR, Chan AW, Lah JJ, Agca Y. Presenilin 1 transgene addition to amyloid precursor protein overexpressing transgenic rats increases amyloid beta 42 levels and results in loss of memory retention. *BMC Neurosci.* 2016;17(1):46.

Chapter 4: The Role of Hypertension in Executive Function and White Matter Astrocytosis

This study set out to evaluate the impact of comorbid pathogenic APP and cerebrovascular stress on executive function (Objective 3). The experiments in this study were conducted prior to our development of set-shifting methodology, thus evaluation of behavioural flexibility was limited to delayed match-sample testing in the MWM, which evaluates both working memory and behavioural flexibility. A manuscript of this study is under review for publication in *Hypertension*.

4.1 Abstract

Hypertension is recognized as a risk factor for Alzheimer disease (AD), but the causal link remains undetermined. Although astrocytes and microglia play an important role in maintaining the neurovascular unit, astrocytes and microglia have been understudied in comorbid models of hypertension and AD. In this study, male transgenic Fischer 344 rats (TgAPP21) overexpressing a pathogenic human amyloid precursor protein received 8 weeks of chronic Angiotensin II (AngII) infusion to increase blood pressure, and the rats were evaluated for astrocytosis, microgliosis, and cognitive function. A linear relationship between astrocytosis and blood pressure was observed in the corpus callosum and cingulum of wildtype rats, with hypertensive wildtype rats matching the elevated baseline astrocytosis seen in normotensive transgenic rats. In contrast, hypertensive transgenic rats did not demonstrate a further increase of astrocytosis, indicating a deficient response. AngII infusion did not affect activation of microglia, which were elevated in the white matter and hippocampus of transgenic rats. AngII infusion did impair both wildtype and transgenic rats' executive functions in the Morris Water Maze. These results present important implications for the interaction between hypertension and pathogenic human amyloid precursor protein expression, as AngII infusion produced cognitive impairments in both genotypes, but transgenic rats were additionally impaired in developing a normal astrocytic response to elevated blood pressure.

4.2 Introduction

Cerebrovascular pathology is commonly observed in all types of dementia. In addition to vascular dementia, this is also apparent in Alzheimer disease (AD), with 80% of cases showing coincident cerebrovascular pathology on autopsy¹. Hypertension is recognized as a leading vascular risk factor for AD²⁻⁴, but the causal link between hypertension and AD has not been identified. Moreover, it remains inconclusive whether anti-hypertensive therapy can offer cognitive protection⁵⁻¹⁰. Observed interactions between AD and vascular pathology has given rise to the Neurovascular Hypothesis of AD¹¹⁻¹³. The Neurovascular Hypothesis proposes that cerebrovascular dysregulation, such as systemic hypertension, disrupts amyloid and tau protein homeostasis, leading to neuronal injury and cognitive impairment. At the same time, amyloid- and tau-mediated injury can disrupt neurovascular coupling. Central to this bi-directional pathology is the neurovascular unit, maintained in part by astrocytes and microglia, which are responsive to hypertension¹⁴⁻¹⁶.

The importance of hypertension as a risk factor for AD is further supported by the close link between hypertension and leukoaraiosis, also known as white matter hyperintensities¹⁷. Leukoaraiosis is associated with disruptions of white matter integrity^{18,19} and is an important predictor for dementias including AD²⁰. These white matter disruptions can cause impairments of executive functions such as working memory and behavioural flexibility¹⁸, which is also seen in patients with hypertension²¹⁻²³. Hypertension disrupts astrocytic polarity and the blood-brain barrier²⁴⁻²⁷, which may be an initiating factor in the development of leukoaraiosis²⁸. Thus, white matter pathology plays an important role in the cognitive effects of hypertension.

Previous animal models of comorbid hypertension and AD have demonstrated that hypertension does exacerbate amyloidopathies and cognitive impairment²⁹⁻³⁴, but these studies did not present data on white matter disruption, executive function, astrocytes, or microglia. In the present study, we investigated the impact of hypertension on the transgenic Fischer 344 rat (TgAPP21) which overexpresses a pathogenic variant of the human amyloid precursor protein (hAPP)³⁵, focusing on astrocytes, microglia, and

executive function. Cerebral amyloid pathology does not occur spontaneously in TgAPP21 but can be induced³⁵⁻³⁷, thus TgAPP21 are ideal for modelling the roles of hypertension and glial cells in the early pre-plaque stages of AD. For 8 weeks, 8 – 10-month-old male wildtype and transgenic rats were chronically infused with either normal saline (Wt & Tg rats) or Angiotensin II (AngII; Wt-AngII & Tg-AngII rats) to elevate blood pressure and model the effects of hypertension³⁸⁻⁴⁰. We expected increased astrocytosis particularly in the white matter regions of Wt-AngII and Tg-AngII, accompanied by executive dysfunction, as both white matter and executive function are particularly vulnerable to hypertension²¹⁻²³. As both hypertension and high levels of amyloid activate astrocytes and microglia^{12,14-16,41-43}, we expected the greatest amount of glial activity in the comorbid Tg-AngII rats.

Indeed, after 8 weeks of blood pressure elevation, we found greater astrocyte reactivity in the corpus callosum and cingulum of Wt-AngII rats. The level of white matter astrocytosis in Wt-AngII rats was similar to Tg rats, which appeared to have an elevated baseline level of reactive astrocytes. However, Tg-AngII rats did not demonstrate a further increase of astrocytosis. AngII infusion did impair both Wt-AngII and Tg-AngII rats in the Morris Water Maze (MWM) adaptation of a delayed match-sample test, a spatial task that also tests working memory and behavioural flexibility. These results present important implications for the interactive effects of hypertension and genetic risk factors for AD, as AngII infusion produced cognitive impairments in both genotypes, but Tg-AngII were additionally impaired in developing a normal astrocytic response to elevated blood pressure.

4.3 Methods

4.3.1 *Animals*

Animal ethics and procedures were approved by the Animal Care Committee at Western University (protocol 2014-016) and are in compliance with Canadian and National Institute of Health Guides for the Care and Use of Laboratory Animals (NIH Publication #80-23). Homozygous TgAPP21 rats were studied to model the effect of increased brain concentrations of pathogenic hAPP³⁵. 26 male wildtype Fischer 344 rats and 29 male TgAPP21 rats were aged to 7.25 months (SD = 0.55 months), weighing an average of 367 g (SD = 38 g), before osmotic pumps were implanted to deliver saline or AngII for 8 weeks. Behavioural testing was performed during the last 2 weeks of saline or AngII infusion.

4.3.2 *Blood Pressure Elevation & Measurement*

With random allocation, 13 wildtype and 14 TgAPP21 rats were infused with normal saline (Wt, Tg); 13 Wt and 15 TgAPP21 rats were infused with AngII to elevate blood pressure (Wt-AngII, Tg-AngII)³⁸⁻⁴⁰. Osmotic pumps (Alzet, model 2004; Cupertino, CA) were filled with a saline-angiotensin II solution (Sigma Aldrich, A9525; Oakville, Ontario) or with normal saline. The angiotensin II solutions were diluted according to lot-specific osmotic pump flow rates and individual rat weight to deliver 10 000 ng/kg/h. The pumps were implanted subcutaneously on the medial dorsum at the level of the scapulae. The pump reservoir allowed for drug or saline delivery for only 4 weeks, so pumps were replaced once to allow delivery for a total of 8 weeks. Volume pressure reading tail cuffs were used to measure arterial tail blood pressure (Kent Scientific, CODA High Throughput)^{44,45}. In between pump implantation and behavioural tests, blood pressure was measured weekly, so that there were 6 measurements during the 8-week period of angiotensin II or normal saline infusion.

4.3.3 *Morris Water Maze*

On the 7th week of osmotic pump infusion of either normal saline or AngII, rats began behavioural testing. In a dimly lit room, a water tank (144 cm diameter) was filled with room temperature water, dyed with black non-toxic acrylic paint, and a target platform (12 cm diameter) was submerged below 3 cm of water. Rats were placed in a fixed start location and had to locate the hidden platform to be removed from the water tank (Figure 5A). The rats were given six 90 s learning trials (with 1 h inter-trial rest intervals) to learn the location of the submerged platform, aided by large distal visual cues; this learning schedule was adapted from Roof et al⁴⁶. Twenty-four hours after the last learning trial, the rats' memory for the platform location was evaluated on a test trial. Rats were also evaluated on a 5-day series of delayed match-sample testing, to test for performance in more challenging spatial shifts (Figure 5B)^{47,48}. Each day, during the 'sample trial', a new start location and a new platform location was used. The rats are tested on these new spatial parameters 6 h later during the 'match trial' and were assessed for improvement in their latency to find the platform. The 6 h delay was used to create a greater working memory challenge⁴⁸. This was repeated with new start and platform locations each day over 5 days.

After MWM testing was complete, potentially confounding differences in visual perception or swim speed were evaluated on cued trials, wherein the location of the platform was visibly marked. All swim paths were tracked using ANYmaze tracking software, version 4.70 (Stoelting Company; Wood Dale, IL), with a top-view webcam (C525, Logitech; Newark, CA). The experimenter was not visible to the rats during testing.

4.3.4 *Open field*

The day after MWM testing was completed, rat exploratory behaviour and anxiety was evaluated in the open field. Rats were placed in a square 45 cm open field with 40 cm black walls and a black floor and permitted to explore freely for 20 mins. A top-view webcam was used for behavioural tracking with ANYmaze software, version 4.70

(Stoelting Company; Wood Dale, IL). The experimenter was not visible to the rats during testing.

4.3.5 Immunohistochemistry & Image Processing

Immediately after all behavioural testing was complete, before pump reservoirs were depleted, rats were euthanized, perfused with 200 ml of 0.01 PBS followed by 200 ml of freshly depolymerized and buffered 4% paraformaldehyde solution (PFA), and brain tissue was collected and stored in 4% PFA for 24 h before transfer to 30% sucrose solution. 30 μm thick coronal sections were prepared from a subset of brains from each group ($n = 8 - 10$) using a cryostat (CryoStar NX50, Thermo Fischer Scientific; Ottawa, ON). DAB-mediated IHC of free floating sections was performed with an ABC-HRP kit (Thermo Fischer Scientific #32020; Ottawa, ON), a 1:1000 concentration of OX6 primary antibody for MHC II to identify activated microglia (BD Biosciences #554926; Mississauga, ON)⁴⁹, and a 1:2000 concentration of GFAP primary antibody to identify reactive astrocytes (Sigma-Aldrich #G3893; Oakville, ON)⁵⁰.

Stitched micrographs of slides were prepared using a 10x objective lens on an upright microscope (Nikon Eclipse Ni-E, Nikon DS Fi2 colour camera, NIS Elements Imaging; Mississauga, ON). Anatomical regions of interest (cingulum, corpus callosum, internal capsule, hippocampus) were captured at coronal sections: Bregma +2.00, +0.00, and -3.00 mm⁵¹. Micrographs were processed and analyzed using ImageJ, version 1.50b; after regions of interest were outlined using the polygon tool, images were converted to 8-bit, processed using the subtract background command, and then thresholded with a fixed grayscale cut-off value of 237. Percentage of area coverage by DAB-positive cells was recorded for each region of interest. The corpus callosum and cingulum were analyzed across 3 coronal planes and an average area coverage was calculated, weighted by cross-sectional area at each plane.

4.3.6 *Data Analysis*

Two-Way ANOVA and linear regressions were used to evaluate the effects of genotype and AngII infusion using GraphPad Prism 7.0 software (La Jolla, CA). ANCOVA models were used to evaluate the effect of blood pressure as a continuous predictor variable with IBM SPSS version 23 (Armonk, NY). The conservative Sidak's post-hoc analysis was used to compare outcome measures within genotype and infusate factors.

4.4 Results

4.4.1 Blood Pressure Elevation and Measurement

Average MAP was significantly elevated during the 8 weeks of AngII infusion (Figure 4-1; $p < 0.0001$, $F(1,51) = 31.52$; 2-Way ANOVA). There were no genotype differences in response to AngII infusion and its effects on MAP, DBP, and SBP. Post-hoc comparisons found a significant MAP increase of 17 ± 5 mmHg and 22 ± 6 mmHg in Wt-AngII and Tg-AngII rats, respectively (\pm SE of difference; Wt-AngII: $p = 0.004$, $t = 3.307$, $df=51$, Tg-AngII: $p < 0.0001$, $t = 4.673$, $df = 51$; Sidak's test). DBP and SBP demonstrated the same pattern of significant changes; DBP respectively increased by 12 ± 5 mmHg and 21 ± 5 mmHg in Wt-AngII and Tg-AngII rats (Wt-AngII: $p = 0.04$, $t = 2.446$, $df = 51$; Tg-AngII: $t = 4.547$, $df = 51$), while SBP respectively increased by 19 ± 5 mmHg and 21 ± 5 mmHg Wt-AngII and Tg-AngII rats (Wt-AngII: $p = 0.004$, $t = 4.039$, $df = 51$; Tg-AngII: $p < 0.0001$, $t = 4.604$, $df = 51$; Sidak's test). There were no group differences in baseline blood pressures, measured prior to pump implantation.

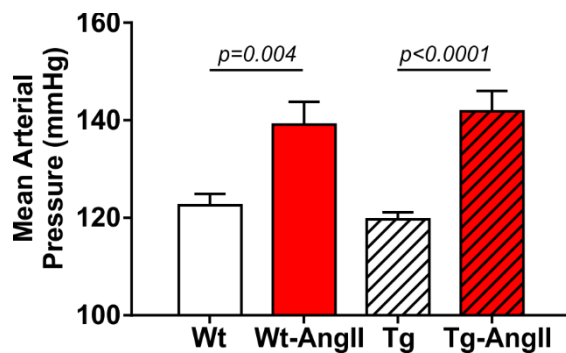


Figure 4-1: Mean Arterial Pressure during 8 weeks of normal saline or AngII infusion.

AngII infusion had a significant effect on mean arterial pressure ($p < 0.0001$). There were no differences in the genotypes' response to AngII.

$n = 13 - 15$; error bars indicate SEM.

4.4.2 Reactive Astrocytes

Reactive astrocytes were found throughout white matter, cortical, subcortical, and hippocampal regions. However, qualitative observations identified more variable degrees of astrocytosis in major white matter tracts (corpus callosum, cingulum, internal capsule) and the hippocampus, so these regions were selected for closer investigation (Figure 4-2). AngII infusion was found to have a significant effect on astrocyte activity in the corpus callosum and cingulum (Figure 4-2B; corpus callosum: $p=0.05$, $F(1,34) = 4.265$; cingulum: $p=0.03$, $F(1,34) = 4.973$; 2-Way ANOVA). This was driven by significant differences between Wt and Wt-AngII rats (corpus callosum: $p=0.03$, $t = 2.537$, $df = 34$; cingulum: $p=0.04$, $t = 2.426$, $df = 34$; Sidak's test). While area coverage by reactive astrocytes increased in the corpus callosum and cingulum of Wt-AngII rats, Tg rats also had elevated astrocytosis that did not increase further in Tg-AngII rats. Astrocytosis in the corpus callosum and cingulum was linearly correlated with MAP in wildtype rats (Figure 4-2C; $R^2 = 0.52$, $p=0.0007$, $df = 18$), but not in transgenic rats. Regardless of whether the corpus callosum and cingulum were pooled or analyzed separately, similar significant relationships were identified and the slopes of the regressions between astrocytosis and MAP were significantly different between wildtype and transgenic rats. Moreover, genotype, MAP, and their interaction were found to have significant effects on astrocytosis in the corpus callosum and cingulum in an ANCOVA model that substituted infusate allocation with MAP as a continuous predictor (genotype: $p = 0.009$, $F(1,34) = 7.568$; MAP: $p = 0.03$, $F(1,34) = 4.893$; genotype*MAP: $p = 0.02$, $F(1,34) = 6.407$; ANCOVA). The same findings of significance were observed when the corpus callosum and cingulum were analyzed separately. Absolute MAP was found to be more informative than individual increases of MAP (as compared to baseline measurements prior to pump implantation), as relative changes in MAP was not a significant predictor of astrocytosis. In Wt rats, blood pressure elevation increased white matter astrocyte reactivity to levels matching Tg and Tg-AngII rats. These findings suggest that white matter astrocyte reactivity was already saturated in Tg rats and could not increase further in response to elevated blood pressure.

In Wt-AngII rats, reactive astrocytes had extensive processes wrapping around blood vessels (Figure 4-2A). In contrast, Tg-AngII rats showed some increase of reactive astrocyte processes wrapping around blood vessels, but not as consistently as Wt-AngII. In comparison to Wt-AngII, astrocytic processes were qualitatively observed to be reduced in Tg-AngII across blood vessels ranging from 4 – 50 μm in diameter. This further supports the interpretation that astrocytes in Tg rats were already reactive at maximum capacity and could not respond to elevated blood pressure in Tg-AngII rats.

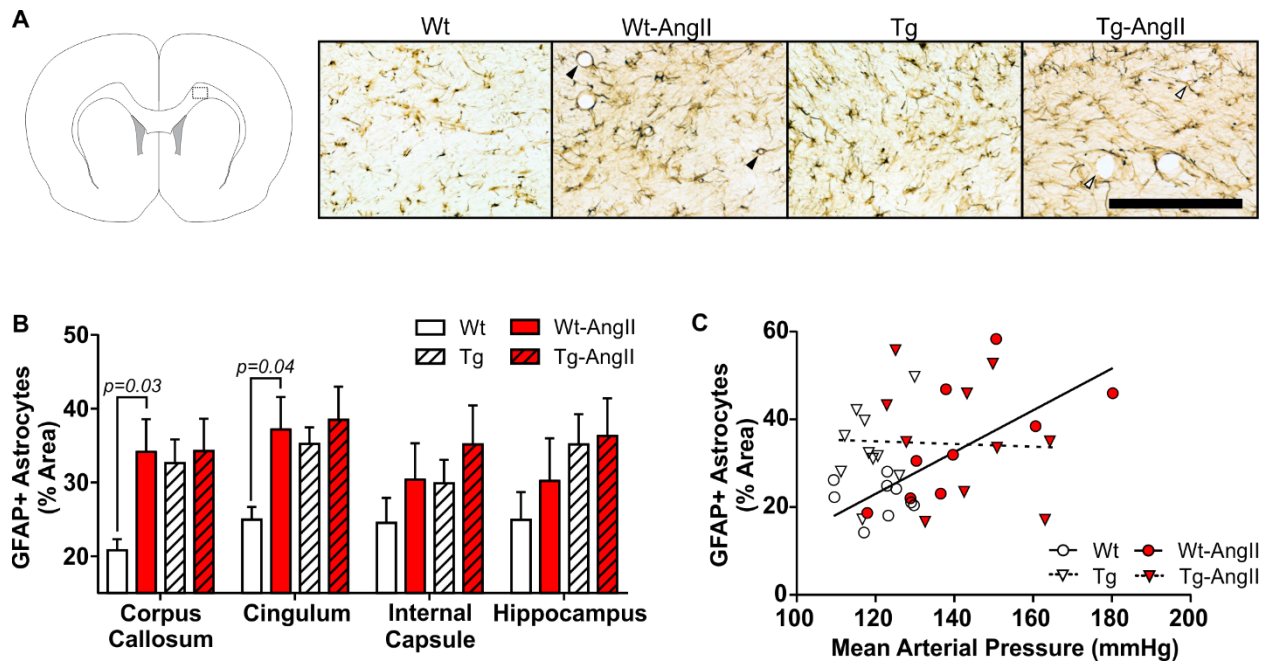


Figure 4-2: Increased white matter reactive astrocytosis in transgenic rats is unresponsive to blood pressure elevation.

Reactive astrocytes were identified using DAB-mediated IHC with a primary antibody for GFAP.

(A) The schematic shows one of the coronal planes on which the corpus callosum was analyzed (Bregma +2.0 mm). Representative images of 30 μ m thick sections were taken from the dotted outline; 200 μ m scale bar. Black triangles identify representative blood vessels with extensive astrocyte wrapping, as commonly observed in Wt-AngII rats; in comparison, white triangles identify representative blood vessels with relatively incomplete astrocyte wrapping, as observed in Tg-AngII rats.

(B) AngII infusion was found to have a significant effect on astrocyte activity in the corpus callosum and cingulum ($p < 0.05$). This was driven by significant differences between Wt and Wt-AngII rats only.

(C) Elevated mean arterial pressure linearly increased reactive astrocytosis in wildtype rats ($R^2 = 0.52$, $p = 0.0007$), but not transgenic rats. $n = 9 - 10$; error bars indicate SEM.

4.3.3 Activated Microglia

Activated microglia were found infrequently in Wt and Wt-AngII rats but they did appear consistently in major white matter tracts and the hippocampus of Tg and Tg-AngII rats (Figure 4-3A). Both Tg and Tg-AngII rats demonstrated a significant increase of microglia activation in the corpus callosum, cingulum, internal capsule, and hippocampus (Figure 4-3B; corpus callosum: $p < 0.0001$, $F(1,33) = 22.02$; cingulum: $p = 0.006$, $F(1,33) = 14.26$; internal capsule: $p = 0.0005$, $F(1,33) = 15.33$; hippocampus: $p = 0.03$, $F(1,33) = 5.248$). Neither AngII infusion nor MAP had any significant relationship with microglia activation in these regions.

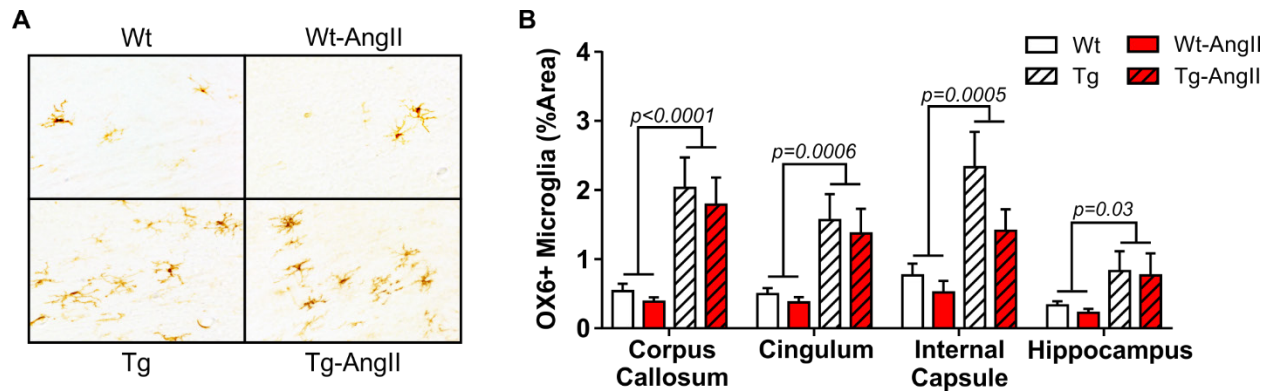


Figure 4-3: Increased white matter and hippocampal microglia activation in transgenic rats.

(A) Representative images show activated pro-inflammatory microglia in the corpus callosum and cingulum, identified using DAB mediated IHC with the OX6 primary antibody for MHC II. 30 μ m thick coronal sections; 200 μ m scale bar.

(B) Genotype was a significant factor in microglial activation in all regions analyzed. n = 8 – 10; error bars indicate SEM.

4.3.4 Open Field

Exploratory behaviour was evaluated by measuring the total distance travelled in the open field test; a subanalysis also evaluated the first 5 min period of the 20 min test, during which relatively more exploration occurs (Figure 4-4A). Genotype was a significant factor, with Tg and Tg-AngII rats having demonstrated less exploration (first 5 min: $p = 0.006$, $F(1,51) = 8.342$; full 20 min: $p < 0.0001$, $F(1,51) = 22.39$; 2-Way ANOVA). AngII infusion did not have an effect on exploratory behaviour. The centre of the field is considered to be anxiogenic, but there were no significant group differences in the proportion of time in the centre during either the first 5 min period or the full 20 min test duration (Figure 4-4B). Thus, anxiety is unlikely to have confounded behavioural measures.

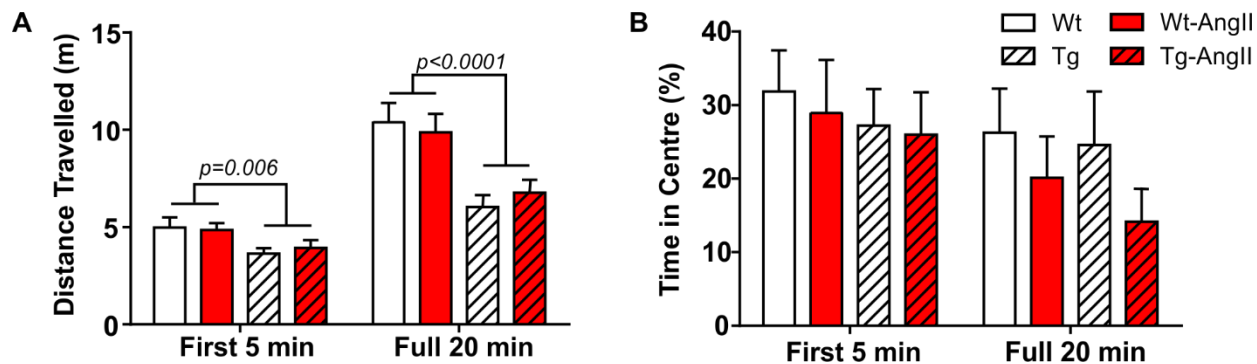


Figure 4-4: Reduced exploratory behaviour in transgenic rats.

(A) Tg and Tg-AngII travelled significantly less during both the first 5 min period of the test and during the full 20 min test, while AngII had no significant effect on distance travelled.

(B) No significant group differences were observed in avoidance of the anxiogenic centre of the open field.

n = 13 – 15; error bars indicate SEM.

4.3.5 Morris Water Maze

No group differences were observed in spatial learning and memory (Figure 4-5A). However, AngII infusion appeared to impair performance on delayed match-sample testing (Figure 4-5B). On the 'sample' trial, rats were challenged to find a new platform location every day from a new platform location for 5 days. Swim time improvement was then evaluated on a 6 h delayed 'match' trial. Trial-unique information of changing spatial parameters every day places demands on spatial reference memory, working memory, and behavioural flexibility^{47,48}. Both Wt and Tg rats demonstrated significant non-zero swim time improvements on the match trial (Wt: $p = 0.003$, $t = 4.482$, $df = 12$; Tg: $p = 0.03$, $t = 3.082$, $df = 13$; one-sample t-test with Bonferonni correction). In contrast, AngII infusion impaired rats of both genotypes, so that Wt-AngII and Tg-AngII did not demonstrate a significant swim time improvement. The frequently changing spatial parameters of delayed match-sample testing placed greater demands on spatial reference memory, working memory, and behavioural flexibility^{47,48}. However, no group differences were observed in spatial reference memory (Figure 4-5A), so AngII infusion is more likely to have impaired working memory and/or behavioural flexibility. During cued trials, no differences were observed in swim time to platform nor swim speed, so visual acuity nor mobility were unlikely to have had any confounding effect.

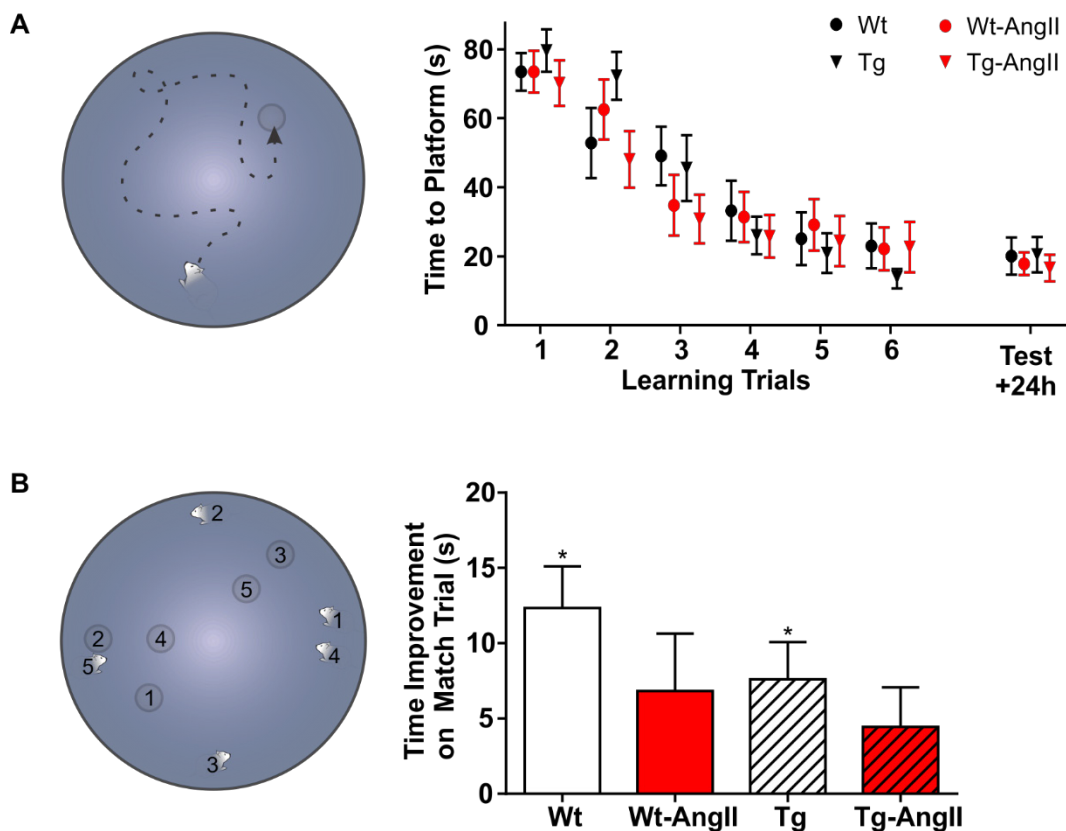


Figure 4-5: AngII infusion impaired behavioural flexibility.

(A) With a fixed start location, rats were given 6 trials to learn the platform location; 24 h later, a test trial evaluated spatial memory. No significant group differences were observed on the learning or test trials.

(B) Every day for 5 days, rats were challenged to learn a new platform location from a new start location. The randomized start and platform locations are indicated by corresponding number pairs. After the first exposure to a new platform location on a 'sample' trial, swim time improvement was measured on a 6 h delayed 'match' trial. * Wt and Tg rats demonstrated a significant swim time improvement on the match trial ($p < 0.03$) but Wt-AngII and Tg-AngII rats did not, suggesting that AngII infusion impaired working memory and/or behavioural flexibility.

$n = 13 - 15$; error bars indicate SEM.

4.5 Discussion

Normotensive Tg rats had an elevated baseline of reactive astrocytes in the corpus callosum and cingulum, while Tg-AngII rats did not show a further increase of astrocytosis. The increase of reactive astrocytes in Wt-AngII rats was accompanied with extensive astrocytic processes around blood vessels, which was less consistent and relatively incomplete in Tg-AngII. This suggested that astrocytes in transgenic rats did not develop a normal response to elevated blood pressure; the role of transgenic hAPP in this insufficient response is supported by previous findings of amyloid overwhelming astrocytes and inducing senescence in astrocytes^{52,53}. AngII infusion impaired both Wt-AngII and Tg-AngII rats in the MWM adaptation of a delayed match-sample test, a spatial task that tests working memory and behavioural flexibility, consistent with the clinical studies on the cognitive effects of hypertension²¹⁻²³. While AngII infusion did not affect activation of microglia in either genotype, Tg and Tg-AngII rats demonstrated significantly more pro-inflammatory activation of microglia in the corpus callosum, cingulum, internal capsule, and hippocampus. This further indicates dysregulation in the cerebral tissue of TgAPP21 rats and implicates pro-inflammatory microglia as an important factor in the early pre-plaque stages of AD^{42,43}. White matter microgliosis has also been identified as an important early factor of neurodegeneration in recent animal and human studies^{54,55}.

Previous studies have found detrimental histological and cognitive effects of AngII infusion or AngII blockade to be independent of blood pressure, which has been attributed to the central effects of AngII⁵⁶⁻⁵⁹. However, these studies did not present data on white matter pathology in particular. In contrast, we observed a linear astrocytic response to blood pressure elevation in the corpus callosum and cingulum of wildtype rats. While pathogenic amyloid may have obscured a linear relationship between blood pressure and white matter astrocytosis in the TgAPP21 rats, as it might in clinical studies, our finding suggests that the neurological benefit of AngII blockade may still be dependent on adequate blood pressure reduction when it comes to white matter integrity. This is particularly important for the ongoing research on therapeutic targets in the management of high blood pressure.

Perspectives

White matter and executive function are particularly vulnerable to hypertension, which is reinforced by the findings of the present study. Future preclinical research on the cerebral and cognitive effects of hypertension should evaluate more specific metabolic parameters of white matter function and the specific cognitive subdomains of executive function. The comorbidity of hypertension and pathogenic amyloid may also have an overwhelming effect on astrocytes, which are central to the maintenance of the neurovascular unit. Thus, identifying specific molecular targets in the astrocyte, such as cell signalling factors, may prove to be crucial to managing the intersection of cerebrovascular and AD-related pathology. Characterizing these dysregulations induced by hypertension and amyloid will be crucial to refining ongoing research on the neuroprotective effects of antihypertensive treatment.

4.6 References

1. Toledo JB, Arnold SE, Raible K, et al. Contribution of cerebrovascular disease in autopsy confirmed neurodegenerative disease cases in the National Alzheimer's Coordinating Centre. *Brain*. 2013;136(Pt 9):2697-2706.
2. Oveisgharan S, Hachinski V. Hypertension, executive dysfunction, and progression to dementia: the canadian study of health and aging. *Arch Neurol*. 2010;67(2):187-192.
3. Iadecola C. Hypertension and dementia. *Hypertension*. 2014;64(1):3-5.
4. Livingston G, Sommerlad A, Orgeta V, et al. Dementia prevention, intervention, and care. *Lancet*. 2017;390(10113):2673-2734.
5. Lithell H, Hansson L, Skoog I, et al. The Study on COgnition and Prognosis in the Elderly (SCOPE); outcomes in patients not receiving add-on therapy after randomization. *J Hypertens*. 2004;22(8):1605-1612.
6. Peters R, Beckett N, Forette F, et al. Incident dementia and blood pressure lowering in the Hypertension in the Very Elderly Trial cognitive function assessment (HYVET-COG): a double-blind, placebo controlled trial. *Lancet Neurol*. 2008;7(8):683-689.
7. McGuinness B, Todd S, Passmore P, et al. Blood pressure lowering in patients without prior cerebrovascular disease for prevention of cognitive impairment and dementia. *Cochrane Database Syst Rev*. 2009(4):CD004034-CD004034.
8. Sörös P, Whitehead S, Spence JD, et al. Antihypertensive treatment can prevent stroke and cognitive decline. *Nat Rev Neurol*. 2013;9(3):174-178.
9. Perrotta M, Lembo G, Carnevale D. Hypertension and Dementia: Epidemiological and Experimental Evidence Revealing a Detrimental Relationship. *Int J Mol Sci*. 2016;17(3):347.
10. Walker V, Davies N, Kehoe P, Martin R. Can treatments for hypertension be repurposed for the treatment of dementia? *Revue d'Épidémiologie et de Santé Publique*. 2018;66:S262-S262.
11. Zlokovic BV. Neurovascular mechanisms of Alzheimer's neurodegeneration. *Trends Neurosci*. 2005;28(4):202-208.
12. Zlokovic BV. Neurovascular pathways to neurodegeneration in Alzheimer's disease and other disorders. *Nat Rev Neurosci*. 2011;12(12):723-738.
13. Kisler K, Nelson AR, Montagne A, Zlokovic BV. Cerebral blood flow regulation and neurovascular dysfunction in Alzheimer disease. *Nat Rev Neurosci*. 2017;18(7):419-434.
14. Tomassoni D, Avola R, Di Tullio MA, Sabbatini M, Vitaioli L, Amenta F. Increased expression of glial fibrillary acidic protein in the brain of spontaneously hypertensive rats. *Clin Exp Hypertens*. 2004;26(4):335-350.
15. Dunn KM, Nelson MT. Neurovascular signaling in the brain and the pathological consequences of hypertension. *Am J Physiol Heart Circ Physiol*. 2014;306(1):H1-14.
16. Shen XZ, Li Y, Li L, et al. Microglia participate in neurogenic regulation of hypertension. *Hypertension*. 2015;66(2):309-316.

17. van Dijk EJ, Breteler MM, Schmidt R, et al. The association between blood pressure, hypertension, and cerebral white matter lesions: cardiovascular determinants of dementia study. *Hypertension*. 2004;44(5):625-630.
18. O'Sullivan M, Morris RG, Huckstep B, Jones DK, Williams SC, Markus HS. Diffusion tensor MRI correlates with executive dysfunction in patients with ischaemic leukoaraiosis. *J Neurol Neurosurg Psychiatry*. 2004;75(3):441-447.
19. Altamura C, Scarscia F, Quattrocchi CC, et al. Regional MRI Diffusion, White-Matter Hyperintensities, and Cognitive Function in Alzheimer's Disease and Vascular Dementia. *J Clin Neurol*. 2016;12(2):201-208.
20. Debette S, Markus HS. The clinical importance of white matter hyperintensities on brain magnetic resonance imaging: systematic review and meta-analysis. *BMJ*. 2010;341(jul26 1):c3666.
21. Raz N, Rodrigue KM, Acker JD. Hypertension and the brain: vulnerability of the prefrontal regions and executive functions. *Behav Neurosci*. 2003;117(6):1169-1180.
22. Vicario A, Martinez CD, Baretto D, Diaz Casale A, Nicolosi L. Hypertension and cognitive decline: impact on executive function. *J Clin Hypertens (Greenwich)*. 2005;7(10):598-604.
23. Li X, Ma C, Sun X, et al. Disrupted white matter structure underlies cognitive deficit in hypertensive patients. *Eur Radiol*. 2016;26(9):2899-2907.
24. Tagami M, Nara Y, Kubota A, Fujino H, Yamori Y. Ultrastructural changes in cerebral pericytes and astrocytes of stroke-prone spontaneously hypertensive rats. *Stroke*. 1990;21(7):1064-1071.
25. Yamagata K, Tagami M, Nara Y, et al. Faulty induction of blood-brain barrier functions by astrocytes isolated from stroke-prone spontaneously hypertensive rats. *Clin Exp Pharmacol Physiol*. 1997;24(9-10):686-691.
26. Tomassoni D, Bramanti V, Amenta F. Expression of aquaporins 1 and 4 in the brain of spontaneously hypertensive rats. *Brain Res*. 2010;1325:155-163.
27. Wang Y, Zhang R, Tao C, et al. Blood-Brain Barrier Disruption and Perivascular Beta-Amyloid Accumulation in the Brain of Aged Rats with Spontaneous Hypertension: Evaluation with Dynamic Contrast-Enhanced Magnetic Resonance Imaging. *Korean J Radiol*. 2018;19(3):498-507.
28. Huang J, Li J, Feng C, et al. Blood-Brain Barrier Damage as the Starting Point of Leukoaraiosis Caused by Cerebral Chronic Hypoperfusion and Its Involved Mechanisms: Effect of Agrin and Aquaporin-4. *Biomed Res Int*. 2018;2018:2321797.
29. Diaz-Ruiz C, Wang J, Ksiezak-Reding H, et al. Role of Hypertension in Aggravating Abeta Neuropathology of AD Type and Tau-Mediated Motor Impairment. *Cardiovasc Psychiatry Neurol*. 2009;2009:107286.
30. Gentile MT, Poulet R, Di Pardo A, et al. Beta-amyloid deposition in brain is enhanced in mouse models of arterial hypertension. *Neurobiol Aging*. 2009;30(2):222-228.
31. Carnevale D, Mascio G, D'Andrea I, et al. Hypertension induces brain beta-amyloid accumulation, cognitive impairment, and memory deterioration through activation of receptor for advanced glycation end products in brain vasculature. *Hypertension*. 2012;60(1):188-197.

32. Csiszar A, Tucsek Z, Toth P, et al. Synergistic effects of hypertension and aging on cognitive function and hippocampal expression of genes involved in beta-amyloid generation and Alzheimer's disease. *Am J Physiol Heart Circ Physiol*. 2013;305(8):H1120-1130.
33. Cifuentes D, Poittevin M, Dere E, et al. Hypertension accelerates the progression of Alzheimer-like pathology in a mouse model of the disease. *Hypertension*. 2015;65(1):218-224.
34. Carnevale D, Perrotta M, Lembo G, Trimarco B. Pathophysiological Links Among Hypertension and Alzheimer's Disease. *High Blood Press Cardiovasc Prev*. 2016;23(1):3-7.
35. Agca C, Fritz JJ, Walker LC, et al. Development of transgenic rats producing human beta-amyloid precursor protein as a model for Alzheimer's disease: transgene and endogenous APP genes are regulated tissue-specifically. *BMC Neurosci*. 2008;9:28.
36. Rosen RF, Fritz JJ, Dooyema J, et al. Exogenous seeding of cerebral beta-amyloid deposition in betaAPP-transgenic rats. *J Neurochem*. 2012;120(5):660-666.
37. Silverberg GD, Miller MC, Pascale CL, et al. Kaolin-induced chronic hydrocephalus accelerates amyloid deposition and vascular disease in transgenic rats expressing high levels of human APP. *Fluids Barriers CNS*. 2015;12(1):2.
38. Crowley SD, Gurley SB, Herrera MJ, et al. *Angiotensin II causes hypertension and cardiac hypertrophy through its receptors in the kidney*. 2006. 0605545103.
39. Osborn JW, Fink GD, Kuroki MT. Neural mechanisms of angiotensin II-salt hypertension: implications for therapies targeting neural control of the splanchnic circulation. *Curr Hypertens Rep*. 2011;13(3):221-228.
40. Lohmeier TE. Angiotensin II infusion model of hypertension: is there an important sympathetic component? *Hypertension*. 2012;59(3):539-541.
41. von Bernhardi R, Eugenin J. Microglial reactivity to beta-amyloid is modulated by astrocytes and proinflammatory factors. *Brain Res*. 2004;1025(1-2):186-193.
42. von Bernhardi R, Eugenin-von Bernhardi L, Eugenin J. Microglial cell dysregulation in brain aging and neurodegeneration. *Front Aging Neurosci*. 2015;7:124.
43. Prokop S, Miller KR, Heppner FL. Microglia actions in Alzheimer's disease. *Acta neuropathologica*. 2013;126(4):461-477.
44. Feng M, Whitesall S, Zhang Y, Beibel M, D'Alecy L, DiPetrillo K. Validation of volume-pressure recording tail-cuff blood pressure measurements. *Am J Hypertens*. 2008;21(12):1288-1291.
45. Kurtz TW, Griffin KA, Bidani AK, et al. Recommendations for blood pressure measurement in humans and experimental animals. Part 2: Blood pressure measurement in experimental animals: a statement for professionals from the subcommittee of professional and public education of the American Heart Association council on high blood pressure research. *Hypertension*. 2005;45(2):299-310.
46. Roof RL, Schielke GP, Ren X, Hall ED. A comparison of long-term functional outcome after 2 middle cerebral artery occlusion models in rats. *Stroke*. 2001;32(11):2648-2657.
47. Vorhees CV, Williams MT. Morris water maze: procedures for assessing spatial and related forms of learning and memory. *Nat Protoc*. 2006;1(2):848-858.

48. Bizon JL, LaSarge CL, Montgomery KS, McDermott AN, Setlow B, Griffith WH. Spatial reference and working memory across the lifespan of male Fischer 344 rats. *Neurobiol Aging*. 2009;30(4):646-655.
49. Wong WT. Microglial aging in the healthy CNS: phenotypes, drivers, and rejuvenation. *Front Cell Neurosci*. 2013;7:22.
50. Sofroniew MV, Vinters HV. Astrocytes: biology and pathology. *Acta Neuropathol*. 2010;119(1):7-35.
51. Paxinos G, Watson C. *The rat brain in stereotaxic coordinates*. 6th ed. Amsterdam ; Boston ;; Academic Press/Elsevier; 2007.
52. Bhat R, Crowe EP, Bitto A, et al. Astrocyte senescence as a component of Alzheimer's disease. *PLoS One*. 2012;7(9):e45069.
53. Sollvander S, Nikitidou E, Brolin R, et al. Accumulation of amyloid-beta by astrocytes result in enlarged endosomes and microvesicle-induced apoptosis of neurons. *Mol Neurodegener*. 2016;11(1):38.
54. Raj D, Yin Z, Breur M, et al. Increased White Matter Inflammation in Aging- and Alzheimer's Disease Brain. *Front Mol Neurosci*. 2017;10(June):206.
55. Hase Y, Horsburgh K, Ihara M, Kalaria RN. White matter degeneration in vascular and other ageing-related dementias. *J Neurochem*. 2018;144(5):617-633.
56. Tedesco MA, Ratti G, Di Salvo G, Natale F. Does the Angiotensin II Receptor Antagonist Losartan Improve Cognitive Function? *Drugs & Aging*. 2002;19(10):723-732.
57. Takeda S, Sato N, Takeuchi D, et al. Angiotensin receptor blocker prevented beta-amyloid-induced cognitive impairment associated with recovery of neurovascular coupling. *Hypertension*. 2009;54(6):1345-1352.
58. Hajjar I, Brown L, Mack WJ, Chui H. Impact of Angiotensin receptor blockers on Alzheimer disease neuropathology in a large brain autopsy series. *Arch Neurol*. 2012;69(12):1632-1638.
59. Takane K, Hasegawa Y, Lin B, et al. Detrimental Effects of Centrally Administered Angiotensin II are Enhanced in a Mouse Model of Alzheimer Disease Independently of Blood Pressure. *J Am Heart Assoc*. 2017;6(4).

Chapter 5: Striatal Ischemic Injury Exacerbates Behavioural Inflexibility

This study set out to evaluate the impact of comorbid pathogenic APP and cerebrovascular injury on executive function (Objective 3) and was conducted in close collaboration with Aaron M Regis, Vineeth Bhoadi, and Dr Seung-Hun Oh. The findings presented here reflect my contribution which focused on behavioural evaluation, namely set shifting. This study was published in *Behavioural Brain Research*.

5.1 Abstract

Alzheimer disease (AD) and stroke coexist and interact; yet how they interact is not sufficiently understood. Both AD and basal ganglia stroke can impair behavioural flexibility, which can be reliably modeled in rats using an established operant based set-shifting test. Transgenic Fischer 344-APP21 rats (TgAPP21) overexpress pathogenic human amyloid precursor protein (hAPP) but do not spontaneously develop overt pathology, hence TgAPP21 rats can be used to model the effect of vascular injury in the prodromal stages of Alzheimer disease. We demonstrate that the injection of endothelin-1 (ET1) into the dorsal striatum of TgAPP21 rats (Tg-ET1) produced an exacerbation of behavioural inflexibility with a behavioural phenotype that was distinct from saline-injected wildtype & TgAPP21 rats as well as ET1-injected wildtype rats (Wt-ET1). In addition to profiling the types of errors made, interpolative modeling using logistic exposure-response regression provided an informative analysis of the timing and efficiency of behavioural flexibility. During set-shifting, Tg-ET1 committed fewer perseverative errors than Wt-ET1. However, Tg-ET1 committed significantly more regressive errors and had a less efficient strategy change than all other groups. Thus, behavioural flexibility was more vulnerable to striatal ischemic injury in TgAPP21.

5.2 Introduction

It is well established that Alzheimer disease (AD) and stroke are frequently coincident and interact mechanistically¹⁻⁹. Stroke is not only a significant risk factor for AD²⁻⁵, but the progression of AD is exacerbated in patients who had previously experienced a stroke^{6,9}. In addition to verbal and episodic memory deficits, AD is associated with impairments in the cognitive processes underlying executive function, such as attention, working memory and behavioral flexibility¹⁰⁻¹⁷. Separately, executive dysfunction can also occur in association with vascular dementia induced by stroke^{18,19}, including covert or 'silent' strokes in the basal ganglia¹⁹⁻²². In cases of comorbid stroke in AD patients, it is known that lacunar infarcts, which affect the basal ganglia, thalamus, or deep white matter, increase the odds of dementia at lower Braak stages^{1,23}. At present, however, it is unclear whether behavioural flexibility, an important component of executive function, is affected by subcortical cerebrovascular injury coupled with AD-related pathology.

Over the past decade, a variety of preclinical rodent models have been developed to investigate the comorbidity of AD and stroke, with focus on characterizing the behavioral deficits associated with learning and memory-based tasks²⁴⁻²⁷. Conversely, behavioural testing of executive function has not been comprehensively investigated in these models even though, clinically, executive dysfunction plays a key role in the cognitive impairment of both AD and stroke. Using operant conditioning-based paradigms, it is possible to screen rodents for executive dysfunction, such as impairments in behavioral flexibility, using tasks requiring set-shifting. Consistent with patients performing the Wisconsin Card Sorting Test (WCST), a neuropsychological assessment of behavioral flexibility, these set-shifting tasks challenge rodents to update their goal-directed strategies when the rules governing what constitutes a correct behavioral response are suddenly changed²⁸. Within this context, it is reasonable to predict that a comorbid rodent model of AD and striatal stroke would lead to significant deficits in behavioral flexibility because AD patients have been found to perform worse on the WCST than age-matched control subjects²⁹⁻³³, and patients with clinical features of stroke in their basal ganglia show an inability to shift strategies during the WCST^{34,35}. Consequently, establishing a preclinical model of executive dysfunction in a comorbid rodent model of AD and stroke will facilitate future

investigations into the underlying mechanisms and offer a platform for evaluating potential therapeutic strategies.

In the present study, we endeavored to characterize behavioral flexibility following focal striatal ischemic injury in aged Fischer 344 rats expressing pathogenic human amyloid precursor protein (hAPP); the transgenic Fischer 344-APP21 rat (TgAPP21) overexpresses hAPP with Swedish and Indiana mutations³⁶. TgAPP21 rats do not develop amyloid plaques spontaneously, but do develop amyloid deposits under physiological cerebral stress^{37,38}, making this an ideal model to investigate the prodromal phases of AD pathogenesis. An operant conditioned lever-pressing task^{39,40} was used to assess the set-shifting ability of 16-month old TgAPP21 rats 3 months after unilateral striatal ischemia was induced with endothelin-1 (ET1) injection. The striatum was selected for ischemic injury due to the clinical link between subcortical lacunar infarcts and post-stroke cognitive impairment in the presence of amyloid pathology [1,9]. To characterize behavioral flexibility, the overall performance and associated error profile of ET1-injected TgAPP21 rats was compared to that of TgAPP21 rats without striatal ET1 injection, as well as age-matched wildtype rats with and without ET1 injection.

Consistent with clinical studies of AD patients, we predicted that the TgAPP21 rats would commit an increased number of errors and show increased perseverance (i.e., a failure to suppress their actions associated with the previously-correct strategy) compared to wildtype controls, and that these deficits in behavioural flexibility would be exacerbated by a unilateral striatal ischemic injury. However, in contrast to our prediction, the ET1-injected TgAPP21 rats committed more regressive errors. We further characterized this unexpected yet robust behavioral phenotype with a logistic exposure-response curve to interpolate group-wise error rates, providing an additional estimate for the efficiency and timing of strategy change. Ultimately, we demonstrated that the combined stress of focal striatal ischemic injury and mutant hAPP overexpression caused an exacerbation of behavioral inflexibility in our comorbid rat model.

5.3 Methods

5.3.1 Animals

Animal ethics and procedures were approved by the Animal Care Committee at Western University (protocol 2014-016) and are in compliance with Canadian and National Institute of Health Guides for the Care and Use of Laboratory Animals (NIH Publication #80-23). All rats used in this study were housed in facilities maintained by Western University Animal Care and Veterinary Services on a 12:12 hour light/dark cycle alternating at 1AM/PM; behavioural testing was conducted during the rats' dark cycle. To model increased brain concentrations of amyloid protein, we used homozygous transgenic Fischer 344-APP21 rats (TgAPP21). Developed by lentiviral infection of zygotes, TgAPP21 rats overexpress a pathogenic human APP sequence with Swedish and Indiana mutations, and produce high levels of beta-amyloid (both 1-40 and 1-42)³⁶. TgAPP21 rats were bred and aged in house, alongside wildtype Fischer 344. TgAPP21 homozygosity was validated using tissue samples from pups. In total, 22 transgenic male (Tg) and 18 male wildtype (Wt) rats with body mass ranging from 340-450g, aged 13 months, were used in this study.

5.3.2 Endothelin-1 Focal Ischemic Injury

Focal striatal ischemia was modelled using a unilateral injection of ET1, a potent vasoconstrictor, into the dorsal striatum of the right hemisphere⁴¹. Wildtype (Wt) and transgenic (Tg) rats were randomly selected for ET1 or saline injection: n = 8 Wt; n = 10 Wt-ET1; n = 9 Tg; and n = 13 Tg-ET1. Surgery was performed with isoflurane anaesthetic (Baxter Corporation, Mississauga, Canada; 4% with 2.0 L/min of oxygen for induction, shifted to 2% isoflurane once in surgical plane). Prior to surgery, 0.03 mg/kg buprenorphine diluted in 0.9% sterile sodium chloride (saline) was administered subcutaneously. Anaesthetized rats were secured in a Kopf stereotaxic frame and a single injection of ET1 (60 pmol dissolved in 3 μ l sterile 0.9% saline) was injected unilaterally over 5 min into the right dorsal striatum (AP: +0.5 mm, ML: 3.0 mm, DV: 5.0

mm relative to Bregma) using a 32-gauge Hamilton syringe (Hamilton Company, Reno, NV). Rats injected with equal volume of sterile saline underwent identical procedures with equivalent time under isoflurane anaesthesia, pre- and post-operative care. Following ET1 or saline injection, rats were injected with 0.03 mL of antibiotic (intramuscular enrofloxacin/Baytril, Bayer Inc., Toronto, Canada), monitored during recovery, single housed, and observed for 3 months. Strategy set shifting tests began 3 months after surgery at 16 months of age, followed by euthanasia at 17 months of age.

5.3.3 Thionine Histochemistry

Thionine staining was used to detect cellular Nissl substance and regions of glial scarring and cell loss due to ischemic injury⁴². 4 months after saline or ET1 injection (following behavioural testing), brain tissue was collected after transcardiac perfusion with freshly depolymerized and buffered 4% paraformaldehyde solution (PFA). The tissue was post-fixed in PFA for 24 h before transfer to 30% sucrose cryoprotectant. 30 µm coronal brain sections were first washed in 0.01 M PBS to remove residual cryoprotectant. Sections were mounted using 0.3% gelatin on SuperFrost Plus slides (VWR International, PA, USA) and left to dry for 24 h prior to staining. Mounted sections were rehydrated from 100% ethanol to ddH₂O, followed by 30 s exposure to a solution of 0.25% thionine (0.25% thionine acetate salt, 0.28% NaOH, 0.9% glacial acetic acid in ddH₂O). Slides were then dehydrated from 50% ethanol to Xylene, followed by cover slipping with DePex mounting medium (DePex, BDH Chemicals, Poole, UK).

5.3.4 Microscopy and Striatal Injury Analysis

Stained sections were analyzed using a Nikon Eclipse Ni-E upright microscope with a Nikon DS Fi2 colour camera head (NIS Elements Imaging), stitched photomicrographs using 2x and 10x objective lenses captured the region of injection, and anatomical identification was verified with a rat brain atlas⁴³. Infarct area was quantified by outlining regions of glial scarring and cell loss; for each rat, infarct areas were averaged from two

adjacent coronal sections at the injection site (AP: 1.92 mm relative to Bregma). Infarct areas were observed in Wt-ET1 and Tg-ET1 rats, but not Wt and Tg rats (n = 6 for all groups). During imaging and infarct area measurement, the experimenter was blinded to rat ID and experimental group.

5.3.5 *Set-Shifting*

The set shifting protocol, which includes side bias determination, is detailed in [2.3.2 Set Shift & Reversal on page 53](#). As the experiments in this chapter were performed prior the experiments of Chapter 2 & 3, the response discrimination retrieval test and reversal sessions were not yet implemented.

Briefly, rats were food restricted and maintained at 85-87% of free-feed mass to ensure motivation for 45mg sucrose pellets (Dustless precision pellets, Bio-Serv; Burlington, ON) during behavioural reinforcement in a sound-attenuated operant conditioning chamber (Med Associates; St. Albans, VT). During all training and testing, lever presses were reinforced with a sucrose pellet using a fixed-ratio 1 schedule. Habituation to the operant-chamber was followed by initial lever-press training; rats were required to lever press on at least 85 of 90 trials of lever presentations, pseudorandomly alternating sides, before progressing to visual cue discrimination.

24 h after initial training, rats were given 100 trials to learn visual cue discrimination. In each trial, both levers were extended but only the lever paired with the cue light, which pseudorandomly alternated sides, would yield a sucrose pellet reward when pressed ([Figure 2-1 on page 58](#)). The passing criterion for visual discrimination was 8 correct consecutive responses. 24 h after meeting criterion, a retrieval session of 20 visual cue discrimination trials was run to evaluate retention. Immediately after the retrieval session, 120 trials of response discrimination were initiated: only one lever would yield a sucrose pellet on all trials, even though the cue light continued to alternate sides. For each rat, the lever opposite a previously determined side bias was selected to be rewarding during response discrimination⁴⁴. This challenged the rats to ignore the previously learned visual cue discrimination and to acquire a spatial strategy, constituting an extra-dimensional set

shift. As described previously⁴⁴, response discrimination trials were binned into 16 trials of 8 congruent and 8 incongruent trials. Perseverative errors were scored when rats reverted to visual cue discrimination on incongruent trials; once rats demonstrated disengagement from visual cue discrimination (5 or fewer errors in a block of 8 incongruent trials), subsequent reversion to visual cue discrimination on incongruent trials was scored as regressive errors. Incorrect lever presses on congruent trials were scored as never-reinforced errors. Omissions (no lever press) were not treated as an error. The passing criterion for response discrimination was 8 correct consecutive responses. We departed from common approaches to operant conditioning chamber based set shifting⁴⁵ in that we allowed rats to complete all 120 trials of response discrimination instead of removing them from the chamber once they achieved criterion. This allowed us to quantify the number of errors committed after criterion, offering a more complete measure of regressive behaviour.

During all discrimination tests (visual cue, response), rats were granted a 10 s response period during which the chamber was illuminated. If the correct lever was pressed, the chamber remained illuminated for another 4 s so that rats could retrieve the sucrose pellet reward. This was followed by a dark inter-trial period so that trials lasted a total of 30 s. Cue lights were presented 3 s before lever extension and extinguished upon lever press or the end of the 10 s response period.

In addition to profiling the types of errors committed, we also applied a logistic modelling of group-wise error rates. This produced an exposure-response learning curve that could be used to interpolate when 50% of a groups' responses had transitioned to the new strategy (equivalent to the IC50 of a logistic curve) and the efficiency of this transition (Hill slope). Logistic modelling allowed for variable slopes and was bound by a 0% and 100% error rate. If a group required more trials to reach 50% strategy change (greater IC50 value), then the group had a delayed strategy change. A shallower exposure-response curve (lower Hill slope), indicated a reduced efficiency of strategy change. All set-shifting behavioural indices are summarized in [Appendix Table A-1 on page 209](#).

5.3.4 *Data Analyses*

All statistical analyses were conducted using GraphPad Prism 7.0 software (GraphPad, La Jolla, CA). Data are summarized in figures as means \pm SEM. Two-way analysis of variance (ANOVA) analyzed the effects of genotype (Wt/Tg) and injection (saline/ET1) and the interaction between these two independent factors; Tukey post-hoc tests were used to compare individual groups where main effects were found to be significant. Significance was determined with $\alpha = 0.05$.

5.4 Results

5.4.1 *Striatal Ischemic Injury*

To quantify the extent of residual striatal ischemic injury 4 months after ET1 injection, thionine staining of Nissl bodies was used to identify regions of glial scarring and cell loss. While saline injected rats (Figure 5-1AC) displayed healthy neuronal cell populations visualized using a 10x microscope objective (Figure 5-1EG), scarring in ET-1 treated rats (Figure 5-1BD) was detected by a loss of neurons and the presence of dense populations of glial cells (Figure 5-1FH). No significant differences were observed between the infarct areas of Wt-ET1 ($0.85 \pm 0.24 \text{ mm}^2$) and Tg-ET1 ($0.59 \pm 0.16 \text{ mm}^2$) rats (Figure 5-1I; unpaired t-test).

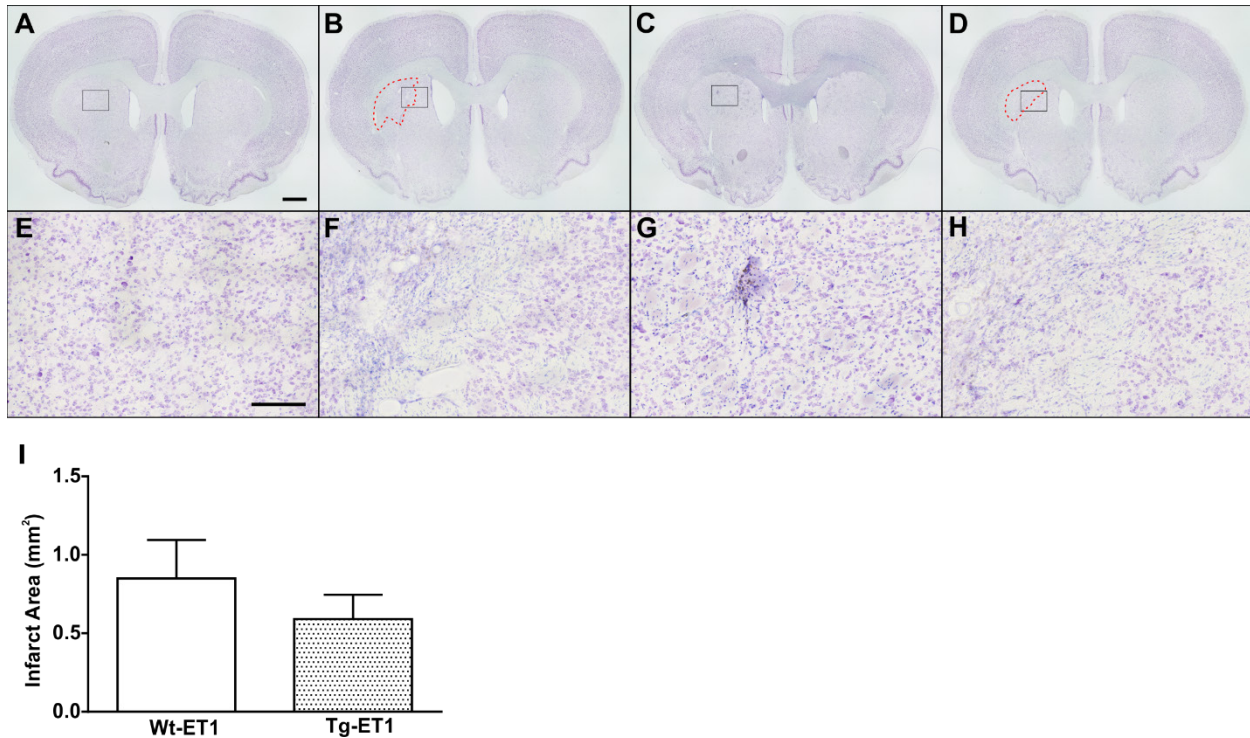


Figure 5-1: Wt-ET1 and Tg-ET1 have equal infarct areas in the ipsilateral striatum

Representative images of thionine stained coronal sections from Wt (A), Wt-ET1(B), Tg (C) and Tg-ET1 (D), captured with a 2x object lens. The black rectangles outline respective images captured with 10x objective lens magnification (E-H). Magnified images of the dorsal striatum reveal typical striatal cellular morphology in saline injected Wt and Tg rats (E,G) while Wt-ET1 and Tg-ET1 rats (F,H) have residual scars and cell loss resulting from ischemic injury; these scars are outlined by red dashes (B,D). Scale bar is 1 mm in 2x photomicrographs (A-D), and 200 μ m in 10x photomicrographs (E-H). Regions of residual scarring and cell loss in ET1 injured rats were used to quantify infarct area in the ipsilateral striatum with n = 6 samples for both groups; mean infarct area did not differ between Wt-ET1 and Tg-ET1 rats (I).

5.4.2 *Visual Cue Discrimination*

The VCD task demonstrated equal capacity for associative learning across all four experimental groups, as a two-way ANOVA revealed no differences in the number of trials needed to achieve the performance criterion (i.e., 8 correct consecutive responses) (Figure 5-2A). To determine whether genotype and/or injection affected memory retrieval of the original VCD strategy, rats were tested on 20 VCD trials the following day, just prior to the RD task (i.e., set-shifting). All groups accurately retrieved the original strategy, selecting the visual-cue paired lever on $\geq 80\%$ 20 VCD trials (Figure 5-2B); no differences were found across groups on the 20 VCD retention trials ($p > 0.05$, two-way ANOVA)

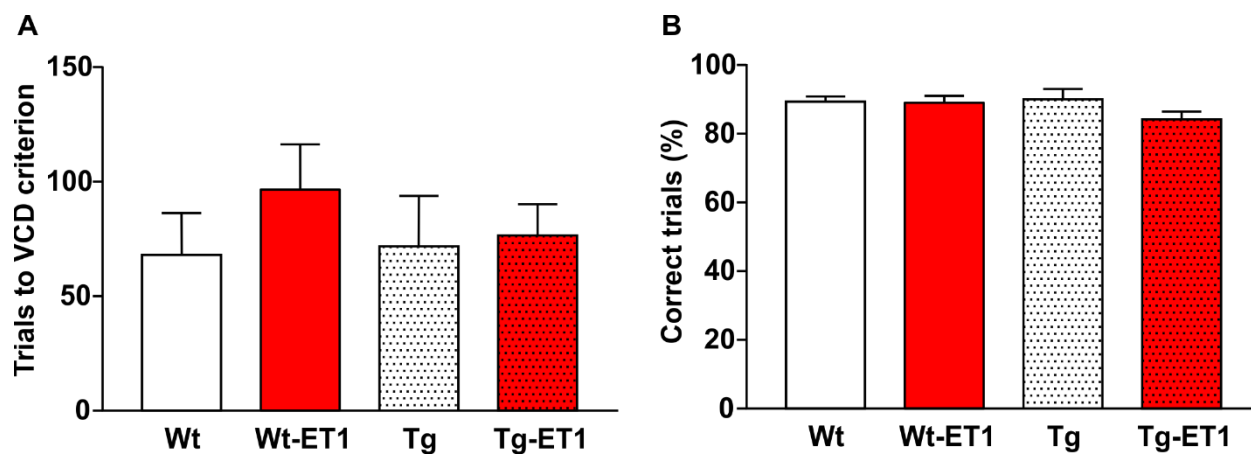


Figure 5-2: Visual cue discrimination learning and memory retrieval

(A) The number of trials before criterion (8 correct consecutive responses) did not differ across groups, indicating no differences in learning of visual cue discrimination (VCD).

(B) On the following day of testing, prior to response discrimination trials, a set of 20 VCD trials were performed. No differences were observed across groups in the number of correct responses, indicating a lack of effect of genotype or injection on the retention of the VCD strategy.

5.4.3 Set-shifting: Response Discrimination

Behavioral flexibility was assessed by comparing each group's ability to set-shift following the transition from the VCD task (i.e., "follow the light) to the RD task (i.e., only the lever opposite the rat's side bias was always correct; [Figure 2-1](#) on page 58). A two-way ANOVA found that ET1 injection caused a delay in the number of trials needed to achieve the performance criterion (8 correct consecutive responses; $F(1,36) = 7.575$, $p = 0.009$), such that Wt-ET1 and Tg-ET1 rats took longer to consistently engage the new strategy ([Figure 5-3A](#)). However, in contrast to our prediction, there were no group differences observed in either the number of errors to criterion ([Figure 5-3B](#)), errors made after achieving the performance criterion ([Figure 5-3C](#)), or total errors committed over the 120 RD trials ([Figure 5-3D](#)).

To further investigate our prediction that the TgAPP21 would demonstrate a greater increase in perseverance following striatal ischemic injury, we compared the error profiles across the treatment groups. A two-way ANOVA revealed a main effect for genotype whereby the transgenic rats actually performed fewer perseverative errors ($F(1,36) = 4.373$, $p = 0.04$), yet more never-reinforced errors ($F(1,36) = 9.04$, $p = 0.005$) and more regressive errors ($F(1,36) = 9.951$, $p = 0.003$) compared to wildtype rats ([Figure 5-4](#)). Moreover, this main effect of genotype to decrease the number of perseverative errors as well as increase the number of regressive errors was driven by the Tg-ET1 group; these rats demonstrated significantly fewer perseverative errors than the Wt-ET1 group ($p = 0.04$; Tukey's post hoc test), and significantly more regressive errors than all the other groups (Wt $p < 0.0001$, Wt-ET1 $p = 0.02$, Tg $p = 0.003$; Tukey's post hoc test). Finally, striatal injection of ET1 also produced an overall increase in the number of regressive errors committed ($F(1,36) = 18.15$, $p = 0.0001$). Collectively, these results suggest an interactive effect of ET1 injection and pathogenic hAPP expression on the error profile; however, instead of increased perseverance, these comorbid rats seemed to show a difficulty in maintaining the new strategy as the task progressed (i.e., they continued to regress to the original strategy).

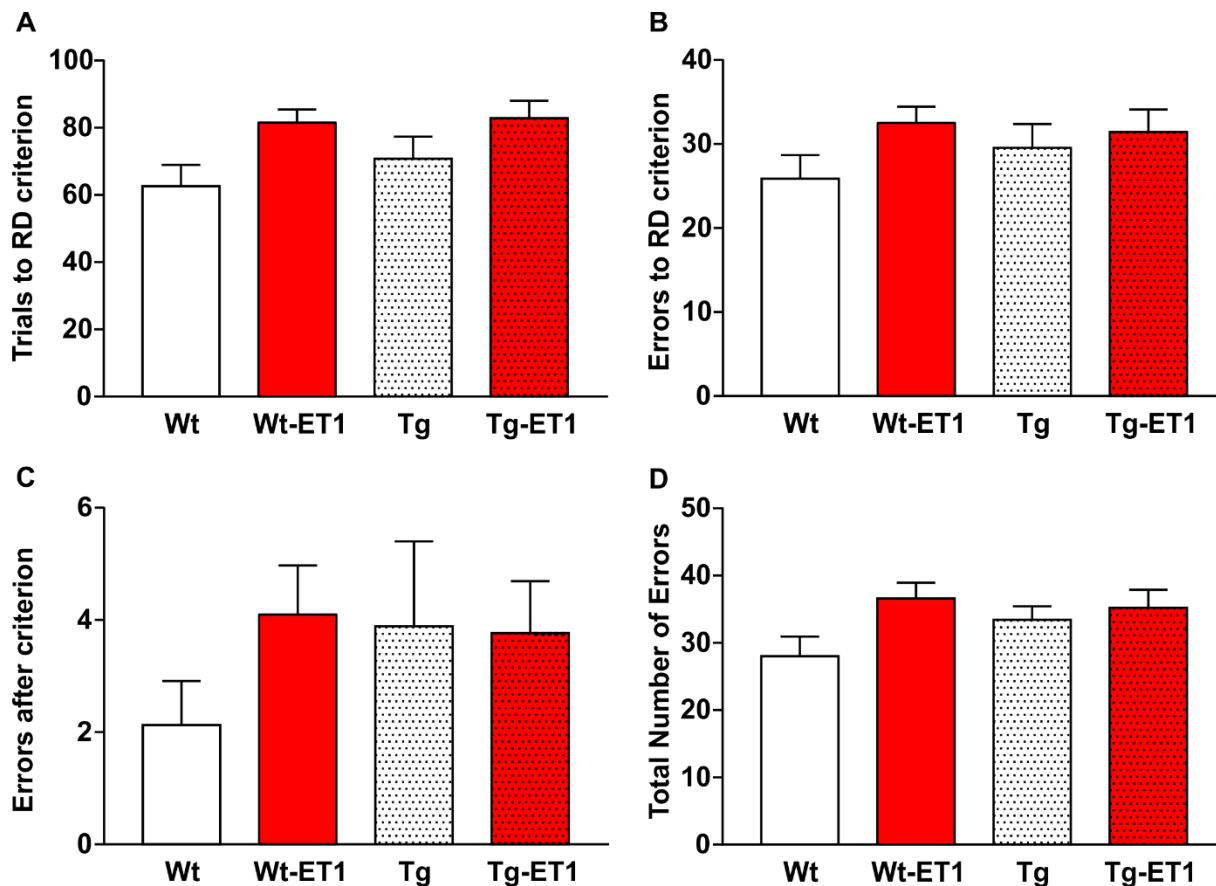


Figure 5-3: Response discrimination learning and number of errors committed during set-shifting

(A) A two-way ANOVA revealed that injection of ET1 significantly increased the number of trials to criterion (8 correct consecutive responses; $p = 0.009$), indicating a broad impairment of cognitive flexibility in ET1 injected rats. No significant effects were observed on the number of errors that were made prior to criterion (B), errors committed after the rats had achieved the test criterion (C), or total errors made over the 120 trials (D).

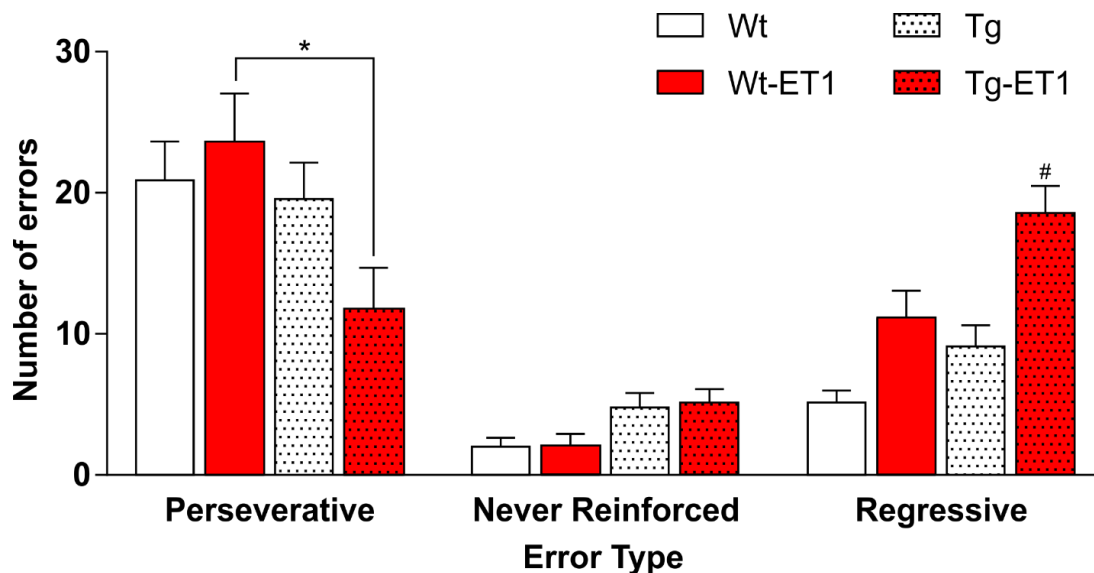


Figure 5-4: Set-shift error profile

The combination of transgene expression and ET1 injection drove the strongest change in the error profile. Among ET1 injected rats, only the Tg-ET1 group demonstrated a change in the number of perseverative errors (* $p = 0.04$, Tukey's post hoc test). Tg-ET1 also showed the greatest increase in regressive errors; #Tg-ET1 committed more regressive errors than Wt, Wt-ET1, and Tg (# $p < 0.0001$, $p = 0.02$, and $p = 0.003$ respectively, Tukey's post hoc tests). Genotype had a significant main effect on the number of perseverative errors, never-reinforced errors, and regressive errors ($p = 0.04$, $p = 0.005$, and $p = 0.003$ respectively), whereas injection type had a significant main effect on regressive errors ($p = 0.0001$).

5.4.4 Logistic Modelling: Exposure-Response Curve

The number of trials to criterion and error profiles do not capture the incremental changes that occur in each trial of RD. In contrast, a logistic model of mean group-wise error rates (Figure 5-5A) produced a behavioural exposure-response learning curve derived from all incongruent trial data (including omission trials), and therefore the incremental effect of each incongruent opportunity could be interpolated. The key indices of the exposure-response learning curves could then characterize each experimental group: the number of trials to 50% strategy change (equivalent to the IC50 of the logistic curve) is an index of when the strategy occurred, and the Hill slope of the logistic curve is an index of how efficiently that strategy change occurred.

The error rates were well modelled by a logistic curve ($R^2 = 0.74 - 0.92$; Figure 5-5A), and both the number of trials to 50% strategy change and Hill Slope were significantly different across groups ($F(6,232) = 14.98, p < 0.0001$). ET1 injection had a significant effect on the number of trials to 50% strategy change ($F(1,36) = 17.36, p = 0.0007$; Figure 5-5B). This reflects a delay in strategy change and coincides with the significant increase in the number of trials to RD performance criterion in Wt-ET1 and Tg-ET1 rats. However, the effect of injection on 50% strategy change was driven by a strong interaction with genotype ($F(1,36) = 17.36, p = 0.0002$); although ET1 injection increased the number of incongruent trials to 50% strategy change in wildtype rats (24.77 for Wt versus 34.46 for Wt-ET1), it had no effect on transgenic rats. The 50% strategy change was significantly greater in Wt-ET1 than all groups (Wt $p < 0.0001$; Tg $p = 0.01$; Tg-ET1 $p = 0.002$; Tukey's post hoc test). The Hill slope was also significantly affected by ET1 injection ($F(1,36) = 12.66, p = 0.0011$; Figure 5-5C) and was also driven by a strong interaction between ET1 injection and genotype ($F(1,36) = 11.45, p = 0.0017$). In contrast to the genotype-dependent effect on 50% strategy change, the Hill slope was reduced in transgenic rats but not in wildtype rats. The Hill slope was significantly less in Tg-ET1 than all other groups (Wt $p = 0.002$; Wt-ET1 $p = 0.001$; Tg $p < 0.0001$; Tukey's post hoc test). Thus, ET1 injection delayed strategy change in wildtype rats but not transgenic rats, and ET1 injection reduced the efficiency of strategy change in transgenic rats but not wildtype rats.

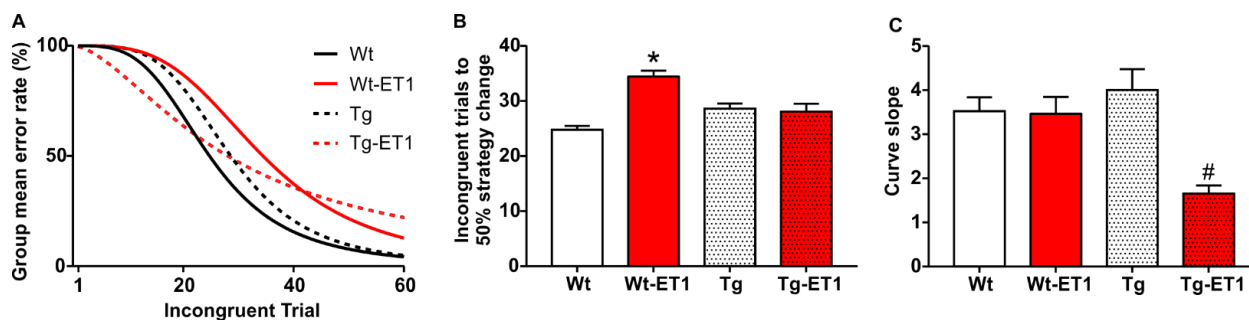


Figure 5-5: Logistic modelling of incongruent trial error rates

In wildtype rats, ET1 injection delayed strategy change, but did not impair the efficiency of strategy change. In transgenic rats, ET1 injection did not delay strategy change but slowed down the efficiency of strategy change.

(A) Logistic exposure-response regression effectively models mean group error rates on incongruent trials ($R^2 = 0.74 - 0.92$).

(B) Number of incongruent trials to 50% strategy change estimates how many response discrimination opportunities are needed for half of a group's responses to demonstrate a strategy change (i.e., when the strategy change occurs). ET1 injection had a significant effect on trials to 50% strategy change ($p = 0.0007$), which was driven by the significant difference between Wt and Wt-ET1 ($p < 0.0001$, Tukey's post hoc test); transgenic rats injected with ET1 showed no change in the mean number of trials to 50% strategy change, reflecting a significant interaction between genotype and injection ($p = 0.0002$). The Wt-ET1 group required significantly more incongruent trials to attain 50% strategy change than Wt, Tg, and Tg-ET1 rats ($*p < 0.0001$, $p = 0.01$, and $p = 0.002$ respectively, Tukey's post hoc tests).

(C) The Hill slope quantifies the steepness of an exposure-response curve, which reflects the efficiency of strategy change (i.e., how fast the strategy change occurs). ET1 injection had a significant effect on the Hill slope ($p = 0.001$), but there was a significant interaction between genotype and injection ($p = 0.002$) such that only transgenic rats demonstrated an effect of ET1 injection. Consequently, the Tg-ET1 group had a significantly lower Hill slope parameter than Wt, Wt-ET1, and Tg rats ($\#p = 0.002$, $p = 0.001$, and $p < 0.0001$ respectively, Tukey's post hoc tests).

5.5 Discussion

In the present study, an operant conditioning-based set-shifting task was used to investigate behavioral flexibility in a novel model of the combined stress of focal striatal ischemic injury and mutant pathogenic hAPP (Swedish/Indiana) expression in aged Fischer 344-APP21 rats (TgAPP21). Our Tg-ET1 rats demonstrated an unexpected increase in regressive errors but not perseverative errors. Studies of other conditions, including acute stress, autism spectrum disorders, mania, and schizophrenia, have also found surprising results regarding behavioural flexibility⁴⁶⁻⁴⁸, including increases of regressive errors⁴⁹⁻⁵⁶. To develop a better understanding of regressive errors, we complemented traditional metrics (the number of trials/errors to criterion; scoring of error types) with a logistic regression model to help quantify the timing and efficiency of strategy change.

5.5.1 Comorbidity of AD and Stroke

Numerous preclinical rodent models have investigated the mechanisms underlying the sensorimotor and cognitive deficits associated with dementia, including comorbidity models which specifically examined the interaction between AD and stroke on the performance of learning and memory-based tasks (for review, see Thiel et al., 2014)^{9,24-27}. Consistent with previous clinical investigations, the collective findings of these rodent comorbidity studies have shown that the nature and extent of the cognitive impairments depends on the age of the animals at the time of insult and assessment, as well as the location and severity of ischemic injury. It is important to note, however, that despite over a decade of animal research devoted to examining the interaction of AD and stroke, to our knowledge, the present study represents the first investigation into the performance deficits associated with set-shifting ability.

Compared to age-matched control subjects, AD patients have been found to commit more total errors in the WCST, largely due to an increase in perseverance^{29,31,32}. Similarly, patients who experienced a clinically-documented stroke in their basal ganglia also showed an inability to flexibly shift attention from one set of rules to another during the

WCST^{34,35}. Based on these clinical studies, we predicted that unilateral striatal ischemic injury would exacerbate the number of perseverative errors committed by the transgenic rats. Surprisingly, traditional error type profiling instead revealed that pathogenic hAPP expression decreased the number of perseverative errors made but increased never-reinforced errors and regressive errors, whereas ET1 injection increased the number of regressive errors only. The combined effect of pathogenic hAPP expression and ET1 injection significantly altered the types of errors committed such that the Tg-ET1 rats made the fewest perseverative errors and the greatest number of regressive errors. Interestingly, this increase in regressive errors is consistent with the error profile observed following bilateral disruption of the dorsal striatum in wildtype rats^{49,52}, even though the Tg-ET1 group had only unilateral ischemic injury.

It is important to note that although the comorbid rats in the present study showed the greatest change in error profile (Figure 5-4), it was not clear from these traditional analyses whether this shift from perseverative errors towards regressive errors truly reflected impaired behavioral flexibility, as the number of errors to criterion as well as the total number of errors committed were not significantly affected by genotype or ET1 injection (Figure 5-3). Thus, we applied a logistic model of group-wise error rates to help characterize whether Tg-ET1 rats demonstrated a true functional impairment of behavioural flexibility.

5.5.2 Logistic Modelling: Exposure-Response Curve

The number of trials or errors to criterion provides some quantification of the timing of strategy change. On the other hand, scoring error types (perseverative, never-reinforced and regressive) helps to profile the components of set-shifting behaviour, but this approach does not offer a clear sense of the timing off these errors. Furthermore, using fixed 16-trial bins to distinguish perseverative and regressive blocks limits the temporal resolution that can capture behavioural change. By interpolating group-wise error rates using a logistic exposure-response regression model derived from all incongruent trials, we could capture trial-by-trial behavioural changes. To that end, the IC50 of the logistic

curve corresponded with when 50% strategy change had been achieved, whereas the Hill slope corresponded with the efficiency of strategy change. We found that Tg-ET1 rats indeed had the most impaired in the efficiency of strategy change (Figure 5-5C); although they appeared to disengage from the visual cue strategy earlier, the Tg-ET1 had a less efficient acquisition of RD. This also raises the possibility that the timing and the efficiency of strategy change may be differentially impaired. These findings demonstrate the added value of analyzing the set-shifting test using logistic modelling (Figure 5-5).

5.5.3 Clinical Relevance of Comorbid Model

In contrast to our predictions, the combined stress of pathogenic hAPP expression and striatal ischemic injury produced a decrease in perseverative errors and a synergistic increase in regressive errors during the set-shifting task. Consequently, it may appear that our model does not replicate the increase of perseverative errors observed in mild cognitive impairment, AD, and striatal stroke²⁹⁻³⁵. However, it is important to acknowledge the possibility that differences in the semantics and paradigms of rodent set-shift tasks and the WCST may prohibit the ability to draw clear parallels for specific components of behavioural flexibility. For example, the WCST literature often describes perseverative errors in a manner that encompasses both the perseverative and regressive errors as classified in the present study^{54,55}. Furthermore, 'non-perseverative' WCST errors can also be subcategorized as 'efficient errors' and 'random errors', each associated with distinct cognitive impairments and neural correlates⁵⁷ that do not have analogous parameters in a two-dimension set-shift paradigm like that of the present study.

In support of the clinical relevance of our rat model, we elected to investigate the impact of unilateral, not bilateral, ET1 injections given that stroke victims are less likely to suffer infarcts of the same anatomy bilaterally. A bilateral injection would likely yield greater impairment of behavioural flexibility, and future studies using bilateral injections could be helpful in revealing the extent of contralateral compensation that may occur in our unilateral injection model. In the present study, rats were tested 3 months after ET1 injection (at 16 months of age) in order to capture the permanent impairment incurred by

striatal ischemia, but also to capture the impact of pathogenic hAPP on longer-term recovery. AD-related pathology has been proposed to impair angiogenesis and repair of vascular injury due to the vasculotoxic accumulation of β -amyloid, which may be an important mechanism by which coincident AD-related pathology and vascular injury have synergistic effects^{58,59}. However, it is noteworthy that infarct sizes did not differ between Wt-ET1 and Tg-ET1 rats 4 months after ET1 injury, thus differences in residual infarct size cannot account for the observed behavioural differences. In future studies, the age at injection and subsequent testing (and the delay period in between) will be additional important variables to consider, as well as the impact of therapeutic intervention and rehabilitation.

5.6 References

1. Snowdon DA, Greiner LH, Mortimer JA, Riley KP, Greiner PA, Markesbery WR. Brain infarction and the clinical expression of Alzheimer disease. The Nun Study. *JAMA*. 1997;277(10):813-817.
2. de la Torre JC. Alzheimer Disease as a Vascular Disorder: Nosological Evidence. *Stroke*. 2002;33(4):1152-1162.
3. Honig LS, Tang MX, Albert S, et al. Stroke and the risk of Alzheimer disease. *Arch Neurol*. 2003;60(12):1707-1712.
4. Gorelick PB, Scuteri A, Black SE, et al. Vascular contributions to cognitive impairment and dementia: a statement for healthcare professionals from the american heart association/american stroke association. *Stroke*. 2011;42(9):2672-2713.
5. de Bruijn RF, Ikram MA. Cardiovascular risk factors and future risk of Alzheimer's disease. *BMC Med*. 2014;12(1):130.
6. Regan C, Katona C, Walker Z, Hooper J, Donovan J, Livingston G. Relationship of vascular risk to the progression of Alzheimer disease. *Neurology*. 2006;67(8):1357-1362.
7. Whitehead SN, Cheng G, Hachinski VC, Cechetto DF. Progressive increase in infarct size, neuroinflammation, and cognitive deficits in the presence of high levels of amyloid. *Stroke*. 2007;38(12):3245-3250.
8. Attems J, Jellinger KA. The overlap between vascular disease and Alzheimer's disease--lessons from pathology. *BMC Med*. 2014;12(1):206.
9. Thiel A, Cechetto DF, Heiss WD, Hachinski V, Whitehead SN. Amyloid burden, neuroinflammation, and links to cognitive decline after ischemic stroke. *Stroke*. 2014;45(9):2825-2829.
10. Binetti G, Magni E, Padovani A, Cappa SF, Bianchetti A, Trabucchi M. Executive dysfunction in early Alzheimer's disease. *J Neurol Neurosurg Psychiatry*. 1996;60(1):91-93.
11. Fox N. Presymptomatic cognitive deficits in individuals at risk of familial Alzheimer's disease. A longitudinal prospective study. *Brain*. 1998;121(9):1631-1639.
12. Sgaramella TM, Borgo F, Mondini S, Pasini M, Toso V, Semenza C. Executive deficits appearing in the initial stage of Alzheimer's disease. *Brain Cogn*. 2001;46(1-2):264-268.
13. Backman L, Jones S, Berger AK, Laukka EJ, Small BJ. Cognitive impairment in preclinical Alzheimer's disease: a meta-analysis. *Neuropsychology*. 2005;19(4):520-531.
14. Baudic S, Barba GD, Thibaudet MC, Smagghe A, Remy P, Traykov L. Executive function deficits in early Alzheimer's disease and their relations with episodic memory. *Arch Clin Neuropsychol*. 2006;21(1):15-21.
15. Grober E, Hall CB, Lipton RB, Zonderman AB, Resnick SM, Kawas C. Memory impairment, executive dysfunction, and intellectual decline in preclinical Alzheimer's disease. *J Int Neuropsychol Soc*. 2008;14(2):266-278.
16. Belleville S, Fouquet C, Duchesne S, Collins DL, Hudon C. Detecting early preclinical alzheimer's disease via cognition, neuropsychiatry, and neuroimaging: Qualitative review and recommendations for testing. Vol 422014:S375-S382.

17. Cloutier S, Chertkow H, Kergoat MJ, Gauthier S, Belleville S. Patterns of Cognitive Decline Prior to Dementia in Persons with Mild Cognitive Impairment. *J Alzheimers Dis.* 2015;47(4):901-913.
18. Stephens S, Kenny RA, Rowan E, et al. Neuropsychological characteristics of mild vascular cognitive impairment and dementia after stroke. *Int J Geriatr Psychiatry.* 2004;19(11):1053-1057.
19. Prins ND, Scheltens P. White matter hyperintensities, cognitive impairment and dementia: an update. *Nat Rev Neurol.* 2015;11(3):157-165.
20. Roman GC, Erkinjuntti T, Wallin A, Pantoni L, Chui HC. Subcortical ischaemic vascular dementia. *Lancet Neurol.* 2002;1(7):426-436.
21. Vermeer SE, Prins ND, den Heijer T, Hofman A, Koudstaal PJ, Breteler MM. Silent brain infarcts and the risk of dementia and cognitive decline. *N Engl J Med.* 2003;348(13):1215-1222.
22. Jokinen H, Kalska H, Mantyla R, et al. Cognitive profile of subcortical ischaemic vascular disease. *J Neurol Neurosurg Psychiatry.* 2006;77(1):28-33.
23. Toledo JB, Arnold SE, Raible K, et al. Contribution of cerebrovascular disease in autopsy confirmed neurodegenerative disease cases in the National Alzheimer's Coordinating Centre. *Brain.* 2013;136(Pt 9):2697-2706.
24. Amtul Z, Nikolova S, Gao L, et al. Comorbid Abeta toxicity and stroke: hippocampal atrophy, pathology, and cognitive deficit. *Neurobiol Aging.* 2014;35(7):1605-1614.
25. Amtul Z, Whitehead SN, Keeley RJ, et al. Comorbid rat model of ischemia and beta-amyloid toxicity: striatal and cortical degeneration. *Brain Pathol.* 2015;25(1):24-32.
26. Au JL, Weishaupt N, Nell HJ, Whitehead SN, Cechetto DF. Motor and Hippocampal Dependent Spatial Learning and Reference Memory Assessment in a Transgenic Rat Model of Alzheimer's Disease with Stroke. *J Vis Exp.* 2016(109):e53089-e53089.
27. Wong RS, Cechetto DF, Whitehead SN. Assessing the Effects of Acute Amyloid beta Oligomer Exposure in the Rat. *Int J Mol Sci.* 2016;17(9):1390-1390.
28. Monchi O, Petrides M, Petre V, Worsley K, Dagher A. Wisconsin Card Sorting revisited: distinct neural circuits participating in different stages of the task identified by event-related functional magnetic resonance imaging. *J Neurosci.* 2001;21(19):7733-7741.
29. Bondi MW, Monsch AU, Butters N, Salmon DP, Paulsen JS. Utility of a modified version of the wisconsin card sorting test in the detection of dementia of the alzheimer type. *Clin Neuropsychol.* 1993;7(2):161-170.
30. Paulsen JS, Salmon DP, Monsch AU, Butters N, Swenson MR, Bondi MW. Discrimination of cortical from subcortical dementias on the basis of memory and problem-solving tests. *J Clin Psychol.* 1995;51(1):48-58.
31. Paolo AM, Axelrod BN, Troster AI, Blackwell KT, Koller WC. Utility of a Wisconsin Card Sorting Test short form in persons with Alzheimer's and Parkinson's disease. *J Clin Exp Neuropsychol.* 1996;18(6):892-897.
32. Nagahama Y, Okina T, Suzuki N, et al. Factor structure of a modified version of the wisconsin card sorting test: an analysis of executive deficit in Alzheimer's disease and mild cognitive impairment. *Dement Geriatr Cogn Disord.* 2003;16(2):103-112.

33. Chen TF, Chen YF, Cheng TW, Hua MS, Liu HM, Chiu MJ. Executive dysfunction and periventricular diffusion tensor changes in amnesic mild cognitive impairment and early Alzheimer's disease. *Hum Brain Mapp.* 2009;30(11):3826-3836.
34. Eslinger PJ, Grattan LM. Frontal lobe and frontal-striatal substrates for different forms of human cognitive flexibility. *Neuropsychologia.* 1993;31(1):17-28.
35. Su CY, Wuang YP, Chang JK, Guo NW, Kwan AL. Wisconsin Card Sorting Test performance after putaminal hemorrhagic stroke. *Kaohsiung J Med Sci.* 2006;22(2):75-84.
36. Agca C, Fritz JJ, Walker LC, et al. Development of transgenic rats producing human beta-amyloid precursor protein as a model for Alzheimer's disease: transgene and endogenous APP genes are regulated tissue-specifically. *BMC Neurosci.* 2008;9:28.
37. Rosen RF, Fritz JJ, Dooyema J, et al. Exogenous seeding of cerebral beta-amyloid deposition in betaAPP-transgenic rats. *J Neurochem.* 2012;120(5):660-666.
38. Silverberg GD, Miller MC, Pascale CL, et al. Kaolin-induced chronic hydrocephalus accelerates amyloid deposition and vascular disease in transgenic rats expressing high levels of human APP. *Fluids Barriers CNS.* 2015;12(1):2.
39. Floresco SB, Block AE, Tse MTL. Inactivation of the medial prefrontal cortex of the rat impairs strategy set-shifting, but not reversal learning, using a novel, automated procedure. *Behav Brain Res.* 2008;190(1):85-96.
40. Desai SJ, Allman BL, Rajakumar N. Combination of behaviorally sub-effective doses of glutamate NMDA and dopamine D1 receptor antagonists impairs executive function. *Behav Brain Res.* 2017;323:24-31.
41. Sozmen EG, Hinman JD, Carmichael ST. Models that matter: white matter stroke models. *Neurotherapeutics.* 2012;9(2):349-358.
42. Popp A, Jaenisch N, Witte OW, Frahm C. Identification of ischemic regions in a rat model of stroke. *PLoS One.* 2009;4(3):e4764.
43. Paxinos G, Watson C. *The rat brain in stereotaxic coordinates.* 6th ed. Amsterdam ; Boston ;; Academic Press/Elsevier; 2007.
44. Levit A, Regis AM, Garabon JR, et al. Behavioural inflexibility in a comorbid rat model of striatal ischemic injury and mutant hAPP overexpression. *Behav Brain Res.* 2017;333(June):267-275.
45. Brady AM, Floresco SB. Operant procedures for assessing behavioral flexibility in rats. *J Vis Exp.* 2015(96):e52387.
46. Durstewitz D, Vittoz NM, Floresco SB, Seamans JK. Abrupt transitions between prefrontal neural ensemble states accompany behavioral transitions during rule learning. *Neuron.* 2010;66(3):438-448.
47. Floresco SB, Zhang Y, Enomoto T. Neural circuits subserving behavioral flexibility and their relevance to schizophrenia. *Behav Brain Res.* 2009;204(2):396-409.
48. Butts KA, Floresco SB, Phillips AG. Acute stress impairs set-shifting but not reversal learning. *Behav Brain Res.* 2013;252:222-229.

49. Ragozzino ME, Jih J, Tzavos A. Involvement of the dorsomedial striatum in behavioral flexibility: role of muscarinic cholinergic receptors. *Brain Res.* 2002;953(1-2):205-214.
50. Zhang Y, Cazakoff BN, Thai CA, Howland JG. Prenatal exposure to a viral mimetic alters behavioural flexibility in male, but not female, rats. *Neuropharmacology.* 2012;62(3):1299-1307.
51. Ballendine SA, Greba Q, Dawicki W, Zhang X, Gordon JR, Howland JG. Behavioral alterations in rat offspring following maternal immune activation and ELR-CXC chemokine receptor antagonism during pregnancy: implications for neurodevelopmental psychiatric disorders. *Prog Neuropsychopharmacol Biol Psychiatry.* 2015;57:155-165.
52. Palencia CA, Ragozzino ME. The influence of NMDA receptors in the dorsomedial striatum on response reversal learning. *Neurobiol Learn Mem.* 2004;82(2):81-89.
53. Ragozzino ME, Ragozzino KE, Mizumori SJ, Kesner RP. Role of the dorsomedial striatum in behavioral flexibility for response and visual cue discrimination learning. *Behav Neurosci.* 2002;116(1):105-115.
54. Hill SK, Reilly JL, Ragozzino ME, et al. Regressing to Prior Response Preference After Set Switching Implicates Striatal Dysfunction Across Psychotic Disorders: Findings From the B-SNIP Study. *Schizophr Bull.* 2015;41(4):940-950.
55. Miller HL, Ragozzino ME, Cook EH, Sweeney JA, Mosconi MW. Cognitive set shifting deficits and their relationship to repetitive behaviors in autism spectrum disorder. *J Autism Dev Disord.* 2015;45(3):805-815.
56. Amodeo DA, Grospe G, Zang H, Dwivedi Y, Ragozzino ME. Cognitive flexibility impairment and reduced frontal cortex BDNF expression in the ouabain model of mania. *Neuroscience.* 2017;345:229-242.
57. Barceló F, Knight RT. Both random and perseverative errors underlie WCST deficits in prefrontal patients. *Neuropsychologia.* 2002;40(3):349-356.
58. Zlokovic BV. Neurovascular mechanisms of Alzheimer's neurodegeneration. *Trends Neurosci.* 2005;28(4):202-208.
59. Zlokovic BV. Neurovascular pathways to neurodegeneration in Alzheimer's disease and other disorders. *Nat Rev Neurosci.* 2011;12(12):723-738.

Chapter 6: Discussion

6.1 Summary

The studies presented in this thesis set out to advance a better understanding of the interactions between pathogenic APP, white matter inflammation, cerebrovascular disease, and executive dysfunction. In particular, these studies test the hypotheses that **ageing and pathogenic APP induces white matter inflammation, resulting in executive dysfunction** and that **vascular injury exacerbates white matter inflammation and executive dysfunction induced by ageing and pathogenic APP**. The TgAPP21 rat model of AD was studied to test these hypotheses and address the following research objectives

- 1) To determine the effect of pathogenic APP on white matter inflammation and executive function ([Chapter 2](#) and [Chapter 3](#))
- 2) To characterize the temporal relationship between age, pathogenic APP expression, white matter inflammation, and executive function ([Chapter 3](#))
- 3) To evaluate the impact of comorbid pathogenic APP and cerebrovascular stress (hypertension; [Chapter 4](#)) or injury (ischemia; [Chapter 5](#)) on executive function

The TgAPP21 rat was found to spontaneously demonstrate a regressive form of behavioural inflexibility, reversal impairments, and increased white matter microglia activation ([Chapter 2](#)). When further characterized across 4 age points, TgAPP21 rats demonstrated precocious white matter microglia activation ([Chapter 3](#)). Regressive behavioural inflexibility and reversal impairments were also observed at an earlier age in TgAPP21 rats (8 months), but Wt rats also demonstrated increased white matter microglial activation with age and a regressive target quadrant preference at 13 months of age. These findings support the hypothesis that both age and pathogenic APP induces white matter inflammation, resulting in executive dysfunction. However, behavioural inflexibility did not continue to increase with age while white matter microglia activation did. Thus, the relationship between white matter inflammation and executive dysfunction may be dynamic and age-dependent.

In studying the impact of cerebrovascular disease, Wt rats demonstrated increased white matter astrocytosis in response to hypertension, while TgAPP21 rats had an elevated baseline of white matter astrocytosis that did not increase further in response to hypertension (Chapter 4). Hypertension impaired the working memory and behavioural flexibility of both Wt and TgAPP21 rats, while striatal ischemic injury exacerbated regressive behavioural inflexibility in the TgAPP21 rats (Chapter 5). Though astrocytosis was correlated with blood pressure in Wt rats, microgliosis did not increase in response to blood pressure elevation in either Wt or TgAPP21 rats, which makes it unclear that hypertension had an effect on white matter inflammation. However, the hypothesis that cerebrovascular disease can exacerbate executive dysfunction, namely behavioural flexibility and working memory, was supported by the MWM delayed match-sample test results. Overall, the results presented in this thesis both support and suggest specific revisions to the initial hypotheses, which are explored in the following sections.

6.2 Regressive Behavioural Inflexibility

Several deviations from common protocols used in behavioural testing proved to be highly insightful. In the MWM, TgAPP21 rats demonstrated a regressive-like preference for the target quadrant. To our knowledge, this behavioural phenomenon in the MWM has not been previously described. While most implementations of the probe tests are performed for only 30 – 60 s in order to avoid extinction^{1,2}, performing the probe test for 90 s was crucial to capturing regressive behaviour in the MWM. This also presents important implications for the interpretation of the MWM test; behavioural inflexibility can confound evaluations of memory in the MWM probe. A conventional interpretation of increased target quadrant preference would suggest that TgAPP21 rats had more robust or precise memory of the learned platform location. The absence of genotype differences on memory dependent tasks, except in 22M Wt and TgAPP21 rats, makes it less likely that the TgAPP21 rats' increased target quadrant preference could be attributed to better memory. At the same time, the TgAPP21 rats' concurrent regressive behaviour during RD supports the interpretation that the TgAPP21 rats' increased preference for the target

quadrant, particularly in the last 30 s of the probe test, could be attributed to regressive inflexibility. Similarly, observing behaviour for a full 120 trials during RD, regardless of when shift criterion was observed, identified differences in the number of errors committed after criterion. In contrast, testing is commonly ceased once criterion is achieved³, although an increase of errors after criterion suggests a highly aberrant regressive inflexibility.

Thus, behavioural testing paradigms may benefit from minor modifications that better capture regressive forms of behavioural inflexibility. This extends to clinical research as well, as current neuropsychological evaluations in human subjects do not distinguish between perseverative and regressive forms of inflexibility⁴⁻⁶. This may be attributed to the recency of the notion of a *regressive* subtype of behavioural inflexibility, which was first explicitly proposed by *Ragozzino et al* in 2002 in a rat model of dorsomedial striatal injury with unimpaired perseverative flexibility but increased regressive inflexibility⁷. However, dissociated impairments analogous to regressive inflexibility have been previously described in patients with Parkinson disease⁷. Similar to the WCST, the computerized Penn Conditional Exclusion Test (PCET) offers evaluation of cognitive flexibility but with added differentiation of perseverative and regressive inflexibility⁸. The application of the PCET in studies of autism spectrum disorder^{5,9} and schizophrenia^{4,10} identified dissociated increases of regressive cognitive flexibility, which were attributed to dysfunction in the striatum and frontostriatal systems. Accordingly, ET1 injury in the TgAPP21 rats' striatum, a region commonly afflicted by SBI, resulted in an exacerbated increase of regressive inflexibility. Other conditions that disrupt the frontostriatal system, which includes extensive reciprocal connections carried in the white matter between the frontal cortex and the striatum, may also feature regressive forms of inflexibility that have been overlooked. This includes major depressive disorder¹¹, schizophrenia¹², bulimia nervosa¹³, attention-deficit/hyperactivity disorder¹⁴, obsessive-compulsive disorder^{14,15}, frontotemporal dementia¹⁶, Parkinson disease^{7,17}, and AD^{18,19}. Thus, evaluation of regressive cognitive flexibility may have far-reaching clinical significance in psychiatry and neurology. In particular, our findings support the evaluation of regressive inflexibility in patients at risk of AD, patients with MCI, or patients with cerebrovascular disease of the frontostriatal system, using methods such as the PCET.

6.3 White Matter Inflammation

While the importance of white matter integrity for executive function is widely supported in the current literature, very few studies have explored the impact of white matter inflammation on executive function in the context of neurodegenerative conditions. This is despite evidence of white matter inflammation as a common feature of both AD^{20,21} and VCI²². As new biomarker technology specific to white matter inflammation emerges, including both PET and MRI²³, and neuropsychological evaluation of both AD and VCI continues to be refined, validating the link between white matter inflammation and cognitive function will be important for evaluating future anti-inflammatory therapeutics. White matter microglial activation has been linked to executive dysfunction in a rodent in a mouse model of carotid artery occlusion²⁴ and in a mouse model of catatonic schizophrenia²⁵. In human post-mortem studies, executive dysfunction was linked to white matter microglia and astrocytic activation in both dementia pugilistica and alcohol-related neuropathology^{26,27}. Our parallel findings of increased and precocious white matter microglia activation and regressive behavioural inflexibility in the TgAPP21 rat contributes to this limited literature and suggest that this neuropathological-cognitive correlate may also present in clinical cases of AD. Microglia activation was not observed in response to blood pressure increase, and reactive astrocytosis was not observed in AngII infused TgAPP21 rats which may have reached an upper limit of astrocyte reactivity independent of blood pressure. However, Wt rats demonstrated a linear increase in white matter reactive astrocytosis in response to MAP increase. At the same time, AngII infused Wt rats failed to demonstrate significant improvement in sample trial swim time in the MWM delayed match-sample test, indicating impaired working memory and behavioural flexibility. While it was less clear that hypertension caused white matter inflammation, as compared to the effect of pathogenic APP expression on microglia activation, chronic astrocytosis due to hypertension could lead to dystrophic astrocytes and dysfunctional inflammation^{20,28}. This is also consistent with the central role of astrocytes in maintaining and recruiting microglia to the NVU²⁹⁻³¹. These findings support further investigation of white matter inflammation as a substrate of cognitive inflexibility and other forms of executive dysfunction in patients diagnosed with or at risk of AD or VCI.

6.4 Mixed Pathology

Large post-mortem studies strongly suggest that AD and VCI are not only frequently coincidental^{32,33}, but also have synergistic effects on cognitive impairment³³⁻³⁵ and neuropathology^{33,36-39}. The significance of a synergistic relationship, as opposed to a merely additive effect of two coincidental categories of neuropathology, is particularly relevant to the development of therapeutic strategies. If mechanisms that link cerebrovascular and AD pathology can be targeted, the burden of comorbidity could be greatly reduced. This is highlighted by the self-propagating pathological cycle of NVU dysfunction, for which targeted therapies are emerging^{40,41}. Further studies are needed to evaluate whether the absence of a white matter astrocytic response to hypertension in AngII-infused TgAPP21 increased the risk of neuropathology. Thus, our current findings are inconclusive on whether hypertension and pathogenic APP expression have synergistic deleterious effects. Our finding of greatly altered pattern of behavioural flexibility in TgAPP21 rats with focal striatal injury, namely an impaired efficiency in set shifting manifesting with decreased perseverative errors and increased regressive errors. The comorbidity of striatal ischemic injury and pathogenic APP expression created a disruption of behavioural flexibility that was distinct from and greater than the effect of either pathology alone. This behavioural disruption in the comorbid group also would not have been predicted from an additive combination of either pathology, suggesting a synergistic effect on cognition.

6.5 Limitations

Although TgAPP21 rats demonstrated greater regressive inflexibility as well as increased and precocious white matter microglia activation, statistical power was not adequate for evaluating direct correlations between behaviour and histology. In 8-month-old rats, reversal errors did correlate with microglia activation in the supraventricular corpus callosum, but this was not observed across all ages. Similarly, group-wise analysis identified significant correlations between forceps minor astrocytosis and the number of regressive errors, but this was not observed within the different age cohorts, including the

8-month-old rats. Furthermore, while white matter microglia activation showed a precocious and greater age-dependent increase in TgAPP21 rats, regressive behaviour peaked at 8 months of age. While this indicates that white matter activated microglia and reactive astrocytes cannot entirely predict behavioural flexibility, it does not preclude a dynamic relationship.

Though genotype differences in white matter astrocytosis was not observed in 8-month-old rats, 9-month-old TgAPP21 rats infused with saline had greater reactive astrocytosis than Wt rats infused with saline. While this difference was not significant, it was still unexpected based on the findings presented in Chapters 2 and 3. This may indicate that the methods used in Chapter 4 (anesthesia, surgery, AngII, or the osmotic minipump) had different and non-benign effects on Wt and TgAPP21 rats, including white matter astrocyte reactivity. Anesthesia and surgery have been found to activate microglia, which can affect astrocyte activity⁴². However, isoflurane has also been shown to *reduce* expression of GFAP in astrocytes⁴³. Additional control groups for the methods of Chapter 4 could have identified whether or not the increased astrocytosis observed in TgAPP21 was truly spontaneous or the result of the methods used. However, controlling for each major methodological variable (anesthesia, surgery, AngII, or the osmotic minipump) in addition genotype and infusate would not have been feasible. Moreover, while these potential confounds may challenge some of the interpretations regarding the direct effects of blood pressure elevations in Wt and TgAPP21 rats, it would still indicate that TgAPP21 rats are more prone to increased astrocyte reactivity. Thus, physiological stressors are still more likely to induce a level of astrocytosis in TgAPP21 rats that results in a ceiling of reactivity, so that further astrocyte reactivity appears not to respond to increased blood pressure.

Quantification of GFAP+ astrocytes and OX6+ microglia relied on cross-sectional area coverage by DAB staining. This approach was decided on the basis that DAB IHC does not follow a linear relationship between antigen quantity and chromogen level⁴⁴⁻⁴⁶, so instead of falsely quantifying the level of GFAP or MHC II (the target of the OX6 antibody), a binary detection of antigen-positive cells was used. This was particularly appropriate with GFAP and MHC II, which respectively differentiate reactive astrocytes and activated

microglia from quiescent astrocytes and microglia with incomplete but informative selectivity^{47,48}. Thus, increased area coverage with these antibodies indicated increased activation of these glial cells, not increased protein expression. However, the dynamic morphology of both astrocytes and microglia presents a major limitation on this method, as ramification or amoeboid phases would alter a single cells' cross-sectional area coverage. The cross-sectional area of a reactive astrocyte is greater than a quiescent astrocyte⁴⁹, while ramified quiescent microglia have a greater mean cross-sectional area than amoeboid microglia⁵⁰. Thus, increased GFAP+ area coverage should reflect either a greater number of reactive astrocytes or more extensive reactivity within the average astrocyte, while the relationship between OX6+ area coverage and microgliosis is less certain. Increased OX6+ area coverage could be due to an increase of quiescent ramified microglia or due to a greater number of activated microglia. Qualitative observation of OX6+ microglia found hyper-ramified or reactive states of activation as the most common phenotype, regardless of the number of cells that were OX6+ positive. Moreover, MHC II expression is linked upregulation of a key pro-inflammatory cytokine (IFN- γ) and downregulation of anti-inflammatory cytokine (IL-10)⁵¹. Thus, while area coverage is an imperfect DAB IHC measure of microglia activation, increased area coverage is still most likely to indicate a pro-inflammatory environment.

Lastly, the TgAPP21 rat expresses a pathogenic variant of APP that is known to cause autosomal dominant-inherited EOAD, which may involve distinct disease mechanisms from LOAD. However, while leukoaraiosis was previously associated more with LOAD, which was attributed to the more multifactorial nature of LOAD⁵², the recent DIAN study found leukoaraiosis to also be a core feature of EOAD⁵³. While the etiology of leukoaraiosis continues to be studied, the TgAPP21 rat model still offers evaluation of the role of white matter microglial activation in white matter integrity, which is pertinent to age-associated cognitive decline, VCI, EOAD, and also LOAD.

6.6 Future Directions

The studies presented in this thesis offer a foundation for several future directions of research. The TgAPP21 rat has demonstrated plaque-independent behavioural inflexibility, increased white matter inflammation, and increased vulnerability to cerebrovascular disease, two expressions of AD that corroborate clinical studies but are considered to be hallmarks of the disease. However, cognitive flexibility is important for maintaining functional independence and both inflammatory processes and vascular disease are responsive to current pharmacological interventions. Moreover, the TgAPP21 rat models early stages of AD, prior to accumulation of senile plaque and NFT; earlier identification and treatment of AD has greater potential to delay cognitive decline⁵⁴. Thus, TgAPP21 rat model offers an important opportunity to learn more of the early stages of AD, for which current diagnostic methods have limited specificity⁵⁴, and to evaluate the potential of therapeutic interventions such as anti-inflammatory medications and anti-hypertensive medications. While the benefit of NSAIDs for preventing AD has been controversial, the most recent meta-analysis of 236 000 participants in 16 cohort studies concluded that NSAID use significantly reduced AD diagnosis rate by 19%, despite considerable heterogeneity in drug and dosing regimen⁵⁵. A randomized-controlled trial did find reduced incidence when NSAID therapy was initiated in asymptomatic participants but increased incidence when treatment was initiated in participants with cognitive impairment or dementia⁵⁶. Thus, *early* intervention may be essential, for which the TgAPP21 rat would be a good model. Other emerging anti-inflammatory interventions for AD, targeting TNF- α and activation of microglia and astrocytes, would be informed by evaluation in the TgAPP21 rat model: rapamycin, minocycline, pioglitazone, thalidomide, etanercept, and celestrol⁵⁷⁻⁵⁹. Investigating the benefit of anti-hypertensive drugs on working memory impairment and astrocyte activity in the comorbid hypertensive TgAPP21 rat could also model whether and how anti-hypertensive medication may offer cognitive protection which currently, continues to be inconclusive⁶⁰⁻⁶⁵. Similarly, studying the effect of therapeutics that may the extent of stroke injury in the TgAPP21 rat may reveal important mechanisms that lead to post-stroke cognitive impairment and dementia. This includes 3K3A-APC, a modified activated protein C which has anticoagulant and

cytoprotective properties that has been shown to protect neurons and endothelial cells following ischemic injury^{66,67}. The modelling and treatment of other comorbidities and risk factors in the TgAPP21 rat that were not evaluated in this thesis, such as hearing loss, obesity, and diabetes mellitus type II⁶⁸, may also be highly informative. Several major categories of existing therapeutics are being evaluated in preclinical and clinical studies for their potential as disease modifying treatments of AD, including medications used to treat hypertension, diabetes, rheumatological conditions, viral infections, and cancer^{57,69,70}; the TgAPP21 rat may be an important preclinical model for this effort, particularly for evaluating intervention in earlier stages of AD and the impact on executive dysfunction and neuroinflammation. Therapeutic studies that show an impact, either directly or indirectly, on white matter microglial activation in the TgAPP21 rat would also offer stronger mechanistic evaluation of the role of white matter inflammation in cognitive impairment.

Establishing priorities for therapeutic intervention should be guided by further characterization of the TgAPP21 rat. While behavioural flexibility and working memory were studied in this thesis, testing paradigms have also been established for evaluation of inhibitory control, namely the stop signal task⁷¹. Astrocyte and microglia were identified using antibodies for GFAP and MHC-Class II but identifying the cell populations activated in the TgAPP21 rat or in response to vascular injury with greater specificity would require more selective molecular targets. In particular, co-labelling astrocytes and blood vessels may focus investigation on astrocytes directly involved in NVU homeostasis; co-labelling astrocytes and A β or other APP products would test whether increased astrocytosis in TgAPP21 rats infused with saline in Chapter 4 was in response to amyloid burden. Identifying subpopulations of activated microglia may also clarify the pro-inflammatory stimulus in TgAPP21 rats. Molecular targets may specify whether activated microglia are responding to amyloid protein (TREM-2, LRP receptors) or degenerated myelin (complement receptors, scavenger receptors, Galectin-3/Mac-2)⁷². Importantly, the impact of white matter microgliosis and astrocytosis on oligodendrocytes and myelin should also be evaluated in the TgAPP21 rat, as demyelination and dysfunctional oligodendrocytes has been observed in rodent models of AD and in post-mortem evaluation of AD cases, though mechanisms remain speculative⁷³. Similarly, the

functional effects of potential axonal injury by microglia and astrocytes could be evaluated by studying synaptic integrity^{74,75} in cortical, subcortical, and hippocampal tissue using IHC^{76,77}, morphological and ultrastructural analysis of synaptic spines^{78,79}, or in vivo with PET^{80,81}. Electrophysiological evaluation would also offer important functional evaluation of axonal and synaptic function⁸². Plaque-independent disruption of synaptic transmission has been observed in mouse models of AD⁸², and white matter microglial activation in the TgAPP21 warrants similar investigation.

PET imaging continues to emerge as a potentially critical diagnostic tool in AD diagnosis. However, the use of PET in clinical AD research is dominated by radiotracers for amyloid and tau protein. To study the role of microglia activation in AD, especially in the context of comorbid cerebrovascular disease, PET offers an important opportunity for in vivo evaluation. Radioligands have been developed to bind the translocator protein (TSPO), an outer-mitochondrial-membrane bound protein that is upregulated in activated microglia and astrocyte⁸³⁻⁸⁷. Preliminary data of the application of this technology in a comorbid TgAPP21 rat with striatal ischemic injury is presented in [Appendix F](#).

6.7 Conclusion

The findings presented in this thesis support the hypothesis that age and pathogenic APP induce behavioural inflexibility and white matter inflammation, as indicated by microglial activation and reactive astrocytes. Pathogenic APP in the TgAPP21 rat both increased the magnitude and accelerated the onset of behavioural inflexibility and white matter inflammation. The additional impact of hypertension as a representative form of cerebrovascular stress did not affect white matter microglia activation. However, hypertension did impair the working memory and behavioural flexibility of both Wt and TgAPP21 rats. While Wt rats demonstrated increased white matter astrocytosis in response to hypertension, TgAPP21 rats appeared to have an elevated baseline level of white matter astrocytosis and did not demonstrate a further astrocytic response to hypertension. Thus, it cannot be concluded that hypertension, a form of cerebrovascular stress, exacerbated white matter inflammation. However, the comorbidity of pathogenic

APP expression and ischemic injury did result in a synergistic impairment of behavioural flexibility; the TgAPP21 rats' vulnerability to cerebrovascular injury was more apparent following focal ischemic injury of the dorsal striatum, which resulted in greatly impaired behavioural flexibility. Thus, the TgAPP21 rat is an important model for studying the complex relationship between age, pathogenic APP, and cerebrovascular disease. The TgAPP21 rat also presents important opportunities for future evaluation of novel therapeutic interventions that target inflammatory processes and the links between AD and cerebrovascular disease. These findings support the emerging significance of white matter inflammation and executive dysfunction in the pathophysiology of ageing, AD, and VCI.

6.7 References

1. Vorhees CV, Williams MT. Morris water maze: procedures for assessing spatial and related forms of learning and memory. *Nat Protoc.* 2006;1(2):848-858.
2. Blokland A, Geraerts E, Been M. A detailed analysis of rats' spatial memory in a probe trial of a Morris task. *Behav Brain Res.* 2004;154(1):71-75.
3. Brady AM, Floresco SB. Operant procedures for assessing behavioral flexibility in rats. *J Vis Exp.* 2015(96):e52387.
4. Hill SK, Reilly JL, Ragozzino ME, et al. Regressing to Prior Response Preference After Set Switching Implicates Striatal Dysfunction Across Psychotic Disorders: Findings From the B-SNIP Study. *Schizophr Bull.* 2015;41(4):940-950.
5. Miller HL, Ragozzino ME, Cook EH, Sweeney JA, Mosconi MW. Cognitive set shifting deficits and their relationship to repetitive behaviors in autism spectrum disorder. *J Autism Dev Disord.* 2015;45(3):805-815.
6. Barceló F, Knight RT. Both random and perseverative errors underlie WCST deficits in prefrontal patients. *Neuropsychologia.* 2002;40(3):349-356.
7. Ragozzino ME, Ragozzino KE, Mizumori SJ, Kesner RP. Role of the dorsomedial striatum in behavioral flexibility for response and visual cue discrimination learning. *Behav Neurosci.* 2002;116(1):105-115.
8. Kurtz MM, Ragland JD, Moberg PJ, Gur RC. The Penn Conditional Exclusion Test: a new measure of executive-function with alternate forms of repeat administration. *Arch Clin Neuropsychol.* 2004;19(2):191-201.
9. D'Cruz AM, Ragozzino ME, Mosconi MW, Shrestha S, Cook EH, Sweeney JA. Reduced behavioral flexibility in autism spectrum disorders. *Neuropsychology.* 2013;27(2):152-160.
10. Nelson CLM, Amsbaugh HM, Reilly JL, et al. Beneficial and adverse effects of antipsychotic medication on cognitive flexibility are related to COMT genotype in first episode psychosis. *Schizophr Res.* 2018.
11. Furman DJ, Hamilton JP, Gotlib IH. Frontostriatal functional connectivity in major depressive disorder. *Biol Mood Anxiety Disord.* 2011;1(1):11.
12. Lin P, Wang X, Zhang B, et al. Functional dysconnectivity of the limbic loop of frontostriatal circuits in first-episode, treatment-naive schizophrenia. *Hum Brain Mapp.* 2018;39(2):747-757.
13. Berner LA, Marsh R. Frontostriatal circuits and the development of bulimia nervosa. *Front Behav Neurosci.* 2014;8:395.
14. Norman LJ, Carlisi CO, Christakou A, et al. Frontostriatal Dysfunction During Decision Making in Attention-Deficit/Hyperactivity Disorder and Obsessive-Compulsive Disorder. *Biol Psychiatry Cogn Neurosci Neuroimaging.* 2018;3(8):694-703.
15. Vaghi MM, Vertes PE, Kitzbichler MG, et al. Specific Frontostriatal Circuits for Impaired Cognitive Flexibility and Goal-Directed Planning in Obsessive-Compulsive Disorder: Evidence From Resting-State Functional Connectivity. *Biol Psychiatry.* 2017;81(8):708-717.

16. Bertoux M, O'Callaghan C, Flanagan E, Hodges JR, Hornberger M. Fronto-Striatal Atrophy in Behavioral Variant Frontotemporal Dementia and Alzheimer's Disease. *Front Neurol*. 2015;6:147.
17. Zgaljardic DJ, Borod JC, Foldi NS, et al. An examination of executive dysfunction associated with frontostriatal circuitry in Parkinson's disease. *J Clin Exp Neuropsychol*. 2006;28(7):1127-1144.
18. Oh H, Madison C, Villeneuve S, Markley C, Jagust WJ. Association of gray matter atrophy with age, beta-amyloid, and cognition in aging. *Cereb Cortex*. 2014;24(6):1609-1618.
19. Buckner RL. Memory and executive function in aging and AD: multiple factors that cause decline and reserve factors that compensate. *Neuron*. 2004;44(1):195-208.
20. Heppner FL, Ransohoff RM, Becher B. Immune attack: the role of inflammation in Alzheimer disease. *Nat Rev Neurosci*. 2015;16(6):358-372.
21. Raj D, Yin Z, Breur M, et al. Increased White Matter Inflammation in Aging- and Alzheimer's Disease Brain. *Front Mol Neurosci*. 2017;10(June):206.
22. Rosenberg GA. Inflammation and white matter damage in vascular cognitive impairment. *Stroke*. 2009;40(3 Suppl):S20-23.
23. Pulli B, Chen JW. Imaging Neuroinflammation - from Bench to Bedside. *J Clin Cell Immunol*. 2014;5.
24. Kim DH, Choi BR, Jeon WK, Han JS. Impairment of intradimensional shift in an attentional set-shifting task in rats with chronic bilateral common carotid artery occlusion. *Behav Brain Res*. 2016;296:169-176.
25. Janova H, Arinrad S, Balmuth E, et al. Microglia ablation alleviates myelin-associated catatonic signs in mice. *J Clin Invest*. 2018;128(2):734-745.
26. Saing T, Dick M, Nelson PT, Kim RC, Cribbs DH, Head E. Frontal cortex neuropathology in dementia pugilistica. *J Neurotrauma*. 2012;29(6):1054-1070.
27. de la Monte SM, Kril JJ. Human alcohol-related neuropathology. *Acta Neuropathol*. 2014;127(1):71-90.
28. Thal DR. The role of astrocytes in amyloid beta-protein toxicity and clearance. *Exp Neurol*. 2012;236(1):1-5.
29. Thurgur H, Pinteaux E. Microglia in the Neurovascular Unit: Blood–Brain Barrier–microglia Interactions After Central Nervous System Disorders. *Neuroscience*. 2018.
30. Barakat R, Redzic Z. The Role of Activated Microglia and Resident Macrophages in the Neurovascular Unit during Cerebral Ischemia: Is the Jury Still Out? *Med Princ Pract*. 2016;25 Suppl 1:3-14.
31. Zenaro E, Piacentino G, Constantin G. The blood-brain barrier in Alzheimer's disease. *Neurobiol Dis*. 2017;107:41-56.
32. Toledo JB, Arnold SE, Raible K, et al. Contribution of cerebrovascular disease in autopsy confirmed neurodegenerative disease cases in the National Alzheimer's Coordinating Centre. *Brain*. 2013;136(Pt 9):2697-2706.

33. Arvanitakis Z, Capuano AW, Leurgans SE, Bennett DA, Schneider JA. Relation of cerebral vessel disease to Alzheimer's disease dementia and cognitive function in elderly people: a cross-sectional study. *Lancet Neurol.* 2016;15(9):934-943.
34. Snowdon DA, Greiner LH, Mortimer JA, Riley KP, Greiner PA, Markesbery WR. Brain infarction and the clinical expression of Alzheimer disease. The Nun Study. *JAMA.* 1997;277(10):813-817.
35. Azarpazhooh MR, Avan A, Cipriano LE, Munoz DG, Sposato LA, Hachinski V. Concomitant vascular and neurodegenerative pathologies double the risk of dementia. *Alzheimer's & Dementia.* 2018;14:148-156.
36. Kisler K, Nelson AR, Montagne A, Zlokovic BV. Cerebral blood flow regulation and neurovascular dysfunction in Alzheimer disease. *Nat Rev Neurosci.* 2017;18(7):419-434.
37. Zlokovic BV. Neurovascular mechanisms of Alzheimer's neurodegeneration. *Trends Neurosci.* 2005;28(4):202-208.
38. Zlokovic BV. Neurovascular pathways to neurodegeneration in Alzheimer's disease and other disorders. *Nat Rev Neurosci.* 2011;12(12):723-738.
39. Iadecola C. Neurovascular regulation in the normal brain and in Alzheimer's disease. *Nat Rev Neurosci.* 2004;5(5):347-360.
40. Carnevale D, Mascio G, D'Andrea I, et al. Hypertension induces brain beta-amyloid accumulation, cognitive impairment, and memory deterioration through activation of receptor for advanced glycation end products in brain vasculature. *Hypertension.* 2012;60(1):188-197.
41. Deane R, Singh I, Sagare AP, et al. A multimodal RAGE-specific inhibitor reduces amyloid beta-mediated brain disorder in a mouse model of Alzheimer disease. *J Clin Invest.* 2012;122(4):1377-1392.
42. Bell JD, Stary CM. Anesthetic neurotoxicity: an emerging role for glia in neuroprotection. *J Mol Med (Berl).* 2017;95(4):349-351.
43. Culley DJ, Cotran EK, Karlsson E, et al. Isoflurane affects the cytoskeleton but not survival, proliferation, or synaptogenic properties of rat astrocytes in vitro. *Br J Anaesth.* 2013;110 Suppl 1:i19-28.
44. van der Loos CM. Multiple immunoenzyme staining: methods and visualizations for the observation with spectral imaging. *J Histochem Cytochem.* 2008;56(4):313-328.
45. Shu J, Dolman GE, Duan J, Qiu G, Ilyas M. Statistical colour models: an automated digital image analysis method for quantification of histological biomarkers. *Biomed Eng Online.* 2016;15:46.
46. Rimm DL. What brown cannot do for you. *Nat Biotechnol.* 2006;24(8):914-916.
47. Sofroniew MV, Vinters HV. Astrocytes: biology and pathology. *Acta Neuropathol.* 2010;119(1):7-35.
48. Wong WT. Microglial aging in the healthy CNS: phenotypes, drivers, and rejuvenation. *Front Cell Neurosci.* 2013;7:22.
49. Rodriguez JJ, Olabarria M, Chvatal A, Verkhratsky A. Astroglia in dementia and Alzheimer's disease. *Cell Death Differ.* 2009;16(3):378-385.

50. Caldeira C, Oliveira AF, Cunha C, et al. Microglia change from a reactive to an age-like phenotype with the time in culture. *Front Cell Neurosci.* 2014;8:152.
51. Frank MG, Barrientos RM, Biedenkapp JC, Rudy JW, Watkins LR, Maier SF. mRNA up-regulation of MHC II and pivotal pro-inflammatory genes in normal brain aging. *Neurobiol Aging.* 2006;27(5):717-722.
52. Andreasen N, Hesse C, Davidsson P, et al. Cerebrospinal fluid beta-amyloid(1-42) in Alzheimer disease: differences between early- and late-onset Alzheimer disease and stability during the course of disease. *Arch Neurol.* 1999;56(6):673-680.
53. Lee S, Viqar F, Zimmerman ME, et al. White matter hyperintensities are a core feature of Alzheimer's disease: Evidence from the dominantly inherited Alzheimer network. *Ann Neurol.* 2016;79(6):929-939.
54. Solomon A, Mangialasche F, Richard E, et al. Advances in the prevention of Alzheimer's disease and dementia. *J Intern Med.* 2014;275(3):229-250.
55. Zhang C, Wang Y, Wang D, Zhang J, Zhang F. NSAID Exposure and Risk of Alzheimer's Disease: An Updated Meta-Analysis From Cohort Studies. *Front Aging Neurosci.* 2018;10:83.
56. Breitner JC, Baker LD, Montine TJ, et al. Extended results of the Alzheimer's disease anti-inflammatory prevention trial. *Alzheimers Dement.* 2011;7(4):402-411.
57. Corbett A, Williams G, Ballard C. Drug repositioning in Alzheimer's disease. *Front Biosci (Schol Ed).* 2015;7:184-188.
58. Calsolaro V, Edison P. Neuroinflammation in Alzheimer's disease: Current evidence and future directions. *Alzheimers Dement.* 2016;12(6):719-732.
59. Decourt B, Lahiri DK, Sabbagh MN. Targeting Tumor Necrosis Factor Alpha for Alzheimer's Disease. *Curr Alzheimer Res.* 2017;14(4):412-425.
60. Lithell H, Hansson L, Skoog I, et al. The Study on COgnition and Prognosis in the Elderly (SCOPE); outcomes in patients not receiving add-on therapy after randomization. *J Hypertens.* 2004;22(8):1605-1612.
61. Peters R, Beckett N, Forette F, et al. Incident dementia and blood pressure lowering in the Hypertension in the Very Elderly Trial cognitive function assessment (HYVET-COG): a double-blind, placebo controlled trial. *Lancet Neurol.* 2008;7(8):683-689.
62. McGuinness B, Todd S, Passmore P, et al. Blood pressure lowering in patients without prior cerebrovascular disease for prevention of cognitive impairment and dementia. *Cochrane Database Syst Rev.* 2009(4):CD004034-CD004034.
63. Sörös P, Whitehead S, Spence JD, et al. Antihypertensive treatment can prevent stroke and cognitive decline. *Nat Rev Neurol.* 2013;9(3):174-178.
64. Perrotta M, Lembo G, Carnevale D. Hypertension and Dementia: Epidemiological and Experimental Evidence Revealing a Detrimental Relationship. *Int J Mol Sci.* 2016;17(3):347.
65. Walker V, Davies N, Kehoe P, Martin R. Can treatments for hypertension be repurposed for the treatment of dementia? *Revue d'Épidémiologie et de Santé Publique.* 2018;66:S262-S262.

66. Guo H, Singh I, Wang Y, et al. Neuroprotective activities of activated protein C mutant with reduced anticoagulant activity. *European Journal of Neuroscience*. 2009;29(6):1119-1130.
67. D. Williams P, V. Zlokovic B, H. Griffin J, E. Pryor K, P. Davis T. Preclinical Safety and Pharmacokinetic Profile of 3K3A-APC, a Novel, Modified Activated Protein C for Ischemic Stroke. *Current Pharmaceutical Design*. 2012;18(27):4215-4222.
68. Livingston G, Sommerlad A, Orgeta V, et al. Dementia prevention, intervention, and care. *Lancet*. 2017;390(10113):2673-2734.
69. Appleby BS, Nacopoulos D, Milano N, Zhong K, Cummings JL. A review: treatment of Alzheimer's disease discovered in repurposed agents. *Dement Geriatr Cogn Disord*. 2013;35(1-2):1-22.
70. Corbett A, Pickett J, Burns A, et al. Drug repositioning for Alzheimer's disease. *Nature Reviews Drug Discovery*. 2012;11(11):833-846.
71. Mayse JD, Nelson GM, Park P, Gallagher M, Lin SC. Proactive and reactive inhibitory control in rats. *Front Neurosci*. 2014;8:104.
72. Fu R, Shen Q, Xu P, Luo JJ, Tang Y. Phagocytosis of microglia in the central nervous system diseases. *Mol Neurobiol*. 2014;49(3):1422-1434.
73. Nasrabady SE, Rizvi B, Goldman JE, Brickman AM. White matter changes in Alzheimer's disease: a focus on myelin and oligodendrocytes. *Acta Neuropathol Commun*. 2018;6(1):22.
74. Terry RD, Masliah E, Salmon DP, et al. Physical basis of cognitive alterations in Alzheimer's disease: synapse loss is the major correlate of cognitive impairment. *Ann Neurol*. 1991;30(4):572-580.
75. Neuman KM, Molina-Campos E, Musial TF, et al. Evidence for Alzheimer's disease-linked synapse loss and compensation in mouse and human hippocampal CA1 pyramidal neurons. *Brain Struct Funct*. 2015;220(6):3143-3165.
76. Masliah E, Terry RD, DeTeresa RM, Hansen LA. Immunohistochemical quantification of the synapse-related protein synaptophysin in Alzheimer disease. *Neurosci Lett*. 1989;103(2):234-239.
77. Ippolito DM, Eroglu C. Quantifying synapses: an immunocytochemistry-based assay to quantify synapse number. *J Vis Exp*. 2010(45).
78. Scheff SW, Price DA. Synaptic pathology in Alzheimer's disease: a review of ultrastructural studies. *Neurobiol Aging*. 2003;24(8):1029-1046.
79. Mancuso JJ, Chen Y, Li X, Xue Z, Wong ST. Methods of dendritic spine detection: from Golgi to high-resolution optical imaging. *Neuroscience*. 2013;251:129-140.
80. Chen MK, Mecca AP, Naganawa M, et al. Assessing Synaptic Density in Alzheimer Disease With Synaptic Vesicle Glycoprotein 2A Positron Emission Tomographic Imaging. *JAMA Neurol*. 2018.
81. Finnema SJ, Nabulsi NB, Eid T, et al. Imaging synaptic density in the living human brain. *Sci Transl Med*. 2016;8(348):348ra396.
82. Hsia AY, Masliah E, McConlogue L, et al. Plaque-independent disruption of neural circuits in Alzheimer's disease mouse models. *Proc Natl Acad Sci U S A*. 1999;96(6):3228-3233.

83. Venneti S, Lopresti BJ, Wiley CA. The peripheral benzodiazepine receptor (Translocator protein 18kDa) in microglia: from pathology to imaging. *Prog Neurobiol.* 2006;80(6):308-322.
84. Chen MK, Guilarte TR. Translocator protein 18 kDa (TSPO): molecular sensor of brain injury and repair. *Pharmacol Ther.* 2008;118(1):1-17.
85. Lavisse S, Guillermier M, Herard AS, et al. Reactive astrocytes overexpress TSPO and are detected by TSPO positron emission tomography imaging. *J Neurosci.* 2012;32(32):10809-10818.
86. Vivash L, O'Brien TJ. Imaging Microglial Activation with TSPO PET: Lighting Up Neurologic Diseases? *J Nucl Med.* 2016;57(2):165-168.
87. Wilson AA, Garcia A, Parkes J, et al. Radiosynthesis and initial evaluation of [18F]-FEPPA for PET imaging of peripheral benzodiazepine receptors. *Nucl Med Biol.* 2008;35(3):305-314.

Appendices

Appendix A: Set Shift Data Extraction	203
A1 MED-PC to Excel Conversion	204
A2 Visual Cue Workbook	205
A3 Response Discrimination Workbook	206
Appendix B: MWM Regressive Preference for Target Quadrant	210
Appendix C: Immunohistochemistry Protocols	211
C1 Solutions	211
C2 Immunohistochemistry Protocol	213
Appendix D: Microscopy and Image Analysis Protocols	214
D1 Threshold Analysis: Detailed Walkthrough	217
D2 Threshold Analysis: Protocol Summary	225
Appendix E: Rat Tail Cuff Blood Pressure Measurement Protocol	226
E1 Background	226
E2 Equipment Use & Maintenance	228
E2.1 Software Set-up	228
E2.2 Recommended Session Parameters	229
E2.3 Warming Platform	229
E2.4 Cuff Replacement	230
E2.5 Cleaning & Storage	230
E2.6 Animal Handling	231
E3 Data Quality & Analysis	231
E4 Operating Summary	234
E5 References	236

	201
Appendix F: PET/MRI Study	237
F1 Introduction	237
F1.1 Objectives	238
F2 Methods	238
F3 Results	240
F4 Conclusions	243
F5 References	244
Appendix G: Animal Use Protocol	246

List of Appendix Tables

Appendix Table A-1: Set Shifting Indices	209
--	-----

List of Appendix Figures

Appendix Figure A-1: MED-PC to Excel Setup	204
Appendix Figure A-2: Sample Visual Cue Discrimination Output	205
Appendix Figure A-3: Sample Response Discrimination Output for Error Profile	207
Appendix Figure A-4: Sample Response Discrimination Output for Logistic Regression of Mean Group Error Rates	208
Appendix Figure D-1: Microscope Imaging Parameters	214
Appendix Figure D-2: Focus Surface Setup	215
Appendix Figure D-3: Micrograph Stitching	216
Appendix Figure D-4: Forceps Minor	219

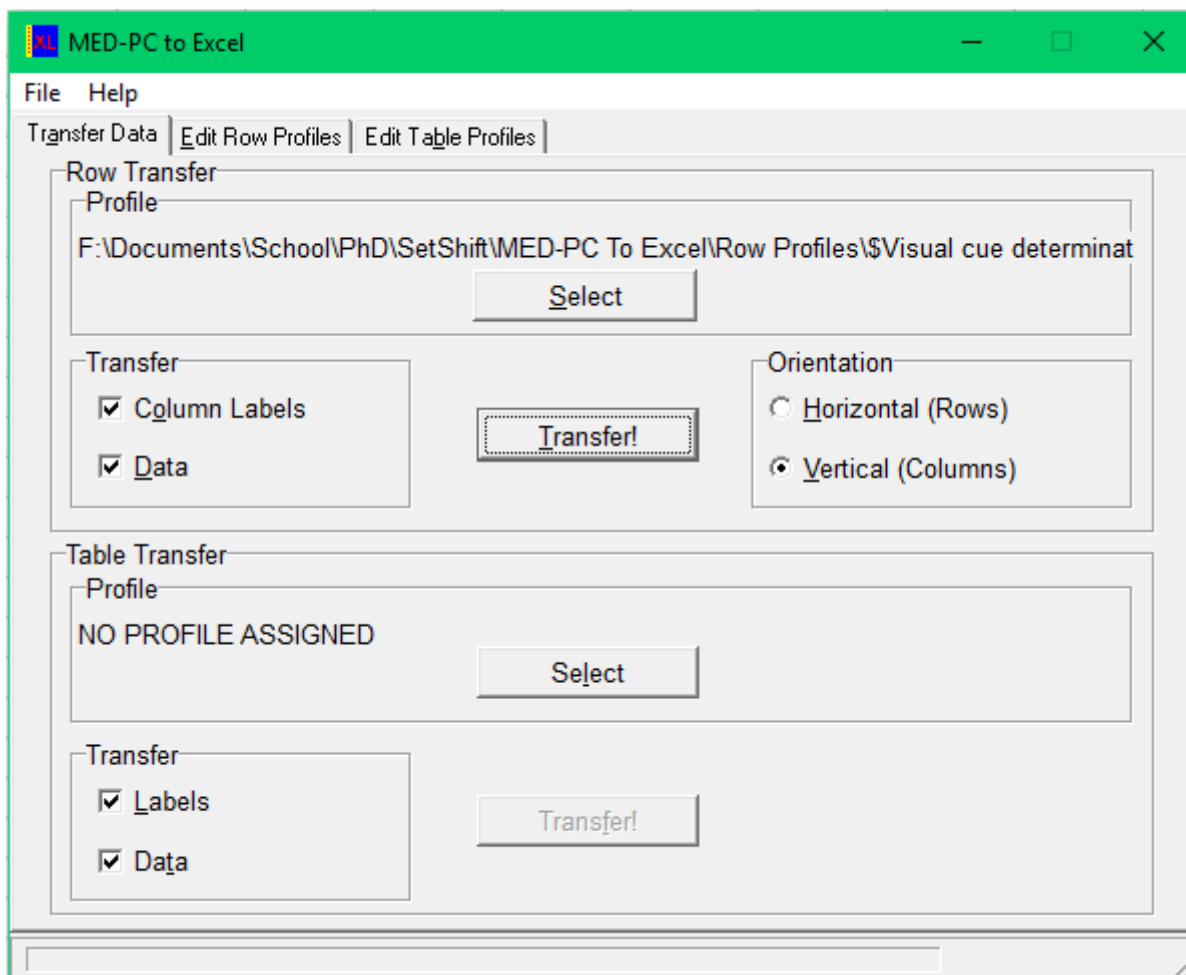
	202
Appendix Figure D-5: Anterior Corpus Callosum	220
Appendix Figure D-6: Anterior Supraventricular Corpus Callosum	220
Appendix Figure D-7: Anterior Cingulum	221
Appendix Figure D-8: Middle corpus callosum, supraventricular corpus callosum, cingulum	221
Appendix Figure D-9: Posterior Corpus Callosum, Cingulum	222
Appendix Figure D-10: Internal capsule	222
Appendix Figure D-11: Anterior Dorsal Hippocampus	223
Appendix Figure D-12: Posterior Dorsal and Ventral Hippocampus	223
Appendix Figure E-1: Cuff Positioning on Restrained Rat's Tail	226
Appendix Figure E-2: Sample channel output for one cycle	227
Appendix Figure E-3: Suggested organization of data	233
Appendix Figure F-1: Endothelin-1 injection into the dorsal striatum	239
Appendix Figure F-2: Brain Segmentation Model	239
Appendix Figure F-3: Immunohistochemistry Corroborates ¹⁸ F-FEPPA-PET/MR Findings	240
Appendix Figure F-4: ¹⁸ F-FEPPA Uptake Following Injury Persists in Anterior White Matter Tracts	241
Appendix Figure F-5: Mean Transit Time Prolonged by Ischemic Injury	241
Appendix Figure F-6: ¹⁸ F-FEPPA Kinetic Profile	242

Appendix A: Set Shift Data Extraction

This appendix details the *Excel* (Microsoft) workbooks that were developed to extract meaningful set shifting data from the raw data generated by *MED-PC* software (Med Associates; St. Albans, VT). The supplemental file, *Visual Cue Workbook.xlsm*, extracts visual cue discrimination data and relies on the import of raw data using the *MED-PC to Excel* tool provided by Med Associates. The supplemental file, *Response Discrimination Workbook.xlsm*, extracts response discrimination data and also relies on the import of raw data using the *MED-PC to Excel* tool provided by Med Associates and includes VBA macros. To ensure the stability of the workbooks, the files are designated as 'read-only'; do not save or overwrite the files and copy any extracted data into separate data files. The workbooks were developed using Excel 2016; the instructions outlined below are specific to Excel 2016.

A1 MED-PC to Excel Conversion

1. Open MPC2XL.EXE (MED-PC to Excel)
2. Under “Row Transfer” in the “Transfer Data” tab, press “Select”
3. Open “\$Visual cue deminationnew.MRP” for visual cue discrimination files, open “\$Shift Response Discrimination.MRP” for response discrimination files.
4. Make sure both “Column Labels” and “Data” are select under the “Transfer” box
5. Select “Vertical (Column)” under the “Orientation” box
6. Open Excel workbook and ensure that the A1 cell on the first tab (*Input*) is selected; this applies to both workbooks. Transferring data into any other cell can cause irreversible malfunction of the workbooks.
7. Return to MED-PC to Excel, press “Transfer”, select raw data file



Appendix Figure A-1: MED-PC to Excel Setup

A2 Visual Cue Workbook

Once data is transferred into *Visual Cue Workbook.xlsx*, key measures will appear in cells E3-5: Trials to Criterion, Errors to Criterion, Errors after Criterion. Criterion is set to 8 consecutive correct response. Omissions do not reset a series of correct responses. Rows 27-426 show raw data with annotations: Trial number, whether criteria have been met, running total counts of errors, and running counts of consecutive correct responses (performance).

	A	B	C	D	E
1	Subject	TGM104.1			
2	StartDate	170509			
3	StartTime	230533		Trials to Criterion	40
4	Experiment	VC1		Errors to Criterion	12
5	Group	4MOB		Errors After Criterion	12
6	Box	1			
7	Comment				
8	Max Number of Trials	100			
9	Min Number of Trails	100			
10	Performance Criterion	10			
11	Stimulus Length (sec)	3			
12	Trial Length (sec)	20			
13	Lever Response Time (sec)	10			
14	Reward Length (sec)	4			
15	Trial #,B(0)	100			
16	Correct Left,B(1)	32			
17	Incorrect Left,B(2)	7			
18	Correct Right,B(3)	42			
19	Incorrect Right,B(4)	17			
20	Omissions,B(5)	2			
21	Avg Lat Corr Lft,B(6)	1.708			
22	Avg Lat Incorr L,B(7)	1.376			
23	Avg Lat Corr Rgt,B(8)	1.007			
24	Avg Lat Incorr R,B(9)	1.028			
25	Reinforcers,B(10)	74			
26	Head Entries,B(11)	0			

Appendix Figure A-2: Sample Visual Cue Discrimination Output

A3 Response Discrimination Workbook

The Excel workbook *Response Discrimination Workbook.xlsm* requires the use of VBA macros. To enable the use of VBA macros in excel, users must first enable the developer tab (see “Show the Developer tab” in Microsoft Office Support documentation) and enable macros (see “Enable or disable macros in Office files” in Microsoft Office Support documentation).

Once Data is transferred into *Response Discrimination Workbook.xlsm*, go to the ‘Developer’ tab and select ‘Macros’. Run *Compiled_Left2* (shortcut key: Ctrl + Shift + E) or *Compiled_Right2* (shortcut key: Ctrl + Shift + R) depending on whether the left or right lever was selected to be rewarding, respectively. If uncertain which lever was selected to be rewarding in a given experiment, the raw data file can be inspected using a text editor such as *Notepad* or *Word* (Microsoft) and the experiment protocol can be found next to ‘MSN:’ as either \$Shift Response Discrimination LEFT or \$Shift Response Discrimination RIGHT corresponding to left or right rewarding levers, respectively. Once the *Compiled_Left/Right2* macro is run, Excel should end on the *Summary* tab with error profile data.

To reset the workbook, run the *Clear All* macro (shortcut key: Ctrl + Shift + C).

To produce a list of errors for each incongruent trial, as required for logistic regression modelling, run *Compiled_Left* (shortcut key: Ctrl + E) or *Compiled_Right* (shortcut key: Ctrl + R) on transferred data. Return to the *Input* tab and copy the data under Column D which will indicate ‘1’ for incorrect lever presses or ‘0’ for correct lever presses or omissions for all incongruent trials in order from the top of the column to the bottom.

	A	B
1	Error Profile	
2	RD - Trials to criterion	73
3	RD - Errors to criterion	28
4	Total Errors	30
5	Errors After Criterion	2
6	Perseverative errors	20
7	Never-reinforced errors	2
8	Regressive errors	8
9		
10	Congruent Latency	1.482667
11	Congruent Correct Latency	1.392931
12	Congruent Incorrect Latency	4.085
13	Incongruent Latency	1.560345
14	Incongruent Correct Latency	1.803
15	Incongruent Incorrect Latency	1.300357
16	Average Latency	1.521051
17	Transition Analysis	
18	VC Disengage	19
19	RD Engage	71
20	Transition Period Length	52
21	VC Engaged Latency	1.249231
22	VC Dis Latency	1.46375
23	RD Engaged Latency	1.929583
24		
25		
26		
27		
28		
29		
30		
31		
32		
33		
34		
35		
36		
37		

Appendix Figure A-3: Sample Response Discrimination Output for Error Profile

	A	B	C	D
1	Subject	TGM104.1		
2	StartDate	170511		
3	StartTime	3515		
4	Experiment	RD LEFT		
5	Group	4MOB		
6	Box	1		
7	Comment			
8	Max Number of Trials	120		
9	Min Number of Trails	120		
10	Performance Criterio	10		
11	Correct Lever	1		
12	Stimulus Length (sec)	3		
13	Trial Length (sec)	20		
14	Lever Response Time	10		
15	Reward Length (sec)	4		
16	A(12)	400		
17	Trial #,B(0)	120		
18	Total Correct,B(1)	88		
19	Tot Incorrect,B(2)	30		
20	Omissions,B(3)	2		
21	Avg Lat Corr,B(4)	1.533		
22	Avg Lat Incorr,B(5)	1.486		
23	Reinforcers,B(6)	88		
24	Head Entries,B(7)		Trial Ty	Error
32	D(7)	2	Incongrue	1
39	D(14)	3	Incongrue	1
53	D(28)	5	Incongrue	1
74	D(49)	8	Incongrue	1
88	D(63)	10	Incongrue	1
102	D(77)	12	Incongrue	1
109	D(84)	13	Incongrue	0
123	D(98)	15	Incongrue	1
144	D(119)	18	Incongrue	1
151	D(126)	19	Incongrue	0
165	D(140)	21	Incongrue	1
179	D(154)	23	Incongrue	1
193	D(168)	25	Incongrue	1
207	D(182)	27	Incongrue	1

Appendix Figure A-4: Sample Response Discrimination Output for Logistic Regression of Mean Group Error Rates

Appendix Table A-1: Set Shifting Indices

Trials & Errors to Criterion	8 correct consecutive responses (irrespective of trial congruency).
Perseverative Errors	Reflect a failure to disengage from the old VCD strategy and occur on incongruent trials, early in set shifting. RD trials were analyzed in blocks of 16; 8 of these trials were incongruent trials. When rats showed adherence to the old strategy by selecting the incorrect lever on 6 or more of a block's 8 incongruent trials ($\geq 75\%$), all incongruent trial errors in that block were characterized as perseverative.
Never-Reinforced Errors	Incorrect lever responses on congruent trials. These errors tend to occur as rats explore new strategies and reflects the ability to filter out non-rewarding options.
Regressive Errors	Reflect a failure to learn or maintain the new RD strategy due to regression towards the old VCD strategy. These occur later in set-shifting on incongruent trials, after the rat had already begun to disengage from VCD. RD trials were analyzed in blocks of 16; 8 of these trials were incongruent trials. If rats demonstrated disengagement from the old VCD strategy (chose the incorrect lever) on 5 or fewer of a block's 8 incongruent trials ($<75\%$), all incongruent trial errors in that block were characterized as regressive. Once a regressive block occurred, all subsequent blocks were considered regressive as well.
Logistic model: Trials to 50% Strategy Change	The interpolated number of incongruent trials needed for half of a group's responses to demonstrate a strategy change during RD; when only 50% of a group's responses follow the old strategy (commit errors). Equivalent to the IC50 of a logistic exposure-response curve.
Logistic model: Hill Slope	The Hill slope of a logistic exposure-response curve quantifies the steepness of the curve, reflecting the efficiency of strategy change.

Since omissions did not clearly indicate which strategy was followed, omissions were not scored as errors in these indices. VCD = Visual Cue Discrimination, RD = Response Discrimination

Appendix B: MWM Regressive Preference for Target Quadrant

Representative recordings of probe test swimming behaviour. Both videos are run at 4x speed and trace respective swim paths in the top left corner. The platform was previously learned to be located in the top-right quadrant.

Appendix C: Immunohistochemistry Protocols

C1 Solutions

Cryoprotectant (1 L)

10 g	PVP-40
500 mL	0.1M Phosphate Buffer (PB) solution (<i>same as 0.1M PBS, but without NaCl</i>)
300 g	Sucrose
300 ml	Ethylene glycol

Solution can take 0.5 – 2 h to dissolve. Recommended order: add PVP to PB, slowly added sucrose and wait for both PVP & Sucrose to dissolve, add ethylene glycol, bring volume up to 1L with PB.

Before use, put a test sample in freezer (falcon tube) ensure that the cryoprotectant does not freeze

DAB Solution

0.05% diaminobenzidine tetrahydrochloride (Sigma-Aldrich #D5637) in 0.01M PBS
stir for 15 min and run through filter paper (Whatman Grade 2/8 μ m)
add 3% H₂O₂ 15 s prior to use, stir.

Gelatin

1.5 g	Powdered Gelatin
500ml	Distilled water

Heat in microwave for ~30s (do not allow water to boil) and stir. Discard if there is any indication that an old solution has spoiled.

Paraformaldehyde Solution (1 L)

40 g	paraformaldehyde
500 mL	distilled water
1 ml	NaOH (or ~15 drops)
100 mL	0.1M PBS
390 mL	distilled water; or enough to form 1 L solution

Adjust pH to 7.35 with HCl

Phosphate Buffered Saline (PBS)

1L 10X PBS Stock Solution (0.1M; 1 L)

90 g NaCl

10.9 g Na₂HPO₄ anhydrous or 20.6 g for Na₂HPO₄ heptahydrate

3.2 g NaH₂PO₄ anhydrous or 3.7 g for NaH₂PO₄ monohydrate

Add distilled water to 1L once dissolved

Adjust pH to 7.35 using HCl and NaOH dropper

1x PBS Working Solution (0.01M)

Dilute 1 part 10X Stock solution with 9 parts distilled water; adjust pH

Phosphate Buffer Saline with 0.2% TritonX detergent (PBST)

add 1 mL TritonX to 500 mL 0.01M PBS

Sucrose 30% (500 ml)

150 g sucrose

Add enough distilled water to make 500 ml solution once sucrose is fully dissolved

For long term storage (> 1 month), add pinch of isoniazid to solution (preservative; caution! Highly toxic)

C2 Immunohistochemistry Protocol

Primary:

OX6 mouse monoclonal (BD Pharmingen #554926); use 1:1000 in primary solution

GFAP mouse monoclonal (Sigma-Aldrich #G3893); use 1:2000 in primary solution

Secondary: Biotinylated Horse anti-mouse IgG (Thermo Fisher Scientific #31806)

Other reagents:

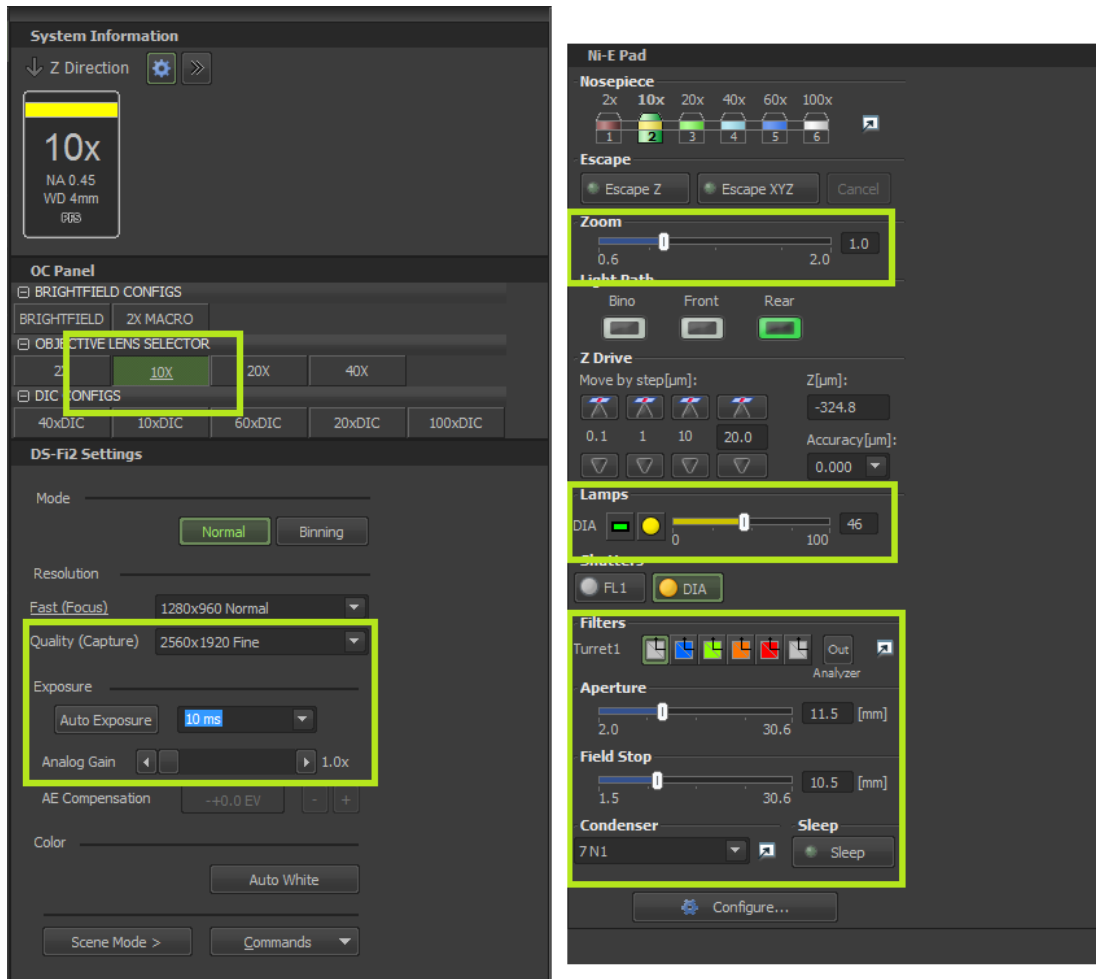
Normal Horse Serum (Abcam #7484)

ABC reagent kit (Thermo Fisher Scientific # 32020)

Day 1	
Wash	0.01M PBS 10 min x 6 times <i>If weak DAB staining due to prolonged storage, may need to wash 10 min x 10 times</i>
Block endogenous peroxidase	1% H ₂ O ₂ 10 min
Wash	0.01M PBS 5 min x 3 times
Block nonspecific antigens	2% horse serum in PBST
Incubate with Primary Antibody	Primary in 2% horse serum in PBST Overnight in 4°C
Day 2	
Wash	0.01M PBS 5 min x 3 times
Incubate with Secondary Antibody	1:500 biotinylated secondary in PBST
Wash	0.01M PBS 5 min x 3 times
Incubate with Horseradish Peroxidase	2 drops of Avidin, 2 drops of Biotin in 10 mL PBST
Wash	0.01M PBS 5 min x 3 times
Incubate with DAB Solution	OX6: 30 s GFAP: 120 s
Wash	0.01M PBS 5 min x 3 times
Mount sections, airdry overnight	
Day 3	
Dehydrate in sequential concentrations	5 min in 50% 70% 95% and 100% Ethanol, then 5 min in 50/50% Ethanol/xylene solution, then 10 min in 100% Xylene; use new xylene if cloudy
Coverslip	DePex Mounting Medium; air dry for >48 h

Appendix D: Microscopy and Image Analysis Protocols

This appendix outlines specific parameters used in acquiring micrographs (Nikon Eclipse Ni-E, Nikon DS Fi2 colour camera, NIS Elements Imaging; Mississauga, ON) and in analysis using ImageJ v1.50b.

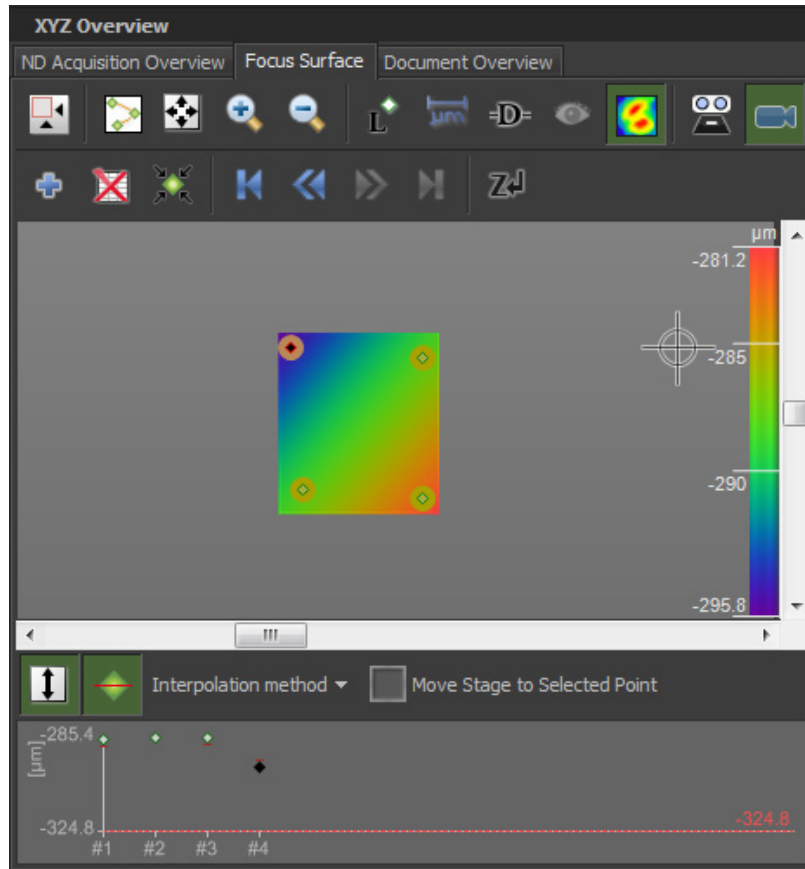


Appendix Figure D-1: Microscope Imaging Parameters

Using the 10x Objective, ensure that the following are set to:

- Quality: 2560x1920 Fine
- Exposure: 10 ms
- Analogue gain: 1.0
- Zoom: 1.0x
- Light: 46
- No filters on Turret1
- Analyzer: Out
- Aperture: 11.5
- Field Stop: 10.5
- Condenser: 7N1
- Neutral Density Filter 8 & 32 *only*;
NCB32 filter should be out.

With every new section, perform white balance correction using a probe on off-tissue direct light as reference

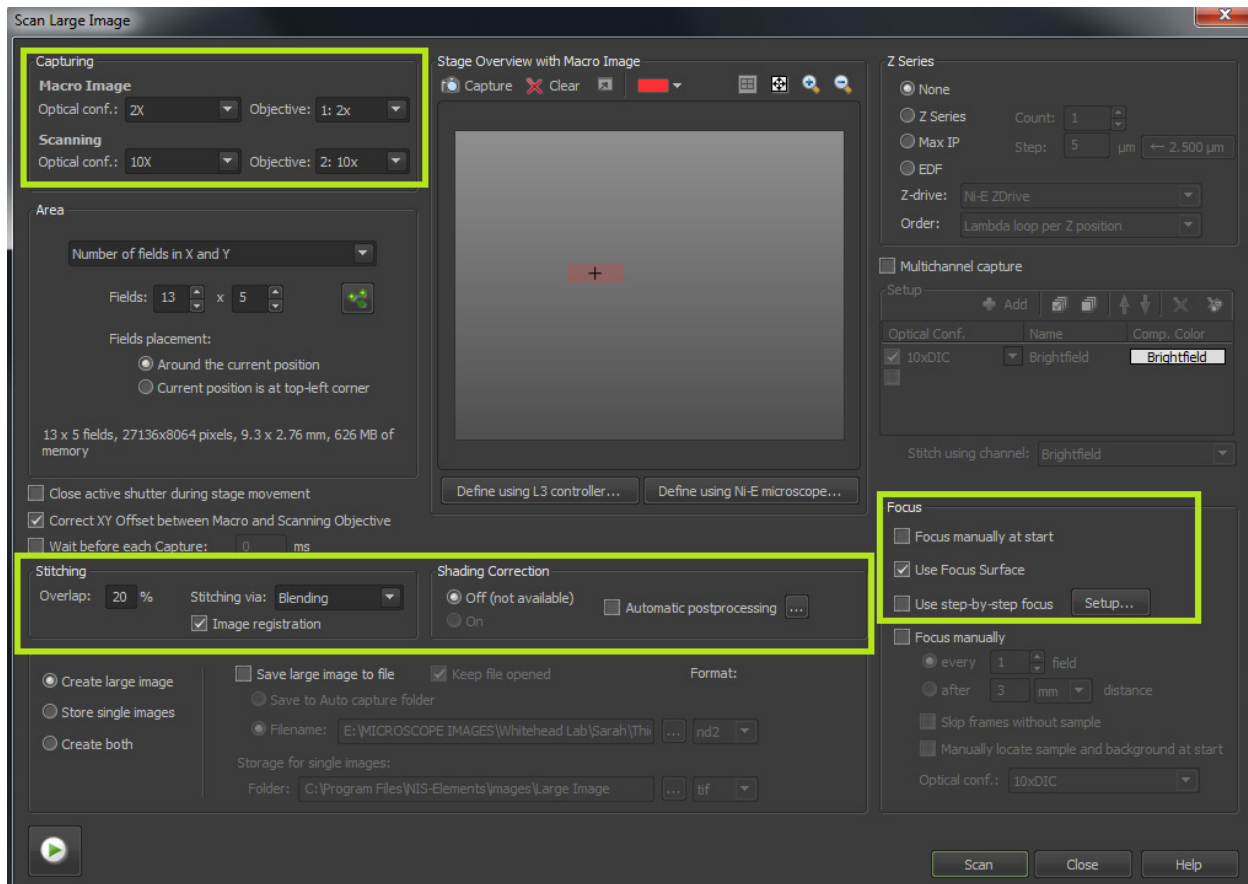


Appendix Figure D-2: Focus Surface Setup

A focus surface allows the software to interpolate optimal focus depths, based on a sampling of points by the user. This corrects for any slant in the stage or slide; this is particularly useful when scanning a large stitched image, e.g. greater than 1 mm in any dimension, with any greater magnification than the 2x objective. Ensure that the interpolation method is selected.

Placing 4-6 focus points around the perimeter of the section and several focus points on ROIs is recommended. A flat focus plane (i.e. colour gradient follows a straight line across the plane) identifies a slide or stage slant; non-flat focus planes (i.e. colour gradient follows a curved line, or a peak/valley is in the middle of the focus plane) may indicate errors in the setting of focus points or in the program's interpolation. If the focus plane does not appear flat, continue to add focus points until the plane is flat – if this does not resolve, use of the focus surface is not advised and automatic step-by-step focus is recommended instead.

Note the range of the focus surface; the difference between the maximum and minimum depth (measured in the z dimension) should not exceed $\sim 50 \mu\text{m}$ across a coronal section of $\sim 15 \text{ mm}$ width. This indicates a major stage or slide slope that will result in blurry artifacts.



Appendix Figure D-3: Micrograph Stitching

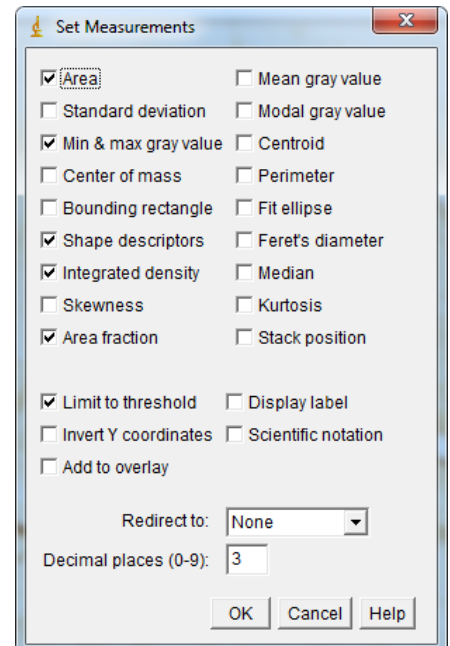
For consistent image sizes, pre-determined X & Y field dimensions are advised. Note that the microscope software (and also ImageJ) does not reliably handle images greater than 28 000 pixels in any dimension.

Select “Focus manually at start”, “Focus Surface” or “Use step-by-step focus” as appropriate.

D1 Threshold Analysis: Detailed Walkthrough

Before starting, set & check the following settings:

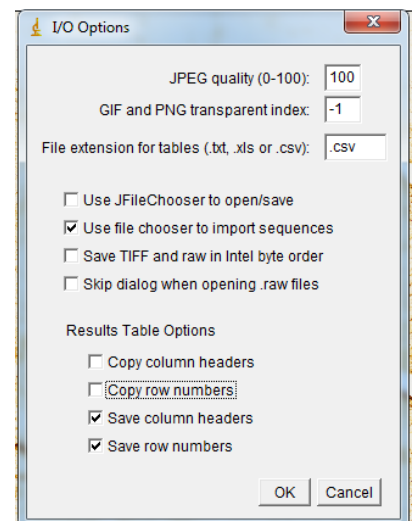
Analyze > Set measurements.



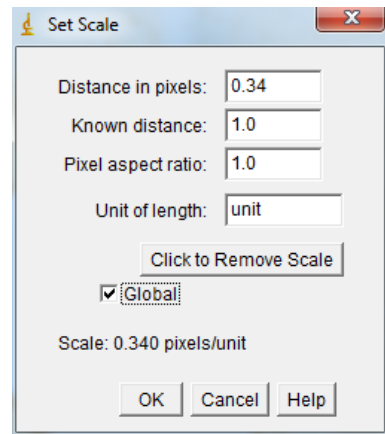
Measure (Ctrl+M);

in the results window, Results>Options:

Make sure JPEG quality is set to 100.



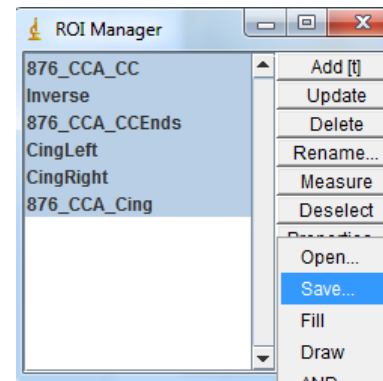
Step 1. Set/check scale for each new image



Step 2. Using the polygon tool, trace out the ROI of interest (start with corpus callosum)

- Do not include edges (tend to be darker than rest of white matter tract)
- Note that anchors can be dragged after selection is complete – careful not to click outside of selection before it is saved (will lose selection)
- When selection is complete, press [T]. ROI manager window will appear
- Select new ROI, and Rename: *ID_Section_Anatomy* eg, *876_CCA_CC*
- Recommended abbreviations:

- FM: Forceps minor	- Cing: Cingulum
- CC: Corpus callosum	- HPC: Hippocampus
- CCEnds: Supraventricular Corpus callosum	- IC: Internal capsule



Measure [M]; paste area to “ROI area” column in appropriate data spreadsheet

- Ensure μm^2 , not pixels! Area value should have decimals.

Save! When all ROIs in the image are outlined and named, select all ROIs in the Manager (click on the list of ROIs, Ctrl + A, or hold Ctrl/Shift as you select the ROIs > More >> Save > Name as *ID_Section* in the image folder

- Avoid large tears, artifacts
- To remove artifacts or tears from selection:
 - If large or extends beyond ROI, make multiple selections to construct ROI of interest
 - If smaller, use freehand tool to outline artifact, save outline of artifact [T], select ROI of interest and artifact outline, more>>XOR, save corrected ROI [T]

Consult Paxinos' & Watsons' 6th edition *The Rat Brain in Stereotaxic Coordinates* to help guide anatomical selection, especially for OX6 staining & IC.



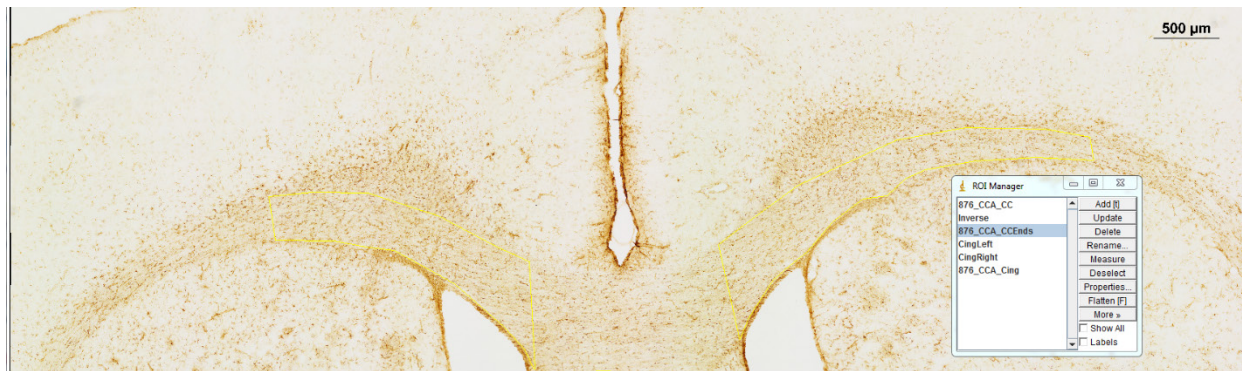
Appendix Figure D-4: Forceps Minor

- Bregma +3.00 mm
- Yellow trace indicates ROI



Appendix Figure D-5: Anterior Corpus Callosum

- Bregma +2.00 mm
- Extend selection to lateral ends of cingulum
- Lateral ends of selection should be roughly parallel to the dorsal/ventral axis
- On anterior corpus callosum, middle of selection should dip down to most ventral reach of the CC



Appendix Figure D-6: Anterior Supraventricular Corpus Callosum

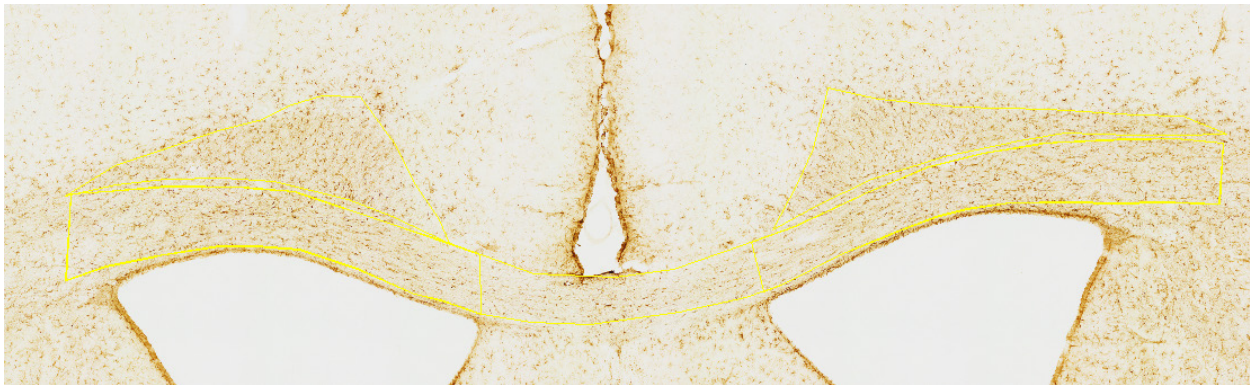
On anterior and middle corpus callosum, remove selection between medial borders of ventricles

1. Outline white matter tract to be deleted; lateral ends of this selection should be roughly parallel with dorsal-ventral axis.
2. Edit > Selection > Make Inverse. Add to manager [T]
3. In ROI manager, select CC and Inverse middle sections, More >> And, add to manager [T], rename as supraventricular corpus callosum (CC Ends)



Appendix Figure D-7: Anterior Cingulum

- Bregma +2.00 mm
- To combine bilateral Cingulum/HPC/IC selections, select both in the manager (hold Ctrl while selecting), More >> OR (Combine), add selection to manager [T]



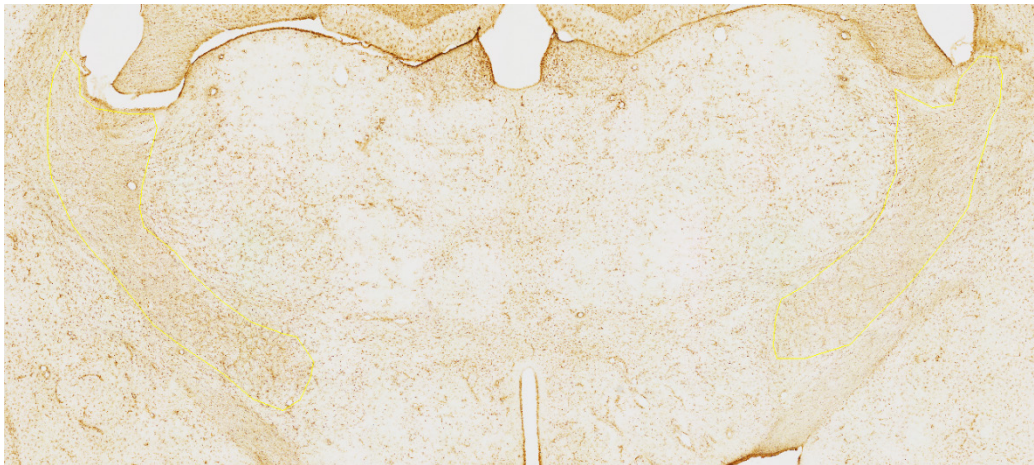
Appendix Figure D-8: Middle corpus callosum, supraventricular corpus callosum, cingulum

- Bregma +0.00 mm



Appendix Figure D-9: Posterior Corpus Callosum, Cingulum

- Bregma -3.00 mm



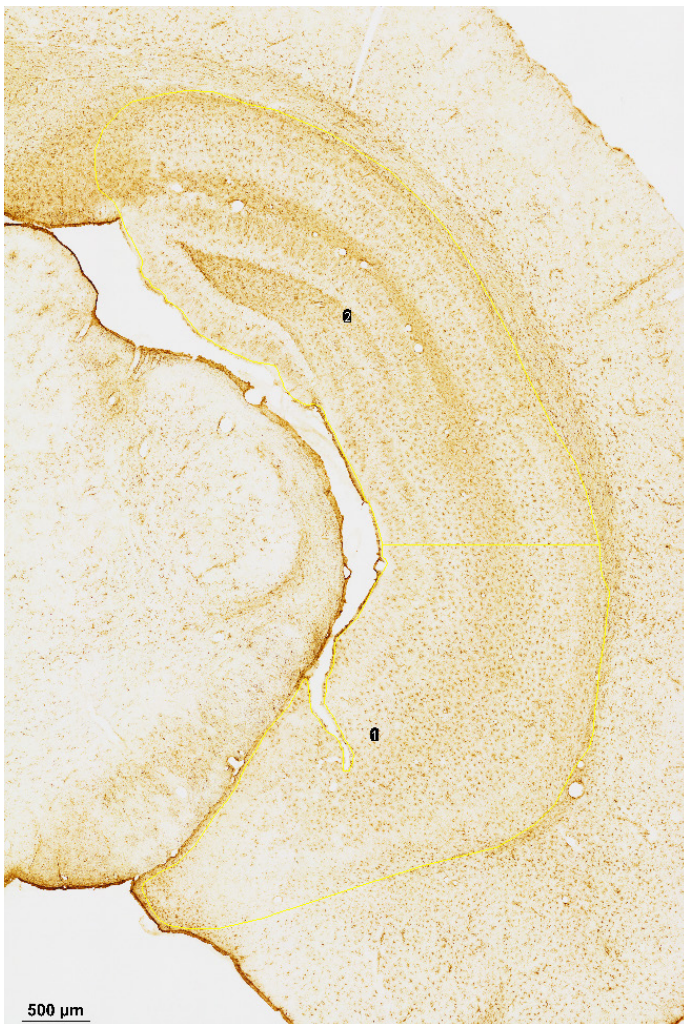
Appendix Figure D-10: Internal capsule

- Bregma -3.00 mm
- Exclude optic tract, ventral and often adjacent to IC.



Appendix Figure D-11: Anterior Dorsal Hippocampus

- Bregma -3.00 mm
- Exclude fimbriae



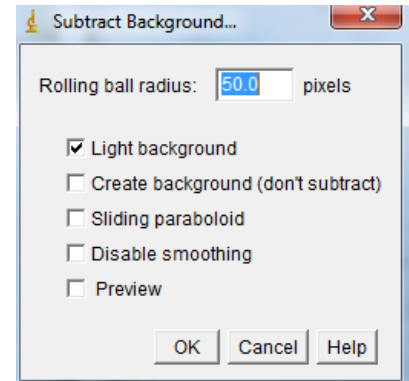
Appendix Figure D-12: Posterior Dorsal and Ventral Hippocampus

- Bregma -5.50 mm
- Horizontal line extending to the most lateral reach of the hippocampus delineated the dorsal and ventral hippocampus.

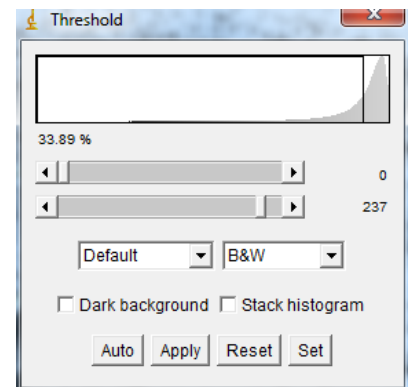
Step 3. Change to 8-bit grayscale (Image > Type > 8-bit)

Step 4. Subtract Background (Process > Subtract Background)

Make sure no ROIs are selected before this step!



Step 5. Threshold (Ctrl + Shift + T); set Max to 237. Do not apply!



Step 6. Measure Thresholded Area

- Select ROI, press [M]
- Ensure measurement is limited to threshold (Area should not be 100%).
- Paste all measurements to data spreadsheet (do not paste over ROI area column).

File	Edit	Font	Results									
	Area	Min	Max	Circ.	IntDen	%Area	RawIntDen	AR	Round	Solidity		
9	19399169.550	44	239	0.406	3915398788.927	0	452620100	2.699	0.371	0.906		
10	61987474.048	67	237	0.070	13483976583.045	32.948	1558747693	3.764	0.266	0.159		

Step 7. Repeat for each ROI of interest

D2 Threshold Analysis: Protocol Summary

Make sure correct measurements & options are set before following summary!

1. Set/Check scale for each new image
 - a. 2.942 “distance in pixels” pixels per 1.00 “Known distance” (μm); 2.942 pixels/unit
 - b. Select “Global”
2. Using the polygon tool, select ROIs.
 - a. Add selections to ROI manager (Shortcut: [T]), name accordingly.
 - b. Measure [M]; paste area to “ROI area” column in appropriate data spreadsheet (ensure μm^2 , not pixels!)
 - c. Select all ROIs, save to image's folder (ROI Manager>More>>Save)
3. Change to 8-bit grayscale (Image>Type>8-bit)
4. Subtract Background (Process>Subtract Background)
 - a. Make sure no ROIs are selected before this step!
5. Threshold (Ctrl+Shift+T); set Max to 237. Do not apply!
6. Measure Thresholded Area (Ensure measurement is limited to threshold).
 - a. Select ROI, press [M]
 - b. Paste measurements to data spreadsheet
7. Repeat step 6 for each ROI on the image

Clear ROI manager before starting on next section

Tips & Useful Keys

(File>Revert) to re-open current image

You can drag and drop Images and ROIs onto the ImageJ toolbar to open them

Custom shortcut keys and Macros can speed up the process (Plugins>Shortcuts/Macros),

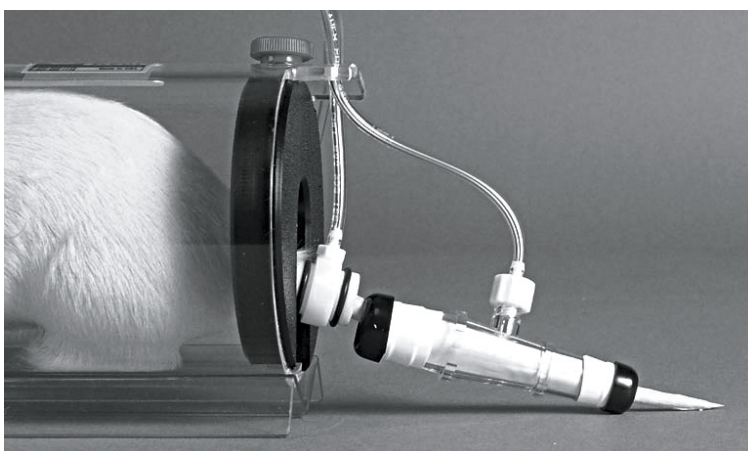
[Space] allows you to drag the picture with your cursor

[+]/[-] for zooming in/out

[Ctrl] + [] to view all ImageJ windows

Appendix E: Rat Tail Cuff Blood Pressure Measurement Protocol

This appendix supplements the methods for blood pressure measurement outlined in [Chapter 4](#). This supplementary guide will include a summary of specific operating details and suggestions for the CODA High Throughput Non-Invasive Blood Pressure system (Kent Scientific; CODA-HT6) that are not found in the equipment user guide. The parameters and suggestions outlined here were followed in generating data for [Chapter 4](#).



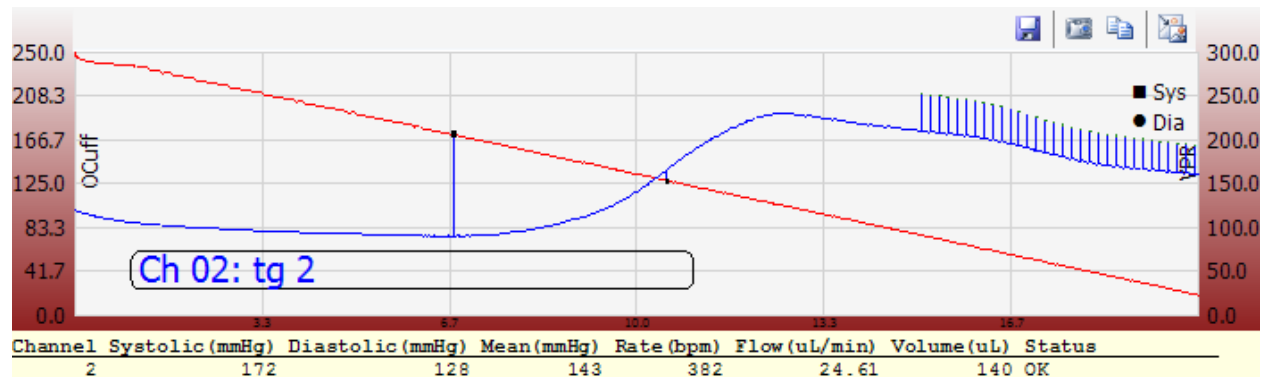
Appendix Figure E-1: Cuff Positioning on Restrained Rat's Tail

Model rat in a restraining tube with an Occlusion cuff (O-Cuff) placed at the base of the tail and a Volume Pressure Recording cuff (VPR-Cuff) distal to the base.

E1 Background

CODA allows non-invasive measurements of rodent blood pressure. This is accomplished by occluding blood flow into and out of the tail using a cuff positioned near the base of the tail, followed by controlled deflation of the occlusion cuff. As this cuff deflates, changes in the volume of the tail are detected by a second cuff positioned distally on the tail. This allows estimation of systolic and diastolic blood pressures. Rodents are held in a tightly fitted tube that isolates the tail and confines the rodent to minimize movement. The confined animals are held on warming platforms that help to increase tail surface temperature, so that changes in tail volume can be more readily measured. The

Whitehead lab's high-throughput CODA equipment can measure 6 channels (i.e. rodents) simultaneously.



Appendix Figure E-2: Sample channel output for one cycle

The horizontal axis denotes the time of the cycle. The red line represents the pressure of the gradually deflating occlusion cuff. The blue line represents the volume recorded by the VPR cuff.

When the O-Cuff (occlusion cuff) inflates to occlude blood flow to and from the tail, tail volume remains constant or decreases, as measured by the VPR (Volume Pressure Recording) cuff (Appendix Figure E-2). The VPR cuff acts as a differential pressure transducer to estimate changes in tail volume. As the pressure of the O-cuff falls below systolic blood pressure, blood begins to flow into the tail. The left (first) blue vertical line indicates this point, which coincides with the minimum of the VPR curve: as flow returns, tail volume increases (Appendix Figure E-2). This is exaggerated by reactive hyperemia. When the O-cuff reaches diastolic pressure, blood flow into and out of the tail reaches a maximum. This is indicated by the right (second) blue vertical line and coincides with the inflection point of the VPR curve (maximum slope of the curve, indicating greatest rate of volume change). Spikes at the right end of the VPR curve are artefacts. Only movement artefacts between or near the systolic and diastolic pressures will interfere with successful measurement. "Precipitous" decreases in O-Cuff pressure or VPR volume indicate a broken/leaking cuff (see page 17-18 of User's Guide and "Cuff Replacement").

The product manufacturers claim to measure heart rate, but these are inaccurate. Mean pressure might also be inaccurate since the equipment does not record the length of systolic or diastolic phases. This is necessary for the most correct estimate of mean pressure. It appears that the program calculates mean pressure using the formula (mean pressure) = $1/3 \times (\text{systolic pressure}) + 2/3 \times (\text{diastolic pressure})$ which is not accurate at increased heart rates.

Several published studies¹⁻⁴ have validated the accuracy of VPR as a method for non-invasive estimation of blood pressure, using arterial catheterization & telemetry as the gold standard for comparison. The systolic pressure estimate is more accurate than the diastolic pressure estimate, and you can expect a slightly greater variance in inter-cycle diastolic blood pressure recordings within individual channels & sessions

E2 Equipment Use & Maintenance

E2.1 Software Set-up

The user's guide has thorough instructions on operating the software, starting on page 8. Each *Session* consists of a user-set number (e.g. 25) of inflation/deflation *cycles* and includes all the channels that were indicated for measurement. Sessions can be further divided into **sets** of cycles. An *experiment* is the collection of all sessions that belong to it; multiple sessions will be run as part of a project. Since sessions will likely be run on multiple dates for multiple animal groups, it is recommended to name the sessions by Date and Animal Group.

CODA Users guide instruction on pages 9-1 &, 19 are useful for first time use. Once an experiment is set up using the *Experiment Wizard*, multiple sessions can be run as part of the same experiment using the *New Session Wizard*. In the new session wizard, *use selected session as template* allows you start a session quickly while keeping the same session parameters as the selected session. Be sure to name new sessions appropriately (e.g. Date and Animal Group) and to allocate the correct animals to their respective CODA channels. It is useful to assign animals to animal groups for ease off initiating sessions.

On the last window of either experiment or new session wizards, do not press “Start” until the cuffs are in place on the animals.

E2.2 Recommended Session Parameters

Acclimation cycles: 0

Number of sets: 1

Time between sets: Default (does not matter if there is only one set)

Cycles per set: 25

Time between cycles: 5 seconds

Deflation time: 20 seconds for smaller rats, 15 second for larger rats (>400g)

Minimum volume: 15 μ L

Display style: Chart for each animal

10 successful cycles are recommended for an accurate mean measurement of blood pressures. Running 25 cycles (without any designated “acclimation” cycles) should produce a sufficient number of successful reads, though this may be reduced if the rats consistently show low inter-cycle variance. Furthermore, the data is organized more simply (fewer spreadsheets) when there are no designated “acclimation” cycles. The program will automatically remove any cycles which are unsuccessful (see error codes in user’s guide), though additional filtering will further reduce the number of successful cycles; see [E3 Data Quality & Analysis](#). With manual filtering of the data, it is not recommended to discard any initial acclimation meet desired data quality.

E2.3 Warming Platform

The user’s guide has thorough instructions on operating the warming platforms, adapted from page 5: begin warming platform by pressing the START/STOP button. Press it again to stop warming. The controls of each warming platform apply to all four channels

(channels cannot be controlled independently). By default, the platform will turn off automatically after 1 hour– adjust the running time using the up and down buttons beside the time display. Be sure that the warming platform will run for sufficient time, so that it does not turn off mid-session. L1 warms up to 32°C, L2 to 35°C, and L3 to 38°C. There are additional levels (L4-6) that can be activated by holding down the up button for 10 seconds (found below the heating level display). L4 is effective for keeping holding tubes warm (i.e. while the rats are habituating to the room) but is often uncomfortable for the animals. When warming is active, the green LED lights will flash when the set temperature level is achieved. When the temperature of a channel falls below the set level, the light will glow steadily. There is a tendency for animals to have lower surface temperature on the leftmost channel (of the left platform) and rightmost channel (of the right platform). For this reason, it is recommended to hold 3 rats on either warming platform on the channels closest to the centre of the cart.

E2.4 Cuff Replacement

Cuffs will need to be replaced. At the time of writing this guide, only a total of four cuffs were replaced over ~3000 cycles. Page 17-18 of the user's guide has good information on when and how to replace the cuff. Testing the cuffs using the device manager before running a session will help prevent mid-session complications.

E2.5 Cleaning & Storage

Do not use alcohol or abrasive detergents on any equipment. Water should suffice for regular cleaning of waste found on warming platforms. Following use, animal holders should be soaked in Sparkleen solution, followed by warm water rinse and dry. Cuffs should be disconnected and stored in a dry storage baggie/container to prevent damage to bladder and tubing. If measurements are taken daily, it may be convenient to keep cuffs connected to the CODA controller. When cuffs are not connected, the CODA controller ports should be protected by the dust covers.

E2.6 Animal Handling

For initial acclimation, the JOVE article recommends²: “To train and improve animal acclimation, add additional cycles to your experiment and run the experiment for five consecutive days. You also can assist with acclimation by placing the animal in the holder for 15 minutes for 3 consecutive days prior to the actual study.”

Appendix Figure E-1 does not offer an accurate representation of the space that a rat should be permitted during testing. Appropriate holding tubes should be selected according to the width of the animals, and the nose cone should be positioned so as to minimize animal movement. This means that the rat nares should be visible at the narrow opening of the nose cone, and the posterior end of the animal should be pressed up against the back cover of the holding tube. This will often require some pressure against the animal when securing the back cover, with care not to pinch any tissue. Advance the nose cone position as necessary if the rat still manages to move excessively or to draw in its tail through the back cover; try not to reinforce this kind of behaviour (e.g. by returning the animal to its cage). Blood pressure may be affected if the chest cavity does not have enough room to expand, and as always, strive to minimize any animal discomfort. Note that animals may also experience discomfort due to excess heating from the warming platform; do not keep animals on L4 for a prolonged amount of time. Movement and apparent stress should subside with repeated sessions. Placing a rat in the same holding tube and warming platform channel for all sessions may reduce stress and makes organization simpler for the experimenter. If randomization of holding tube and placement is desired, take note of the holding tube numbers and platform channels.

E3 Data Quality & Analysis

The CODA software will automatically remove any cycles that do not meet its standards for reliability; see error codes on page 16 of the user guide. Note that the program may sometimes accept clearly inaccurate cycles and may occasionally reject seemingly accurate measurements. It is worthwhile taking note of any cycles that were wrongfully rejected/accepted for later filtering. Once the full report is exported to an excel file, data should be transferred to spreadsheets that will organize sessions from multiple dates

across multiple tabs. Data sheets should be organized such that excel functions can be formulated to calculate: means, standard deviations, standard errors for systolic, diastolic, and mean blood pressures, as well as tail volume (Appendix Figure E-3).

From consultation with the representative for the company that developed and distributes the CODA equipment, it was recommended that any cycles with a volume reading of 15 or less should be discarded. The program is supposed to do this automatically (as per session parameters), but it does not do so. Tail blood volume fluxes can readily reach into the 100's of μL , if enough time is granted during and before sessions (see operating "operating summary"). The following are additional standards that can be met to help ensure reliability of blood pressure measurements, though the values may need to be adjusted with different groups of animals:

- SD of pressure measurements for each channel should be less than 20
- Total number of successful counts after automatic and manual filtering of cycles should be greater than 15.
- Mean volume across cycles should be greater than 50.

These values were based on subjective evaluation of data reliability. Another source recommended deleting measurements if the standard deviation is greater than 30^2 . When data does not meet these standards despite filtering for cycles with volume measurements <15 , it may not be necessary to exclude the final pressure means of individual channels/animals; it only suggests that more time and care should be given during future sessions. Ultimately, the mean systolic, diastolic and mean pressure measurement given for each channel should be used a single data point (not as a sample with variance, since cycles are not independent of each other).

	A	B	C	D	E	F	G	H	I	J
1	2.7 Ch 1	Systolic	Diastolic	Mean	Rate	Flow	Volume		2.8 Ch2	Systolic
2	1	157	94	115	0	3.33	28.74		1	1
3	2	164	98	120	0	3.4	30.2		2	1
4	3	136	107	116	0	4.3	29.4		3	1
5	4	138	97	110	0	4.87	33.36		4	1
6	5	154	110	124	0	3.34	27.64		5	1
7	6	139	105	116	0	3.37	24.13		6	1
8	7	139	86	103	0	3.61	25.51		7	1
9	8	138	102	114	272	3.96	26.79		8	1
10	9	144	104	117	0	4.43	33.79		9	1
11	10	147	88	107	0	5.74	42.85		10	1
12	11	138	81	100	0	7.27	49.46		12	1
13	12	137	89	105	0	4.05	26.95		13	1
14	13	129	88	101	258	4.81	28.5		14	1
15	15	184	108	133	215	11.36	97.77		15	1
16	16	147	97	113	0	8	52.32		16	1
17	17	178	123	141	363	17.24	117.91		17	1
18	18	174	123	140	388	19.05	120.21		18	1
19	19	163	124	137	434	27.56	138.78		19	1
20	20	192	130	150	428	18.11	125.12		20	1
21	21	189	135	153	430	23.1	144.59		21	1
22	22	207	145	165	314	21.15	143.63		23	1
23	23	203	148	166	437	23.24	163.05		24	1
24	24	205	153	170	457	27.15	166.86		25	1
25	25	172	133	146	420	26.26	112.14			
26										
27	Mean	161.4167	111.1667	127.5833	184	11.6125	74.57083		Mean	149.43
28	SD	24.85071	21.13655	21.8053	196.4684	9.120159	52.76549		SD	7.2540
29	Count	24	24	24	24	24	24		Count	
30	SEM	5.072631	4.31448	4.450988	40.10394	1.861645	10.77071		SEM	1.5125
31		!!!	!!!	!!!						
32										
33										

Appendix Figure E-3: Suggested organization of data

Each spreadsheet tab includes CODA data from a different date, for all channels/animals. Rows 27-30 show the outputs of automated formulas (X corresponds to respective columns):

Row 27: =AVERAGE(X2:X26)

Row 28: =STDEV.S(X2:X26)

Row 29: =COUNT(X2:X26)

Row 30: =X28/SQRT(X29)

Additionally, automated cells can be added to notify when a column does not meet the quality standards mentioned above. In this figure, B31-B33 indicate when the SD of respective columns are too high (greater than 20) using the following code =IF(B28>20, "!!!", ""). B32 indicates when the total number of successful cycles (post manual filtering) is too low (less than 15) using the following code =IF(B29<15, "!!!", ""). G31 indicates when the mean volume reading is too low (less than 50) using the following code

=IF(G27<50,"!!!",""). This template, including notification cells, can then be replicated (copied and pasted) for each channel across multiple sessions.

E4 Operating Summary

1. **Place rats in testing room to habituate to the room.** Dim/red lighting is recommended. Make sure that drinking water is accessible to the rats. Allow one hour before placing rats into holding tubes.
2. **Turn on warming platform to L4** with holding tubes and cuffs on the platform. Warmer tubes will help the rats reach sufficient surface temperatures. (see [E2.3 Warming Platform](#))
3. **Test connected cuffs** using the device manager. Replace cuffs as necessary (see [E2.4 Cuff Replacement](#)).
4. After allowing the rats to habituate to the room for one hour, **allow them to enter the holding tubes**. If removed from their cage, the rats will readily enter the holding tubes. This should be accomplished with ease on a flat surface (such as the top of a cart). Be sure not to pinch any fat, paws, or testicles when securing back of tube. See [E2.6 Animal Handling](#) for more details.
5. **Place cuffs onto rat tails.** O-cuffs may reach the base of the tail and will work well if they can be advanced to anywhere on the proximal third of the tail. Ensure that O-cuffs stop at minimal resistance and are not too tight on the tail. The same applies to VPR cuffs (placed distal to the O-cuff). The higher up the VPR cuff is placed, the more blood volume will be measured; however, the two cuffs should not be in contact with each other as this can affect inflation/deflation of the bladders and produce measurement artefacts.
6. **Turn warming platforms down to L3** or even lower if animals show distress from heat (persistently vocalizing stress, moving tails off of the heated platform, unusually active). Cover tails with the black blanket for efficiency of heating and to provide some weight against tail movement. It is recommended to keep the blanket over the tails during the course of all sessions, though it may be removed at the user's discretion.
7. **Wait 10-15 minutes** to allow tail surface temperatures to reach levels that facilitate sufficient tail blood volume for BP measurements. Note that tail surface temperatures (measured at base of tail) do not always correlate well with volumes seen in BP measurement. The CODA user's guide recommends 32-35°C. See trade-off note in step 8. Waiting may not be necessary with larger tails (greater blood volumes may be more readily measured), remove or reduce the wait time in step 7 if it does not help with initial measurements.

8. Run cycles.

- Pause as necessary to reposition cuffs or rats, though excessive handling can increase fluctuations in blood pressure; handling of cuffs and animals should be avoided unless necessary (cuffs fall off or shift to positions where insufficient volume is measured, or a tail is withdrawn into the holding tubes).
- You may also need to pause in between cycles to allow tail volumes to increase gradually. Tail volume seems to increase with repeat inflation/deflation cycles, so you can use the first several cycles to help increase tail volume to satisfactory levels.
- If tail volumes are resistant to increase as cycles are being run, consider increasing the heating level of the warming platform.
- Recognize the trade-off: as the rats are held on the warming platform for longer, tail volume may increase, but the rats may also become agitated and movement artifacts or cuff displacement can result.
- See [E2.1 Software Setup](#) for recommendations on number of cycles to run.

9. Remove cuffs, return rats to cage. Be mindful of any feces and urine and avoid contact of rat waste with cuff material.**10. Save & Back Up data.** Experiment Manager> navigate to session of interest> produce a full report and export to excel. When the excel file opens, be sure to save it. The CODA software keeps a copy of all data for later retrieval, including measurement charts.**11. Consider rewarding rats with sunflower seeds.****12. Wash holding tubes** with Sparkleen detergent and rinse with warm water, dry with paper towel. A mouse shoebox cage is useful for soaking holding tubes in detergent.**13. Wash warming platform.** Water & paper towel usually suffices.

E5 References

1. Feng M, Whitesall S, Zhang Y, Beibel M, D'Alecy L, DiPetrillo K. Validation of volume-pressure recording tail-cuff blood pressure measurements. *Am J Hypertens*. 2008;21(12):1288-1291.
2. Daugherty A, Rateri D, Hong L, Balakrishnan A. Measuring blood pressure in mice using volume pressure recording, a tail-cuff method. *J Vis Exp*. 2009(27).
3. Kurtz TW, Griffin KA, Bidani AK, et al. Recommendations for blood pressure measurement in humans and experimental animals. Part 2: Blood pressure measurement in experimental animals: a statement for professionals from the subcommittee of professional and public education of the American Heart Association council on high blood pressure research. *Hypertension*. 2005;45(2):299-310.
4. Malkoff J. Non-invasive blood pressure for mice and rats. (Whitepaper) *Animal Lab News*, Kent Scientific Corporation. 2005:1-8.

Appendix F: PET/MRI Study

The following appendix outlines a pilot study of in vivo measurement of microglia activation in the TgAPP21 rat following ET1 ischemic injury of the dorsal striatum. PET imaging with a radioligand that localizes to activated microglia and reactive astrocytes was complemented with MR and CT imaging to improve anatomical localization.

F1 Introduction

Subcortical infarcts indicate a greater risk for future strokes and cognitive impairment, even when patients do not initially present with symptoms^{1,2}. This sequela is thought to be mediated in part by secondary chronic inflammation, particularly in the white matter, which may also interact with other neurodegenerative conditions such as AD³⁻⁵. White matter pathology initiated by small vessel disease or infarcts is predictive for cognitive decline⁶⁻¹⁰ and involves inflammatory processes¹⁰⁻¹³. In vivo imaging of an animal model of ischemic subcortical injury would be instrumental for characterizing secondary inflammation and for testing therapeutic interventions.

¹⁸F-FEPPA is a PET-ligand that binds to the translocator protein (TSPO), an outer-mitochondrial-membrane bound protein that is upregulated in activated microglia and astrocytes¹⁴⁻¹⁸. This radiotracer was injected into 8 – 12-month-old male Fischer 344 rats following ischemic injury of the dorsal striatum. Following dynamic 90 min PET, the rats also underwent 3T MRI and contrast-enhanced CT-perfusion imaging to help localize radiotracer uptake and to explore additional in vivo imaging correlates of neuroinflammation. To corroborate multimodal imaging findings, brain tissue was analyzed using immunohistochemistry for microglia activation and reactive astrocytosis.

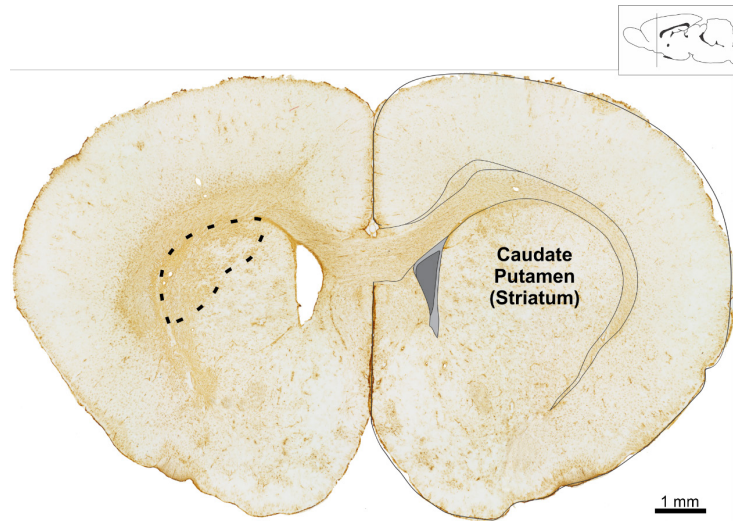
As integrity of prefrontal-subcortical circuits are particularly critical to cognitive status following stroke,^{2,19} differences in ¹⁸F-FEPPA uptake were compared across white matter segments anterior, proximal, or posterior to the site of injury. Blood sampling offers important corrections to radiotracer input functions, but it is challenging in rodents; an accurate population-derived input function would forego the need for future manual blood sampling.

F1.1 Objectives

- Establish protocol for multimodal imaging (^{18}F -FEPPA-PET/MR/CT) of a rodent ischemic stroke model.
- Determine spatial and temporal progression of white matter injury and inflammation.
- Evaluate the kinetics of ^{18}F -FEPPA and develop a population-derived input function

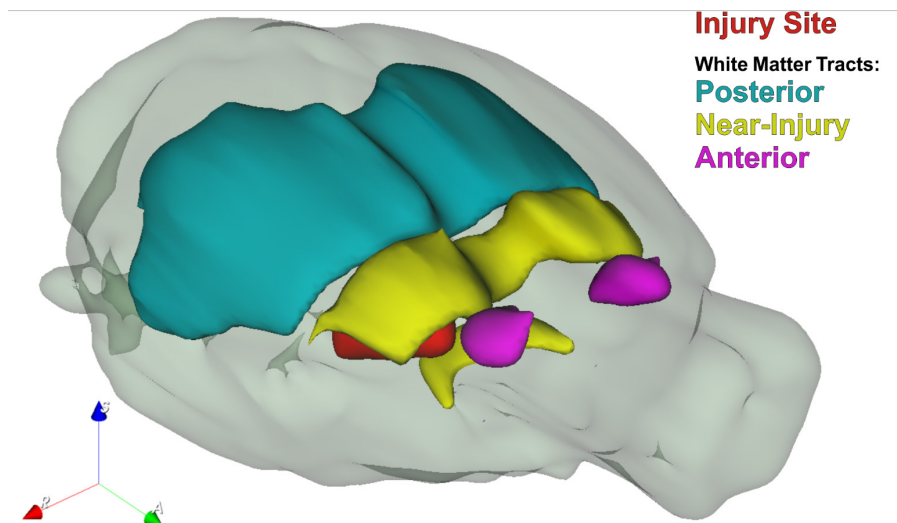
F2 Methods

8 – 12-month-old TgAPP21 rats were imaged 7 – 10 days prior to focal ischemic injury of the dorsal striatum (baseline imaging), 7 days following injury, and 30 days following injury. To model focal ischemic injury, unilateral ET1 (60 pmol dissolved in 3 μl sterile 0.9% saline) was injected into the dorsal striatum of ($n = 6$), as described in [5.3.2 Endothelin-1 Focal Ischemic Injury](#). On each of the 3 imaging days, ^{18}F -FEPPA was produced at an onsite cyclotron. Injected doses averaged 29.6 MBq, ranging from 22.4 – 37.6 MBq. Immediately following ^{18}F -FEPPA injection, a dynamic 90 min PET scan (Siemens Inveon) was initiated, followed by a 40 min MR imaging sequence (Siemens Biograph mMR), and then iopamidol (Isovue®)-enhanced CT (GE VCT). Dynamic PET data was manually registered to subsequently acquired T2-weighted MR images. CT analysis of cerebral circulation was focused on mean transit time (MTT), which estimates the average time needed for blood to pass through tissue and corresponds to the ratio of cerebral blood volume : flow. During baseline and 30-day post-injury imaging, arterial blood samples were acquired from 5 subjects at 2, 8, 16, 64, and 90 min after ^{18}F -FEPPA injection. The ratio of unmetabolized ^{18}F -FEPPA in plasma and blood was determined by solid-phase extraction chromatography^{20,21}. Following imaging 30 days after ET1 ischemic injury, rats were euthanized, and brain tissue was collected for IHC, as described in [2.3.5 Immunohistochemistry & Image Processing](#).



Appendix Figure F-1: Endothelin-1 injection into the dorsal striatum

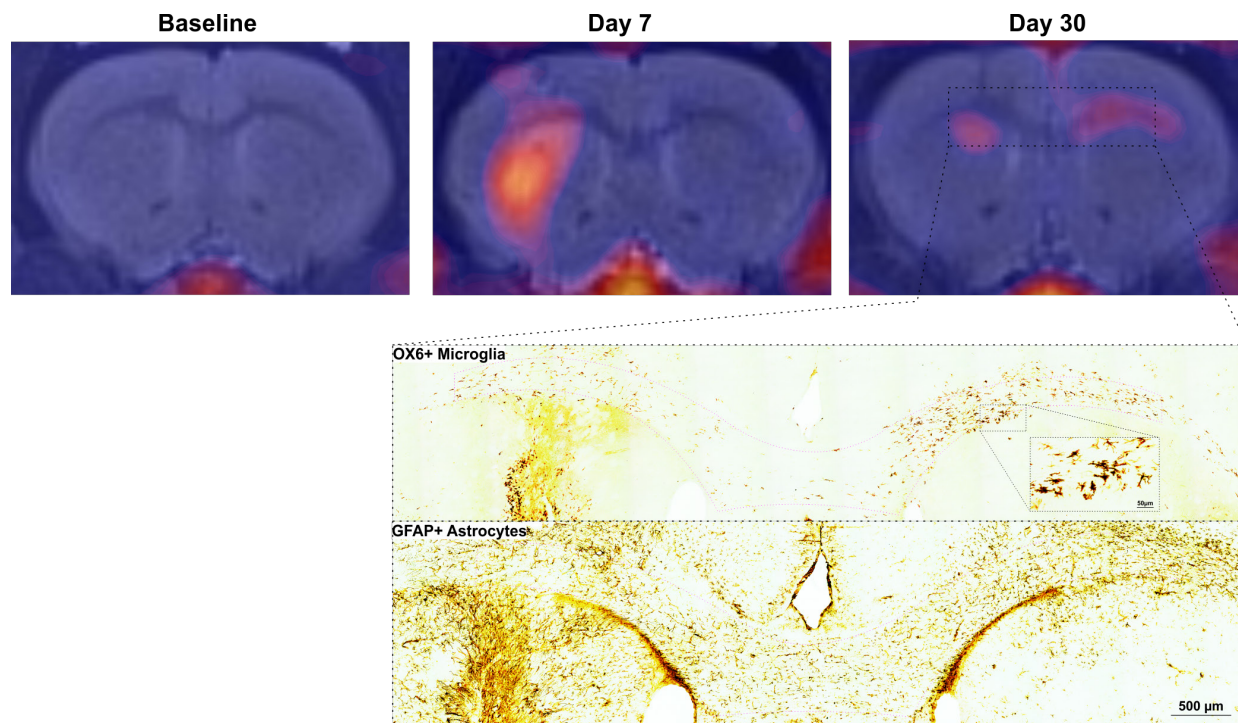
Dashed outline identifies glial scar formed after ET1 injection, observed on DAB-IHC with a primary antibody for GFAP (30 μ m coronal section).



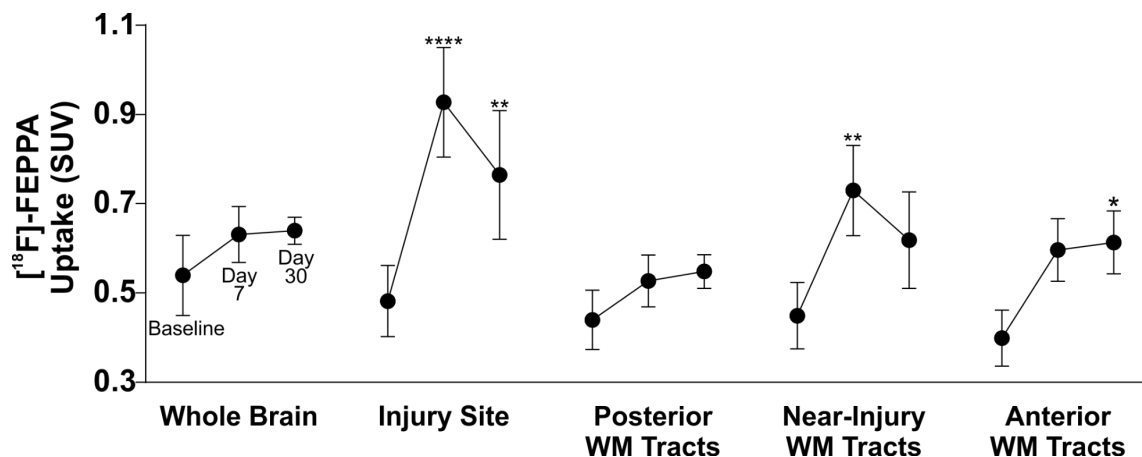
Appendix Figure F-2: Brain Segmentation Model

Neuroanatomy and injury site identified by T2-weighted MRI; these segments were then applied to co-registered PET data.

F3 Results

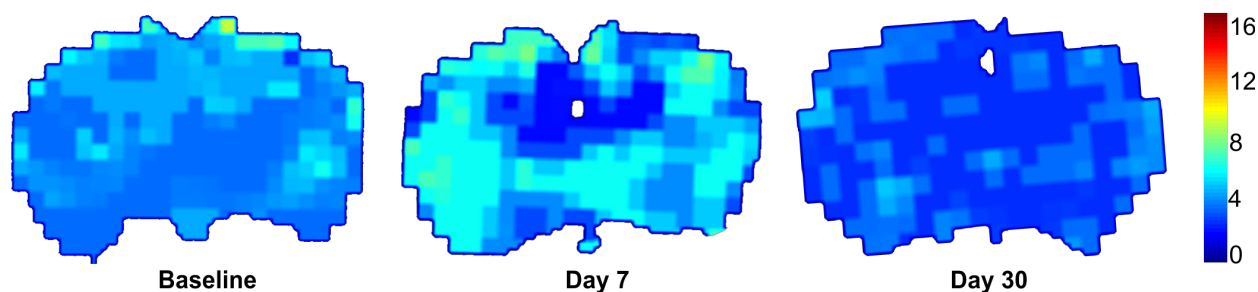
**Appendix Figure F-3: Immunohistochemistry Corroborates ^{18}F -FEPPA-PET/MR Findings**

High penumbral ^{18}F -FEPPA uptake was observed 7 days after ET1-ischemic injury of the dorsal striatum. Localization of increased uptake corresponded with OX6+ activated microglia more consistently than GFAP+ reactive astrocytes. 30 days following injury, continued uptake and microglial activation was observed distal to the injury site, particularly in white matter tracts.



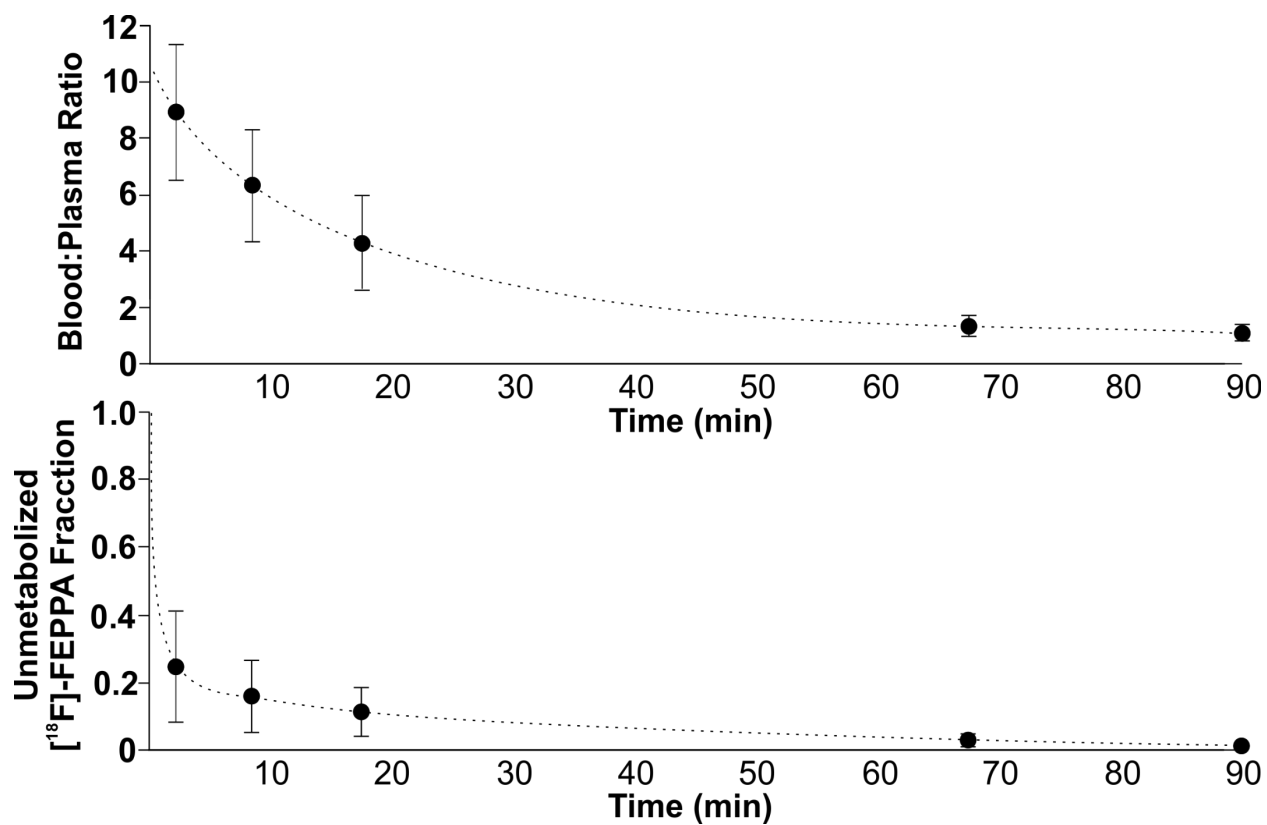
Appendix Figure F-4: ^{18}F -FEPPA Uptake Following Injury Persists in Anterior White Matter Tracts

^{18}F -FEPPA uptake was significantly increased around the injury site and proximal white matter (WM) following injury. 30 days after injury, uptake in these regions reduced from levels seen at day 7 but was still relatively increased throughout the brain, especially in anterior white matter. * $p < 0.05$, ** $p < 0.01$, **** $p < 0.0001$ compared to baseline. $n = 6$, error bars = SEM



Appendix Figure F-5: Mean Transit Time Prolonged by Ischemic Injury

These experiments were conducted following PET & MR imaging, thus anesthesia time and quality was likely an important variable that affected cerebral circulation. Despite this confound, MTT was found to be prolonged in the penumbral region 7 days after injury and normalized by day 30. Axial resolution = 500 μm , scale = time (s)



Appendix Figure F-6: ¹⁸F-FEPPA Kinetic Profile

The blood:plasma-bound ratio of the ¹⁸F-FEPPA radiotracer was well modelled by a bi-exponential function ($R^2 = 0.87$), while the unmetabolized fraction of the radiotracer was well modelled by a Hill function ($R^2 = 0.92$). These population-derived kinetic models will be applied to future arterial input functions in dynamic PET.

n = 5, error bars = SD.

F4 Conclusions

This study demonstrates the feasibility of ^{18}F -FEPPA-PET as an effective method for in vivo imaging of microglia activity in a rat model of ischemic stroke. The localization of microglia activity was further improved with MRI co-registration. Qualitative evaluation of immunohistochemistry revealed that ^{18}F -FEPPA uptake corresponded better with increased microglia activation than reactive astrogliosis (Appendix Figure F-3). PET findings indicated sustained wide spread inflammation, especially in anterior white matter, following ischemic injury of the dorsal striatum (Appendix Figure F-4).

Reduced MTT warrants further investigation of the impact of disrupted perfusion and circulation on radiotracer uptake (Appendix Figure F-5). This also raises the question of whether BBB disruption following ischemic injury may confound the distribution of ^{18}F -FEPPA in the brain^{22,23}. Despite these limitations, the methods described here will enable comparative investigation, such as the comparison of Wt and TgAPP21 rats' response to ischemic injury and the effect of anti-inflammatory interventions. Future studies can apply the population-derived ^{18}F -FEPPA kinetics to arterial input functions (Appendix Figure F-6), foregoing the need for further blood sampling.

F5 References

1. Vermeer SE, Longstreth WT, Jr., Koudstaal PJ. Silent brain infarcts: a systematic review. *Lancet Neurol.* 2007;6(7):611-619.
2. Kalaria RN, Akinyemi R, Ihara M. Stroke injury, cognitive impairment and vascular dementia. *Biochimica et biophysica acta.* 2016;1862(5):915-925.
3. Thiel A, Cechetto DF, Heiss WD, Hachinski V, Whitehead SN. Amyloid burden, neuroinflammation, and links to cognitive decline after ischemic stroke. *Stroke.* 2014;45(9):2825-2829.
4. Mijajlović MD, Pavlović A, Brainin M, et al. Post-stroke dementia - a comprehensive review. *BMC Medicine.* 2017;15(1):1-12.
5. Qi J-P, Wu H, Yang Y, et al. Cerebral ischemia and Alzheimer's disease: the expression of amyloid-beta and apolipoprotein E in human hippocampus. *Journal of Alzheimer's disease : JAD.* 2007;12(4):335-341.
6. Silbert LC, Dodge HH, Perkins LG, et al. Trajectory of white matter hyperintensity burden preceding mild cognitive impairment. *Neurology.* 2012;79(8):741-747.
7. Smith EE, Egorova S, Blacker D, et al. Magnetic resonance imaging white matter hyperintensities and brain volume in the prediction of mild cognitive impairment and dementia. *Arch Neurol.* 2008;65(1):94-100.
8. Cloutier S, Chertkow H, Kergoat MJ, Gauthier S, Belleville S. Patterns of Cognitive Decline Prior to Dementia in Persons with Mild Cognitive Impairment. *J Alzheimers Dis.* 2015;47(4):901-913.
9. Maier-Hein KH, Westin CF, Shenton ME, et al. Widespread white matter degeneration preceding the onset of dementia. *Alzheimers Dement.* 2015;11(5):485-493 e482.
10. Lee S, Viqar F, Zimmerman ME, et al. White matter hyperintensities are a core feature of Alzheimer's disease: Evidence from the dominantly inherited Alzheimer network. *Ann Neurol.* 2016;79(6):929-939.
11. Rosenberg GA. Inflammation and white matter damage in vascular cognitive impairment. *Stroke.* 2009;40(3 Suppl):S20-23.
12. Wardlaw JM, Valdés Hernández MC, Muñoz-Maniega S, Valdes Hernandez MC, Munoz-Maniega S. What are white matter hyperintensities made of? Relevance to vascular cognitive impairment. *J Am Heart Assoc.* 2015;4(6):1140-1140.
13. Raj D, Yin Z, Breur M, et al. Increased White Matter Inflammation in Aging- and Alzheimer's Disease Brain. *Front Mol Neurosci.* 2017;10(June):206.
14. Venneti S, Lopresti BJ, Wiley CA. The peripheral benzodiazepine receptor (Translocator protein 18kDa) in microglia: from pathology to imaging. *Prog Neurobiol.* 2006;80(6):308-322.
15. Chen MK, Guilarte TR. Translocator protein 18 kDa (TSPO): molecular sensor of brain injury and repair. *Pharmacol Ther.* 2008;118(1):1-17.

16. Lavisse S, Guillermier M, Herard AS, et al. Reactive astrocytes overexpress TSPO and are detected by TSPO positron emission tomography imaging. *J Neurosci*. 2012;32(32):10809-10818.
17. Vivash L, O'Brien TJ. Imaging Microglial Activation with TSPO PET: Lighting Up Neurologic Diseases? *J Nucl Med*. 2016;57(2):165-168.
18. Wilson AA, Garcia A, Parkes J, et al. Radiosynthesis and initial evaluation of [18F]-FEPPA for PET imaging of peripheral benzodiazepine receptors. *Nucl Med Biol*. 2008;35(3):305-314.
19. Duering M, Zieren N, Hervé D, et al. Strategic role of frontal white matter tracts in vascular cognitive impairment: a voxel-based lesion-symptom mapping study in CADASIL. *Brain*. 2011;134(8):2366-2375.
20. Rusjan PM, Wilson AA, Bloomfield PM, et al. Quantitation of translocator protein binding in human brain with the novel radioligand [18F]-FEPPA and positron emission tomography. *J Cereb Blood Flow Metab*. 2011;31(8):1807-1816.
21. Katsifis A, Loc'h C, Henderson D, et al. A rapid solid-phase extraction method for measurement of non-metabolised peripheral benzodiazepine receptor ligands, [(18)F]PBR102 and [(18)F]PBR111, in rat and primate plasma. *Nucl Med Biol*. 2011;38(1):137-148.
22. Boutin H, Prenant C, Maroy R, et al. [18F]DPA-714: direct comparison with [11C]PK11195 in a model of cerebral ischemia in rats. *PLoS One*. 2013;8(2):e56441.
23. Boutin H, Murray K, Pradillo J, et al. 18F-GE-180: a novel TSPO radiotracer compared to 11C-R-PK11195 in a preclinical model of stroke. *Eur J Nucl Med Mol Imaging*. 2015;42(3):503-511.

Appendix G: Animal Use Protocol



AUP Number: 2014-016

PI Name: Whitehead, Shawn N

AUP Title: Role of vascular risk factors in cognitive decline

Official Notification of AUS Approval: A MODIFICATION to Animal Use Protocol 2014-016 has been approved.

The holder of this Animal Use Protocol is responsible to ensure that all associated safety components (biosafety, radiation safety, general laboratory safety) comply with institutional safety standards and have received all necessary approvals. Please consult directly with your institutional safety officers.

Submitted by: Kinchlea, Will D
on behalf of the Animal Use Subcommittee

Curriculum Vitae

Alexander Levit

Degrees

MD/PhD, Schulich School of Medicine & Dentistry, University of Western Ontario	2013 – 2020
PhD research in the Department of Anatomy & Cell Biology, 2015-2018. Supervisors: Dr Shawn Whitehead & Dr Vladimir Hachinski	
Honours Bachelor of Science, University of Toronto	2009 – 2013
Specialist degree in Neuroscience, Major degree in Physiology, Minor degree in Psychology. Graduated with High Distinction.	

Honours and Awards

Queen Elizabeth II Graduate Scholarship in Science and Technology, 15 000.	2017 – 2018
Ontario Graduate Scholarship, 15 000.	2016 – 2017
CIHR Frederick Banting and Charles Best Canada Graduate Scholarship, 17 500.	2015 – 2016
Western Graduate Research Scholarship (3x), 13 500.	2015 – 2018
Schulich Graduate Scholarship (3x), 6000.	2015 – 2018
Ontario Graduate Scholarship (Declined), 15 000.	2015 – 2016
Horace and Clarice Wankel Memorial Award for Cardiovascular Research, 300.	2015
R. John & Agnes M. Adams Summer Medical Student Scholarship, Heart and Stroke Foundation of Canada, 4500.	2015
Jack Banham Hargreaves/Jessie Louisa Florence Hargreaves MD Award, 10 000.	2014 – 2015
Summer Research Training Program Award, 4500.	2014
New College In-Course Scholarships (Received Annually 3x), 4000 in total.	2010 – 2013
Dean's List Scholar (Received Annually 4x).	2009 – 2013
NSERC Undergraduate Student Research Award, 5750.	2011
University of Toronto Scholar Award, 5000.	2009 – 2010
New College Admission Scholarship, 5000.	2009 – 2010

Journal Publications – Original Research

Behavioural inflexibility in a comorbid rat model of striatal ischemic injury and mutant hAPP overexpression
 Alexander Levit, Aaron M. Regis, Jessica R. Garabon, Seung-Hun Oh, Sagar Desai, Nagalingam Rajakumar, Vladimir Hachinski, Yuksel Agca, Cansu Agca, Shawn N. Whitehead, Brian L. Allman.
Behavioural Brain Research, 2017 Aug 30; 333:267-275

Other Publications

Scientific Overview on CSCI-CITAC Annual General Meeting and 2017 Young Investigators' Forum
 Kristen I Barton, Xiya Ma, Ege Babadagli, PhD, Nicolas Tonial, Christopher Newell, Abdullah Ishaque, Heather Leduc-Pessah, Tina Binesh, Sarah Mirali, Elina K Cook, Alexander Levit, Sachin Kumar, Patrick Steadman, Josh Abraham. *Clinical and Investigative Medicine*, 2018 Oct 5; 41(3):E156-E164

The promise of natural language processing in healthcare

Rohin Attrey & Alexander Levit. *University of Western Ontario Medical Journal*, 2018; 87(2): (in review)

Going blind: UWOMJ's updated review process

Alexander Levit. *University of Western Ontario Medical Journal*, 2016; 87(1): 5

Knowledge translation and UWOMJ's expanded authorship

Alexander Levit. *University of Western Ontario Medical Journal*, 2016; 85(1):4

Modifications in anesthesia for geriatric patients

Brandon Chau, Alexander Levit. *University of Western Ontario Medical Journal*, 2015; 84(2): 10-11

Tick tock: Thrombolysis & acute management of ischemic stroke

Alexander Levit, Brandon Chau. *University of Western Ontario Medical Journal*, 2015; 84(1): 7-9

Surgical hygiene: refining the WHO Safe Surgery Saves Lives guidelines

Alexander Levit, Denise Darmawikarta. *University of Western Ontario Medical Journal*, 2014; 83(2): 9-10

The Baby Blues: Challenges and limitations of delivering obstetrics care in rural Canada

Denise Darmawikarta, Alexander Levit. *University of Western Ontario Medical Journal*, 2014; 83(1): 27-29

Platform Presentations

The White Matter Menace: Susceptibility to Cognitive impairment in the TgAPP21 Rat

Department of Anatomy & Cell Biology Seminar Series; London ON: May 04, 2018

No Escape: Regressive search strategy and inflexibility in a transgenic rat model of Alzheimer disease

Department of Anatomy & Cell Biology Research Day; London ON: Oct 27, 2017

Behavioural and white matter changes in a transgenic rat model of prodromal Alzheimer disease

Clinician Scientist Trainee Symposium; London ON: Aug 22, 2017

Poster Presentations

Age-Dependent White Matter Inflammation and Cognitive Impairment in the TgAPP21 Rat Model of Alzheimer Disease

Alexander Levit, Brian L. Allman, Nagalingam Rajakumar, Vladimir Hachinski, Shawn N. Whitehead.

- Canadian Association for Neuroscience Annual General Meeting; Vancouver, BC: May 13-16, 2018
- London Health Research Day; London, ON: May 10, 2018
- American Academy of Neurology Annual General Meeting; Los Angeles, CA: Apr 21-27, 2018.

Received travel award from Department of Anatomy & Cell Biology

Multimodal Imaging of White Matter Inflammation in a Rat Model of Striatal Ischemic Stroke

Alexander Levit, Matthew S. Fox, Qi Qi, Vladimir Hachinski, Jonathan D. Thiessen, Shawn Whitehead.

American Academy of Neurology Annual General Meeting; Los Angeles, CA: Apr 21-27, 2018.

Received travel award from Department of Anatomy & Cell Biology

Correcting the Arterial Input Function for Dynamic 18F-FEPPA PET in Transgenic Fischer 344 Rats with Manual Blood Sampling

Qi Qi, Matthew S. Fox, Alexander Levit, Shawn N. Whitehead, Ting-Yim Lee, Jonathan D. Thiessen.

Imaging Network Ontario Annual Symposium; Toronto, ON: March 28-29, 2018

Regressive behavioural inflexibility and white matter inflammation in the TgAPP21 rat model of Alzheimer disease

Alexander Levit, Aaron M Regis, Vladimir Hachinski, Brian L Allman, Shawn Whitehead

Clinician Investigator Training Association of Canada Annual Scientific Meeting; Toronto ON: Nov 20-22, 2017

Novel analyses of cognitive flexibility in a transgenic hAPP rat model with comorbid striatal ischemic stroke

Aaron Regis, Alexander Levit, Vladimir Hachinski, Brian Allman, Shawn Whitehead

- Canadian National Medical Student Research Symposium; Winnipeg, MB: Jun 5-8, 2017.
Received travel award from Schulich School of Medicine & Dentistry
- Clinician Investigator Training Association of Canada Annual Scientific Meeting; Toronto ON: Nov 21-23, 2016

Investigating the effects of hypertension on a transgenic rat model of Alzheimer disease

Alexander Levit, Sonny Cheng, Andrew Gibson, Murad Ahmad, Olivia Hough, Vladimir Hachinski, Shawn Whitehead

- Alzheimer's Drug Discovery Foundation Neurodegeneration Conference; San Diego, CA: Feb 12-14, 2017. **Received ADDF Young Investigator Scholarship**
- Society for Neuroscience Annual Meeting; San Diego, CA: Nov 12-16, 2016

The role of hypertension and inflammation in an Alzheimer disease rat model

Alexander Levit, Vladimir Hachinski, Shawn Whitehead.

- The International Society of Vascular Behavioural and Cognitive Disorders Congress; Amsterdam, Netherlands: Oct 13-15, 2016
- Department of Anatomy & Cell Biology Research Day; London, ON: Oct 21, 2016
- Canadian Association for Neuroscience Annual Meeting; Toronto, ON: May 29-Jun 1, 2016

White matter inflammation in a comorbid rat model of hypertension & Alzheimer disease

Alexander Levit, Vladimir Hachinski, Shawn Whitehead

Southern Ontario Neuroscience Association Annual Meeting; Waterloo, ON: May 6, 2016

Modelling the role of hypertension in the pathogenesis of Alzheimer disease

Alexander Levit, Vladimir Hachinski, Shawn Whitehead

- London Health Research Day; London, ON: Mar 29, 2016
- Clinician Investigator Trainee Association of Canada Annual General Meeting; Toronto, ON: Nov 23-25, 2015

Teaching & Educational Leadership

Student Representative, CBME Pedagogy Committee

2018 – ongoing

Contributed to the development of a competency-based curriculum for the Schulich School of Medicine & Dentistry's MD Program. The committee was tasked with analyzing and proposing strategies for integrating Competency-Based Medical Education (CBME) and the evaluation of entrustable professional activities (EPAs) into current pedagogical approaches including independent learning, small group learning, and large group learning.

Certificate in University Teaching and Learning

2016 – 2018

Offered by the Teaching Support Centre, Western University, the certificate program allowed me to enhance my teaching and presentation skills through hands-on practice, mentorship, and peer feedback. The program facilitated reflective learning on pedagogical strategies, including a teaching philosophy component; my teaching philosophy emphasizes *discovery-based learning*, and can be provided upon request. Workshops attended:

<i>Threshold Concepts: Teaching Troublesome Knowledge in the Disciplines</i>	Nov 25, 2016
<i>Guiding Students through Problem Solving in STEM</i>	Oct 17, 2016
<i>Avoiding the Blank Stare: Great Ideas for Engaging Students in Tutorials Across Disciplines</i>	Oct 17, 2016
<i>Incorporating Indigenous Methodologies and Ways of Knowing into the Curriculum</i>	Aug 30, 2016
<i>Getting Feedback on Your Students? Learning and Your Teaching</i>	Aug 30, 2016
<i>Lessons from WALs: Engaging Students Outside Active Learning Classrooms</i>	Aug 30, 2016
<i>Great Ideas for Teaching: Panel Presentation</i>	Jan 30, 2016
<i>Putting Together a Teaching Dossier</i>	Jan 30, 2016
<i>Supporting Undergraduate Writing in the Humanities: Perspectives from Philosophy & English</i>	Jan 30, 2016
<i>The Graduate Game Plan: Strategies for Success</i>	Jan 30, 2016

Teaching Assistant, Managing Health Services MPH9010 2018

Class size: 60

This core course of the new Masters of Public Health program focused on the governing, financing, and organizational structures of health systems. As the only TA for MPH9010, my primary responsibility was the evaluation of written assignments. I identified several student submissions with concerns of plagiarism and developed a follow-up plan to handle this concern, meeting with students to clarify expectations for academic writing. In addition to my responsibilities as TA, I took the initiative to evaluate oral presentations, improving grading objectivity and consistency.

Teaching Assistant, Neuroscience for Rehabilitation Sciences ACB9531 2016 – 2017

Class size: 70

ACB9531 was a core first year course for the Master of Physical Therapy program (Faculty of Western Health Sciences), offered by Department of Anatomy & Cell Biology (Schulich School of Medicine & Dentistry). Course content included the function and organization of the central and peripheral nervous system, with a focus on knowledge application by rehabilitation professionals. During both terms, I led self-learning anatomy lab sessions.

- In the 2017 fall term, I enhanced students' learning experiences by addressing their specific questions in micro-teaching sessions, engaging smaller groups of students and encouraging active participation. Threshold concepts were brought up and addressed with the whole class. I also improved in-class evaluations by taking up and discussing quiz answers.
- In the 2016 Fall term, I graded essay assignments and led the development of a detailed rubric to improve grading consistency among TAs. I met with students to clarify assignment expectations, opportunities for improvement, and to address concerns about plagiarism.

Guest Lecturer, Neuroscience for Rehabilitation Sciences ACB9531 2016

Class size: 70

Led a 2-hour lecture on *Synaptic Transmission, Neurotransmitters and Receptors* and another 2-hour lecture on the *Cerebellum & Diencephalon*. Engaged students using classroom assessment techniques, including live question polling.

Editorial Experience & Peer Review

Editorial Review Board, *Clinical & Investigative Medicine* 2018 – ongoing

Contributed peer review of manuscripts submitted to CIM, the official journal of the Canadian Society for Clinical Investigation

Co-Editor-In-Chief, *University of Western Ontario Medical Journal* 2017 – 2018

Oversaw the publication of 3 issues, including themed issues: *Pain Management and Robotics, AI & Big Data*, and coordinated the responsibilities of the entire UWOMJ team of 33 colleagues, including editors, IT directors, finance officers, and staff writers. Introduced blinded peer-review and DOI indexing

Senior Associate Editor, *University of Western Ontario Medical Journal* 2016 – 2017

Oversaw the publication of 3 issues, including themed issues: *Trauma & Disaster Medicine* and *Healthcare Systems*. Directly involved in peer review, copy-editing, and establishing stylistic standards

Junior Associate Editor, *University of Western Ontario Medical Journal* 2015 – 2016
Oversaw the publication of 3 issues, including themed issues: *Preventive Medicine* and *Drugs*. Directly involved in peer review and copy-editing. Expanded journal authorship to graduate research students.

Editorial Review Board, *Journal of Undergraduate Life Science* 2011 – 2012
Contributed to peer review

Training Seminars & Other Conferences

Applied Suicide Intervention Skills Training (ASIST); London, ON	May 26 – 27, 2018
Heart & Stroke Clinical Update; Toronto, ON	Dec 8 – 9, 2017
Principles & Practice of Clinical Research; Burlington, ON	Sep 21 – 22, 2017
American Psychiatric Association Annual Meeting; Toronto, ON	May 16 – 20, 2015
Point of Care Ultrasound Medical Student Summer Symposium; London ON	Aug 23 – 24, 2014

Public Advocacy & Community Engagement

Social Media Manager, Schulich Political Advocacy Committee (PAC) 2018
Set up and coordinated Schulich PAC's social media campaigns, including the successful 2018 municipal lobby initiative to promote naloxone kit availability in public buildings.

CIM-Liaison, CITAC 2018 – ongoing
Acting as liaison between the *Clinical & Investigative Medicine* journal and the Clinician-Investigator Trainee Association of Canada, I promoted CIM to Canadian medical students and residents across Canada and founded publication awards to recognize outstanding healthcare research conducted by medical students and residents.

Municipal Lobbyist, Schulich Political Advocacy Committee (PAC) 2017
Participated in lobby and communications training programs led by the Ontario Medical Association and Schulich School of Medicine & Dentistry's medical student-led Political Advocacy Committee. Met with municipal city councilor to advocate for our ask: expand municipal funding for *My Sister's Place*, a women's shelter that provides essential support services for housing and mental health.

Co-Chair, Retiring With Strong Minds 2015 – 2017
Retiring With Strong Minds is a graduate student led program that aims to promote knowledge exchange between university students and older adults.

- Partnered with local communities to provide accessible venues and promote monthly seminars.
- Recruited graduate student from all academic faculties to present their expertise.
- Consulted presenters on communication of expert knowledge to a layman audience Facilitated discussions about sensitive health issues and research